

Impacts of Climate Change on Canadian Airport Pavements

by

Edward Alexander Abreu

A thesis
presented to the University of Waterloo
in fulfillment of the
thesis requirement for the degree of
Master of Applied Science
in
Civil Engineering

Waterloo, Ontario, Canada, 2019

© Edward Alexander Abreu 2019

AUTHOR'S DECLARATION

I hereby declare that I am the sole author of this thesis. This is a true copy of the thesis, including any required final revisions, as accepted by my examiners.

I understand that my thesis may be made electronically available to the public.

Abstract

Greenhouse gasses (GHG) emitted by the burning of fossil fuels and supplementary anthropogenic activities are on the rise since the industrial revolution. The world is becoming warmer and more polluted with such gases, which have also caused notable changes in the climate. The environment has been affected by this situation and Canadian airports are no exception. This research aims to present numerous changes of climate at different airports located in various provinces and territories of Canada. The extent of precipitation and risk of flooding, the highest and lowest annual temperatures, the fluctuation of freeze-thaw cycles, and the variation of permafrost are all considered. In addition, this research analyzes the impact of these changes on the operation and/or performance of the airside infrastructure at the selected airports and provides recommended considerations for mitigation and adaptation strategies.

The correlation between the changes in climate and the impacts of these to the airfield infrastructure was assessed by an array of laboratory tests in which the samples were subjected to conditions simulating: moisture damage, rise of temperature, and the fluctuation of freeze-thaw cycles. The Hamburg wheel tracking test (HWTT) was performed to evaluate rutting under various temperatures as well as different quantities of freeze-thaw cycles. The tensile strength ratio (TSR) was developed to assess the reduction of indirect tensile strength (ITS) due to freeze-thaw cycles. The ITS results were used to calculate a crack propagation index called IDEAL CT-Index which provided insights into how freeze-thaw cycles affect the crack propagation of flexible airfield pavement infrastructures.

The findings of the research indicate that Canadian airports are indeed experiencing a rise of both the maximum and the minimum temperature which is inducing the amount of rainfall to rise as well. Snowfall, on another hand, is varying depending on the locations, being Montreal airport the one experiencing the largest reduction while Winnipeg airport has the most significant growth over the analysed period of 70 years (1950-2019). Considering the developed freeze-thaw cycle analysis, the results did not show a significant increase or decrease, just fluctuations among the years. However, it was noticed that depending on the location, the amount of annual Freeze-Thaw cycles varied significantly starting from Yellowknife international airport, with an annual average of 9 cycles per year, to Halifax international airport which registered an average of 22 cycles per year. Furthermore, the permafrost analysis presented that Yellowknife and Whitehorse airports are build on top of discontinuous and sporadic permafrost, which makes them susceptible to settlement and fatigue cracking due to the lost of support caused by the reduction of permafrost.

The results from the laboratory tests performed on airfield asphalt samples indicated that freeze-thaw cycles and high temperatures induce the asphalt mix to become softer making it more susceptible to rutting and shoving. Freeze-thaw cycles increased premature rutting failure compared to the one for temperature variation. Apart from the fact that as the number of freeze-thaw cycles increased the tensile strength was reduced. It is significant to note that the relationship was non proportional. Hence, the higher the amount of freeze-thaw cycles induced, the less impact they will have on the mix. Additionally, it is substantial to note that freeze-thaw cycles make the asphalt sample softer, also in a non-proportional way. The CT-index increased as the tensile strength was reduced due to the freeze-thaw cycles. As the samples becomes softer, the energy of fracture dissipates which implies a less brittle performance; hence, less susceptibility for the cracks to propagate.

Acknowledgements

This research would have not been possible without the contributions of several companies, institutions, and people that selflessly contributed with funding, materials, data, and advices. Among them:

- Dr. Sina Varamini from McAsphalt is to be acknowledge for his guidance, help, and support with the laboratory tests, especially the crack propagation.
- Chris Stewart, Myron Thiessen, and Jared Mitchell from the Canadian airfield pavement technical group (CAPTG) which stand out because, more than the funding provided, they allowed me to present the preliminary results of this research at SWIFT Conference, Vancouver 2019.
- The contributions from David Boccia, Jeremy Demelio, and Tejinder Bhelley from PaveAl with the airfield asphalt mixes accompany with all the properties and design details were highly significant.
- Environment Canada and Elena Butz from Meteoblue ought to be acknowledge for being the main source of environment data.
- Misha Kuzma from the geospatial department at the University of Waterloo provided meaningful guidance and assistance to develop several of the maps presented on this research using GIS.

Lastly but, in fact, the most important, I have to acknowledge my supervisor Professor Susan Tighe for making this research possible as well as for her wise advices and life lessons.

Dedication

I would like to dedicate this thesis to my beloved wife and my parents as they have been, and will always be, the foundation that carry all my loads providing support, care, and love.

Table of Contents

AUTHOR’S DECLARATION	ii
Abstract	iii
Acknowledgements	iv
Dedication	v
List of Figures	ix
List of Tables	xiii
List of Images	xiv
Chapter 1	1
Introduction	1
1.1 Introduction.....	1
1.2 Objectives.....	2
1.3 Thesis Methodology	2
1.4 Chapter Summary	3
Chapter 2	4
Literature Review	4
2.0 Climate Change.....	4
2.1 Climate Change effects in the Transportation industry in Canada.....	7
2.2 Canadian Airfield Infrastructure, Design, and Implications.....	8
2.3 Consideration of Climate Change by Canadian Airport Authorities	11
2.4 Current distresses due to Climate Change in Canadian Airport Pavements.....	15
2.4.1 Stripping.....	15
2.4.2 Thermal Cracking.....	16
2.4.2 Rutting.....	16
2.4.4 Frost Heaving	17
2.4.5 Shoving	18
2.4.6 Settlement	18
2.4.7 Fog and Lost of Skid Resistance	19
2.5 Methods of Assessing Rutting, Stripping, Tensile Strength, and Crack Propagation	19
2.5.1 Hamburg Wheel Tracking Test under Water (AASHTO T 324)	20
2.5.2 Modified Lottman Test (AASHTO T 283)	21
2.5.3 Ideal Cracking Test	21
2.6 Chapter Summary	23
Chapter 3	24
Climate Data and Material Collection and Design	24
3.1 Locations	24
3.2 Material Design and Collection	26

3.3 Chapter Summary	27
Chapter 4	28
Wind, Temperature, and Precipitation Analysis and Results	28
4.1 Wind Analysis	28
4.2 Temperature Analysis.....	31
4.2.1 Ambient and Pavement Temperature Results	31
4.2.2 Annual Number of Freeze-Thaw Cycles	36
4.3 Permafrost Analysis.....	39
4.4 Precipitation Analysis and Results	41
4.4 Chapter Summary	44
CHAPTER 5	45
Laboratory Testing Analysis and Discussions	45
5.1 Extraction and Gradation	46
5.2 Hamburg Wheel Tracking Test (AASHTO T 324) modifications, Analysis, and Discussions	48
5.2.1 Rutting and Freeze-Thaw Cycles Evaluation/Correlation.....	48
5.2.2 Rutting and Temperature Rise Evaluation/Correlation	49
5.3 Modified Lottman Test (AASHTO T 283)	52
5.3.1 ITS's Variation due to Freeze-Thaw Cycles	52
5.3.2 ITS's Variation due to Freeze-Thaw Cycles and Faster Compaction	54
5.3.2 ITS's Variation due to the Reduction of the Freeze-Thaw Cycles' Period and Faster Compaction	55
5.4 Ideal Cracking Test.....	55
5.6 Chapter Summary	56
CHAPTER 6	57
Conclusions and Recommendations	57
6.1 Considerations for Mitigation and Adaptation Strategies.....	57
6.1 Conclusions	59
6.2 Future Work and Recommendations.....	60
REFERENCES	61
APPENDIX A	65
Environmental Analysis Results	65
Temperature Results	65
Toronto Pearson International Airport	66
Vancouver International Airport.....	67
Montreal Trudeau International Airport.....	68
Halifax Stanfield International Airport.....	69
Calgary International Airport.....	70

Saskatoon International Airport.....	71
Winnipeg International Airport	72
Moncton International Airport.....	73
Whitehorse International Airport.....	74
Yellowknife International Airport.....	75
Iqaluit Airport	76
Freeze-Thaw Cycles Algorithm	77
Values' Description:	77
Excel Algorithm:.....	77
Freeze-Thaw Cycles Results	78
Precipitation Results	83
Toronto Pearson International Airport	83
Vancouver International Airport.....	84
Montreal Trudeau International Airport.....	85
Halifax Stanfield International Airport	86
Calgary International Airport.....	87
Saskatoon International Airport.....	88
Winnipeg International Airport	89
Moncton International Airport.....	90
Whitehorse International Airport.....	91
Yellowknife International Airport.....	92
Iqaluit Airport	93
APPENDIX B	94
Laboratory Results	94
Hamburg Wheel Tracking Test Results	94
Temperature Variation	95
Freeze-Thaw Cycles Variation	96
Tensile Strength Ratio Results	97
Modified Lottman Test – 50 mm/min – Freeze-Thaw Cycles Variation	98
Modified Lottman Test – 50 mm/sec – Freeze-Thaw Cycles Variation.....	99
Modified Lottman Test – 50 mm/sec – Half Freeze-Thaw Cycles Variation	100
Ideal Cracking Test Results.....	101

List of Figures

Figure 1.1 Research Methodology	2
Figure 2.1 Surface Temperature Anomalies Relatives to 1951-1980 (A) Global Annual Mean Anomalies. (B) Temperature anomalies for the first half decade of the 21st century (James Hansen, 2006).....	4
Figure 2.2 Carbon Dioxide Level During Ice Ages and Warm Period for the Past 800,00 years (National Oceanic and Atmospheric Administration, 2018).....	5
Figure 2.3 Carbon Dioxide Level During the Past 8,000 years (Cook, 2010).....	5
Figure 2.4 Global Climate Projections (Bush & Lemmen, 2019).....	6
Figure 2.5 Average Artic Sea Ice Since 1980 (NSIDC/NASA, 2019).....	7
Figure 2.6 Sample Distribution of a Typical Airport (Aehnelt, 2016).....	9
Figure 2.7 Airfield Pavement Infrastructure Design Examples using FAARFIELD 1.42 (A) Flexible Pavement, (B) Rigid Pavement.....	10
Figure 2.8 Consideration of Climate Change on the Decision Making.....	12
Figure 2.9 Climate Change Consequences on Airfield Pavements.....	12
Figure 2.10 Climate Change Phenomenon’s Perspective.....	13
Figure 2.11 Main Barriers to Contemplate Climate Change Risk and Adaptation/Mitigation in the Day-to-Day Activities for Pavements.....	14
Figure 2.12 Adaptation to Climate Change Risk for Airfield Pavements.....	14
Figure 2.13 Tensile Strength Ratio Conditioned Samples and Compaction Equipment.....	21
Figure 2.14 Crack Propagation, Ideal CT Principle.....	22
Figure 4.1 Wind Rose Diagram Representation.....	29
Figure 4.2 Runway Usage with cumulative data from 1985 to 2019.....	29
Figure 4.3 Airside Infrastructure Annual Usage for YYZ and YOW.....	30
Figure 4.4 Average Minimum and Maximum Monthly Temperatures and Trendlines from 1937 to 2013 for YVR (Vancouver Airport)	31
Figure 4.5 Average Maximum Temperature Trendlines.....	32
Figure 4.6 Average Minimum Temperature Trendlines.....	32
Figure 4.9 Ambient and Surface Temperature Correlation.....	34
Figure 4.10 Annual Maximum Ambient and Surface Temperatures at YYZ.....	35
Figure 4.11 Five years Cumulative Annual Freeze-Thaw Cycles at the Selected Airports.....	36
Figure 4.12 Annual Freeze-Thaw Cycles at the Selected Airports since 1950 to 2018.....	37
Image 4.2 Ice rich ground section near Yellowknife, NWT (Morse, 2017).....	39
Figure 4.13 Permafrost Composition and Inequality at the Selected Airports (Bone, 2019).....	40

Figure 4.14 Decennial Precipitation at the Selected Airports since 1950.....	41
Figure 4.15 Decennial Rainfall at the Selected Airports since 1950.....	42
Figure 4.16 Decennial Snowfall at the Selected Airports since 1950.....	42
Figure 5.1 Gradation Test’s Results.....	47
Figure 5.2 Rutting Propagation versus Freeze-Thaw Cycles.....	48
Figure 5.3 Rutting at 10,000-Wheel Passes versus Freeze-Thaw Cycles.....	49
Figure 5.4 Rutting Propagation versus Temperature.....	50
Figure 5.5 Rutting after 10,000 passes versus Temperature.....	50
Figure 5.6 Tensile Strength Reduction due to Freeze-Thaw Cycles.....	53
Figure 5.7 Tensile Strength versus Number of Freeze-Thaw Cycles.....	54
Figure 5.8 Tensile Strength with Faster Compaction versus Number of Freeze-Thaw Cycles.....	54
Figure 5.9 Tensile Strength with Faster Compaction and half period of Freeze-Thaw Cycles.....	55
Figure 5.10 Indirect Tensile Strengths and Cracking Test Indexes.....	56
Figure A.1 Monthly Ambient Temperature at YYZ from 1938 to 2012.....	66
Figure A.2 Decade Average Temperature Trendlines for YYZ from 1940-1949 to 2010-2019...66	66
Figure A.3 Monthly Ambient Temperature at YVR from 1937 to 2013.....	67
Figure A.4 Decade Average Temperature Trendlines for YVR from 1930-1939 to 2010-2019...67	67
Figure A.5 Monthly Ambient Temperature at YUL from 1942 to 2013.....	68
Figure A.6 Decade Average Temperature Trendlines for YUL Since 1940-1949 to 2010-2019...68	68
Figure A.7 Monthly Ambient Temperature at YHZ from 1961 to 2019.....	69
Figure A.8 Decade Average Temperature Trendlines for YHZ from 1960-1969 to 2010-2019...69	69
Figure A.9 Monthly Ambient Temperature at YYC from 1900 to 2012.....	70
Figure A.10 Decade Average Temperature Trendlines for YYC Since 1900-1909 to 2010-2019.70	70
Figure A.9 Monthly Ambient Temperature at YXE from 1900 to 2006.....	71
Figure A.10 Decade Average Temperature Trendlines for YXE Since 1900-1909 to 2010-2019.71	71
Figure A.11 Monthly Ambient Temperature at YWG from 1939 to 2008.....	72
Figure A.12 Decade Average Temperature Trendlines for YWG Since 1940-1949 to 2010-2019.	72
Figure A.13 Monthly Ambient Temperature at YQM from 1939 to 2010.....	73
Figure A.14 Decade Average Temperature Trendlines for YQM Since 1940-1949 to 2010-2019.	73
Figure A.15 Monthly Ambient Temperature at YXY from 1942 to 2009.....	74

Figure A.16 Decade Average Temperature Trendlines for YXY Since 1940-1949 to 2010-2019.	74
Figure A.17 Monthly Ambient Temperature at YZF from 1942 to 2006.....	75
Figure A.18 Decade Average Temperature Trendlines for YXY Since 1940-1949 to 2010-2019.	75
Figure A.19 Monthly Ambient Temperature at YFB from 1945 to 2008.....	76
Figure A.20 Decade Average Temperature Trendlines for YFB Since 1950-1959 to 2010-2019.....	76
Figure A.21 Annual Freeze-Thaw Cycles for Yellowknife International Airport.....	78
Figure A.22 Annual Freeze-Thaw Cycles for Iqaluit Airport.....	78
Figure A.23 Annual Freeze-Thaw Cycles for Winnipeg International Airport.....	79
Figure A.24 Annual Freeze-Thaw Cycles for Saskatoon International Airport.....	79
Figure A.25 Annual Freeze-Thaw Cycles for Whitehorse International Airport.....	80
Figure A.26 Annual Freeze-Thaw Cycles for Montreal Trudeau International Airport.....	80
Figure A.27 Annual Freeze-Thaw Cycles for Toronto Pearson International Airport.....	81
Figure A.28 Annual Freeze-Thaw Cycles for Moncton International Airport.....	81
Figure A.29 Annual Freeze-Thaw Cycles for Calgary International Airport.....	82
Figure A.30 Annual Freeze-Thaw Cycles for Halifax Stanfield International Airport.....	82
Figure A31 Annual Precipitation, Rainfall, and Snowfall for YYZ from 1937 to 2011.....	83
Figure A32 Annual Precip, Rainfall, and Snowfall Trends from YYZ from 1940-1949 to 2010-2019.....	83
Figure A33 Annual Precipitation, Rainfall, and Snowfall for YVR from 1939 to 2011.....	84
Figure A34 Annual Precip, Rainfall, and Snowfall Trends from YVR from 1940-1949 to 2010-2019.....	84
Figure A35 Annual Precipitation, Rainfall, and Snowfall for YUL from 1941 to 2012.....	85
Figure A36 Annual Precip, Rainfall, and Snowfall Trends from YUL from 1940-1949 to 2010-2019.....	85
Figure A37 Annual Precipitation, Rainfall, and Snowfall for YHZ from 1960 to 2017.....	86
Figure A38 Annual Precip, Rainfall, and Snowfall Trends from YHZ from 1960-1969 to 2010-2019.....	86
Figure A39 Annual Precipitation, Rainfall, and Snowfall for YYC from 1900 to 2012.....	87
Figure A40 Annual Precip, Rainfall, and Snowfall Trends from YYC from 1940-1949 to 2010-2019.....	87
Figure A41 Annual Precipitation, Rainfall, and Snowfall for YXE from 1900 to 2006.....	88
Figure A40 Annual Precip, Rainfall, and Snowfall Trends from YXE from 1900-1909 to 2010-2019.....	88

Figure A43 Annual Precipitation, Rainfall, and Snowfall for YWG from 1937 to 2007.....	89
Figure A44 Annual Precip, Rainfall, and Snowfall Trends from YXE from 1940-1949 to 2010-2019.....	89
Figure A45 Annual Precipitation, Rainfall, and Snowfall for YQM from 1939 to 2011.....	90
Figure A46 Annual Precip, Rainfall, and Snowfall Trends from YQM from 1940-1949 to 2010-2019.....	90
Figure A47 Annual Precipitation, Rainfall, and Snowfall for YXY from 1942 to 2006.....	91
Figure A48 Annual Precip, Rainfall, and Snowfall Trends from YXY from 1950-1959 to 2010-2019.....	91
Figure A49 Annual Precipitation, Rainfall, and Snowfall for YZF from 1943 to 2006.....	92
Figure A50 Annual Precip, Rainfall, and Snowfall Trends from YZF from 1940-1949 to 2010-2019.....	92
Figure A51 Annual Precipitation, Rainfall, and Snowfall for YFB from 1945 to 1995.....	93
Figure A52 Annual Precip, Rainfall, and Snowfall Trends from YFB from 1950-1959 to 2010-2019.....	93
Figure B.1 Rutting Propagation versus Temperature Variation.....	95
Figure B.2 Rutting Propagation versus Freeze-Thaw Cycles' Variation.....	96
Figure B.3 ITS versus Displacement Variations due to F-T Cycles.....	98
Figure B.4 ITS versus Displacement Variations due to F-T Cycles (Higher Speed of Loading)..	99
Figure B.5 ITS versus Displacement Variations due to Half F-T Cycles (Higher Speed of Loading).	100
Figure B.6 Ideal CT Index Variations due to F-T Cycles and Speed of Loading.....	102
Figure B.7 Ideal CT Report for the Non-Condition Samples.....	103
Figure B.8 Ideal CT Report for the Samples with one Freeze-Thaw Cycle.....	104
Figure B.9 Ideal CT Report for the Samples with two Freeze-Thaw Cycle.....	105
Figure B.10 Ideal CT Report for the Samples with three Freeze-Thaw Cycle.....	106

List of Tables

Table 2.1 Traffic Distribution For Examples (A) And (B) Of Figure 2.7	10
Table 3.1 Selected Airport Names, Provinces/Territories, And Iata Codes	24
Table 3.2 Asphalt Mix Design And Gtaa Requirements.....	26
Table 4.1 Ambient And Surface Temperature Relationship.....	34
Table 4.2 Summary Of The Annual Number Of Freeze-Thaw Cycles At The Selected Airports Since 1950 To 2018.....	38
Table 4.3 Cumulative Precipitation, Rainfall, And Snowfall Trendlines From 1950-2019.....	43
Table 5.1 Laboratory Tests Matrix.....	45
Table B.1 Tensile Strength and Ideal Cracking Test Average Results.....	102

List of Images

Image 2.1 Arctic Sea Ice Reduction from Sep 1984 to Sep 2016 A. 1984; B. 2016 (NASA, 2016).	7
Image 2.2 Canadian National Airport System and Examples (Transport Canada, 2017) (Google Earth Pro, 2019).....	9
Image 2.3 Stripping A and B are core holes showing stripping at the bottom of the layer (Pavement Interactive, 2019).....	15
Image 2.4 Low Temp Transverse Cracking Example at YXU Airport (Google Earth Pro, 2019).	16
Image 2.5 Moderate Rutting (PPRA, 2018).....	17
Image 2.6 Frost heaving creation in a flexible pavement A. New Pavement; B. Frozen Pavement Structure; C. Pavement Structure After Thawing (Minnesota Department of Transportation, 2013).....	17
Image 2.7 Frost heaving creation in a rigid pavement (ACPA, 2013).....	17
Image 2.7 Shoving at YYZ Taxiways, 2007 (Stewart, 2010).....	18
Image 2.8 Lidar Point Cloud 20x Vertical Exaggeration of Yellowknife’s Surface Profile in 2015 (Reggin, 2019).....	18
Image 2.9 Foggy Runway (Murmakova, 2017).....	19
Image 2.10 Hamburg Wheel Tracking Test A. CPATT’s Hamburg Wheel Tracking Device; B. Asphalt Samples inside the HWTD after Being Tested.....	20
Image 3.1 Selected Airport per Province/Territory for Case Studies.....	25
Image 3.2 Selected Airports from Southern Ontario for Wind Analysis (Google Earth Pro, 2019).....	25
Image 3.3 Material Pick-up and Storage.....	27
Image 4.1 Ottawa and Toronto Runways’ Direction and Distribution, Respectively (Google Earth Pro, 2019).....	30
Figure 4.7 Difference in Maximum Temperature Trendlines since 1950.....	33
Figure 4.8 Difference in Minimum Temperature Trendlines since 1950.....	33
Image 5.1 Extraction and gradation tests process.....	46
Image 5.3 Hamburg Wheel Tracking Test Samples Tested at Different Temperatures.....	51

Chapter 1

Introduction

This chapter contains the introduction, the objectives, and the research methodology of the thesis.

1.1 Introduction

Over the last centuries, population and technology growth, the industrial revolution which improved the automation of processes intensified the development of the economy and the production of products and assets. Since this period, the concentration of greenhouse gases (GHGs) started to increase significantly resulting in changes in the standard deviation of the climate worldwide (Masters W. P., 2010). Therefore, climate change is an imperative matter that requires the collaboration of all the possible fields (Engineering, Environment, Politics, Economics, Health, Science, and so on) working together to find mitigation strategies to reduce the impacts of the changing climate as well as adaptation strategies to learn how to live with the changes that affect the world in the present.

From an engineering perspective, which involves the planning, design, construction, and maintenance of assets, climate change impacts all the phases before mentioned and is continuing to do so. There is a mathematical approach to measure human impacts to the environment denoted as I=PAT, meaning that these impacts are equal to the Population multiplied by the Affluence (consumption-production per capita) and multiplied by the Technology (environmental impacts per unit of consumption/production), being engineers accountable for this last one. (Holdren, Daily, & Ehrlich, 1995) Hence, it is engineer's responsibility to, first understand but to act against this worldwide challenge; climate change.

Canada is affected by the changes in climate. The expected location of weather events has changed as well as the intensity of these occurrences causing more severe floods and hurricanes, greater droughts, and considerable damages to infrastructures. (Gopalakrishnan, Steyn, & Harvey, 2014) The Canadian airside pavements are being also affected by the variations in climate provoking planning, design, construction, and maintenance's modifications to protect the resiliency of the infrastructure. These modifications represent a significant challenge for decision makers because of sustainability reasons. Hence, the modifications have to make the infrastructure more resistant against the present and future climate while the negative socio-economic and environmental impacts must be kept constant or reduced.

Understanding how the climate is changing, not just in a holistic perspective, but more specifically, how it is varying depending on the location, the weather event, the time period, and so on, can make of decision-making processes significantly easier. This research has focused on evaluating the changes in temperature and precipitation, the fluctuation of freeze-thaw cycles and wind rose diagrams, and the variation of permafrost areas, and how are these events impacting the Canadian airside infrastructure. To assess these impacts, different laboratory tests were conducted on an airside surface material inducing distinct environmental conditions to the samples, aiming to exemplify changes in climate, in order to obtain objective outcomes more than subjective ones.

1.2 Objectives

This research aims to achieve the following objectives:

- Present the changes in climate at different airports located in distinct territories and provinces of Canada
 - Changes in wind direction and strength
 - The variation of precipitation
 - The behaviour of maximum and minimum temperatures
 - The fluctuation of freeze-thaw cycles
 - The lost of permafrost.
- Analyze the impact of these changes on the performance and/or operation of the airside infrastructure of the selected airports by developing laboratory tests
- Provide recommended mitigation and adaptation strategies to overcome or dissipate these impacts.

1.3 Thesis Methodology

This investigation intends to serve as a call of action for Canadian airport authorities and consultants to have a more objective understanding of the impact of climate change on airport pavement infrastructure. It aims to evaluate performance impacts and relate those to operation impacts. This research does not intend to delve into each specific problem but to evaluate them in a cause and consequence perspective. This will help to develop superior considerations for mitigation and adaptation strategies. The different steps that correspond to the methodology of this project are presented in Figure 1.1.

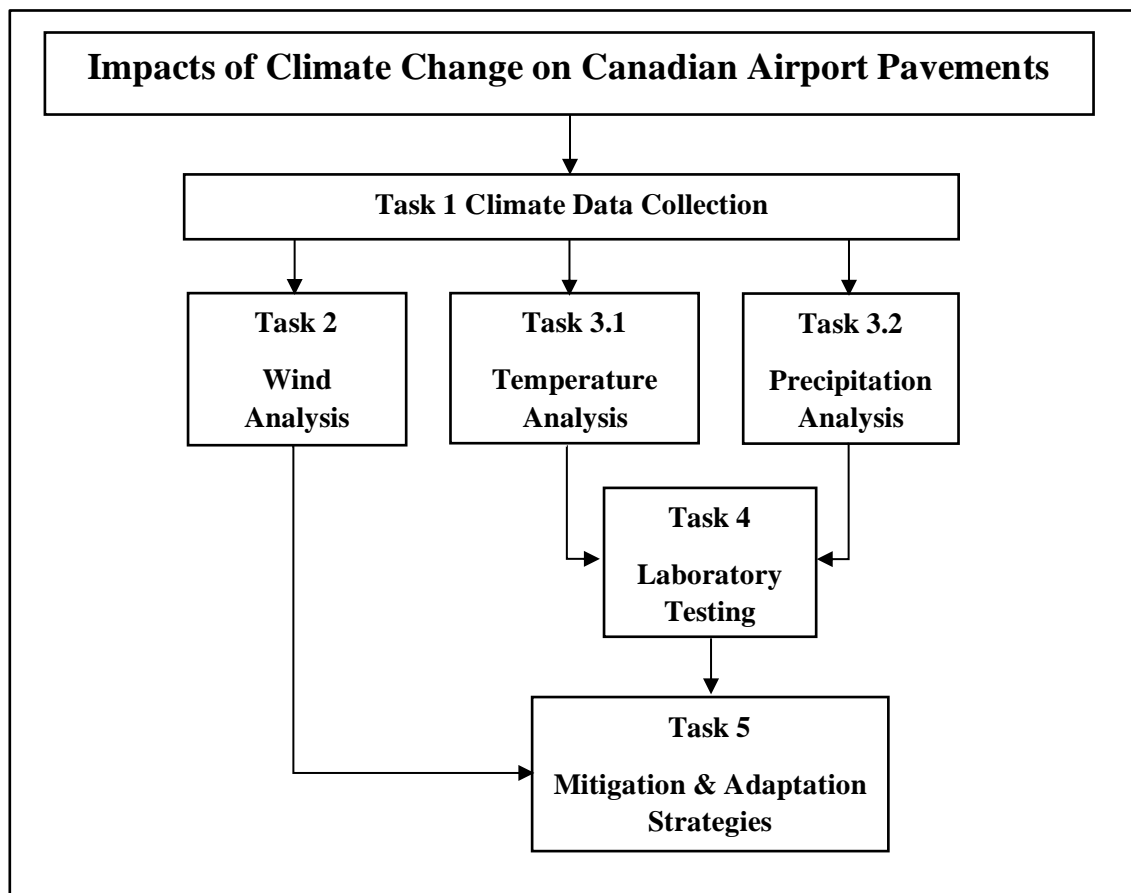


Figure 1.1 Research Methodology

Task 1: The first part of the methodology of this research consists of collecting the climate data around different significant airports from distinct provinces and territories of Canada. The main set of data is obtained from Environment Canada and data from Meteoblue is used for the wind analysis.

Task 2: To evaluate the impact of wind on the operation of the airports, annual wind rose diagrams collected from Meteoblue stations since 1985 are analysed to calculate the usage that the selected airports have been able to provide to their runways against crosswind. This illustrates and quantifies the winds induced changes to the operation of the runways. The results are used to develop mitigation strategies against the fluctuation of wind speed and directions.

Task 3.1: The temperature analysis presents the impacts of the different changes in temperature on the airside pavement infrastructure. Therefore, each specific pavement section examines distinct behaviours. A freeze-thaw cycle analysis is conducted on the development of a calculation program to compute the quantity of cycles per year in each specific airport evaluated. This consists of using performance data to develop a temperature transmission formula to get the surface temperatures of the pavement from the ambient temperature. The main objective of the analysis is to examine how the number cycles per year are changing.

Task 3.2: The precipitation analysis, similar to the temperature analysis, correlates the temperature changes with the changes in precipitation, rainfall, and snowfall depending on the province and or territory. This task aims to quantify the changes in precipitation, rainfall, and snowfall.

Task 4: The laboratory testing is the continuity of the temperature and precipitation analysis that mainly consist on developing moisture and temperature susceptibility tests including the Hamburg Wheel Tracking Test (HWTT) to measure rutting and stripping, as well as the Indirect Tensile Strength (ITS) to measure the Tensile Strength Ratio (TSR) on an airside asphalt mixture by inducing different conditionings of freeze-thaw cycles and saturation to the samples. The ITS data will be used to develop an IDEAL CT which is the calculation of a cracking propagation index to evaluate the impact of freeze-thaw cycles on the formation and/or propagation of cracks.

Task 5: Once the main outcomes of the analysis are obtained considering the literature review, mitigation and adaptation strategies will be proposed for the different scenarios studied and described in the tasks above.

1.4 Chapter Summary

This chapter encompassed the introduction, objectives, and the methodology of this research. It explained how the main cause of climate change comes from anthropogenic actions as well as the responsibility of mitigating it falls in people's hands too. In other words, human impacts to environment are measured by the population, the affluence, and the technology for which engineers have power over the last one. Canadian airport pavements are being affected by the changes in environmental loads causing design, construction, and maintenance's adaptations to keep the resiliency of the infrastructures. It is of paramount importance to understand the changes in climate at the specific locations to make the decision-making processes easier and more reliable. The main objectives of this research are to present different changes in climate at the selected airports located in distinct territories and provinces of Canada as well as to analyze the impact of these changes on the performance and/or operation of the airside infrastructure of the selected airports by correlating environmental analysis with several laboratory tests. Additionally, to provide considerations for mitigation and adaptation strategies to overcome or dissipate these impacts.

Chapter 2

Literature Review

The purpose of this chapter is to provide background information concerning climate change, airport pavements, and the impact of climate change on the transportation industry in Canada. Furthermore, to present the research gaps on investigating the impacts of the changing climate on the Canadian airport pavement's operation and/or performance. In addition, to evaluate the best practices on assessing climate impacts developing laboratory tests.

2.0 Climate Change

The term climate change has gain substantial popularity in the past decades but people continues to confuse it with the weather definition. Weather, is a description of a short-term variation of the state of the atmosphere while climate, is a long-term average of the weather. (Climate Atlas of Canada, 2019) Weather has drastically varied; nonetheless, it created a pattern of statistical distribution. Hence, climate change refers to a variation of the statistical distribution of the weather patterns. (Masters W. P., 2010)

The first steps on noting the significant changes of the climate started at Sweden in 1896 with Svante Arrhenius, a physicist and a chemist that discovered that putting significant amounts of CO₂ in the atmosphere could cause the planet to become warmer. (Barral, 2019) In addition, in 1938 Guy Stewart Callendar started evaluating the changes of global temperature since Arrhenius' times (1880) to his date. He revealed that The Earth was indeed getting warmer mostly due to the industrial processes of burning coal and oil. (Applegate, 2013) Figure 2.1A illustrates that the global annual temperature is rising which is subsequently causing the intensification of other climate events such as precipitation, wind, freeze-thaw cycles, among others. (James Hansen, 2006) In addition, the main changes, as presented in Figure 2.2B, are happening in northern areas of the planet which considerably increases the probability/intensity of the mentioned events in Canada.

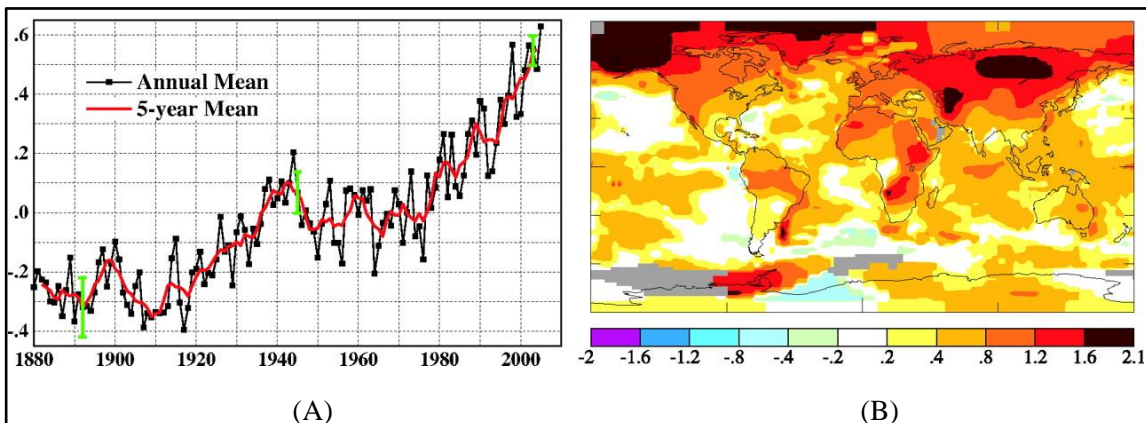


Figure 2.1 Surface Temperature Anomalies Relatives to 1951-1980 (A) Global Annual Mean Anomalies. (B) Temperature anomalies for the first half decade of the 21st century (James Hansen, 2006)

This situation has resulted in the retention of heat in The Earth’s lower atmosphere caused by the increase of greenhouse gases (GHG) emitted by human activities which, since the industrial revolution, the concentration of these gases started to growth significantly. It has changed the green house effect and induced meaningful changes on the climate. (TAC Urban Transportation Council, 1998) Figure 2.2 presents the variability of the concentration of carbon dioxide for the past 800,000 years. As it can be seen, the concentration of this gases has been fluctuating with a sinusoidal behaviour with a regularly constant amplitude; nonetheless, in the past 300 years, as it can be seen in Figure 2.3, the humanity overcame the record of 300 ppm of concentration of CO2 having reached in the present a value of approximately 407 ppm (National Oceanic and Atmospheric Organization, 2019). As the major cause of climate change can be attributed to the emissions of mainly carbon dioxide, the main mitigation to reduce the future impacts is to diminish the emissions of this gas and similar ones as they stay in the atmosphere for centuries. (Environment Canada, 2019)

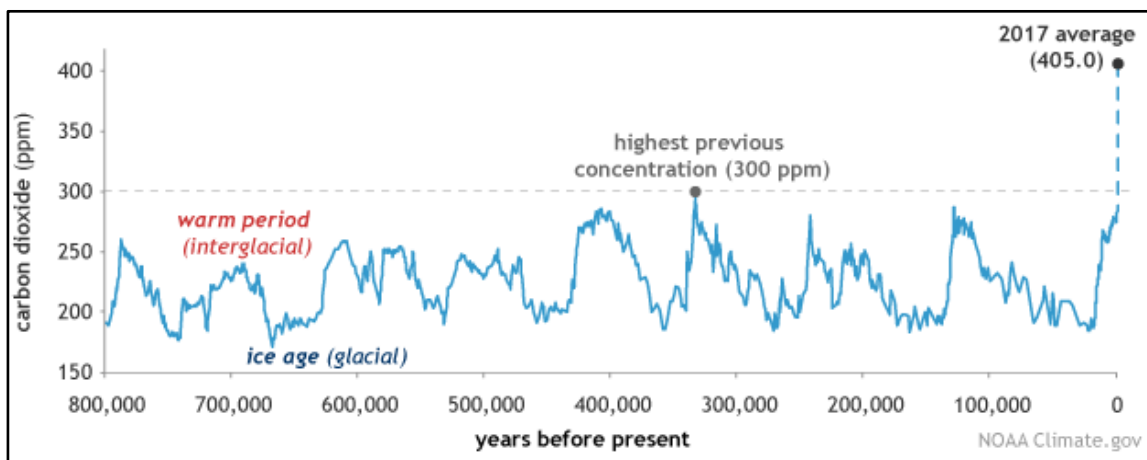


Figure 2.2 Carbon Dioxide Level during Ice Ages and Warm Period for the Past 800,000 years (National Oceanic and Atmospheric Administration, 2018)

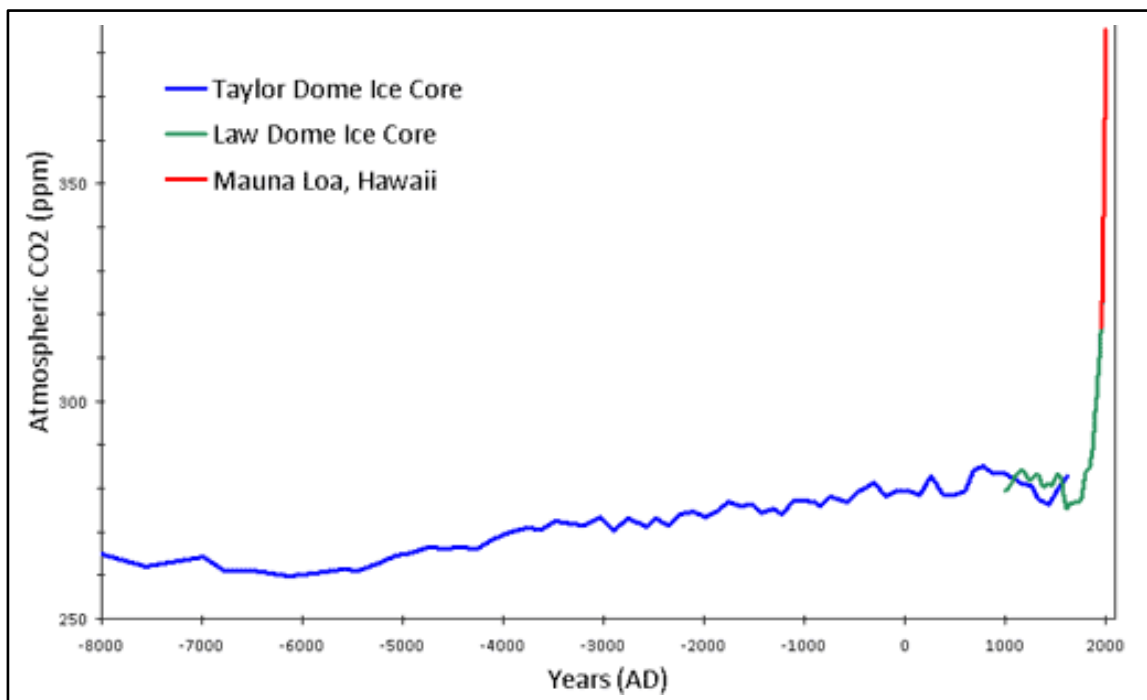


Figure 2.3 Carbon Dioxide Level during the Past 8,000 years (Cook, 2010)

When examining climate change, it is crucial to mention the Intergovernmental Panel on Climate Change (IPCC). Perhaps the most recognized international body focused and working on climate change, it was launched in 1988 with the purpose of understanding climate change through high level research and science and be able to provide mitigation and adaptation strategies to prevent or reduce its impacts. (Bush & Lemmen, 2019) One of the major outcomes of the IPCC is the different climate change scenarios that mainly depend on the carbon dioxide equivalent concentration for the year 2,100. These scenarios are known as representative concentration pathways (RCP's) and they vary from 2.6 W/m² of radiative forcing, remarkably optimistic, to 8.5 W/m² of radiative forcing, exceedingly pessimistic. Figure 2.4 presents the projected changes in climate depending on the concentration pathway. Undeniably, the consequences of following the RCP 8.5, more than preoccupying, are calamitous.

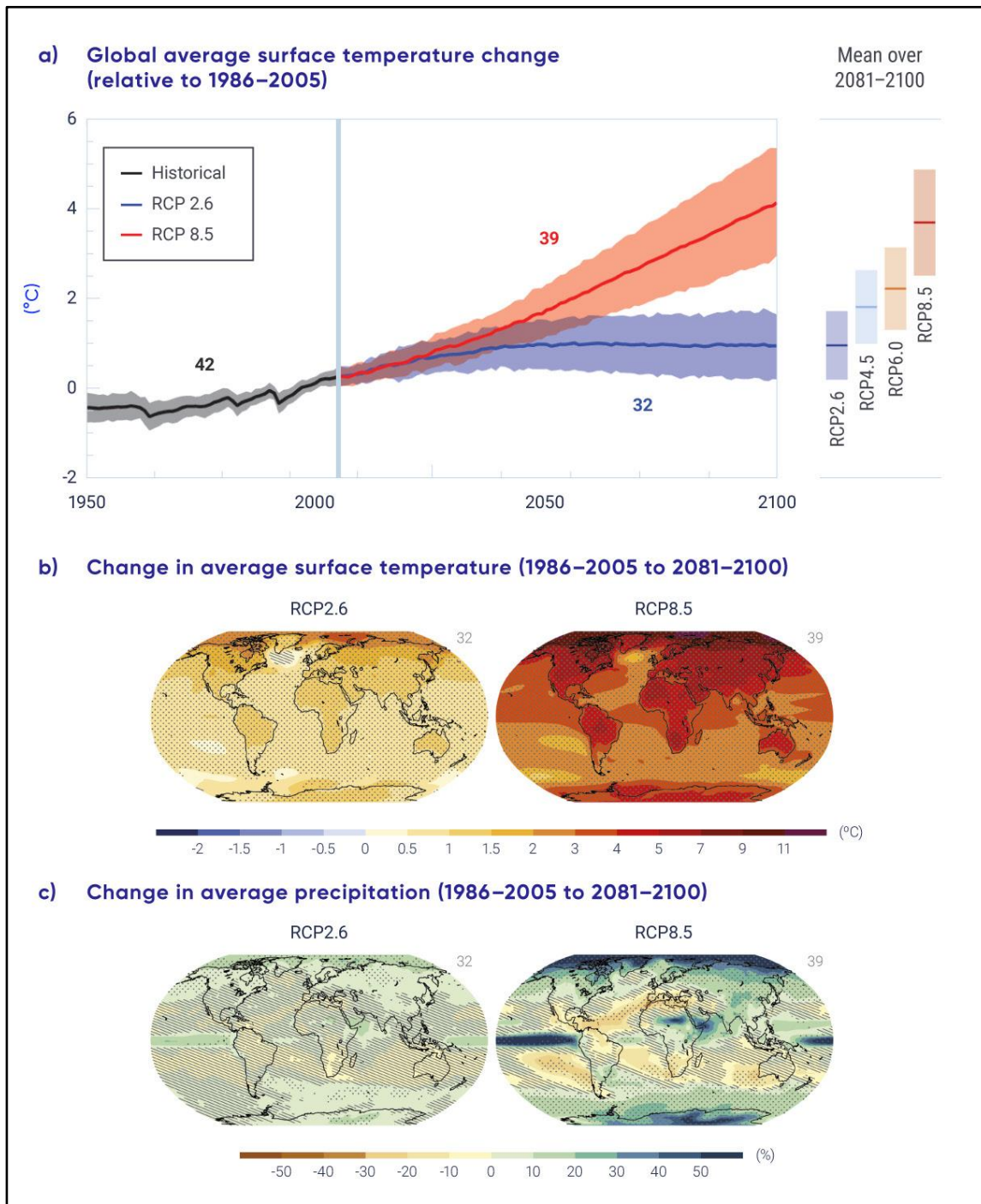


Figure 2.4 Global Climate Projections (Bush & Lemmen, 2019)

2.1 Climate Change effects in the Transportation industry in Canada

One of the main consequences of climate change is the reduction of the sea ice in the Arctic, that, according to the National Aeronautic and Space Administration (NASA), it is currently dipping with a rate of 12.8% per decade. (NSIDC/NASA, 2019) Figure 2.5 and Image 2.1 show the significant reduction of the arctic sea ice which, as a consequence of climate change, represents the input for many other outcomes affecting the planet, being Canada no exception. The main consequences are the rise of the sea level that increases the probability of flooding in coast and plain areas. Additionally, the substantial intensification of temperature caused by the reduction of the reflectiveness of the surface of the planet (albedo) and the increment of GHGs which increases the surface radiation absorb by the atmosphere. (Masters W. P., 2010)

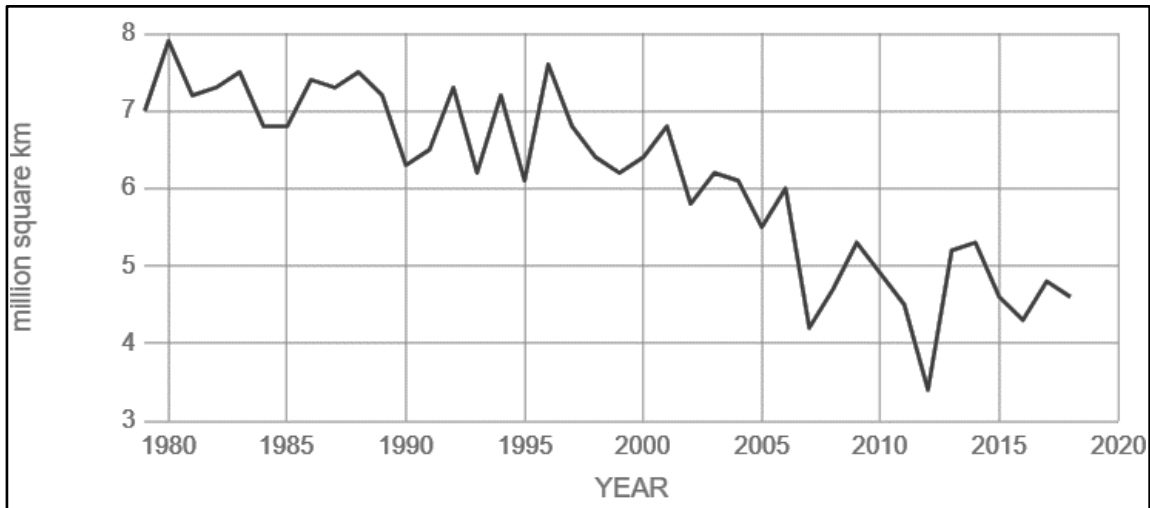


Figure 2.5 Average Arctic Sea Ice since 1980 (NSIDC/NASA, 2019)

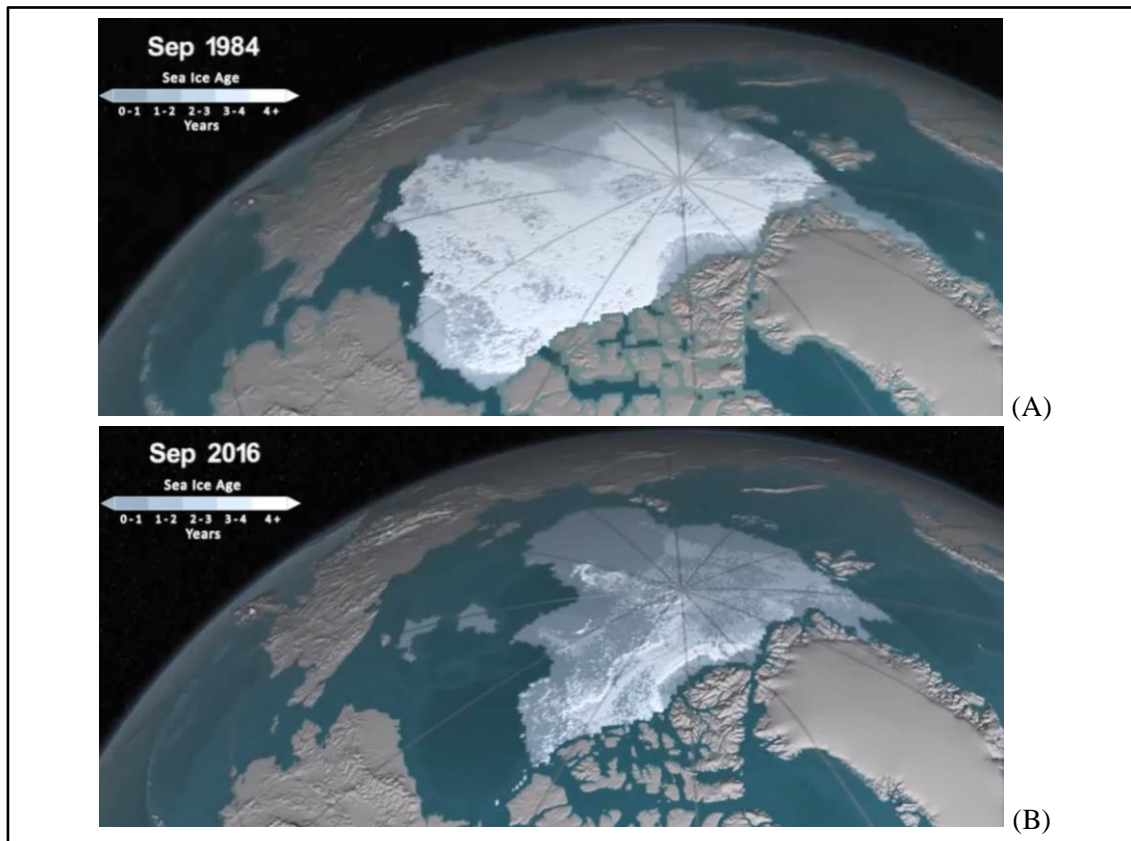


Image 2.1 Arctic Sea Ice Reduction from Sep 1984 to Sep 2016 | A. 1984; B. 2016 (NASA, 2016)

These situations also scatter into other changes such as more frequent extreme snow events, floods, hurricanes, and more importantly, the change of location of weather events. Long term designs significantly depend on the behavior of the climate where meaningful changes in weather events can cause the failure of some infrastructures. The increment of precipitation, the freeze-thaw cycles fluctuation, and the melting of permafrost cause a massive impact on the transportation industry infrastructures in Canada by increasing the frequency and the intensity of distresses.

Emery noted that by 2010 Canada already had a road system value of approximately \$100 billion dollars with significant sensitivity to climate hazards such as the ones mentioned above but adding fog, high wind speed, and heavy ice storms. Climate change, Canada wide, can cause changes in length and quality of construction season as well as variations in the maintenance and design's best practices. In Northern Canada, permafrost degradation and freeze-thaw cycles can trigger infrastructure damage. In the southern part of Canada, changes are expected on the winter maintenance costs for roads and airfield pavements. (Emery, 2012)

According to Warren and Lemmen, Canada has become warmer and will continue to become warmer. It has also become wetter as annual precipitation has increased in recent decades. Annual snowfall has declined in southern Canada. Permafrost has warmed and is projected to continue warming/thawing exponentially. The sea level has changed as it is rising in a 3 mm/year in the Atlantic Canada and 1.6 mm/year in the Pacific coast. Future expectations lead approximately a meter higher in the next 80 years for the Atlantic, Pacific, and Beaufort coast, but a meter lower in the central Arctic. (Warren and Lemmen, 2014)

All these changes mentioned above, create or intensify pavement distresses which is directly related to the maintenance, rehabilitation, and/or reconstruction (MRR) costs. They also create disruption during flooding or hurricane events that provoke a higher user cost and diminish the salvage value at the end of the infrastructure service life due to the fact that, in the long run, significant distresses are found in the granular layers; mainly in the subgrade. Additionally, one of the main climate change distress' trigger and factor of deterioration can be attributed to freeze-thaw cycles. (Haas, Falls, Macleod, & Tighe, 2004) Furthermore, flexible pavements will be less prompt to low temperature cracking; however, rutting distresses might be aggravated due to climate change. (Mills, Tighe, Andrey, Smith, & Huen, 2009) In the end, climate change is affecting the transportation industry and the economy of Canada; hence, understating the impacts of these changes is of paramount importance.

2.2 Canadian Airfield Infrastructure, Design, and Implications

According to the Canadian Justice Law, an airport is an aerodrome powered by a Canadian aviation document; and, an aerodrome is an infrastructure planned, designed, and build for the purpose of arrival, departure, or movement of aircrafts. (Government of Canada, 2018) Airports can be divided in two main areas; land side and airside. The first one is open to the public and the second one is private and with limited access. (Robert E. Hom and J. C. Orman, 1974) The airfield infrastructure correspond to the pavement structure inside the airside area that is envisioned to have aircrafts as the main traffic; see Image 2.2 for examples. These airside infrastructures are as well divided into three main sections; the runway, the taxiway, and the apron, as it can be seeing in Figure 2.6.



Image 2.2 Canadian National Airport System and Examples (Transport Canada, 2017) (Google Earth Pro, 2019)

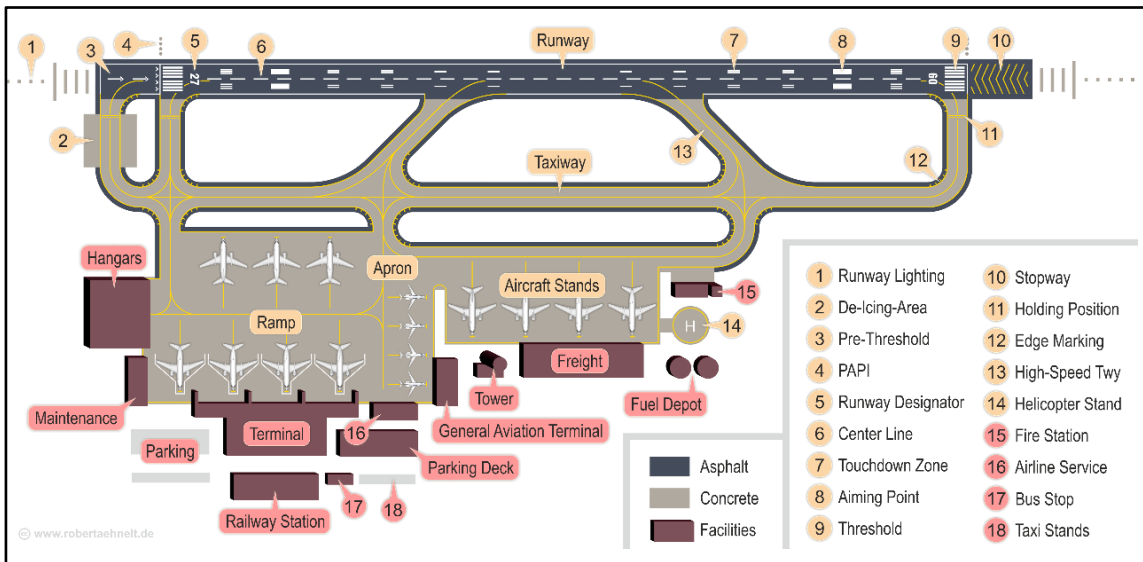


Figure 2.6 Sample Distribution of a Typical Airport (Aehnelt, 2016)

The runway is the section of the airport pavement where the airplanes arrive and depart, which means that are highly susceptible to massive loads with a superior speed of loading, shear stresses, strong winds due to the turbines, among other loads. The apron is the pavement area where the planes are loaded and unloaded inducing heavy and static loads. Furthermore, there are the taxiways which are the part of the airside pavement structure that aim to connect the apron to the runway. Hence, having slow moving and heavy static loads.

Having said that, each of these sections require a distinct design due to the different type of loads that are intended to receive/support. The simplest example corresponds to the aprons that due to the significant amount of stationary load caused by the loading and unloading of passengers and/or goods, they require an infrastructure less susceptible to stationary loads and high temperatures; most commonly concrete pavements. In the case of the runway and taxiways, the pavement type varies between, asphalt, concrete, gravel, or a composite pavement, being this last one a combination of an old rigid pavement with an overlay of HMA on top or vice-versa.

Figure 2.7 shows an example of a flexible and a rigid airfield pavement infrastructure design using the software FAARFIELD 1.42. The traffic distribution and the annual growth are described in Table 2.1 considering the exponential augmentation of airfield transportation in the past decades. Both designs are laying on an equal subgrade and count on the same availability of base and subbase materials. The main difference is in the surface materials and thickness, as the asphalt layer only requires 200mm while the Portland cement concrete (PCC) necessitates 556mm. However, it is significant to mention that the service life of this flexible pavement is around 20 years when the one for the rigid pavement is 30 years.

Table 2.1 Traffic Distribution for Examples (A) and (B) of Figure 2.7

Airplane Name	Gross Taxi Weight (Tons)	Annual Growth
DC3	11.5	0
B737-100	50.5	1
A320 Bogie	74	1.5
DC8-43	144.5	1.5
B787-8	228.5	2.5
B777-300 ER	352.5	3
B747-8F	450	3.5
B747-8F Belly	450	3.5
A380	562	3.5
A380 Belly	562	3.5

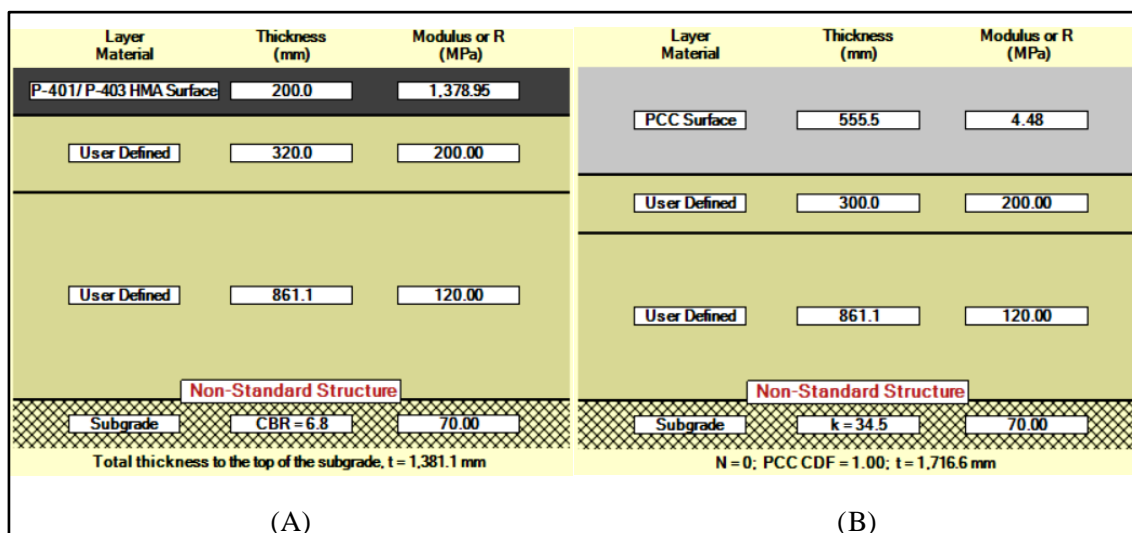


Figure 2.7 Airfield Pavement Infrastructure Design Examples using FAARFIELD 1.42

(A) Flexible Pavement, (B) Rigid Pavement

Concerning the airport design, Transport Canada Civil Aviation (TCCA) correspond the main institution in Canada to develop the standards that describe the design specifications for these infrastructures. The main documents regarding the airside infrastructure are the Advisory Circulars (AC) No. 302-011, 302-016, and 300-004 regarding Airport Pavement Bearing Strength,

Management System, and unpaved runway surfaces respectively, as well as the manual of pavement structural design ASG-19 developed in July 1992.

Transport Canada design method is based on the aircraft load rating (ALR), the freezing index in the location of the airport, the ground vehicle loading group, the tire pressure of the aircraft, and the subgrade bearing strength. Therefore, the climate and the traffic are two significant sections that are not being fully considered on this design specifications as the only climate consideration is the freezing index, which only contemplates temperature changes, and the traffic input is based on the design aircraft loadings. (Public Works Canada, 1992)

Other international design methods that are also considered by Canadian airport authorities are the Federal Aviation Administration (FAA) design method which can be used as a software called FAARFIELD, currently version 1.42. In addition, the Asphalt Institute (AI) SW-1 and the Australian Airport Pavement Structural Design System (APSDS) for flexible pavements, as well as the FAA Finite Element Design (FEDFAA) and the American Concrete Pavement Association AIRPAVE 11 for rigid pavements. (Leanne Whiteley, 2006)

None of these structural airfield pavement design methods combine calculated stresses, strains, and deflections with measured response and field observation of performance of other airports in view of location and other correlated factors; therefore, the above-mentioned design methods are not mechanistic-empirical. Furthermore, they do not contemplate the variation in the statistical distribution of climate patterns; hence, climate change. The consideration of these factors could provide superior performance for future airside infrastructure as these will be significantly more resilient and prepared for present and future loads and hazards.

2.3 Consideration of Climate Change by Canadian Airport Authorities

The airside infrastructure designs, internationally, do not directly consider climate change as an input, and Canada is no exemption. [Section 2.1](#) describes how the climate is changing in Canada and how these variations are indeed compromising the transportation industry and the economy in Canada. The Centre for Pavement Transportation and Technology (CPATT) at the University of Waterloo developed a survey in 2016 designed for Canadian airport authorities to express their perspective about climate change. (Lu & Dutton, 2017) It is important to mention that the amount of answers was not enough to reach statistical significance; nonetheless, it is still essential to present the standpoint of many Canadian airport authorities about climate change to show their awareness regarding this matter. The question varied from general to specific; the subjective answers are to be presented separated into provinces and/or territories as follow:

- Consideration of climate change on decision making (Figure 2.8)
- Climate change consequences on airfield pavements (Figure 2.9)
- Climate change phenomenon's perspective (Figure 2.10)
- Main barriers to contemplate climate change risk and adaptation/mitigation in the day-to-day activities for pavements (Figure 2.11)
- Adaptation to climate change risk for airfield pavements (Figure 2.12).

Figure 2.8 presents how all of the provinces and territories of Canada that answered the survey do consider Climate Change in their decision-making process. More information can be found in the next Figures, being important to mention that for Figures 2.9 to 2.11, the higher the bar, the more the airport authority/province/territory agrees that the matter is increasing and vice versa. Additionally, for Figure 2.12, the indication is how the airport may best adapt to climate change risk for airfield pavement and therefore,

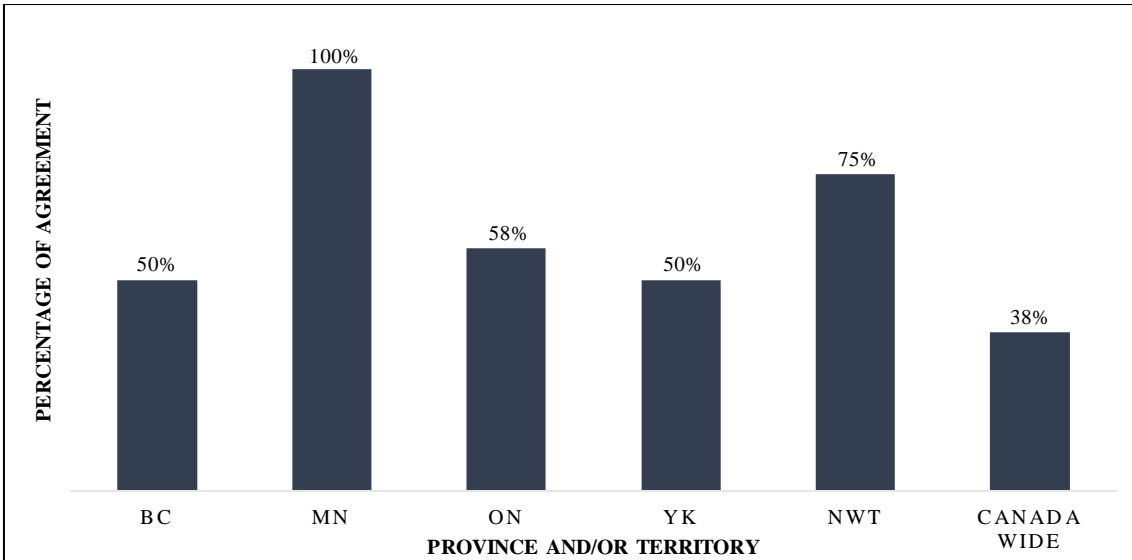


Figure 2.8 Consideration of Climate Change on the Decision Making

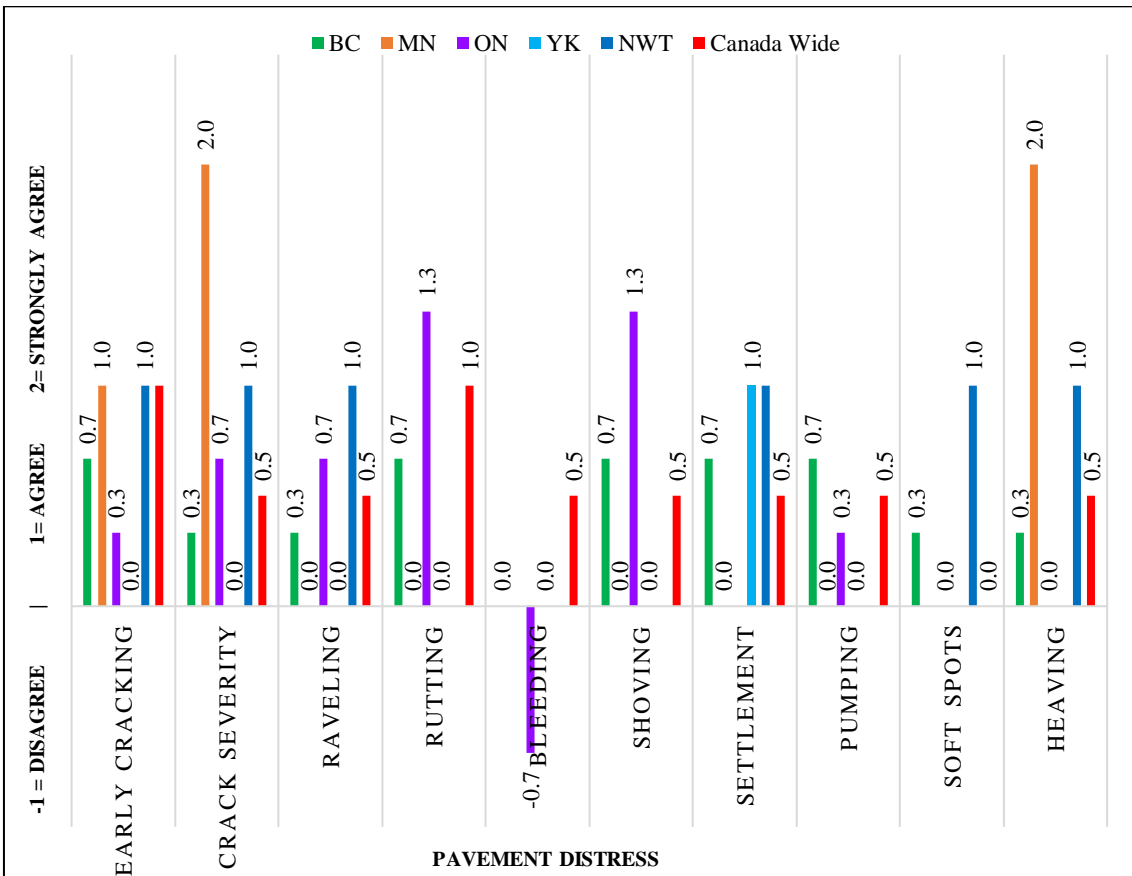


Figure 2.9 Climate Change Consequences on Airfield Pavements

Figure 2.9 shows the perspective of some Canadian airport authorities under climate change consequences on airfield pavement structures. As it can be seen, distresses such as early cracking and crack severity are impacting all airports in Canada, but specially those in northern Canada. Yukon’s airport authorities did not provide a respond on this area as their pavement structure, back at the moment when the survey was active, corresponded to a gravel runway. Rutting, as shown, affects more the provinces of Ontario and British Columbia; therefore, those in southern Canada.

In another hand, settlement and heaving are affecting more the airports in northern Canada as they primarily occur due to the melt or discontinuity of active permafrost layers and the freeze-thaw cycles at the geo-structures which fluctuates the porous pressure constantly modifying the effective stress of the soil layers. It is also important to highlight that some airports at British Columbia, a province with a superior precipitation, are having pumps which is a pavement distress mainly caused by moisture damage.

Figure 2.10 provides some measurements of the perspective of airport authorities on several environmental causes of pavement distresses. As it can be seen, the main causes are the intensity of precipitation, the maximum temperatures, significantly more than the minimum ones, and the number of freeze-thaw cycles as the main one.

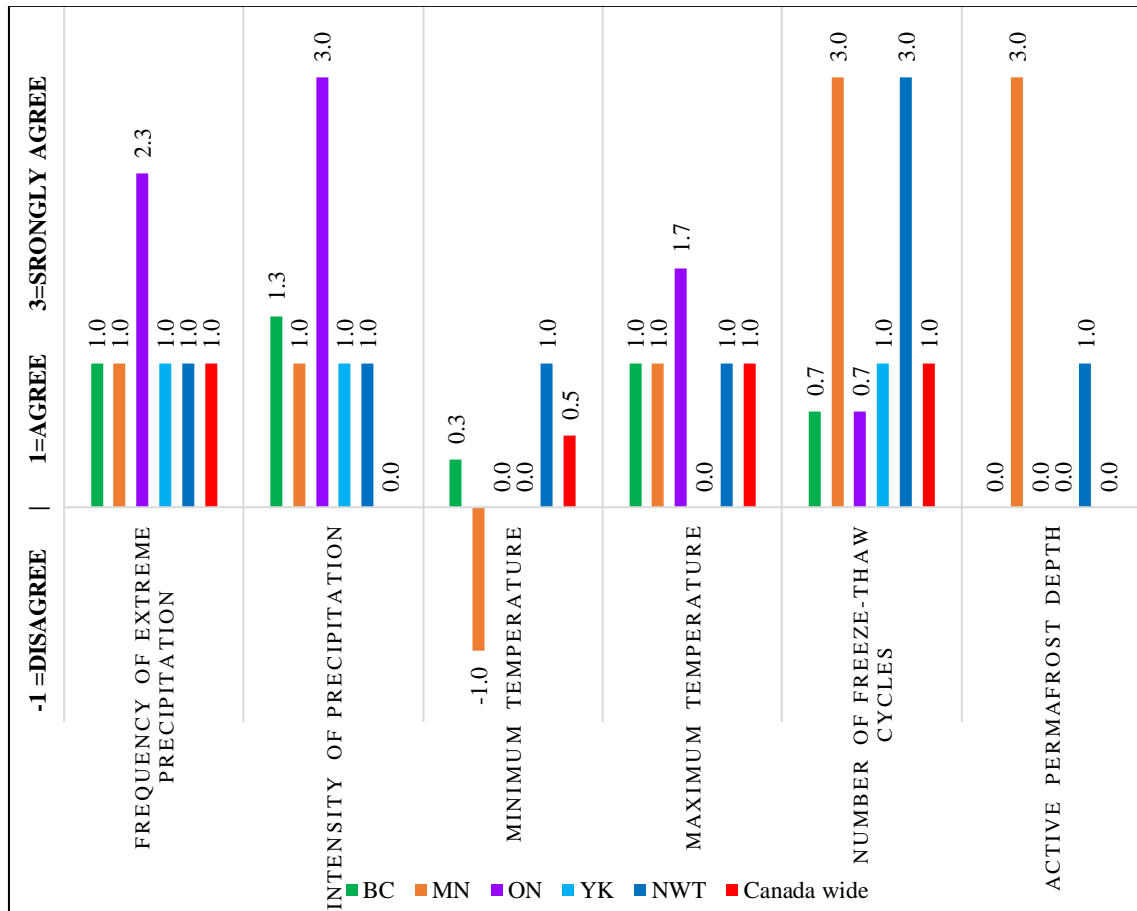


Figure 2.10 Climate Change Phenomenon’s Perspective

The following Figures, 2.11 and 2.12 describe the perception of various airport authorities on several possible mitigation barriers and climate change adaptation strategies. It can be perceived that insufficient funds might be the main obstacle on making the Canadian airside infrastructures more resilient against climate change as well as a lack of adequate climate data which mainly refers on the deficiency and uncertainty of future climate projections. It is significant to notice that all the airport authorities agree that climate change do have a meaningful effect in their practices, especially those from colder regions. Concerning the adaptation strategies, new design technologies appear to be the most preferable option. As an example, aluminum panels are being evaluated to be used as a surface layer for runways in Northern Canada to mitigate surface distresses and the development of foreign object debris (FOD). These panels can also be conceived as an adaptation strategy against the unavailability of construction materials for Northern Canada.

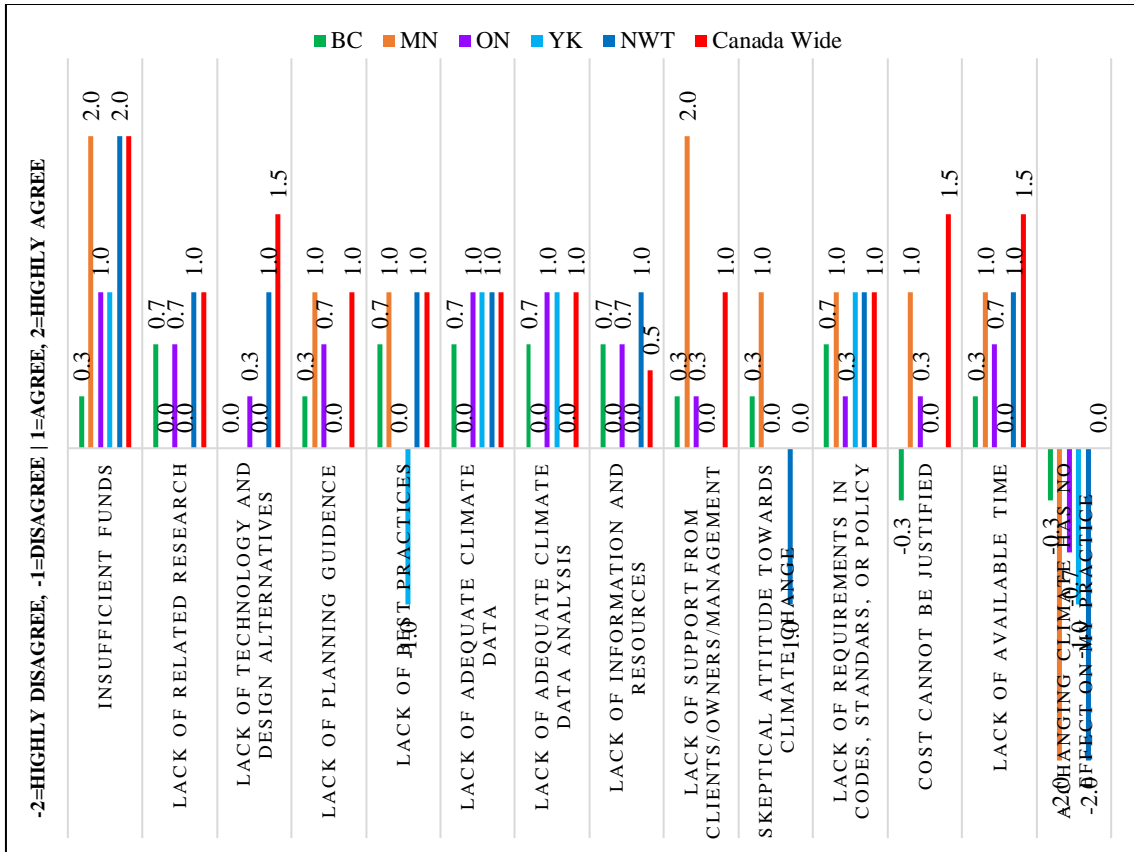


Figure 2.11 Main Barriers to Contemplate Climate Change Risk and Adaptation/Mitigation in the Day-to-Day Activities for Pavements

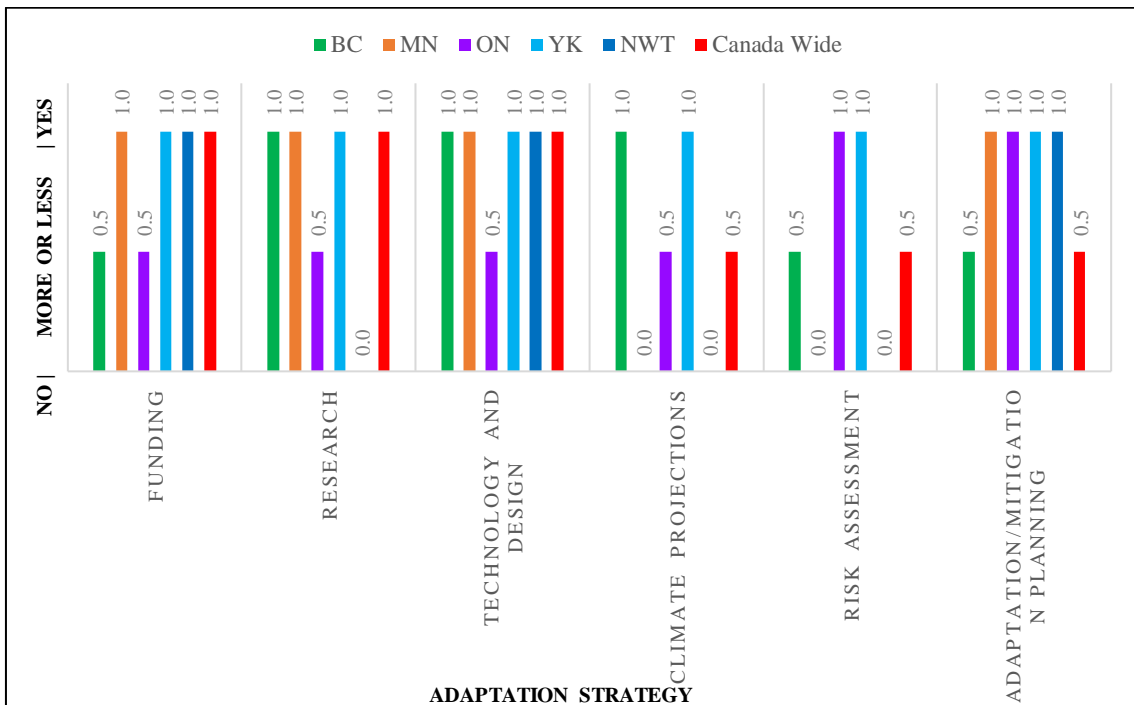


Figure 2.12 Adaptation to Climate Change Risk for Airfield Pavements

The main conclusion of the survey, as presented by Lu and Dutton at CAPTG workshop held during the 2017 annual SWIFT conference, show that climate change is inducing meaningful distresses to the airfield pavement infrastructure, predominantly rutting, shoving, and ravelling

for what mitigation and adaptation strategies are being considered. Additionally, there is yet a lack of risk assessment on the vulnerability of pavements exposed to extreme weather events. The research of experimental designs and new technologies is of paramount importance for airport engineering as well as the education of future leaders as well as researchers and industry should work together to enhance the transfer of technology and best practices. Lastly, new materials and design should be evaluated and/or adopted. (Lu & Dutton, 2017)

2.4 Current distresses due to Climate Change in Canadian Airport Pavements

As it has been presented in this literature review, the climate is changing and those variations do have an effect in the airfield infrastructure of Canadian airports. The main distresses considered by Canadian airport authorities, as presented in Figure 2.9 of the previous section, were the early crack propagation and intensification, rutting and shoving, settlement and frost heaving, and stripping. Furthermore, other distresses that perhaps does not affects the structural integrity of the airfield pavement but do affect the operation of it, are the fog and the lost of skid resistance due to the presence of ice in the surface. Below a description of each type of distress as well as an explanation of its relationship with the changing climate.

2.4.1 Stripping

This pavement distress can be defined as the loss of bonding between the asphalt cement and the aggregates generating moisture damage in the asphalt mix, mainly starting from the bottom of the layer. (Solaimanian, Bonaquist, & Tandon, 2007) It is mainly caused by constant moisture and/or deficient aggregate surface chemistry, and it is detriment for the pavement as it diminishes the structural support and induces cracks and potholes if is not treated. (Pavement Interactive, 2019) The increment of precipitation can induce an intensification of this distress. Refer to image 2.3 for a superior illustration.

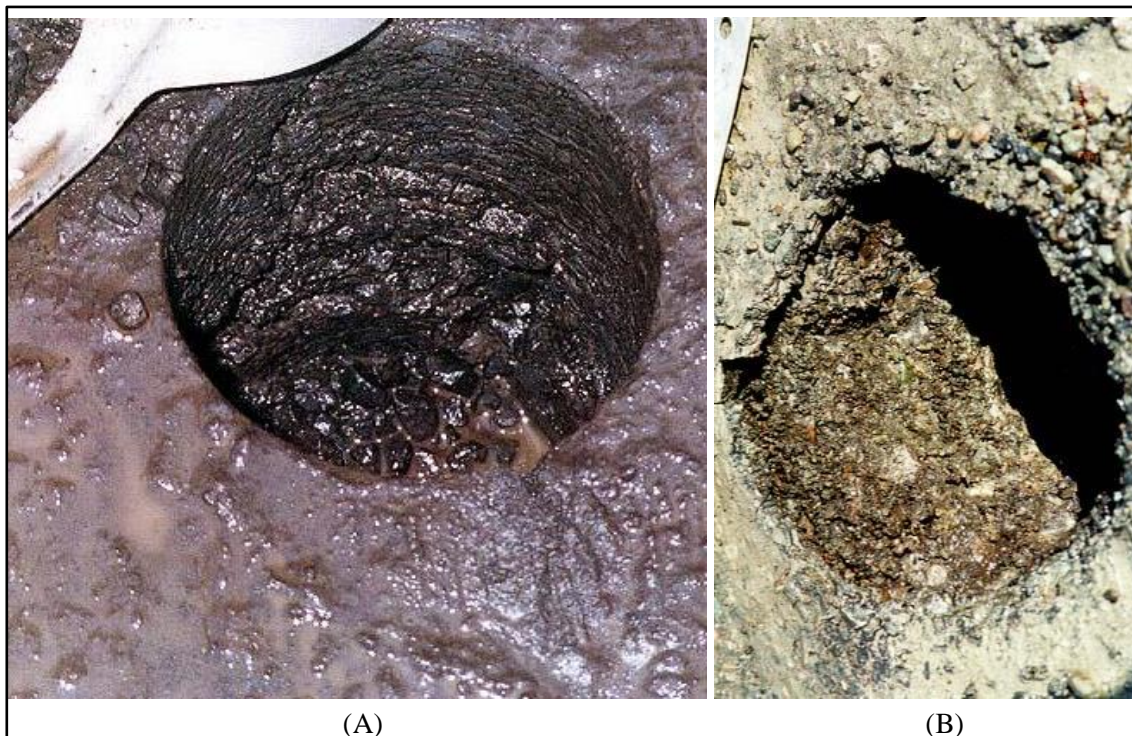


Image 2.3 Stripping | A and B are core holes showing stripping at the bottom of the layer (Pavement Interactive, 2019)

2.4.2 Thermal Cracking

This type of crack occurs due to the expansion and contraction of the pavement structure during the cold and hot periods of the year. In winter, the pavement structure shrinks as well as it becomes stiffer, this also makes the pavement structure harder and therefore more susceptible to crack. There are two types of thermal cracks, the low temperature transverse cracks and the thermal fatigue cracking which is mainly caused by aging and degradation due to cumulative thermal cycles. (Mills, et al., *The Road Well-Traveled: Implications of Climate Change for Pavement Infrastructure in Southern Canada*, 2007)

As the roads/runways are long infrastructures in a 2-dimensional perspective (plant view), when shrinking, the cracks propagate perpendicular to the direction of the way. Then, eventually during the spring, the temperature raises and the pavement goes back to its original shape alleviating stresses but unfortunately, allowing the cracks to originate. Image 2.4 provides a better perspective of how this distress appears.

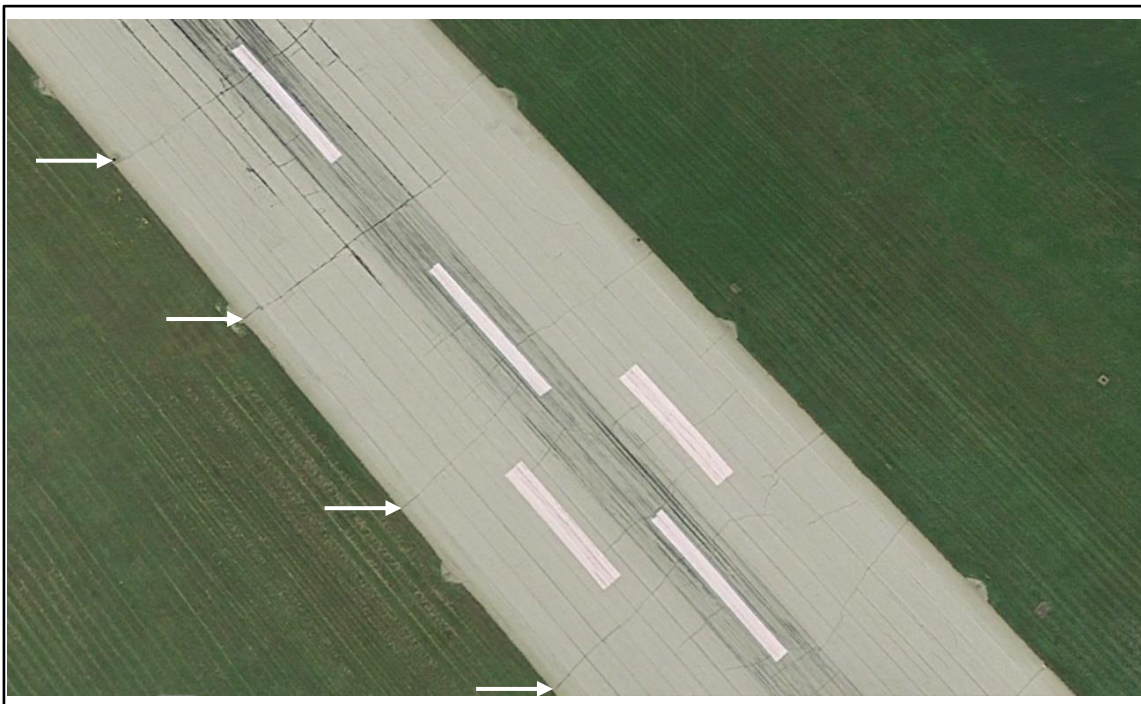


Image 2.4 Low Temp Transverse Cracking Example at YXU Airport (Google Earth Pro, 2019)

2.4.2 Rutting

This distress is a longitudinal permanent deformation caused by repetitive heavy traffic loads combined with a softening of the surface layer. (Khan, Nagabhushana, Tiwan, & Jain, 2013) It can also be caused by a failure in the granular layers due to multiple reasons such as a loss of support of the soil caused by fatigue, significant changes on the ground water table (GWT), and the melt of permafrost. Even though the likelihood of experiencing rutting is not elevated, it represents a risk for airport pavements due to the combination of complex operations and the type of maintenance required by this distress. (White, 2018) In Canada, due to the colder climate, rutting does not represent a substantial distress; nonetheless, because of climate change, the south of Canada is becoming warmer which makes of this distress a potential threat. Image 2.5 can serve as an example of a moderate rutting.

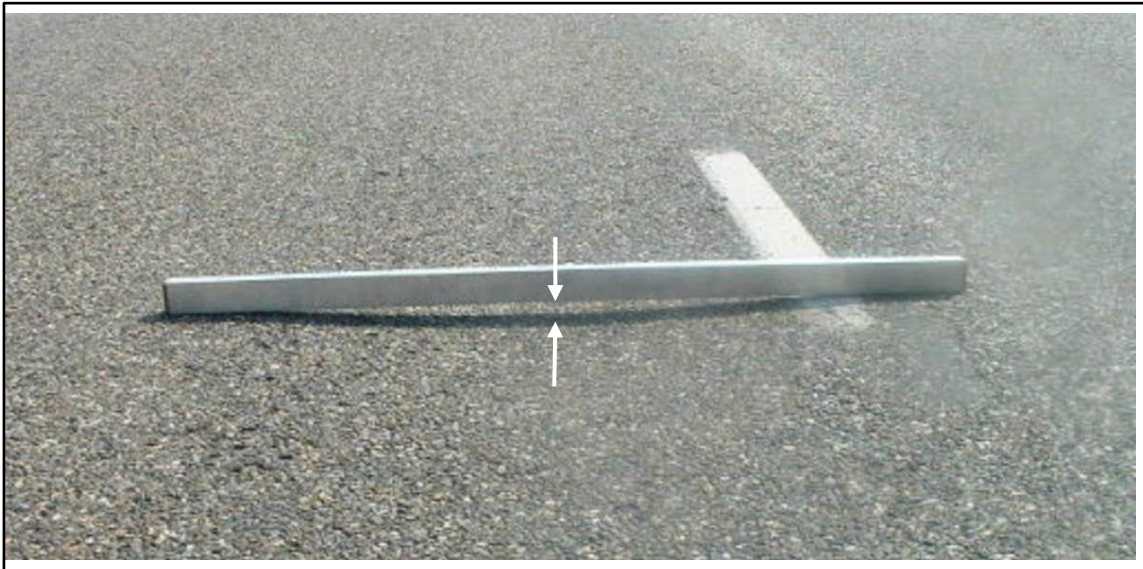


Image 2.5 Moderate Rutting (PPRA, 2018)

2.4.4 Frost Heaving

Frost heaving is a type of pavement distress that is mainly caused by the creation of ice lenses inside the base, subbase, or subgrade layers during the wintertime. The pavement structure in general compresses due to the low temperature; nonetheless, the water inside the soil, as of the properties of water, expands approximately by 9% inducing the heaving. When the water inside the pavement structure thaws during the spring, the deformations that were caused by the stresses that the expanded frozen water induced are not fully repaired, meaning that the pavement structure experiences a permanent deformation after each winter which mainly depends on the length of the winter, the temperature differences, and, indeed, the resiliency of the pavement structure. Images 2.6 and 2.7 present how the frost heaves are developed in flexible and rigid pavements respectively.

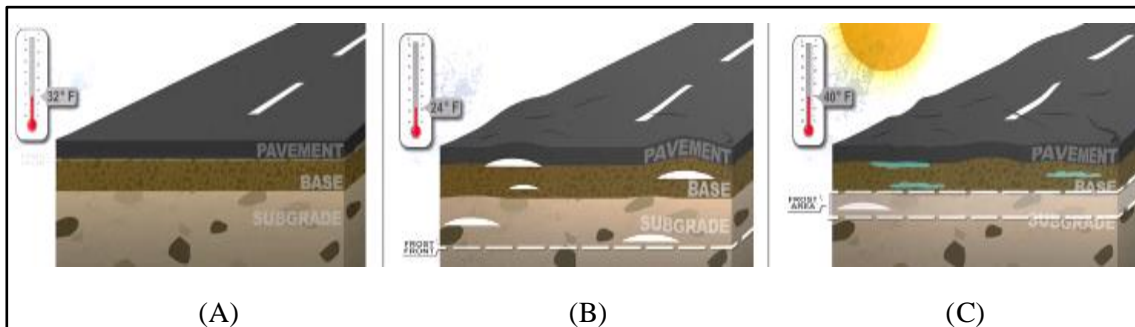


Image 2.6 Frost heaving creation in a flexible pavement | A. New Pavement; B. Frozen Pavement Structure; C. Pavement Structure after Thawing (Minnesota Department of Transportation, 2013)

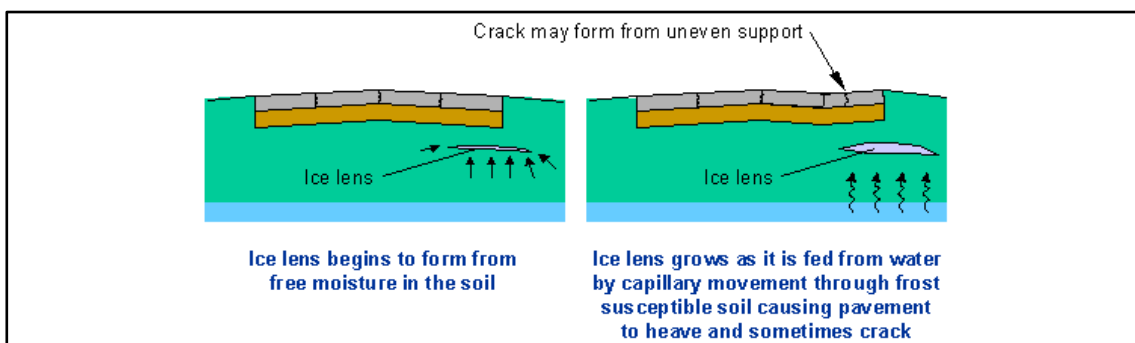


Image 2.7 Frost heaving creation in a rigid pavement (ACPA, 2013)

2.4.5 Shoving

The Cambridge dictionary defines the word shove as to roughly push someone or something. (Cambridge Dictionary, 2019) Hence, this pavement distress, which is more common in flexible pavements, is mainly caused by pushing forces; therefore, heavy breakings inducing substantial shear stresses, and the softening of the asphalt mix instigated by a significant increment of temperature. That being said, this is a type of distress that can be found in the airside areas subjected to critical shear stresses, lofty torsions, and high temperatures; consequently, the runway and taxiway's entrances/exits. Image 2.7 presents shoving areas located at one of Toronto airport' taxiways in June 2007.



Image 2.7 Shoving at YYZ Taxiways, 2007 (Stewart, 2010)

2.4.6 Settlement

This distress can be defined as the subsidence of the ground or the structure above it. Hence, settlement can happen at any layer of the pavement structure but it will affect, sooner or later, the layers above. The main cause of this distress is a reduction on the bearing capacity of the subgrade in many cases due to fatigue, the constant repetition of loads, or, as it is the case of northern Canada, due to a difference in the internal stresses of the soil caused by the thawing of permafrost. For this last possible cause, climate change is responsible because, as the planet warms, the permafrost that used to be continuous becomes discontinuous or sporadic befitting a great cause for future or present settlement. Figure 2.13 presents a vertical exaggeration of the surface profile of Yellowknife airport developed by points cloud data collected by TetraTech using LiDAR in 2015.

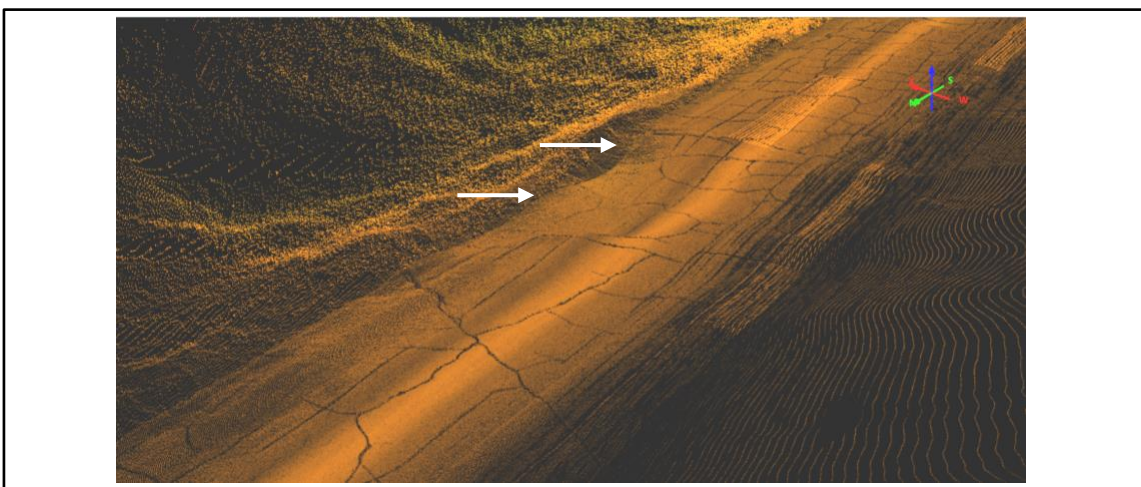


Image 2.8 Lidar Point Cloud 20x Vertical Exaggeration of Yellowknife's Surface Profile in 2015 (Reggin, 2019)

2.4.7 Fog and Lost of Skid Resistance

Among all the distresses that can impact the airfield pavement infrastructure due to environmental conditions and loads, fog represents a significant one for certain locations in Northern Canada. Essentially, due to the increment of temperature and precipitation, the ice cover of rivers is being reduced creating fog, then this fog condenses causing the surface of the pavement to freeze which subsequently diminish the skid resistance of the airfield pavement and rises the necessity for winter maintenance and operations. The lost of skid resistance represent a meaningful thread putting the safety of the users of the airport in jeopardy. Hence, winter operations have to be executed, being the most frequent one for this case to broom the airfield infrastructure. Consequently, the micro texture is reduced, opposite to the macro texture, which perpetually affects the skid resistance. (Konarski, 2014) Image 2.9 presents an example of a foggy runway.

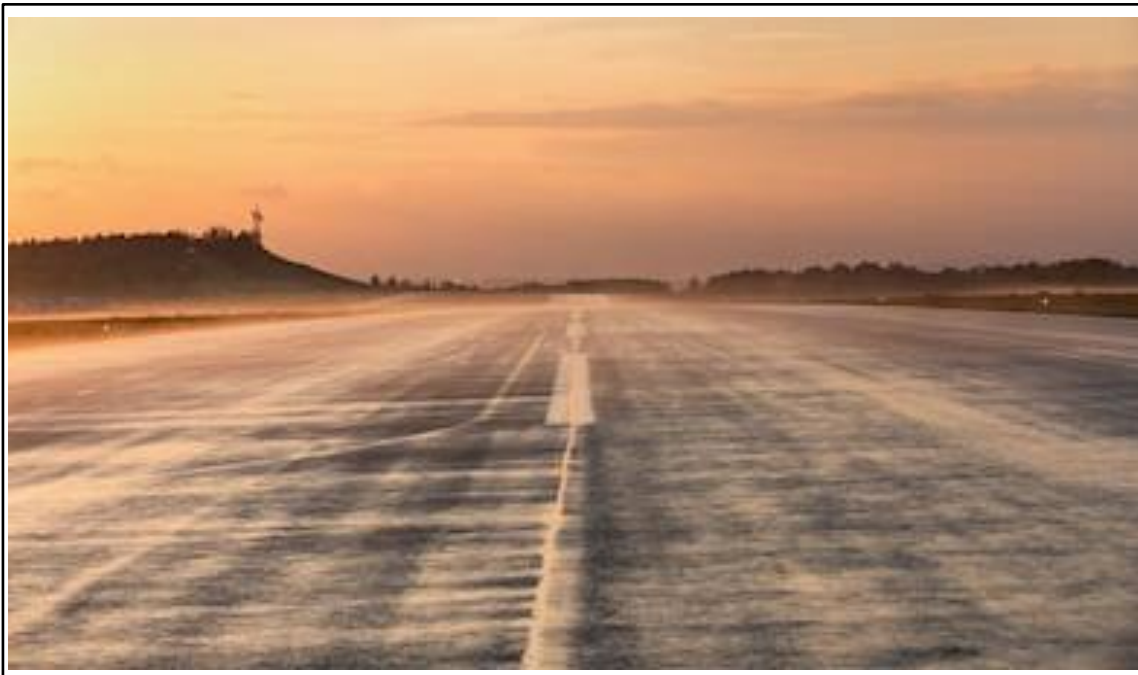


Image 2.9 Foggy Runway (Murmakova, 2017)

2.5 Methods of Assessing Rutting, Stripping, Tensile Strength, and Crack Propagation

Figure 2.12 presented some of the main distresses that Canadian airports are experiencing, depending on their location such as the crack's early propagation and severity for the entire country, rutting and shoving for southern provinces, and heaving and settlement for northern Canada. Because the last two distresses have a different formation that depends more on the characteristics of the soils and the climate at those locations, the methods to assessing these distresses fall out of the scope of this project. Therefore, the distresses that will be assessed are those that occur at the flexible pavements' surface due to environmental loads.

Rutting and shoving will be assessed through the AASHTO T-324, named Hamburg Wheel Tracking Test (under water), Stripping and Tensile Strength will be evaluated by conducting the test AASHTO T-283 called Modified Lottman Test, and lastly, the results from the Tensile Strength Ratio will be used to calculate a crack propagation index from a test developed in 2017 called Ideal Cracking Test. More details of the test can be found below.

2.5.1 Hamburg Wheel Tracking Test under Water (AASHTO T 324)

The Hamburg wheel tracking test (HWTT) is a test that is conducted to measure the susceptibility of asphalt mixes against longitudinal permanent deformation and moisture damage. (Walabita, et al., 2018) The test consists of 4 cylindrical asphalt samples of 150 mm of diameter and 63 mm of height, subjected to a constant dynamic load which exemplifies traffic. The wheels that induces the moving load to the samples are loaded with a weight of 158 ± 1 lb which moves back and forward on top of the asphalt samples creating a track of permanent deformation. The Hamburg Wheel Testing Device (HWTD) keeps the temperature at 50°C , as it is commonly used, and constantly measures the deformation of the samples after certain quantity of cycles until reaching the final value of 10,000 or 20,000 cycles. (American Association of State Highway and Transportation Officials, 2016) The following images illustrate the shape of the device and an example of the samples after being tested.

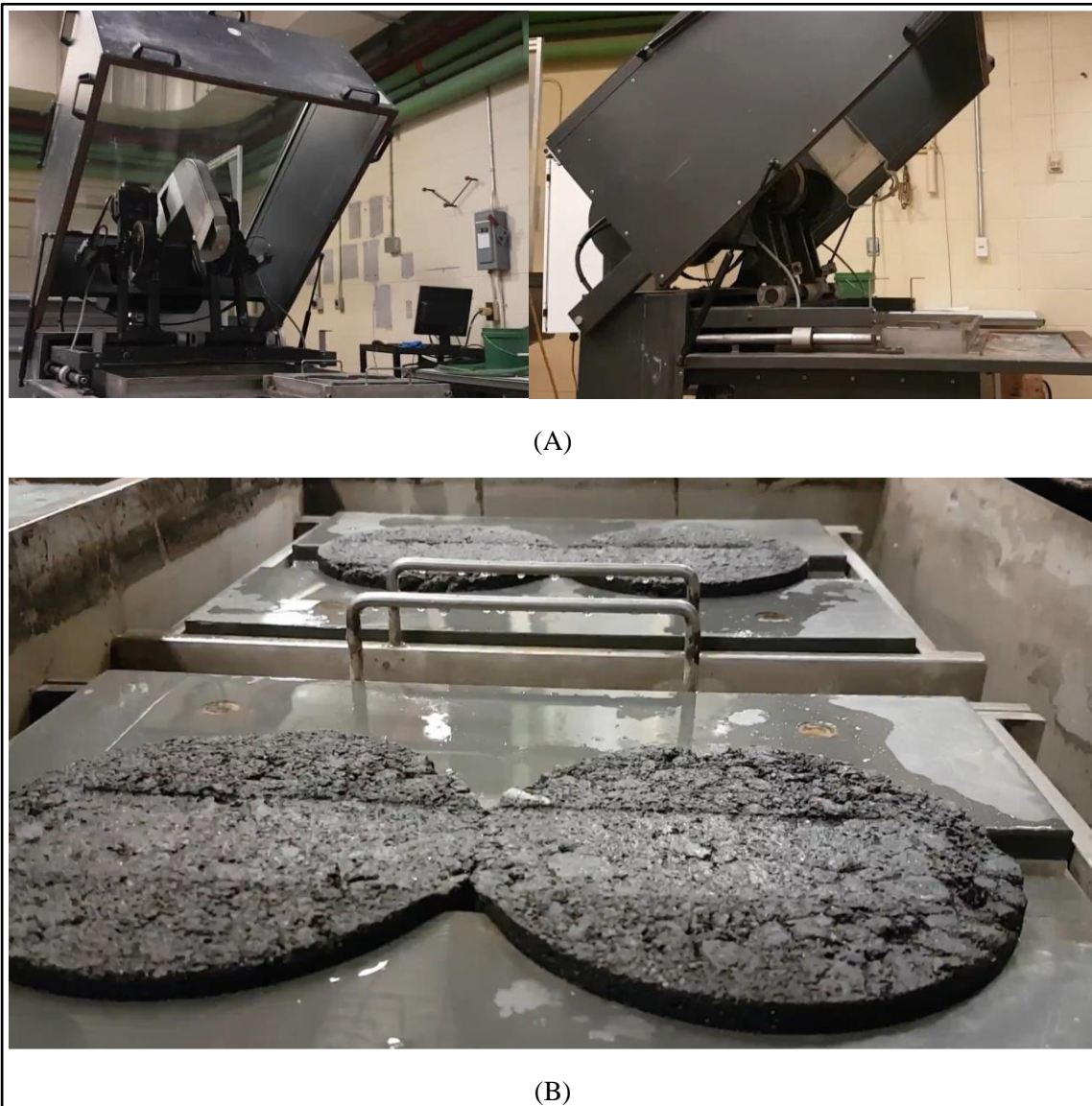


Image 2.10 Hamburg Wheel Tracking Test | A. CPATT's Hamburg Wheel Tracking Device; B. Asphalt Samples inside the HWTD after Being Tested

2.5.2 Modified Lottman Test (AASHTO T 283)

The main purpose of this test is to measure the susceptibility to moisture damage, stripping, and freeze-thaw cycles by inducing climate conditions to the asphalt mix. It requires to separate the samples that will not be conditioned from the ones to be subjected to all the conditioning methods. The samples to be conditioned must be saturated between 70% to 80% as well as subjected to 24 hours of freezing at -18°C and 16 hours of thawing at 60°C to exemplify a year condition (winter-summer). Once the samples have been conditioned, then all of them are brought to 25°C by using a conditioning chamber or by placing them under water at the mentioned temperature for 2 hours. Having all the samples at 25°C, the indirect tensile strength (ITS) test is conducted on them. The test is seeking to measure the ratio of change between the samples that were not conditioned from the ones that did. Image 2.12 provides more details of the test and the samples. (American Association of State Highway and Transportation Officials, 2003)



Figure 2.13 Tensile Strength Ratio Conditioned Samples and Compaction Equipment

2.5.3 Ideal Cracking Test

It is a test that was developed by the Texas A&M Transportation Institute and the Tongji University in Shanghai, China. It mainly consists on using the results from the ITS test (load versus displacement relationship) to evaluate the crack propagation of the mix and categorize the crack susceptibility of it by calculating the CT-index. This index considers mainly the energy of fracture, being this one the area under the curve of the load versus displacement graph, as well as different slopes of the curve from distinct points which describes the behavior of the mix. Additionally, it considers the asphalt content of the mix, the volume of the samples, the air voids, and the maximum specific gravity of the mix (G_{mm}); therefore, it takes into consideration the volumetric details of the mix. (Zhou, Im, Sun, & Scullion, 2017) The next Figure describes superiorly what was detailed in this paragraph.

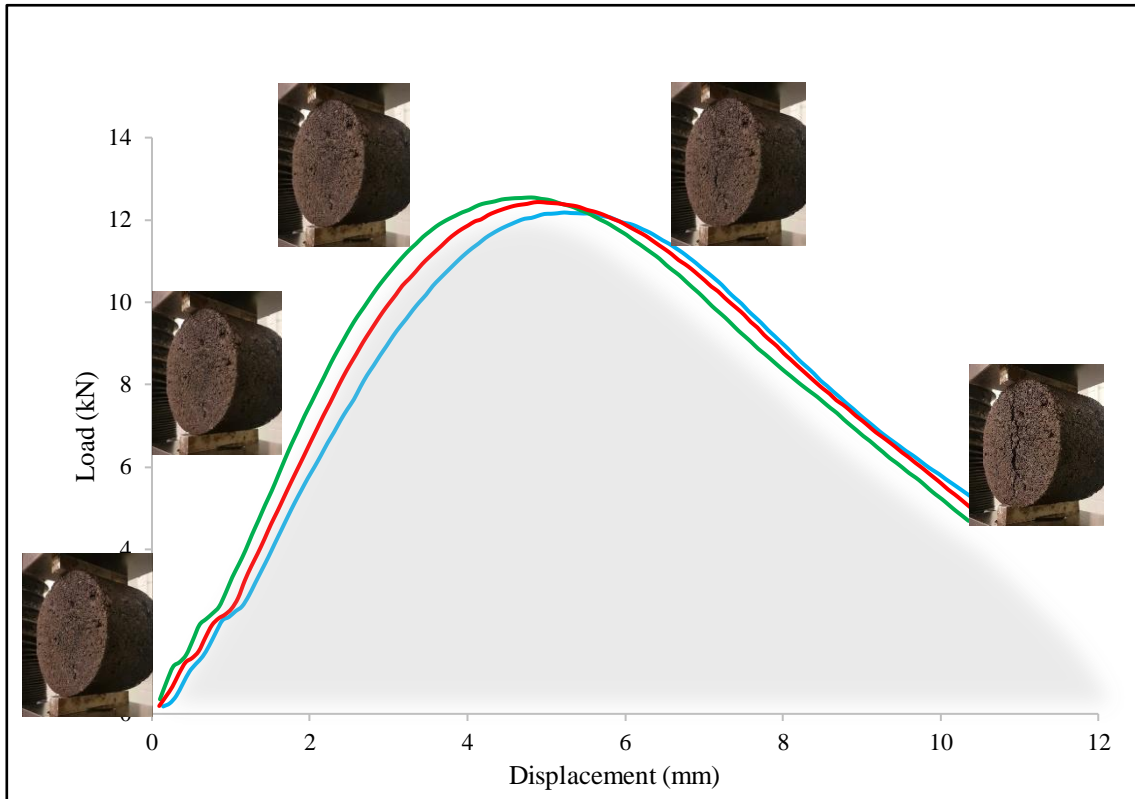


Figure 2.14 Crack Propagation, Ideal CT Principle

According to Zhou, Im, Sun, and Scullion, the cracking test index can be obtained with the following equation:

$$CT\ Index = \frac{t}{62} \times \frac{G_f}{\frac{P}{l}} \times \frac{l}{D} \quad (1)$$

Where t = sample thickness, G_f = fracture energy, P = Applied load, l = measured vertical deformation, D = diameter of the sample. The $\frac{P}{l}$ represents the modulus (slope of the load-displacement curve) and the $\frac{l}{D}$ represents the deformation tolerance under a load.

2.6 Chapter Summary

Climate change, better defined as the variation of the statistical distribution of the weather patterns, has mainly been caused by anthropogenic reasons since the industrial revolution. The increment of the concentration of CO₂ equivalent emissions has grown exponentially in the past 300 years, causing the Earth to retain more heat in the atmosphere which is generating a significant increment of its mean temperature, a meaningful thaw of the arctic sea ice, and many other consequences that have drastically changed the planet as it used to be. Canada, indeed, not an exception, has also suffered many consequences due to climate change, being the main ones, the increment of temperature and precipitation, the higher intensity of floods and hurricanes, the frequent extreme snow events, and more importantly, the change of location of weather events. All these alterations create or intensify pavement distresses which are directly related to a rise of the maintenance, rehabilitation, and/or reconstruction (MRR) costs.

Airports are aerodromes planned, designed, and built for the purpose of arrival, departure, or movement of aircrafts. Moreover, the airfield pavement refers to the infrastructure that sustains the loads induced by these aircrafts. This infrastructure is mainly divided into three main areas; the runway, the taxiway, and the apron. The runway is the arrival and departure zone, the taxiway represents the alignments that connect the runway to the apron, being this last one the area of enplaned and deplaned passengers and/or goods. Equally as having different purposes, they require distinct pavement designs, especially the runway and the apron that mainly consist of a flexible design and a rigid one, respectively.

The Canadian airfield pavement infrastructure design consists of a series of requirements that the future pavement will have to meet, but there is currently not a method to design airfield pavements. This lack of design method leads the airport authorities and consult companies to use international design methods such as FAARFIELD 1.42, the AI SW-1, and APSDS for flexible pavements, as well as the FEDFAA and AIRPAVE 11 for rigid pavements. Unfortunately, none of these structural airside pavement design methods are mechanistic-empirical nor contemplate climate change. The consideration of these factors could provide superior performance for future airside infrastructure as these will be significantly more resilient and prepared for present and future loads and hazards.

As described in [section 2.3](#), several Canadian airport authorities do not fully understand climate change for the process of decision making yet; however, they do agree that having a changing climate does have an effect on their practices. It was presented that distresses such as early cracking and crack severity are impacting all airports in Canada, but specially those in northern Canada. Rutting is affecting more the provinces of Ontario and British Columbia; therefore, those in southern Canada. Settlement and heaving are affecting more the airports in northern Canada as they primarily occur due to the melt or discontinuity of active permafrost layers and the freeze-thaw cycles at the geo-structures. Lastly, it was shown that some airports in British Columbia, a province with a superior precipitation, are experiencing pumps which is a pavement distress mainly caused by moisture damage.

The distresses that were considered to be affecting the most the Canadian airfield pavements were rutting, shoving, stripping, frost heaving, settlement, temperature cracking, and fog, which were superiorly described in [section 2.4](#). Hence, [section 2.5](#) illustrated the methods of assessing these distresses through laboratory tests. Consequently, the Hamburg Wheel Tracking Test (HWTT) was used to evaluate rutting and shoving under different amounts of freeze-thaw cycles and temperatures, the Indirect Tensile Strength test was applied to measure freeze-thaw cycle susceptibility as well as to evaluate the crack propagation by using the IDEAL CT index approach.

Chapter 3

Climate Data and Material Collection and Design

The climate data was collected from Environment Canada as the main source, used for the temperature, precipitation and freeze-thaw cycles' analysis, and from Meteoblue as a secondary one, for the wind analysis. The Meteoblue data set consisted of annual average wind direction and speed from 1985 to 2019. The Environment Canada's data encompassed the maximum, minimum, and average daily temperature, as well as the sum of monthly/annual precipitation divided into total precipitation, rainfall, and snowfall. In another hand, data was collected from temperature sensors located in Yellowknife, NWT to correlate the ambient temperature and the temperature at the surface layer of the pavement structure. Furthermore, an Excel algorithm to obtain freeze-thaw cycles was developed to present the variation of these in the past 50 to 70 years.

Environment Canada, especially on airport locations, have available data varying from 1880-1960 until the current date. The accessibility of the data makes the process smoother; nonetheless, the obtainability of it requires a significant amount of time as the daily data is to be download annually and each year will be a separate excel file. Once all the years to be evaluated are downloaded, the whole set of data is to be concatenated. To complete this assignment with higher efficiency, an algorithm was developed by Dr. Hamed Shahrokhi using the software Spyder (Python 3.7) to complete the task of concatenating the data for each specific location.

3.1 Locations

As stated in the scope of this project, solely airports that belong to the category of National Airport System (NAS); therefore, those with a annual number of passengers higher than 200,000 (Government of Canada, 2010), are to be evaluated and use as examples for a relative province or territory. Image 3.1 and table 3.1 present the airports that were selected as case studies for this project considering only one per province or territory. The represented airport was chosen based on the annual amount of aircrafts or the transportation of freights. Hence, the chosen airports are or have being the busiest ones of their province and/or territory.

Table 3.1 Selected Airport Names, Provinces/Territories, and IATA Codes

Airport Name	Province/Territory	IATA Code
Whitehorse International Airport	Yukon	YXY
Yellowknife International Airport	North West Territories	YZF
Iqaluit International Airport	Nunavut	YFB
Vancouver International Airport	British Columbia	YVR
Calgary International Airport	Alberta	YYC
Saskatoon International Airport	Saskatchewan	YXE
Winnipeg International Airport	Manitoba	YWG
Toronto Pearson International Airport	Ontario	YYZ
Montreal Trudeau International Airport	Quebec	YUL
Moncton International Airport	New Brunswick	YQM
Halifax Stanfield International Airport	Nova Scotia	YHZ

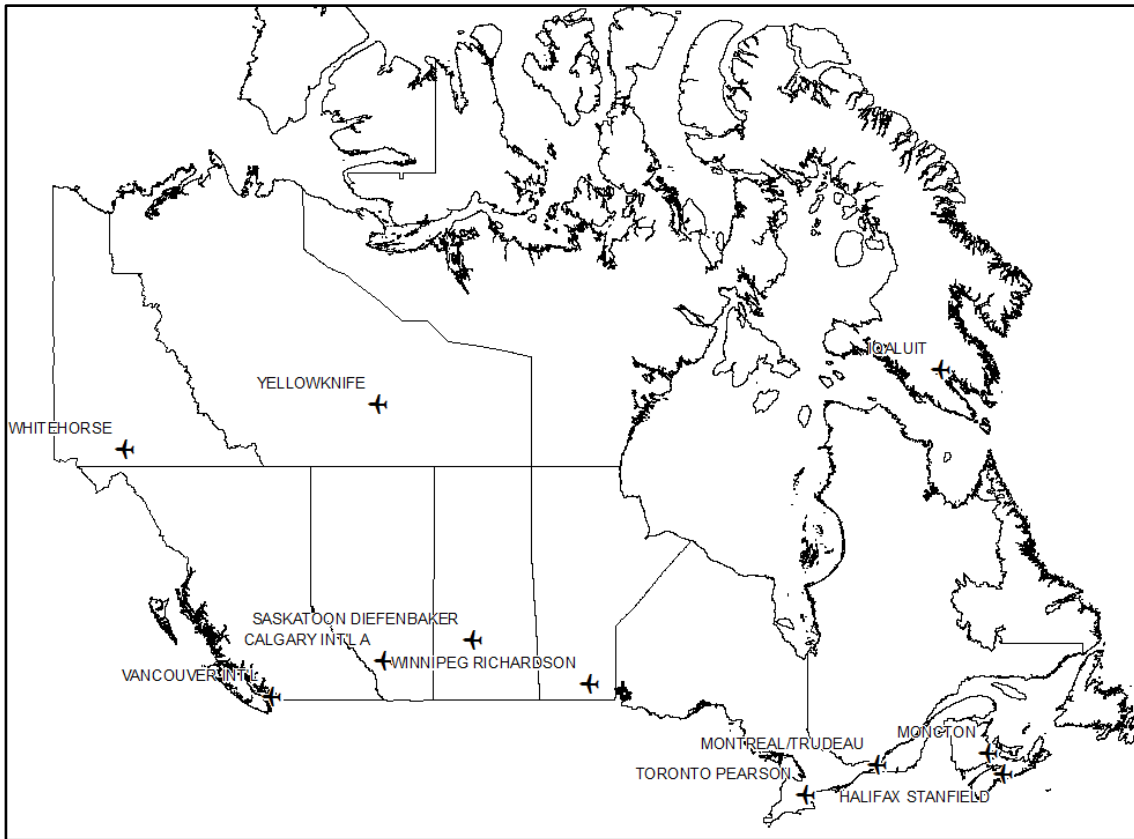


Image 3.1 Selected Airport per Province/Territory for Case Studies

Concerning the wind analysis, only the province of Ontario was considered, more specifically the southern portion of Ontario, for which only three airports were chosen due to the availability of data. Image 3.2 shows the location of the airports that were considered for this analysis. These airports were selected based on the number on runways and the different direction of its. As it can be perceived, Toronto Airport counts on 5 runways, Ottawa Airport have 2 runways, and the Canadian Force Base in Trenton, only have one runway.



Image 3.2 Selected Airports from Southern Ontario for Wind Analysis (Google Earth Pro, 2019)

3.2 Material Design and Collection

The following asphalt mix design was to be used at one of the taxiways of Toronto Pearson International Airport. The main points to consider of the asphalt mix design are the performance grade of the asphalt cement, the content of it, and the aggregate's types and gradation. The mix used for the laboratory tests, as observed in Figure 3.1 and 3.2, represents a PG 70-28J with a 5.2% of asphalt cement. It used three different aggregates 47% of CA#1, 42% of FA#1, and 11% of FA#2, all with distinct gradations that, together, optimize the future performance of the mix and meets the requirements of the Greater Toronto Airport Authorities.

Table 3.2 Asphalt Mix Design and GTAA Requirements

Property		Design ¹ (%)	GTAA ² Gradation Requirements	
Gradation (% Passing)	Sieve Size (mm)		Maximum (%)	Minimum (%)
		26.5	-	-
		19	-	100
		16	100	95
		13.2	98	90
		9.5	80.3	75
		4.75	54.3	45
		2.36	38.7	35
		1.18	25.3	25
		0.600	17.5	15
		0.300	10.3	7
		0.150	5.5	1
	0.075	3	1	
Air Voids (%) at N_{des}³		3.9	5	3
Voids in Mineral Aggregate, VMA (%)		16.5	14.4	
Reclaimed Asphalt Pavement, RAP (%)		0	0	
Performance Grade, PG		70-28J	-	-
Asphalt Cement Content (%)		5.2	-	-
Recommended Compaction Temp. (°C)		147	-	-
Recommended Mixing Temp. (°C)		163	-	-

¹ Engtec Design, ² Greater Toronto Airport Authorities, ³ N_{des} is the number of gyrations at the design compaction

The airfield asphalt mix was produced by Pave-All Limited located in Mississauga. Once produced, the material was picked-up and stored in boxes at the Centre for Pavement and Transportation Technology's warehouse. See Image 3.3 for more details about the process of obtaining and storing the material.



Image 3.3 Material Pick-up and Storage

3.3 Chapter Summary

The purpose of this chapter was to present the data collection and sources as well as the collection and source of the asphalt mix samples that were obtained to develop the laboratory tests.

The main data source was Environment Canada. It was used to develop the temperature and precipitation analysis. Additionally, Meteoblue data was utilized for the wind analysis. Environment Canada's data was collected for a minimum period of 70 years ago; hence, since 1950. The wind data, as provided by Meteoblue was collected since 1985; therefore, a period of approximately 35 years. For the temperature and precipitation analysis, eleven airports from different provinces and/or territories of Canada were selected based on the annual aircraft movement. Nonetheless, for the wind analysis, only three airports were studied due to data availability which were mainly selected based on the number of runway directions.

The material to be used for the laboratory tests was envisioned and design for Toronto Pearson International Airport (YYZ)'s airfield infrastructure. It was obtained from PaveAI and it mainly consisted of an SP 12.5 with 5.2% of a PG 70-28J modified asphalt cement with a compaction temperature of 147°C. The gradation contained three distinct aggregates, 47% of CA#1, 42% of FA#1, and 11% of FA#2 to optimize the future performance of the pavement structure and/or to meet the design requirements of YYZ.

Chapter 4

Wind, Temperature, and Precipitation Analysis and Results

The following chapter presents a runway performance analysis, for the three airports located in the province of Ontario considering the crosswind fluctuations in the past 35 years. Moreover, it presents numerous environmental analysis contemplating temperature and precipitation as data foundation. The main outcomes were the following:

- The average maximum and minimum temperature trendlines as well as the temperature difference, since 1950 until 2019
- A correlation between the ambient temperature and the surface temperature for flexible pavements
- The fluctuation of freeze-thaw cycles for the mentioned period of time at the selected airports
- The permafrost distribution and variation in Canada as well as the possible airports susceptible to suffer distresses due to these changes
- The average precipitation, rainfall, and snowfall trendlines and differences since 1950 until 2019
- A discussion on what are these changes inducing to the airside pavement infrastructure of Canadian Airports depending on each specific location.

4.1 Wind Analysis

The wind can blow at any direction and speed any moment and it is very complex to predict its behaviour in the short term. However, in the long term, it creates a pattern of statistical distribution making the process of predicting the wind's behaviour easier. A wind rose diagram is a graphical description of the wind comportment during certain period of time to determine the best runway orientation. (Mohamed, Osman, & El-monem, 2011)

The objective of this analysis was to present an estimation of the availability or usage of the airport during certain period of time due to wind speed and direction. To estimate this operation percentage, wind rose data from 1985 until the current date of evaluation was required. Additionally, the direction of the runways of the considered airports and the construction's year of the runways was needed. The main concept of the analysis was based on measuring the percentage of the year on which the combination of the wind speed and direction created both a higher cross wind than the threshold of 27.6 km/h for the aircrafts to use the runway safely.

A similar computer model than the one developed by Chang for multiple runway orientations was used. (Chang, 2015) It mainly consists of an excel sheet that comprehend the wind rose diagram data separating it into different sections as it can be seen in Figure 4.1. Considering the angle between the direction of the runway and the velocity of the wind. The following concept was used to calculate the adjustment factor, meaning each division presented in Figure 4.1, which considers the sections that are covered, not covered, and partially covered.

$$\text{If } V_b \times |\sin\theta| \geq V_c \rightarrow f = 1,$$

$$\text{If } V_a \times |\sin\theta| < V_c \rightarrow f = 0,$$

$$\text{If } V_b \times |\sin\theta| < V_c \leq V_H \times |\sin\theta| \rightarrow f = \frac{V_a \times |\sin\theta| - V_c}{V_a \times |\sin\theta| - V_b \times |\sin\theta|}$$

Where, f = adjustment factor for a sector, V_a = Highest wind speed in a sector, V_b = Lowest wind speed in a sector, V_c = Allowable crosswind speed limit, and θ = Angle between wind direction and the predefined runway. (Chang, 2015)

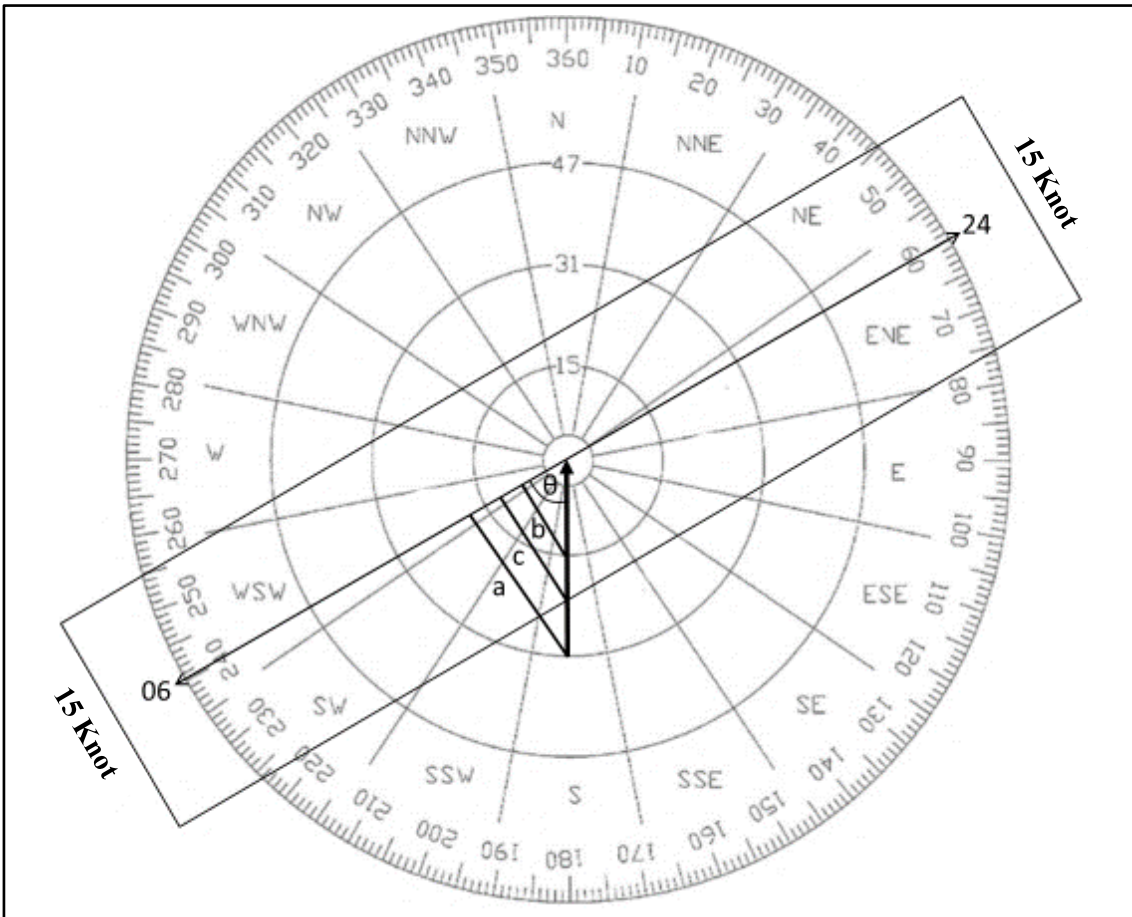


Figure 4.1 Wind Rose Diagram Representation

Figure 4.2 presents the relationship between the amount of runway directions and the annual usage that the airport can provide to them. When the number of runway's directions increases, the airport becomes less susceptible against crosswind as if one runway is unsafe to be used due to crosswind, most likely one of the other runways will be less susceptible at the moment, mitigating safety and improving the usage.

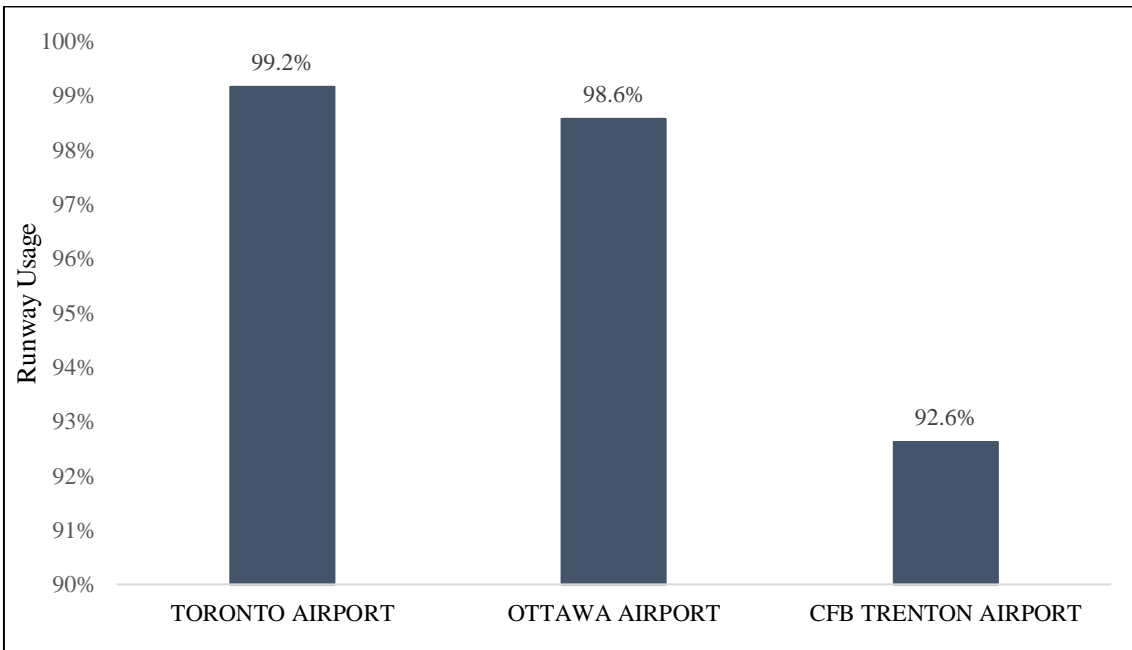


Figure 4.2 Runway Usage with cumulative data from 1985 to 2019

Figure 4.3 describes the annual usage of YYZ and YOW's runways since 1985 until 2018. Ottawa's Airport, compared to Toronto's airport have a more constant behaviour against crosswind due to the fact that both runways are not completely perpendicular but with a 110° difference, meaning that those extra 20° mitigate superiorly the crosswind, as it can be seen in Image 4.1. Same happens with Toronto Airport, specifically on 1997 after the construction of their 4th runway with a 3rd different direction. The runway 06L-24R was shifted 10° from the principal runway 05-23. These 10° improved the usage almost 3% allowing Toronto airport to use its runways up to a 99% of the year.

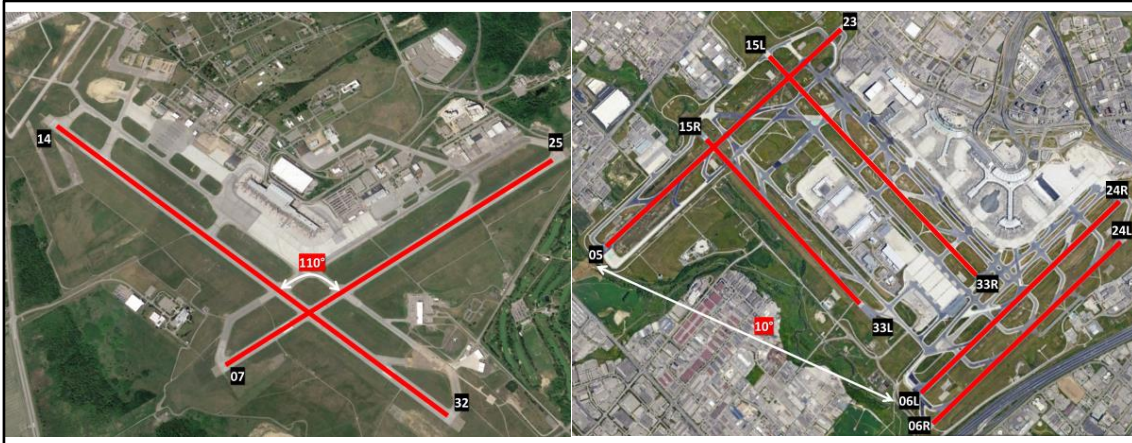


Image 4.1 Ottawa and Toronto Runways' Direction and Distribution, Respectively (Google Earth Pro, 2019)

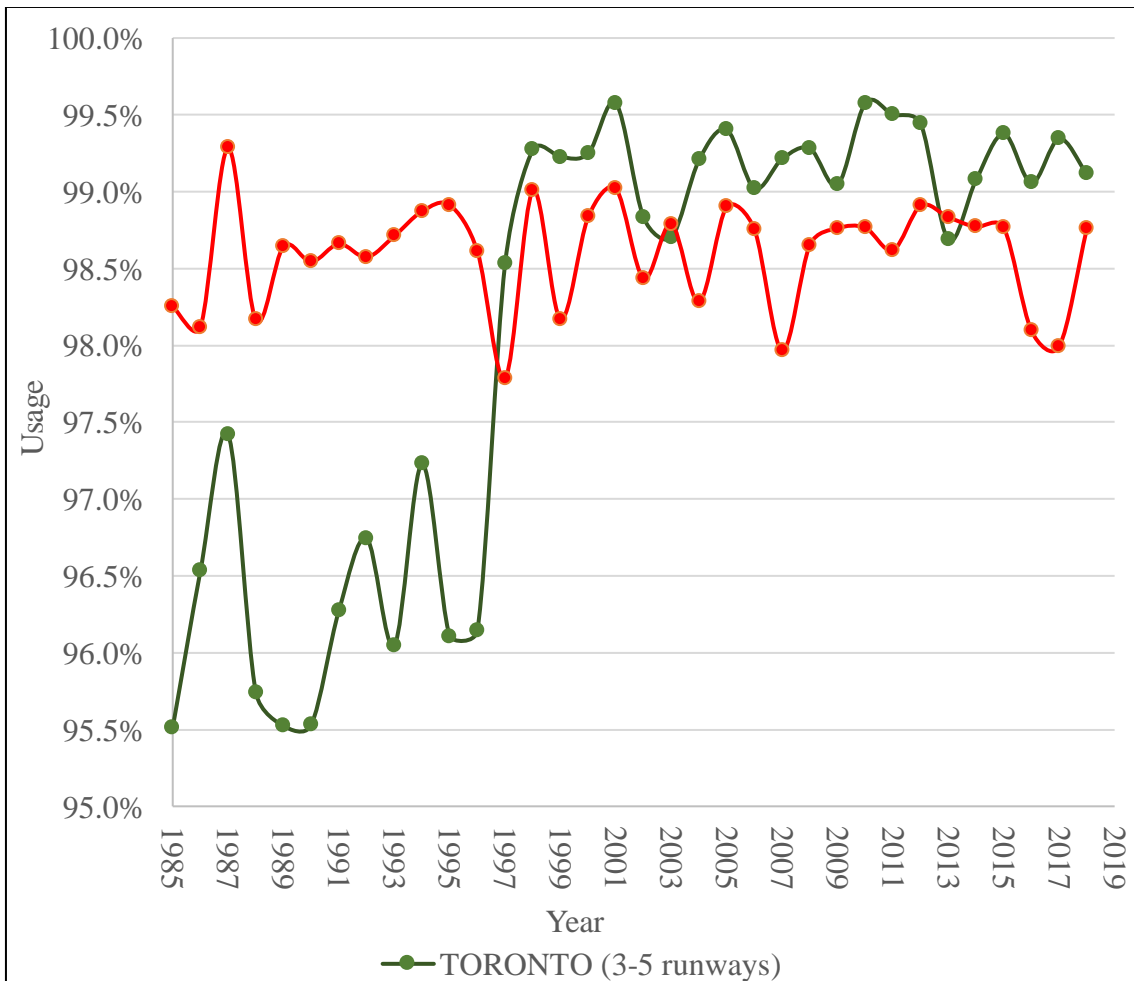


Figure 4.3 Airside Infrastructure Annual Usage for YYZ and YOW

4.2 Temperature Analysis

The analysis is to be made at the selected Canadian airports for a period of 70 years. It will mainly consist of concatenating the data and summarize it into a graph and/or a GIS map animation. The main focus is in evaluating the rise of temperature as well as the fluctuation of freeze-thaw cycles. To get this second one, an algorithm was developed using Microsoft Excel considering a freeze as when the pavement temperature becomes negative in degree Celsius and a thaw when the opposite. Some other assumptions had to be made as, in order to consider a freeze or thaw, the temperature range had to be between -15°C to 15°C and the difference in average temperature from one day and the other had to be greater than 0.2°C. If all the factors and assumptions complied, then it was considered for the calculation of annual freeze-thaw cycles.

4.2.1 Ambient and Pavement Temperature Results

The main purpose consisted of evaluating the temperatures changes on the selected airport's locations in terms of maximum and minimum temperatures, which are the ones that affect the pavement structure the most. Figures 4.5 and 4.6 present the average maximum and minimum temperature trendlines for the 11 airport locations presented [above](#). Figure 4.4 shows Vancouver maximum and minimum monthly temperatures as an example of how the trendlines were develop. Each of the presented trendlines represent a linear regression of the form $Y=AX+B$, where Y signifies the temperature, X is the year, A is the rate of change, and B is the average temperature for the month of January of the first year of evaluation, in the case of Figure 4.4, 1937.

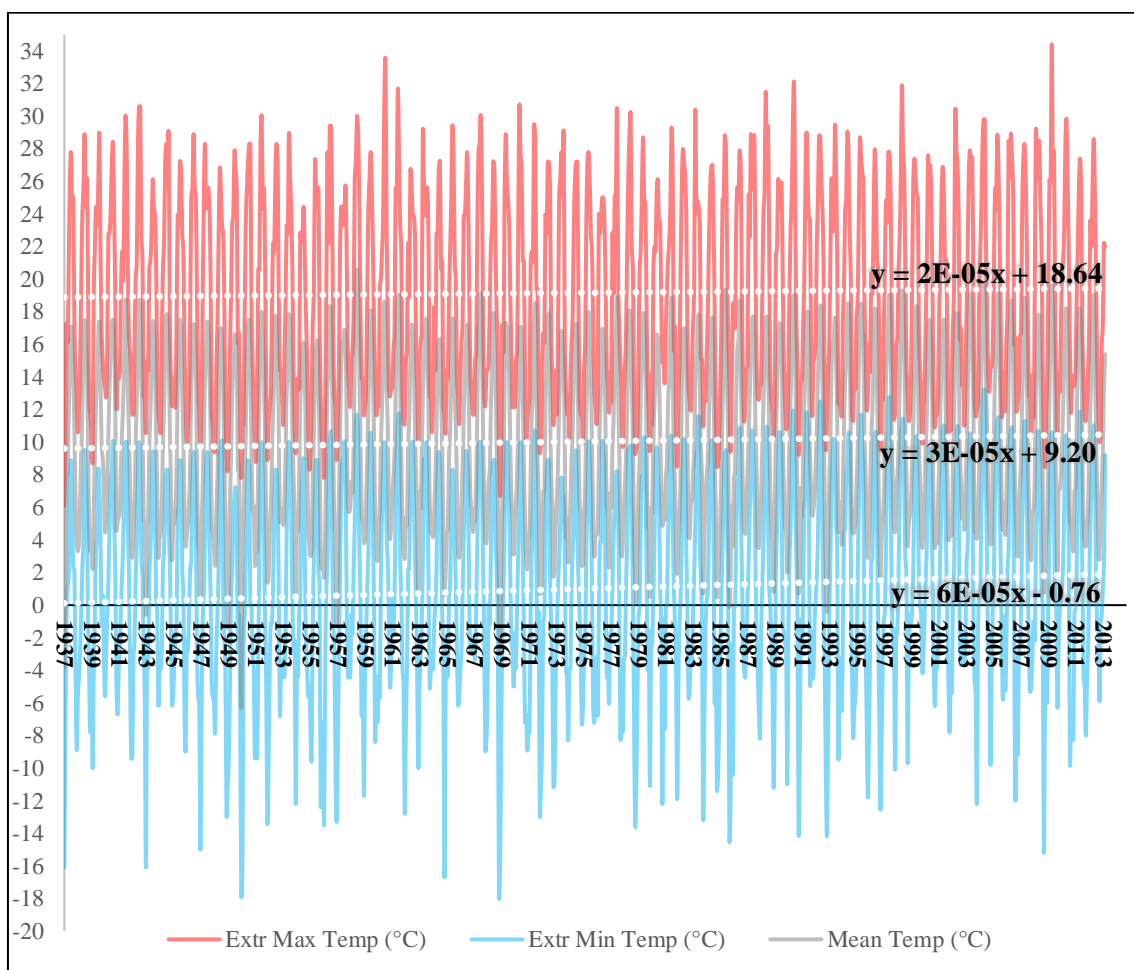


Figure 4.4 Average Minimum and Maximum Monthly Temperatures and Trendlines from 1937 to 2013 for YVR (Vancouver Airport)

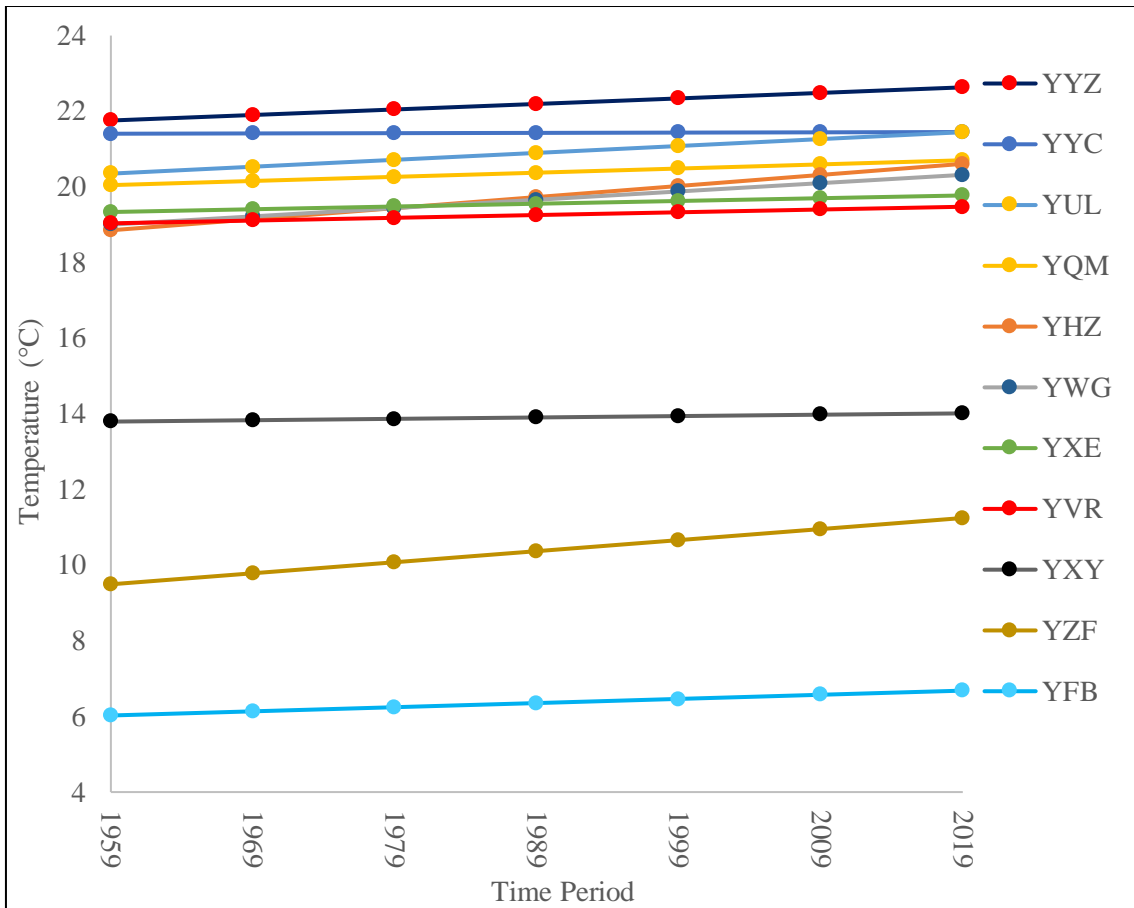


Figure 4.5 Average Maximum Temperature Trendlines

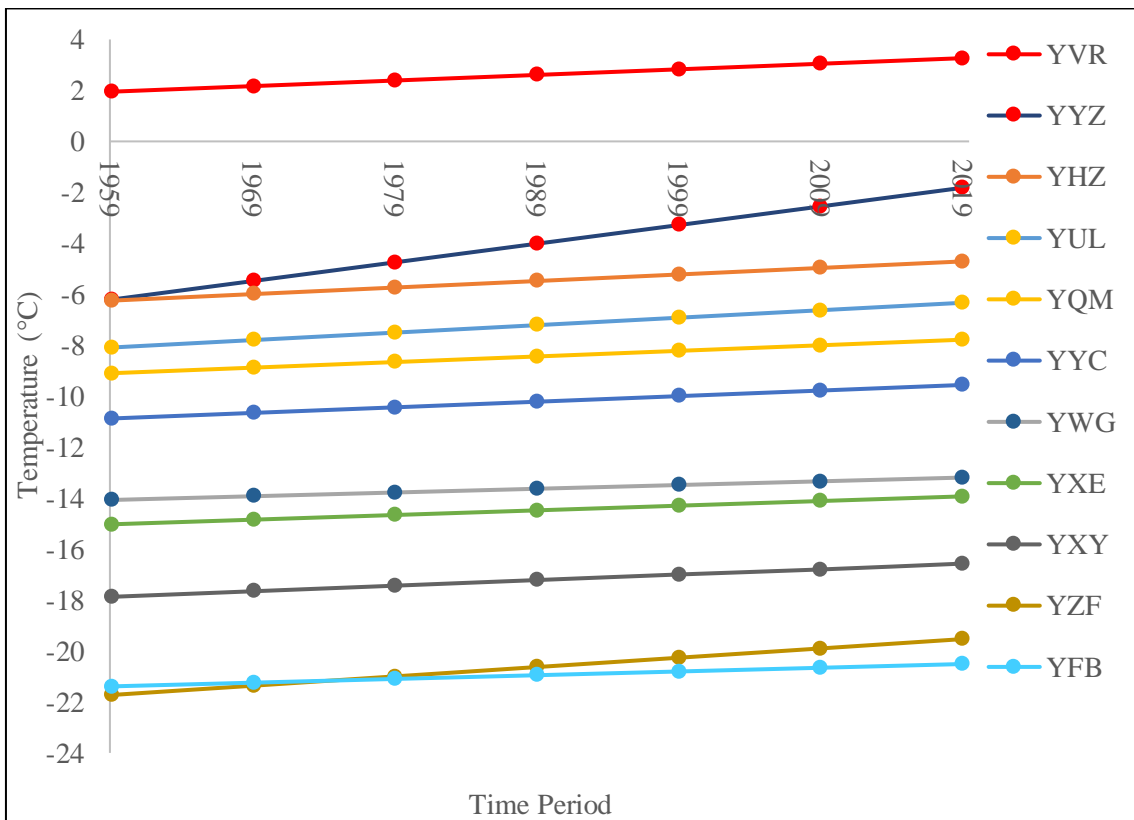


Figure 4.6 Average Minimum Temperature Trendlines

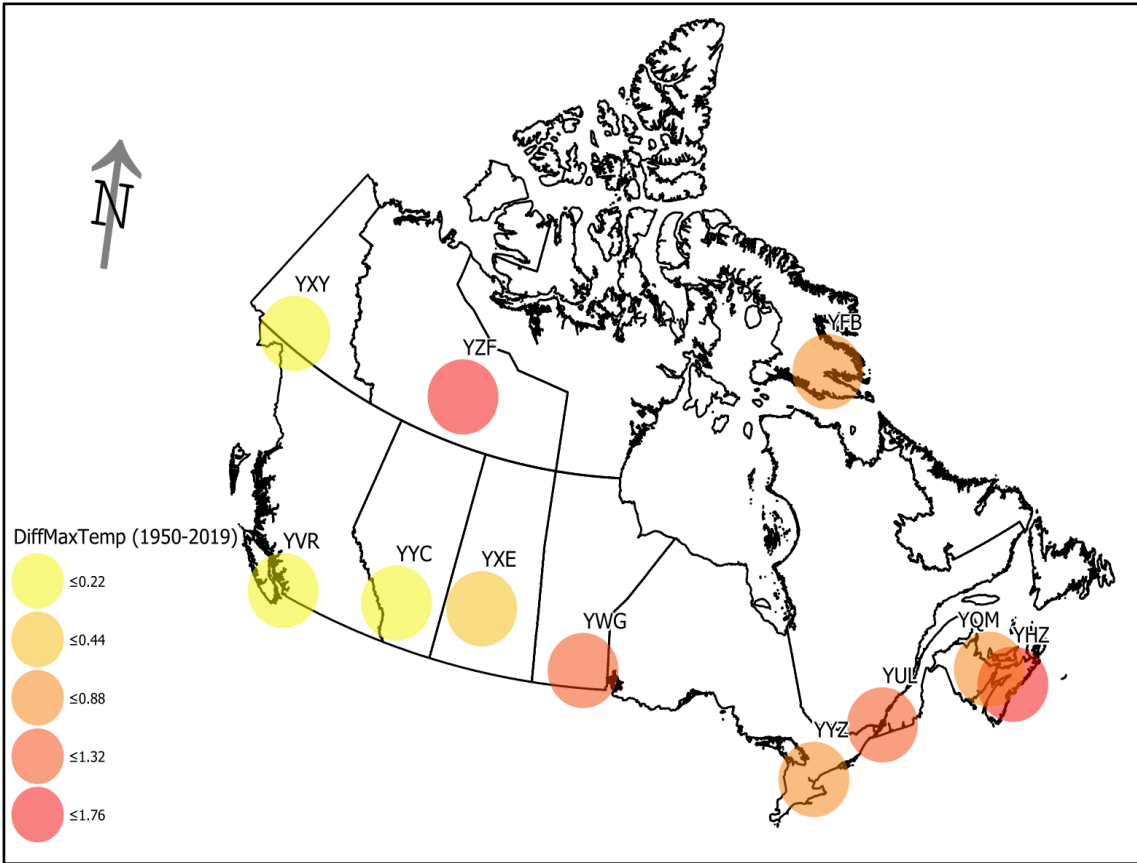


Figure 4.7 Difference in Maximum Temperature Trendlines since 1950

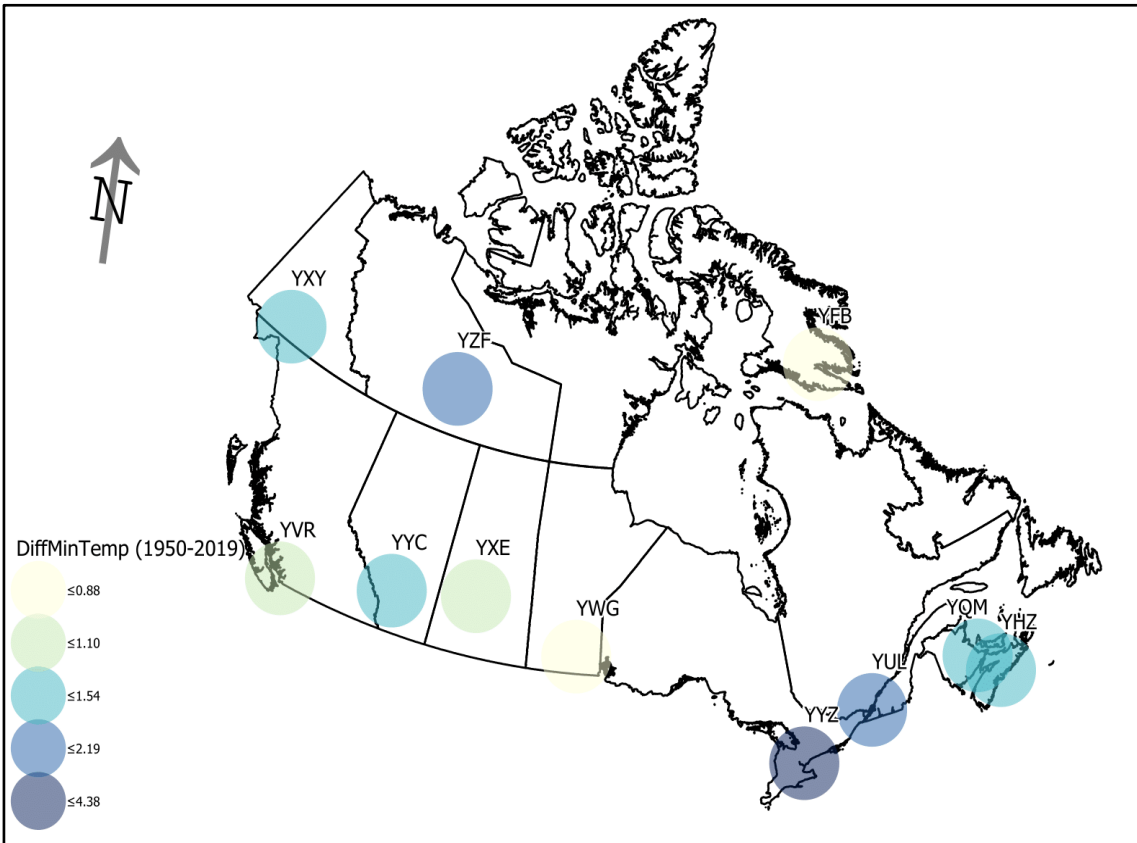


Figure 4.8 Difference in Minimum Temperature Trendlines since 1950

Understanding the effects of climate change at the specific location benefits the decision making for the airport authorities. From Figures 4.5 and 4.6 can be concluded that the hottest airport in Canada are located in southern Ontario as Toronto Pearson Airport, among all the airports evaluated, was the one with the highest temperature. It is also important to recall that Halifax (YHZ) and Yellowknife (YZF) airports were the ones with the highest rate of change, having increase their temperature 1.75°C since the year 1950 as it can be noticed in Figure 4.7.

The evaluated airport with the current lowest temperatures was Iqaluit airport (YFB); however, it is important to reference that more than 5 decades ago, YZF was recording lowest temperatures than Iqaluit. The rate at which the minimum temperature is increasing at YZF may be the cause of the melting of permafrost, which will be presented in [section 4.3](#), soils which is leading to different pavement distresses, mainly settlements and cracks. Furthermore, it is also substantial to discern that Toronto Pearson Airport (YYZ) has experienced a significantly higher increment of its lowest temperature reaching a difference of 4.4°C in the past 70 years, as it is presented in Figure 4.8.

To correlate the ambient temperature changes with what is occurring in the surface of the pavement structure, ambient and surface pavement temperature were obtained from the weather and data collection station located in Yellowknife airport. By having this relationship, the annual freeze-thaw cycles were able to be calculated. The following Figure shows the obtained relationship between the ambient and surface temperature of the pavement. As it can be seen, at low temperatures, the ambient and surface temperatures do not differ considerably; however, at high temperatures, the difference between both temperatures is highly significant. Refer to Table 4.1 for an easier interpretation.

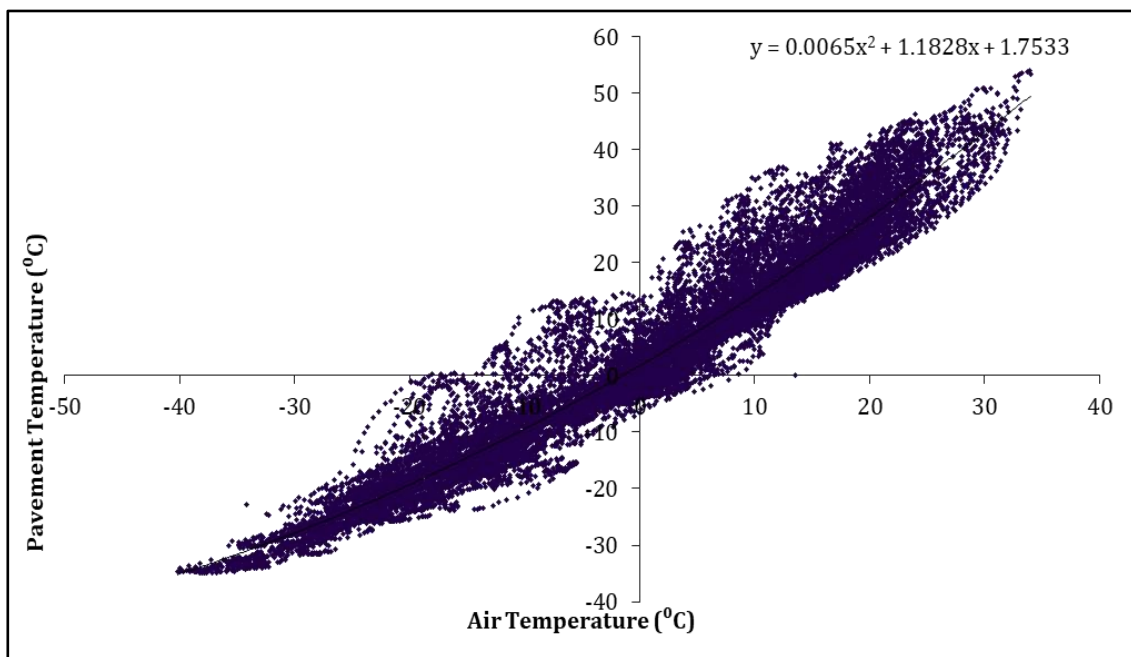


Figure 4.9 Ambient and Surface Temperature Correlation

Table 4.1 Ambient and Surface Temperature Relationship

Ambient Temperature (°C)	-40	-35	-30	-25	-20	-15	-10	-5	0	5	10	15	20	25	30	35	40
Surface Temperature (°C)	-35.2	-31.7	-27.9	-23.8	-19.3	-14.5	-9.4	-4.0	1.8	7.8	14.2	21.0	28.0	35.4	43.1	51.1	59.5

Figure 4.10 presents the annual maximum ambient and surface temperature for Toronto Pearson International Airport which illustrates the significant variations of both temperatures throw out the years, as well as it shows the pavement temperature difference from 1950, 2020, and 2040 following the trendline. These results will be used as an example further in this research.

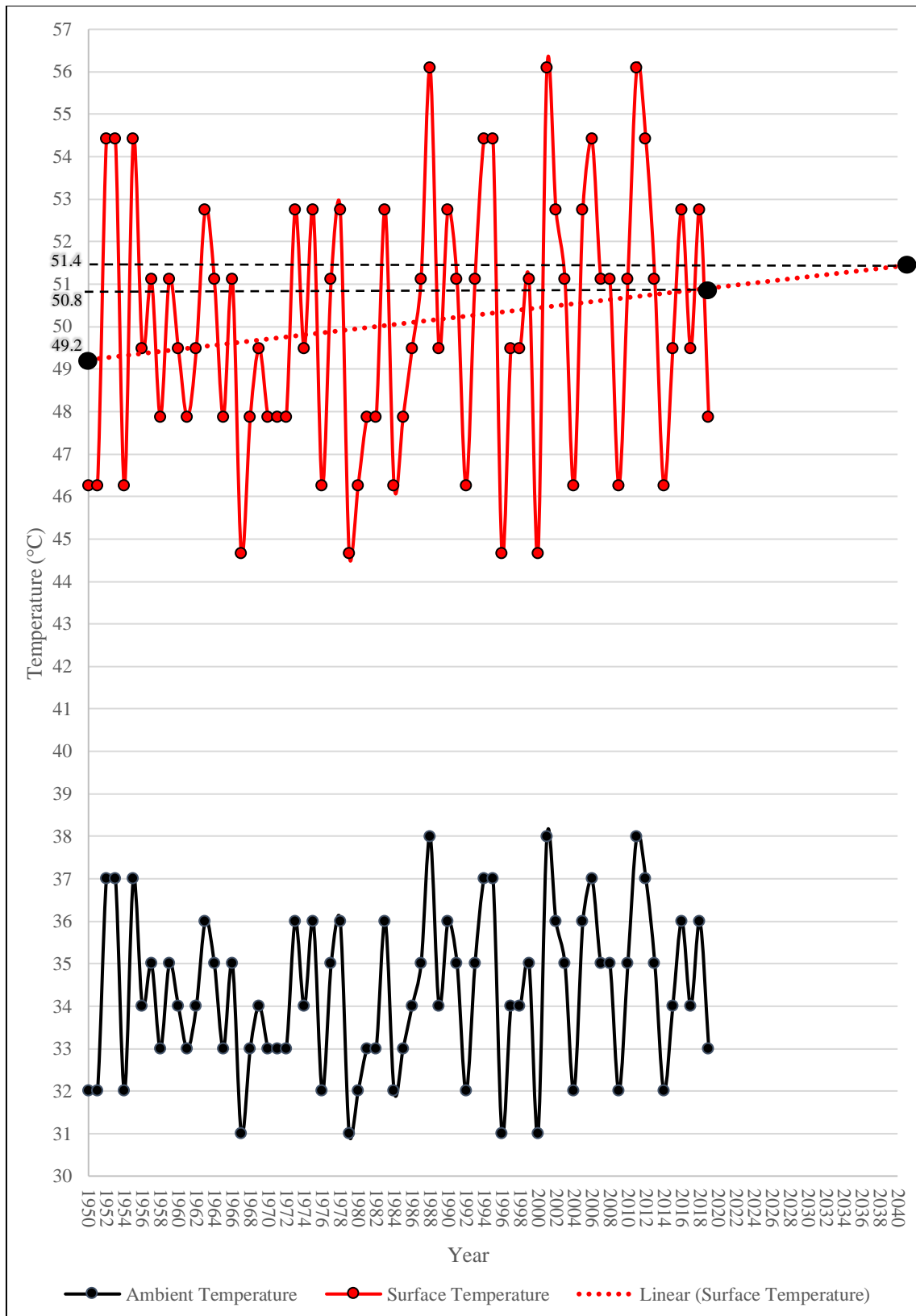


Figure 4.10 Annual Maximum Ambient and Surface Temperatures at YYZ

4.2.2 Annual Number of Freeze-Thaw Cycles

For the purpose of this investigation, a freeze-thaw cycle was considered to be a fluctuation of the pavement surface's temperature shifting from positive to negative and backwards. The annual freeze-thaw cycles were calculated for each selected airport being the results summarized in Figure 4.11 to 4.12.

- Figure 4.11 shows how the freeze-thaw cycles, for a cumulative period of five year, are significantly fluctuating from one period and the next. The main aspect to distinguish is how these cycles vary per location which can be better understood from Figure 4.10 as it meaningfully grows depending the airport.
- Figure 4.12 and Table 4.2 summarize the annual number of freeze-thaw cycles at the selected airports since 1950-2018 starting from Yellowknife, being the less susceptible, until Halifax which is the one with the highest number and increment of free-thaw cycles per year.

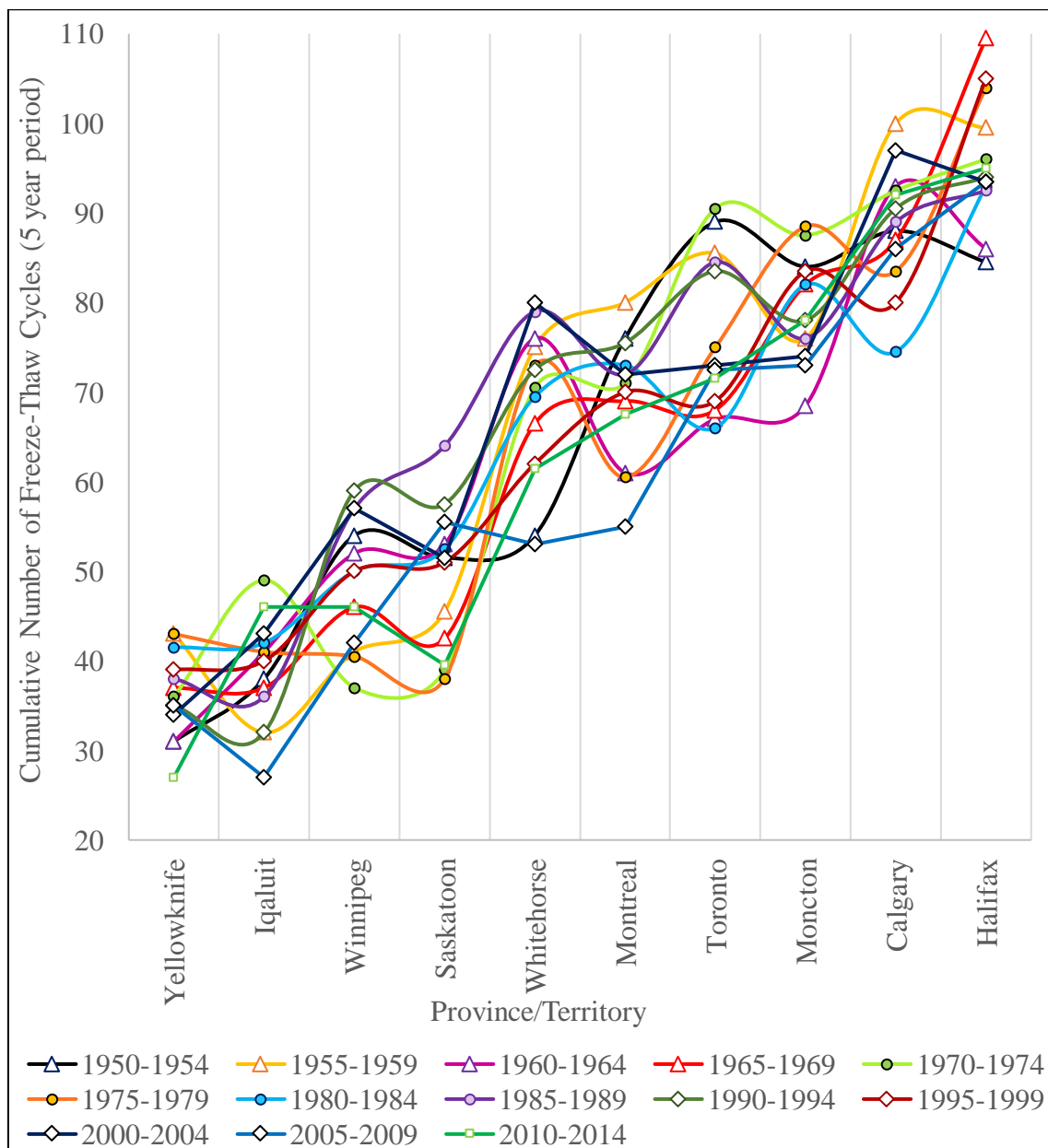


Figure 4.11 Five years Cumulative Annual Freeze-Thaw Cycles at the Selected Airports

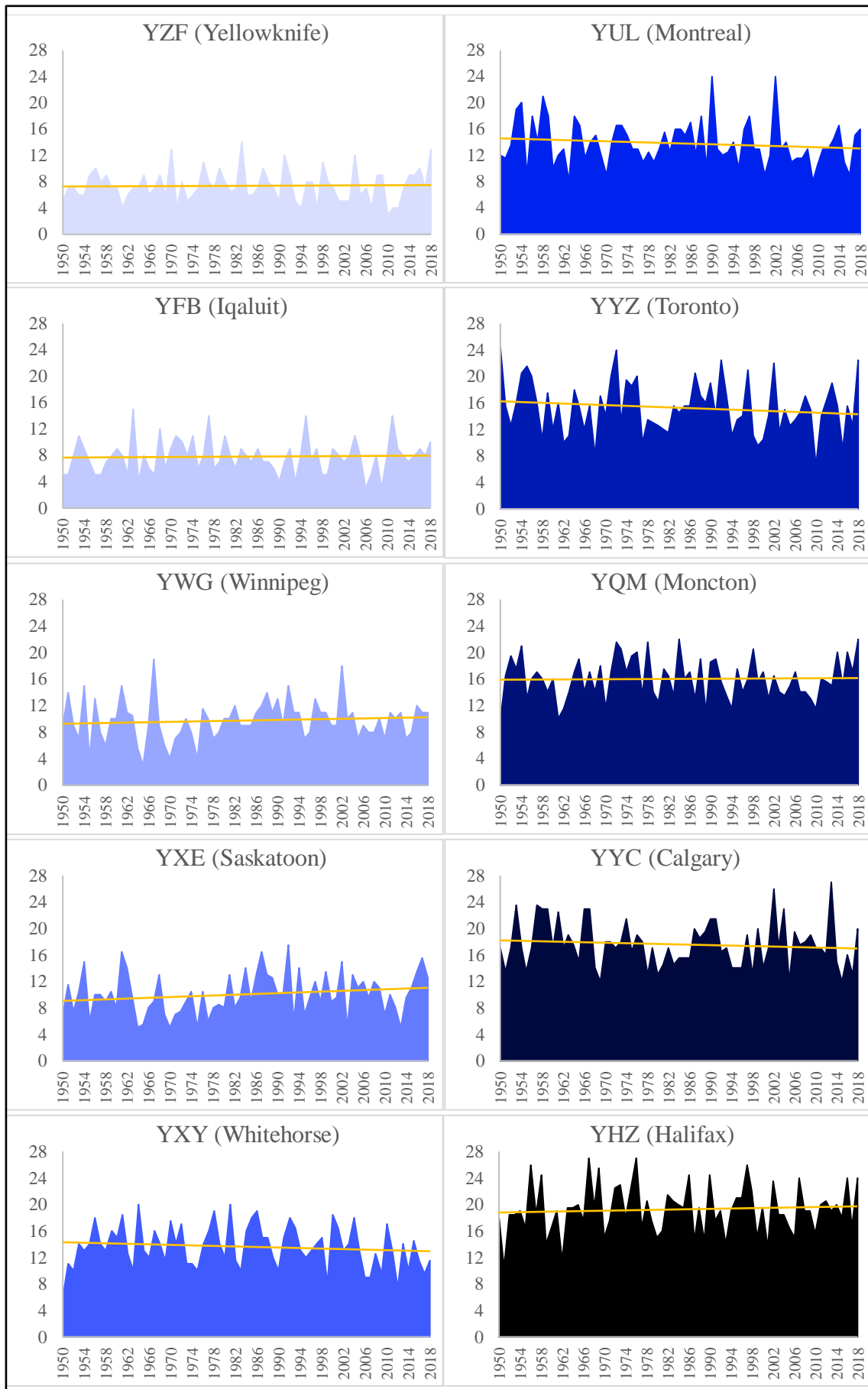


Figure 4.12 Annual Freeze-Thaw Cycles at the Selected Airports since 1950 to 2018

Table 4.2 Summary of the Annual Number of Freeze-Thaw Cycles at the Selected Airports since 1950 to 2018

Year	YZF	YFB	YWG	YXE	YXY	YUL	YYZ	YQM	YYC	YHZ
1950	5	5	9	7	6	12	25	10	17	18
1951	7	5	14	12	11	12	16	17	14	11
1952	7	8	9	8	10	14	13	20	17	19
1953	6	11	7	11	14	19	16	18	24	19
1954	6	9	15	15	13	20	21	21	17	19
1955	9	7	4	6	14	9	22	13	14	17
1956	10	5	13	10	18	18	20	16	17	26
1957	8	5	8	10	14	14	16	17	24	19
1958	9	7	6	9	13	21	11	16	23	25
1959	7	8	10	11	16	18	18	14	23	14
1960	7	9	10	8	15	10	12	16	17	17
1961	4	8	15	17	19	12	16	10	23	19
1962	6	5	11	14	13	13	10	12	17	12
1963	7	15	11	10	10	8	11	14	19	20
1964	7	4	6	5	20	18	18	17	18	20
1965	9	8	3	6	13	17	16	19	15	20
1966	6	6	9	8	12	12	12	14	23	18
1967	7	5	19	9	16	14	16	17	23	27
1968	9	12	9	13	14	15	8	14	14	20
1969	6	6	6	7	12	12	17	18	12	26
1970	13	9	4	5	18	9	14	12	18	15
1971	4	11	7	7	14	14	20	17	18	18
1972	8	10	8	8	17	17	24	22	17	23
1973	5	8	10	9	11	17	13	21	18	23
1974	6	11	8	11	11	15	20	17	22	18
1975	7	6	4	5	10	13	19	20	17	23
1976	11	8	12	11	14	13	20	20	19	27
1977	8	14	10	6	16	11	10	14	18	17
1978	7	6	7	8	19	13	14	22	13	21
1979	10	7	8	9	14	11	13	14	17	18
1980	8	11	10	8	12	13	13	13	13	15
1981	7	8	10	13	20	16	12	18	15	16
1982	7	6	12	8	12	13	12	17	17	22
1983	14	9	9	10	10	16	16	14	15	21
1984	6	8	9	14	16	16	15	22	16	20
1985	6	7	9	9	18	15	16	16	16	20
1986	7	9	11	13	19	17	16	17	16	25
1987	10	7	12	17	15	12	21	13	20	15
1988	8	7	14	13	15	18	17	19	19	20
1989	7	6	11	13	12	10	16	11	20	15
1990	5	4	13	10	10	24	19	19	22	25
1991	12	7	9	10	15	13	14	19	22	18
1992	9	9	15	18	18	12	23	16	17	19
1993	5	4	11	6	17	13	17	14	17	14
1994	4	8	11	14	13	14	11	12	14	19
1995	8	14	7	7	12	10	14	18	14	21
1996	8	7	8	10	13	16	14	14	14	21
1997	4	9	13	12	14	18	21	16	19	26
1998	11	5	11	9	15	13	11	21	13	22
1999	8	5	11	14	8	13	10	16	20	15
2000	7	9	9	9	19	9	11	17	14	20
2001	5	8	9	10	17	12	14	13	17	14
2002	5	7	18	15	13	24	22	17	26	24
2003	5	8	10	5	14	13	12	14	17	19
2004	12	11	11	13	18	14	15	14	23	19
2005	6	8	7	11	13	11	13	15	12	17
2006	7	3	9	12	9	12	14	17	20	15
2007	4	5	8	10	9	12	15	14	18	24
2008	9	8	8	12	13	13	17	14	18	19
2009	9	3	10	11	10	8	15	13	19	19
2010	3	8	7	7	17	11	7	12	17	16
2011	4	14	11	10	13	13	14	16	17	20
2012	4	9	10	8	8	13	17	16	16	21
2013	7	8	11	5	14	15	19	15	27	19
2014	9	7	7	10	10	17	16	20	15	20
2015	9	8	8	11	15	11	9	15	12	18
2016	10	9	12	14	12	9	16	20	16	24
2017	7	8	11	16	10	15	13	17	13	17
2018	13	10	11	13	12	16	23	22	20	24

4.3 Permafrost Analysis

The following analysis was developed with the purpose of correlating the before-presented changes in temperature with some of the distresses that airports in the north of Canada are experiencing. Apart from the cracks, as explained in [section 2.4.6](#) of the literature review, settlement is a significant distress that is mainly caused by a significant reduction of the bearing capacity of the subgrade due to a variation of the porous pressure of the subsequent layers of the pavement, meaning a reduction of the ground water table or the thaw of permafrost soils. Image 4.2 shows an example of a permafrost layer located near Yellowknife, NWT.

Figure 4.13 shows more details about the different type of permafrost compositions varying from glaziers, 100% permafrost, to isolated patches, 0-10%. Iqaluit airport is located in a continuous permafrost zone, and the temperature analysis presented before showed that the changes in temperature at this airport are minimum. Hence, Iqaluit may not be considered susceptible to suffered distresses due to permafrost fluctuations. However, Yellowknife and Whitehorse international airports are located in discontinuous and sporadic permafrost areas, meaning that the airside pavement infrastructure is subjected to meaningful expansions and contractions caused by the discontinuity of the permafrost. Lastly but not less important, Calgary and Vancouver airports are close to isolated patches of permafrost areas, but these isolated patches are situated at the mountain areas, not at the plains where the airports are.

An interesting example, perhaps out of the selected scope, is Cambridge Bay Airport where the centre for pavement and transportation technology at the University of Waterloo develop field work during the 2019. The observations concluded that the gravel runway is not experiencing settlement but a considerable amount of low temperature cracking. Figure 4.13 stand out the location of Cambridge Bay Airport with a blue rectangle. As it can be seen, it is situated in the upper north of Canada, but more importantly, on top of a continuous permafrost structure.



Image 4.2 Ice rich ground section near Yellowknife, NWT (Morse, 2017)

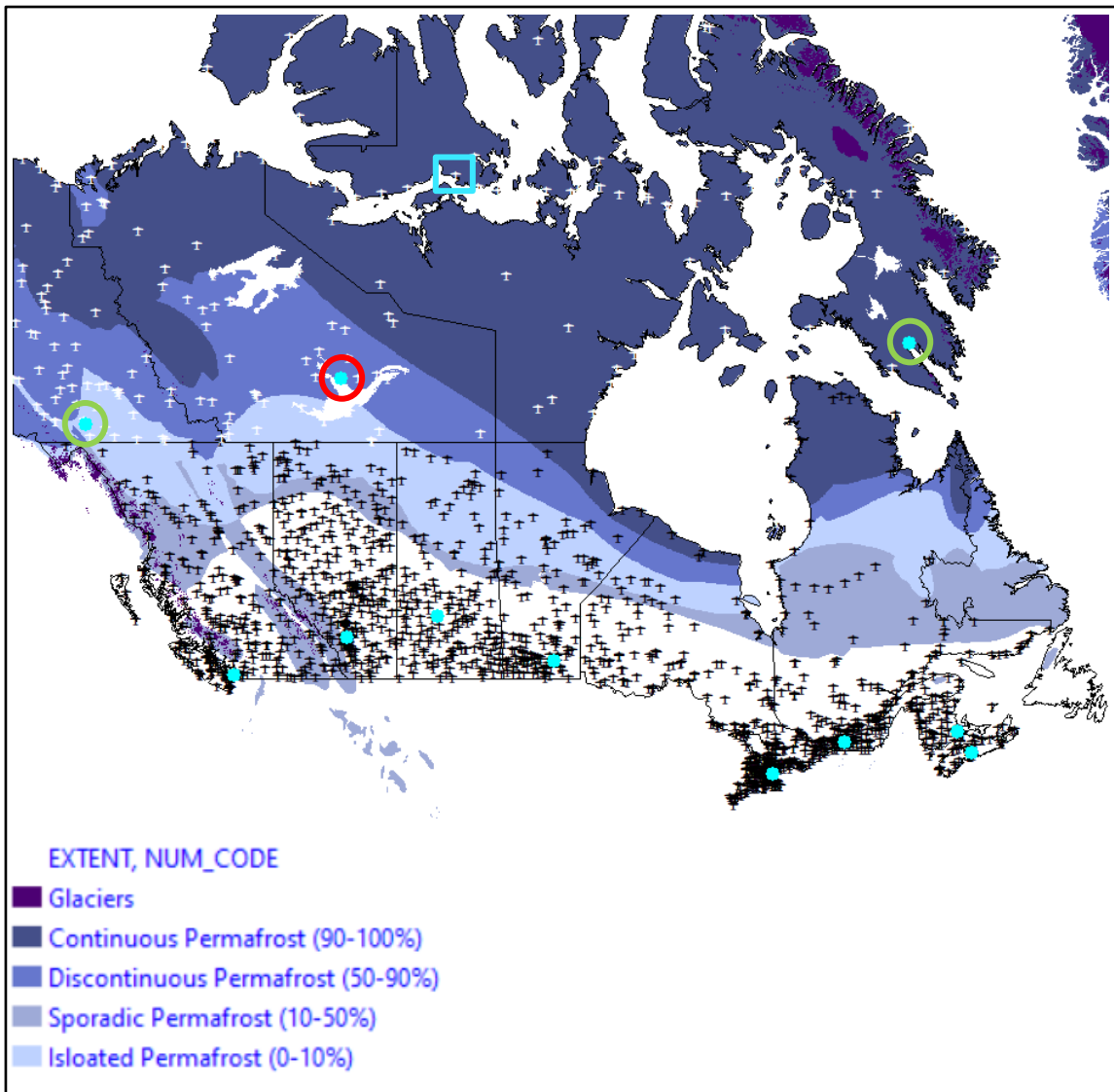


Figure 4.13 Permafrost Composition and Inequality at the Selected Airports (Bone, 2019)

4.4 Precipitation Analysis and Results

The Cambridge Dictionary defines precipitation as “the water that falls from the clouds towards the ground, especially as rain or snow”. (Cambridge Dictionary, 2019) Therefore, it is important to separate the rain, the snow, and the total precipitation analysing each one separately for the selected airports. Figure 4.14, 4.15, and 4.16 present the cumulative amount of precipitation, rain, and snow per decade, respectively. Hence, each point represents how much precipitation, rain, or snow, fell during the entire decade, being the first period from Jan-1950 to Dec-1959.

Many conclusions can be derived from Figure 4.14 being perhaps the main ones that Vancouver, Montreal, and Toronto airports receive a significant amount of precipitation annually, making of these three airports the most susceptible ones to suffer moisture damage. Contrarily, and fairly unexpected, Halifax airport shows to be the one with the smallest amount of precipitation making this airport meaningfully less prone to stripping failure. Figure 4.15 shows a large difference between Vancouver’s airport rainfalls compared to the other ones. It is important to recall as well that the rate of growth for the Vancouver and Montreal’s airport is significantly elevated which means that the probability for these airports to be affected by floods also increases.

Figure 4.16 provides a superior idea of the precipitation behaviour during winter where Moncton airport stands out with a meaningful amount of snow. This directly affects the operation’s difficulty and cost for the airport as it has to be more constantly removing snow form the airside infrastructure. Montreal airport can also be highlighted with a substantial reduction of snow with an annual rate of approximately 0.7cm less. Lastly, it is important to mention that Vancouver airport, being the one with the highest precipitation and rainfall, is the second one with the lowest amount of snow per year because of its high average minimum temperature as presented in [section 4.2.1](#).

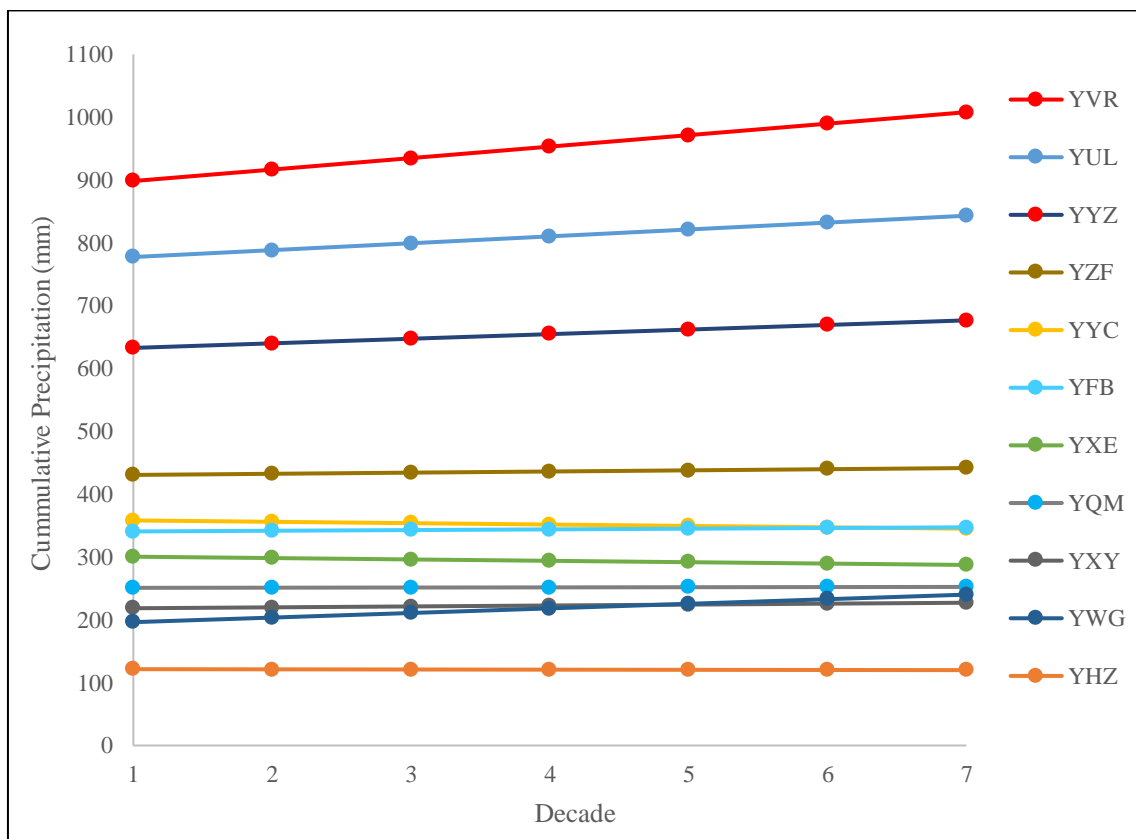


Figure 4.14 Decennial Precipitation at the Selected Airports since 1950

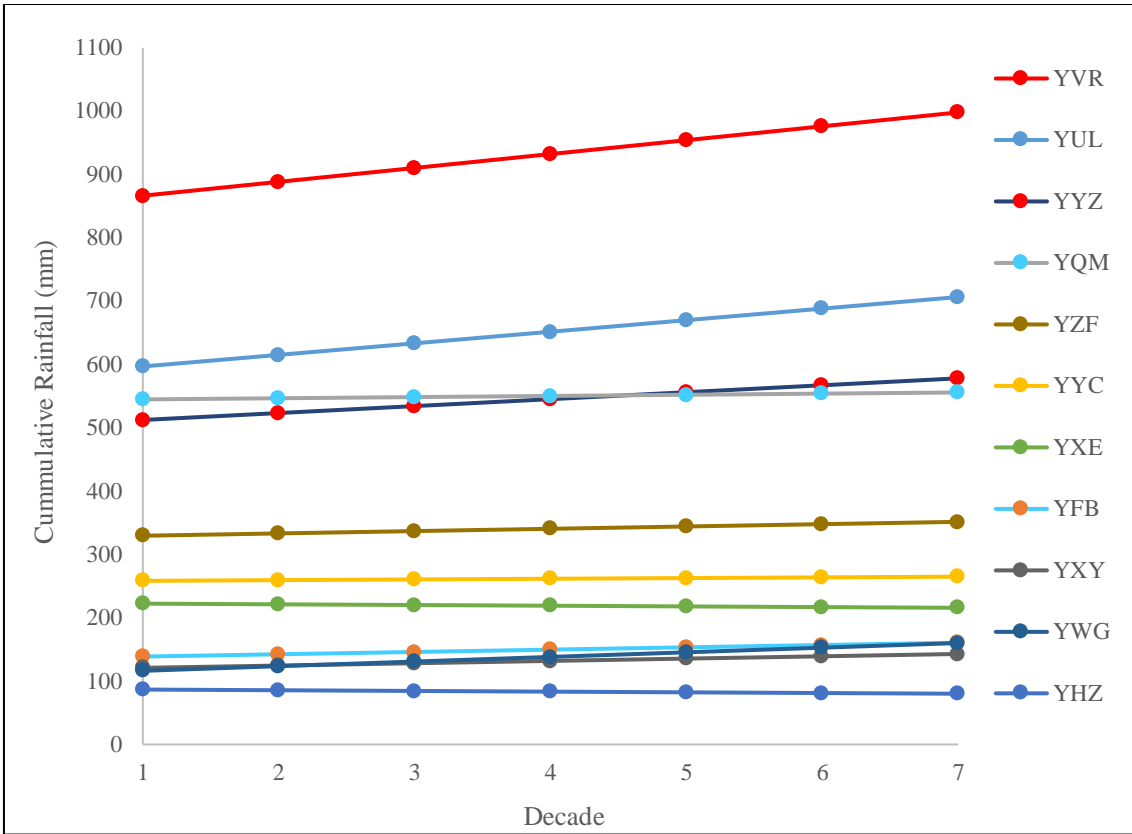


Figure 4.15 Decennial Rainfall at the Selected Airports since 1950

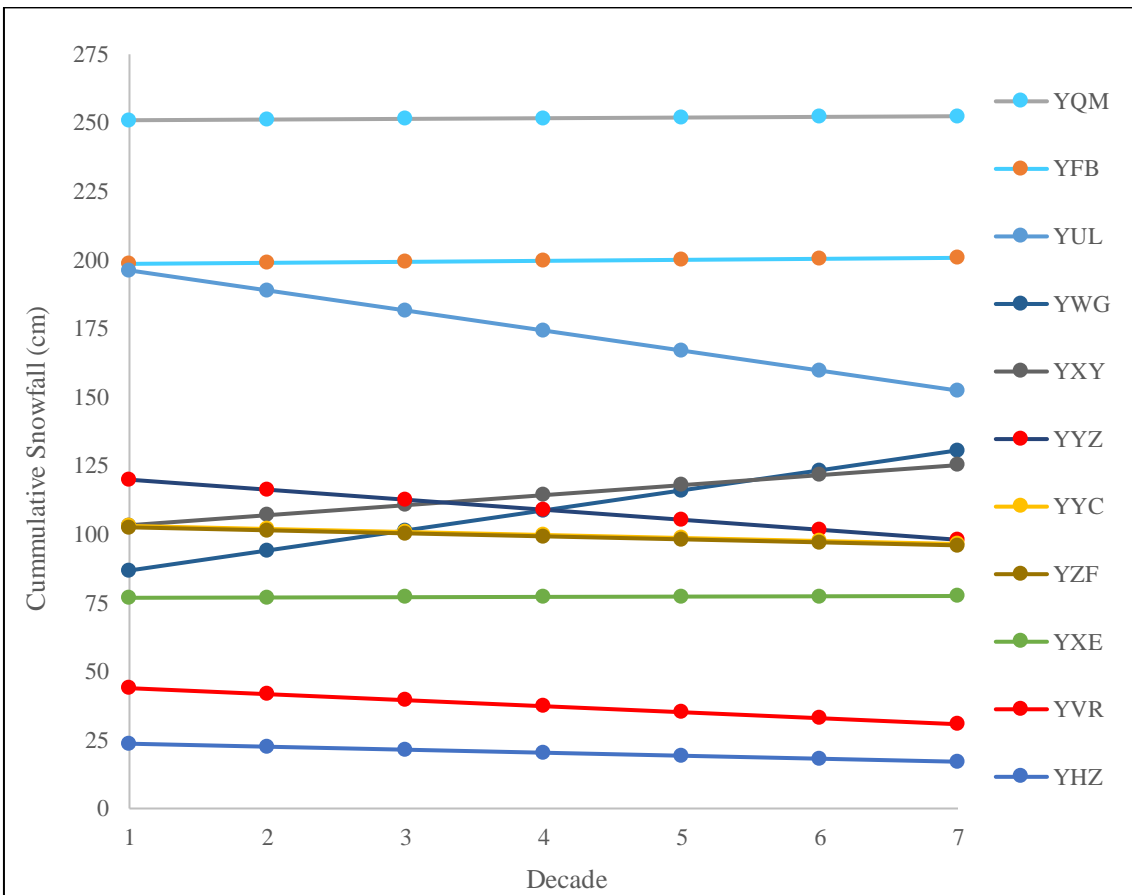


Figure 4.16 Decennial Snowfall at the Selected Airports since 1950

Table 4.3 summarizes Figures 4.14, 4.15, and 4.16 supplementing the discussions mentioned at the beginning of the precipitation analysis. Additionally, it presents the difference of precipitation, rainfall, and snowfall between the decade of 1950-1959 and the current decade (2010-2019).

Table 4.3 Cumulative Precipitation, Rainfall, and Snowfall Trendlines from 1950-2019

AVERAGE <u>PRECIPITATION</u> CUMMULATIVE TRENDLINE												
Start Date	End Date	YYC	YHZ	YFB	YQM	YUL	YXE	YYZ	YVR	YXY	YZF	YWG
1/1/1950	31/12/1959	358	122	341	251	777	301	633	898	218	431	196
1/1/1960	31/12/1969	356	121	342	251	788	298	640	917	220	432	204
1/1/1970	31/12/1979	354	121	343	251	799	296	647	935	221	434	211
1/1/1980	31/12/1989	352	121	344	252	810	294	655	953	223	436	218
1/1/1990	31/12/1999	349	120	345	252	821	292	662	971	224	438	226
1/1/2000	31/12/2009	347	120	346	252	832	290	669	990	226	440	233
1/1/2010	31/12/2019	345	120	347	252	843	287	677	1008	227	442	240
Diff since 1950		-13	-2	7	1	66	-13	44	0	9	11	44

AVERAGE <u>RAINFALL</u> CUMMULATIVE TRENDLINE												
Start Date	End Date	YYC	YHZ	YFB	YQM	YUL	YXE	YYZ	YVR	YXY	YZF	YWG
1/1/1950	31/12/1959	258	87	139	545	597	222	512	866	121	330	116
1/1/1960	31/12/1969	259	86	142	547	615	221	523	888	125	333	124
1/1/1970	31/12/1979	261	84	146	548	633	220	534	910	128	337	131
1/1/1980	31/12/1989	262	83	150	550	652	219	545	932	132	341	138
1/1/1990	31/12/1999	263	82	153	552	670	218	556	954	136	344	146
1/1/2000	31/12/2009	264	81	157	554	688	217	567	976	139	348	153
1/1/2010	31/12/2019	265	80	161	556	706	216	578	998	143	351	160
Diff since 1950		7	-7	22	11	110	-7	66	131	22	22	44

AVERAGE <u>SNOWFALL</u> CUMMULATIVE TRENDLINE												
Start Date	End Date	YYC	YHZ	YFB	YQM	YUL	YXE	YYZ	YVR	YXY	YZF	YWG
1/1/1950	31/12/1959	103	24	199	251	196	77	120	44	103	103	87
1/1/1960	31/12/1969	102	23	199	251	189	77	116	42	107	101	94
1/1/1970	31/12/1979	101	21	199	251	182	77	113	39	111	100	101
1/1/1980	31/12/1989	100	20	200	252	174	77	109	37	114	99	109
1/1/1990	31/12/1999	99	19	200	252	167	77	105	35	118	98	116
1/1/2000	31/12/2009	98	18	200	252	160	77	102	33	122	97	123
1/1/2010	31/12/2019	96	17	201	252	152	77	98	31	125	96	131
Diff since 1950		-7	-7	2	1	-44	1	-22	-13	22	-7	44

4.4 Chapter Summary

This chapter presented the results of numerous environmental analysis for Canada or specific Canadian airports contemplating wind, temperature, freeze-thaw cycles, permafrost, and precipitation.

One of the main considerations during the planning or design stages of an airport runway is the wind behaviour. For this reason, a historic wind rose diagram is developed for which the direction/s that will provide the highest efficiency to the airport are designed. Three airports from the province of Ontario were selected (YYZ, YOW, and YTR) to evaluate the historic usage that the airports were providing to their runways considering the crosswind threshold of 15 Knots (27.6 km/hr). The main results presented that Ottawa airport have a consistent usage of approximately 98% as the direction of its runways was significantly well design, with 110° of difference which, for the case of Ottawa airport, it mitigates the crosswind satisfactorily. Toronto airport, significantly increased its usage after the construction of its 4th runway (06L-24R) as it represented the third distinct direction, rising the usage from approximately 96% to 99%.

The selected Canadian airports for the other environmental analysis were located in Whitehorse (YXY), Yellowknife (YZF), Iqaluit (YFB), Vancouver (YVR), Calgary (YYC), Saskatoon (YXE), Winnipeg (YWG), Toronto (YYZ), Montreal (YUL), Moncton (YQM), and Halifax (YHZ). The main environmental results indicated that YYZ is the one experiencing the highest temperatures, differing from YFB that recorded the lowest ones. In another perspective, YVR presented to be the airport with the lowest thermal loads as its temperature range is meaningfully low compared to the other airports evaluated. Additionally, YHZ and YZF's highest temperature has increased 2°C in the past 70 years; in case of the lowest temperatures, YYZ has risen 4.4°C more in the past 70 years as well. All these changes induce variations to current performances as well as future design specifications and requirements. Considering the developed freeze-thaw cycle analysis, the results did not presented a significant increment or reduction of them, just noteworthy fluctuations among the years; however, it was noticed that depending on the location, the amount of annual freeze-thaw cycles varied significantly starting from YZF airport with a annual average of 9 cycles per year to YHZ airport which registered an average of 22 cycles per year, and growing.

Furthermore, the permafrost analysis consisted of placing the selected airports in the permafrost distribution map which defines the areas that correspond to glaziers or continuous permafrost as well as those that denote discontinues, sporadic, and isolated patches permafrost. Essentially, Iqaluit, Yellowknife, and Whitehorse airports, which are those from the selected airports located in the Canadian territories, are build on top of permafrost, making them susceptible to suffer settlement and fatigue cracking. Except for Iqaluit airport; because it is located on top of a continues-permafrost, its volume is not likely to vary in the approximate future; hence, not vulnerable to the before-mentioned pavement distresses.

Concerning the precipitation analysis, it is indeed increasing in Canada, specially focusing in the rainfall. It was concluded that airports located in the southwest of British Columbia, especially YVR, are experiencing a substantial increment of the rainfall making them more susceptible to have floods and to suffer moisture damage such as stripping or pumping. YUL and YYZ also presented a considerable increment of precipitation. Regarding the snowfall, it was interesting to see how much it is varying depending on the location. The most remarkable cases were for Montreal and Toronto airport having a paramount reduction of the snowfall compared to Winnipeg which is experiencing a massive increment of snowfall. The mentioned airports may consider these outcomes for future mitigations, in the case of Winnipeg, and adaptation strategies, in the case of Montreal.

CHAPTER 5

Laboratory Testing Analysis and Discussions

This chapter aims to correlate the relationship between the outcomes presented in chapter 4 with some distresses that flexible Canadian airside infrastructures are facing due to climate change. Hence, a quantification of the impacts of climate change. Three laboratory tests were performed, as described in [section 2.5](#), the Hamburg wheel tracking test (HWTT), the tensile strength ratio (TSR), and the ideal cracking test (IDEAL CT). The first one to evaluate rutting susceptibility, the second to measure and/or quantify the lost of tensile strength on the pavement surface due to freeze-thaw cycles. Lastly, a crack propagation evaluation was performed using the results from the TSR test.

Table 5.1 presents the matrix for the laboratory tests considering the number of samples, the test's temperatures, the level of saturation, and the amount of freeze-thaw cycles to be induced to the samples. The tensile strength ratio test was modified both for the compaction speed and the time period for the freeze-thaw cycles. The TSR modified refers to an equal tensile strength ratio test but with a compaction speed of 50 mm/sec instead of 50mm/min. The purpose behind this modification was to exemplify the faster speed of loading that runway pavements are subjected to during the departure and/or landing of aircrafts. The other modification, TSR Modified 2, consisted of inducing shorter freeze-thaw cycles to the samples to evaluate the susceptibility of flexible pavements, not only against freeze-thaw cycles itself, but against the time period between one cycle and the other. For this modification, instead of inducing 16 hours of freezing at 18°C and 24 hours of thawing at 60°C, the periods were reduced by half. Hence, 8 hours of freezing and 12 hours of thawing.

Table 5.1 Laboratory Tests Matrix

Test	No. of samples	Test Temperature (°C)	Saturation (%)	Amount of Freeze-Thaw Cycles
HWTT	8	50	-	0
	4	60	-	0
	4	65	-	0
	4	70	-	0
	4	50	70-80	1
	4	50	70-80	2
	4	50	70-80	3
TSR	6	25	-	0
	3	25	70-80	1
	3	25	70-80	2
	3	25	70-80	3
TSR (Speed of Loading Modification)	3	25	70-80	1
	3	25	70-80	2
	3	25	70-80	3
TSR (Frequency Modification)	3	25	70-80	(1/2)
	3	25	70-80	2 (1/2)
	3	25	70-80	3 (1/2)
	3	25	70-80	4 (1/2)

5.1 Extraction and Gradation

The asphalt tested in this research was plant mix-laboratory tested (PMLT). It was mixed in a contractor's plant but tested in the CPATT laboratory. The obtained samples were tested against the mix design for which extraction and gradation tests were performed. The extraction test consists of separating the asphalt cement from the aggregate through using chemicals that induces this reaction as well as equipment that facilitate the process. Image 5.1 illustrates the process to develop the extraction, aggregate gradation, and asphalt cement recovery. (AASHTO T 164, 2014) (AASHTO T 27, 2014)

- A. Primary open centrifuge machine used to separate the asphalt cement from the aggregate. At this step the solvent is added to the loose asphalt mix for specific times of 5-10mins. After waiting the appropriate time for each cycle, the equipment gyrates removing the solvent and asphalt cement from the aggregates.
- B. Residual aggregate after the extraction.
- C. Secondary open centrifuge equipment used to remove the fine aggregates inside the solvent and the asphalt cement. It gyrates significantly faster than the primary one allocating the fines and colloids' particles inside the bullet and the solvent with asphalt cement in a flask.
- D. Bullet where the fines are allocated once separated from the solvent and asphalt cement. The bullet is meant to be weighted before and after the test to obtain the weight of fine particles.
- E. Different sieves used to obtain the gradation of the aggregates varying from 16mm to 0.075mm. The aggregate presented in image B, after being washed, dried, and weighted, is poured inside the sieve column which will separate the particles by size. This will create an envelope that should meet the design specifications.
- F. This last sieve represents the pan that will contain the particles that passes the sieve No. 200 (0.075mm). Hence, the other fine particles that were not mixed with the solvent and asphalt cement in the first step.
- G. After step "D", a rotary evaporator recovery test is conducted to separate the solvent from the asphalt cement. As the evaporation temperature of the solvent is different from that of the asphalt cement, the mix is placed in an oil bath to evaporate the solvent.
- H. This solvent, in gas state, reaches this point on which is cooled down through internal water pipes to change the state of the solvent back to liquid.
- I. Ultimately, the solvent is allocated in the flask until is mostly separated from the asphalt cement. At this point, the aggregates, the asphalt cement, and the solvent are being already separated.

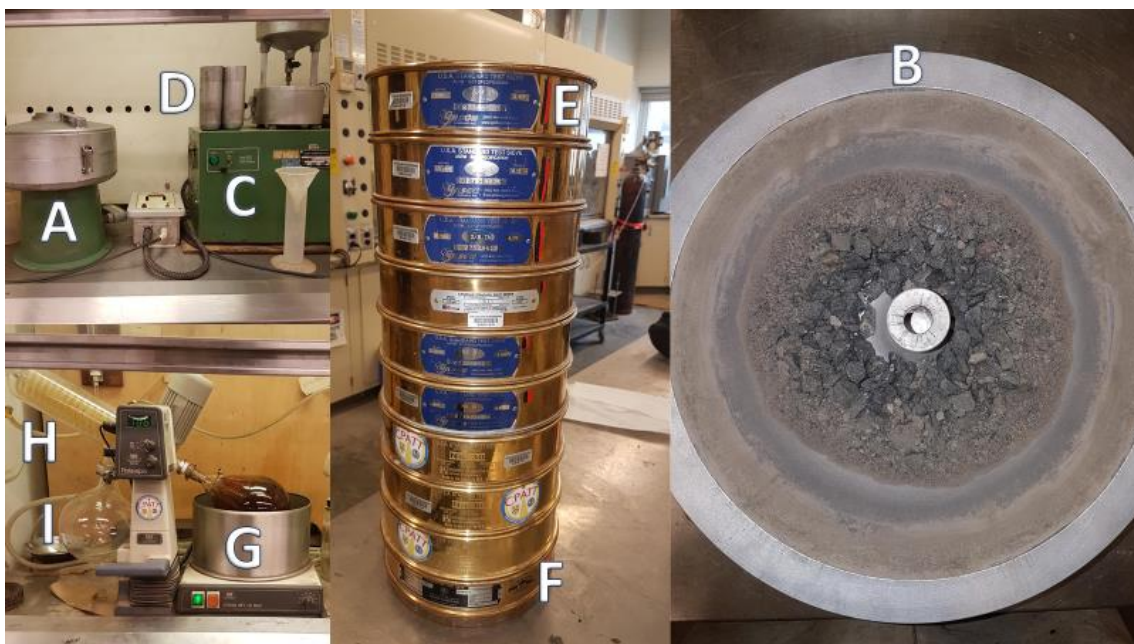


Image 5.1 Extraction and gradation tests process

As the main purpose of the test was to evaluate the asphalt cement content and the gradation of the mix, Methylene Chloride was used to separate the asphalt cement from the aggregate. Many pros and cons exist from using this solvent. The main advantages are that it has a similar extractability index compared to other solvents, for example the Trichloroethylene, but for a much lower price. The main disadvantage is that the asphalt cement hardens and, therefore, no performance test should be made to it after it is extracted and separated from the solvent. If the Trichloroethylene is used, then the asphalt cement, once separated from this solvent through a recovery test, can be further tested. (Cipione, Davrson, Burr, Glover, & Bullin, 1991)

The obtained results were 5.1% of asphalt cement for both trials, which is significantly accurate as the expected amount was 5.2%. Additionally, during the test, a small percentage of asphalt can be loose due to the chemical reaction with the methylene chloride and also the test itself which requires moving the sample from one equipment to another, among other reasons. It can be concluded that the obtained mix's asphalt cement content correlates with the mix design.

For the gradation test, once the aggregates are separated from the asphalt cement, the test requires these to be cleaned using water and with the help of the sieve No. 200 to make sure that the test is to be performed for the aggregates greater than 0.075mm. Considering what was retained in the filter and the bullet during the extraction test as well as the weights before and after cleaning the aggregates, the percentage of colloids can be obtained. The obtained envelopes were very close to the design one, but two percent less fines and aggregates passing the 4.75mm sieve were lost. Nonetheless, the material meets the gradation requirements stated by Toronto Pearson International Airport. (Uzarowski & Tighe, 2016) Figure 5.1 present the results of the gradation test and the thresholds requirements.

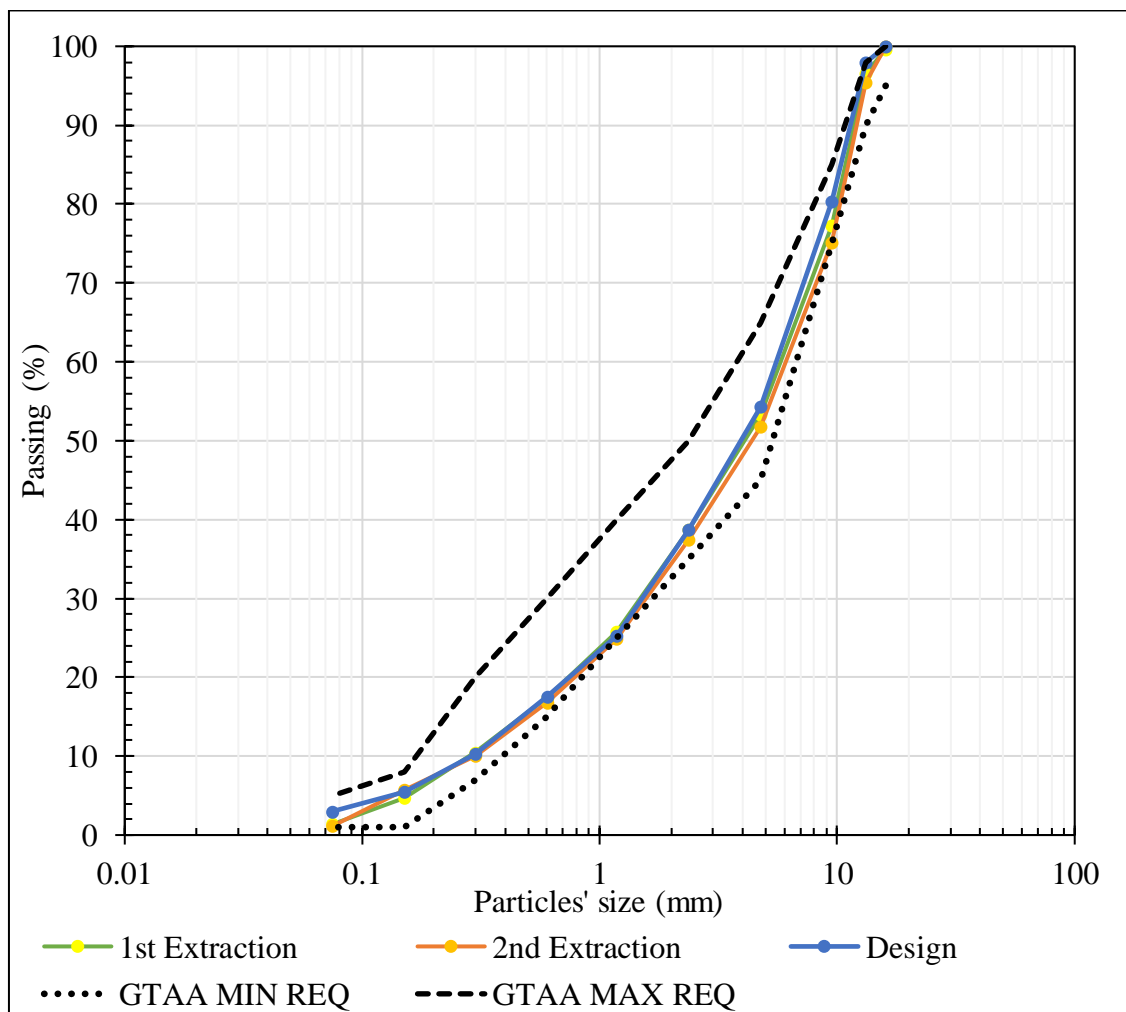


Figure 5.1 Gradation Test's Results

5.2 Hamburg Wheel Tracking Test (AASHTO T 324) modifications, Analysis, and Discussions

[Section 2.5.1](#) explained that this test seeks to evaluate the susceptibility of the mix to permanent deformation under traffic and conditioning loading. It is mainly used to compare different asphalt mixes or to assess if the asphalt mix meets the specifications; nonetheless, the purpose of using this test was to evaluate the same mix under distinct conditions. The threshold of 5 millimeters was considered based on several Canadian airport authorities' requirements/specifications. The control mix was the one with no environmental conditioning and being tested at 50°C. Hence, two main variations were assessed:

1. The conditioning of the samples as more than one freeze-thaw cycle was induced to correlate with the fluctuation of these cycles as well as the relationship with them and the permanent deformation occurring mostly in southern Canada.
2. The temperature of the test, to exemplify and correlate with the rise of temperature that climate change is inducing as it was presented in [section 4.2.1](#).

This analysis helps to objectively understand how climate change is impacting the propagation or occurrence of rutting and possibly shoving at the Canadian airfield pavement infrastructure.

5.2.1 Rutting and Freeze-Thaw Cycles Evaluation/Correlation

An explanation of what happens to the pavement surface during a freeze-thaw cycle is that there is a fluctuation of compression and tension inside the pavement structure which indeed induces changes in the properties of the materials. What this part of the test wants to measure is the rate of change of rutting resistance induced by the different quantity of years that the pavement surface is exposed to winter's hardening and summer's softening of the asphalt mix. By following the conditioning standards of the AASHTO T 283, the samples were tested until up to 3 freeze-thaw cycles as, after this quantity, the structural integrity of the samples was compromised during the conditioning phase. Meaning, other distresses were starting to occur, such as stripping, small cracks, and weathering. Figure 5.2 presents the rutting propagating on 4 different samples with distinct conditions by inducing constant number of wheel passes.

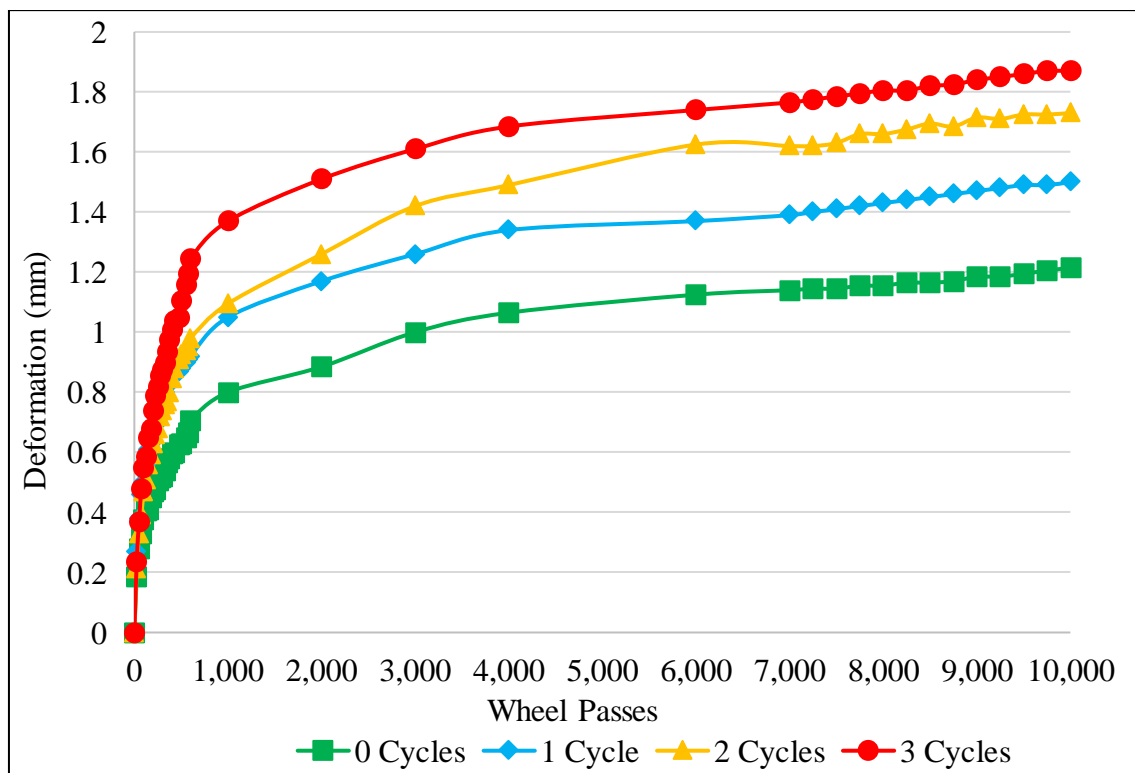


Figure 5.2 Rutting Propagation versus Freeze-Thaw Cycles

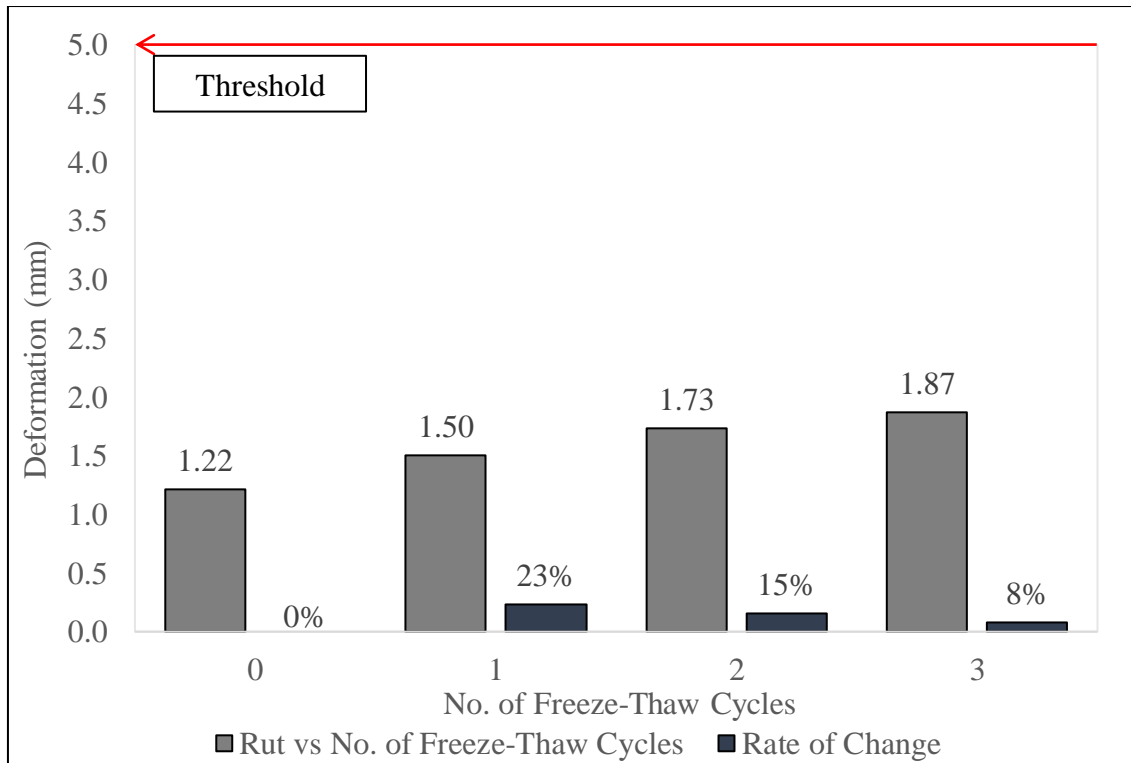


Figure 5.3 Rutting at 10,000-Wheel Passes versus Freeze-Thaw Cycles and Rate of Change

Figure 5.2 present the results of rutting propagation versus the conditioning of the samples under a different quantity of freeze-thaw cycles. As it can be seen, when the number of freeze-thaw cycles increases, the rutting steadily increases; therefore, a non proportional relationship on which the more freeze-thaw cycles the pavement surface is subjected, the less impact these will induce to the rutting resistance. The same can be concluded from Figure 5.3 as it shows that the first years of exposure to freeze-thaw cycles to the pavement surface will be the ones causing the highest damage noting that the rate of change reduces while the number of freeze-thaw cycles increases.

5.2.2 Rutting and Temperature Rise Evaluation/Correlation

Being the rise of temperature one of the main consequences of climate change, not just in Canada, but worldwide, this project decided to assess the rutting susceptibility of the flexible pavement's surface by modifying the temperature on which the HWTT is required to be done. Instead of running the test on non conditioned samples at 50 degrees Celsius, the test was performed as well at approximately 60, 65 and 70 degrees Celsius. This last number being selected for two main reason. First, because the highest ambient temperature that Canada has recorded was 45°C in 1937, Saskatchewan (Ozborn, 2019), which being converted into pavement surface temperature, it approximates the 70°C, and second, due to the logistic of the test, as it is conducted under water and it last approximately 7 hours, if the temperature increases to more that 80°C the water could start evaporating too fast which may induce anomalies in the results and/or complications on the testing machine.

Figure 5.4 presents the rutting propagation as the amount of wheel passes increases. Similar to Figure 5.2, the propagation under temperature variation compared to freeze-thaw cycles variation had a resembling behaviour. Nonetheless, comparing the final rutting after 10,000-wheel passes presented in Figures 5.3 and 5.5 it can be seen how as the temperature rises the rutting susceptibility increases faster. The opposite happens with the number of freeze-thaw cycles, the higher the amount, the less effect these have over the rutting susceptibility.

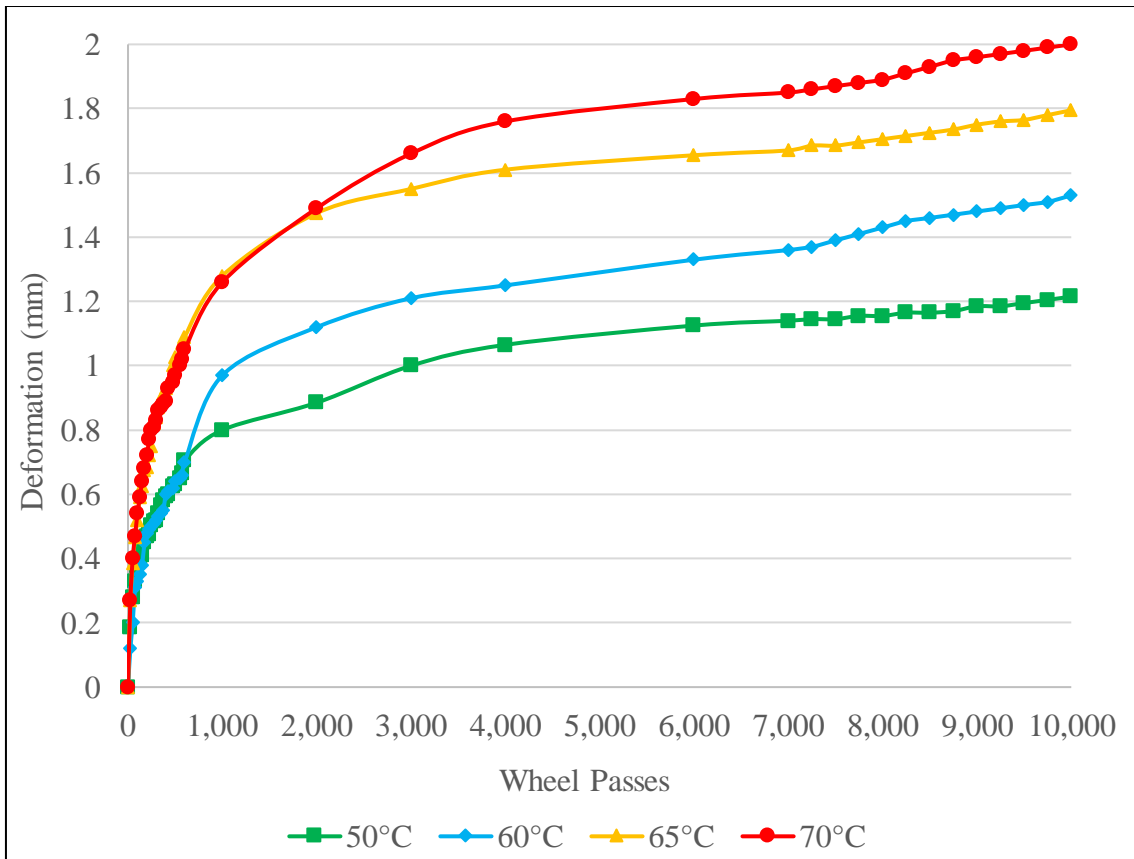


Figure 5.4 Rutting Propagation versus Temperature

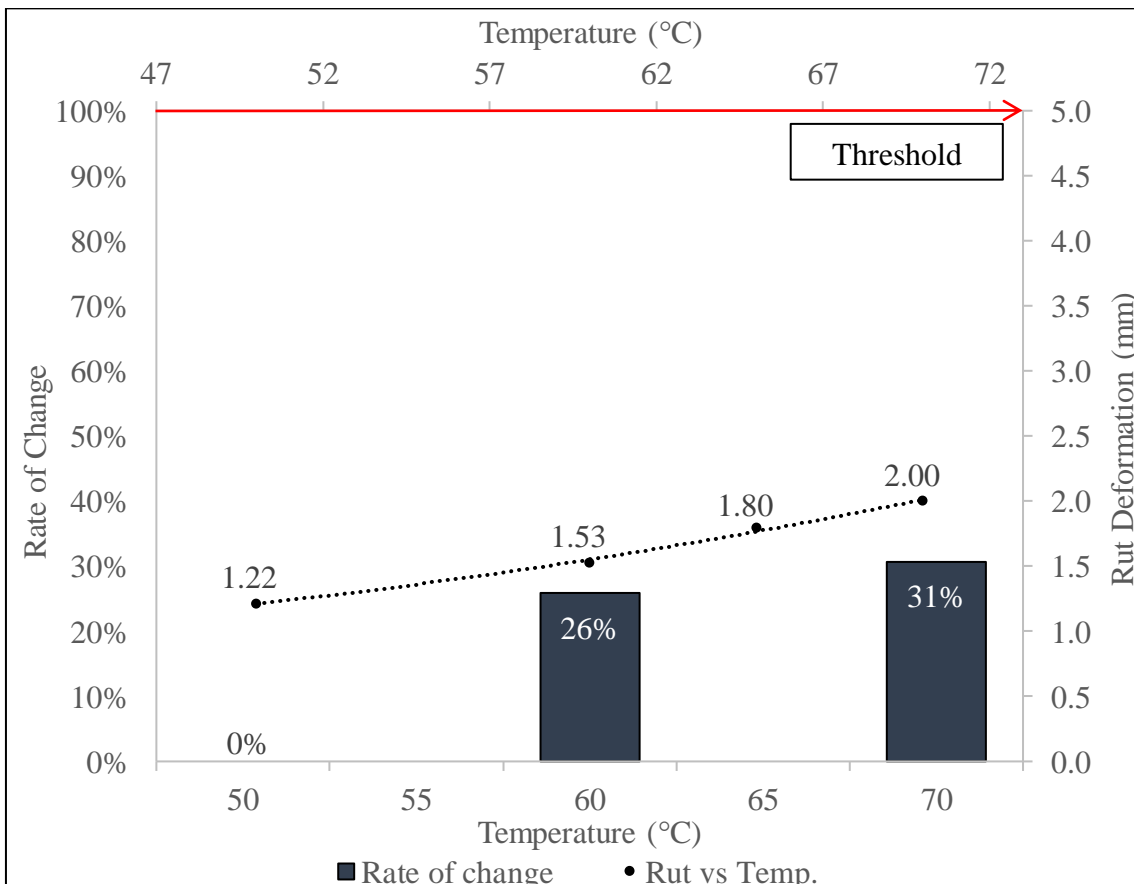


Figure 5.5 Rutting after 10,000 passes versus Temperature and Rate of Change

The following images provides a superior insight of the difference between the samples being tested against freeze-thaw cycles, image 5.2, compared to the ones being tested against the rise of temperature, image 5.3. From image 5.2, it can be noticed that the samples tested after two and three freeze-thaw cycles did not just experience rutting but also were starting to shove and weather. Differing from the freeze-thaw cycle's samples, the ones presented in image 5.3 experienced a more linear wheel track deformation.

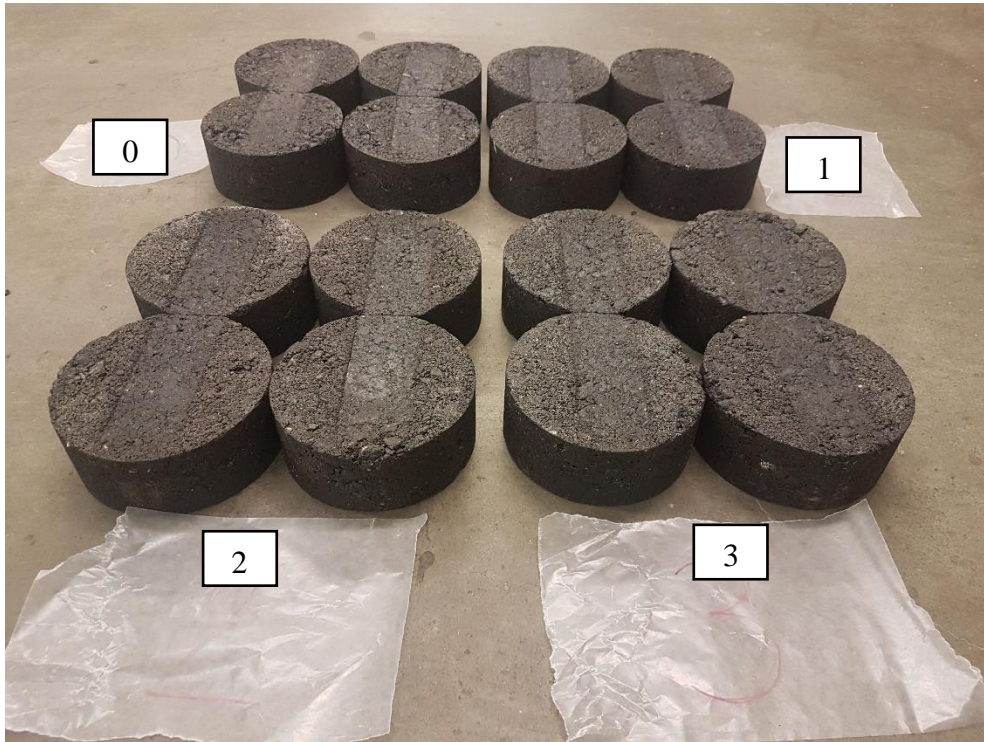


Image 5.2 Hamburg Wheel Tracking Test Samples Tested After Freeze-Thaw Cycles

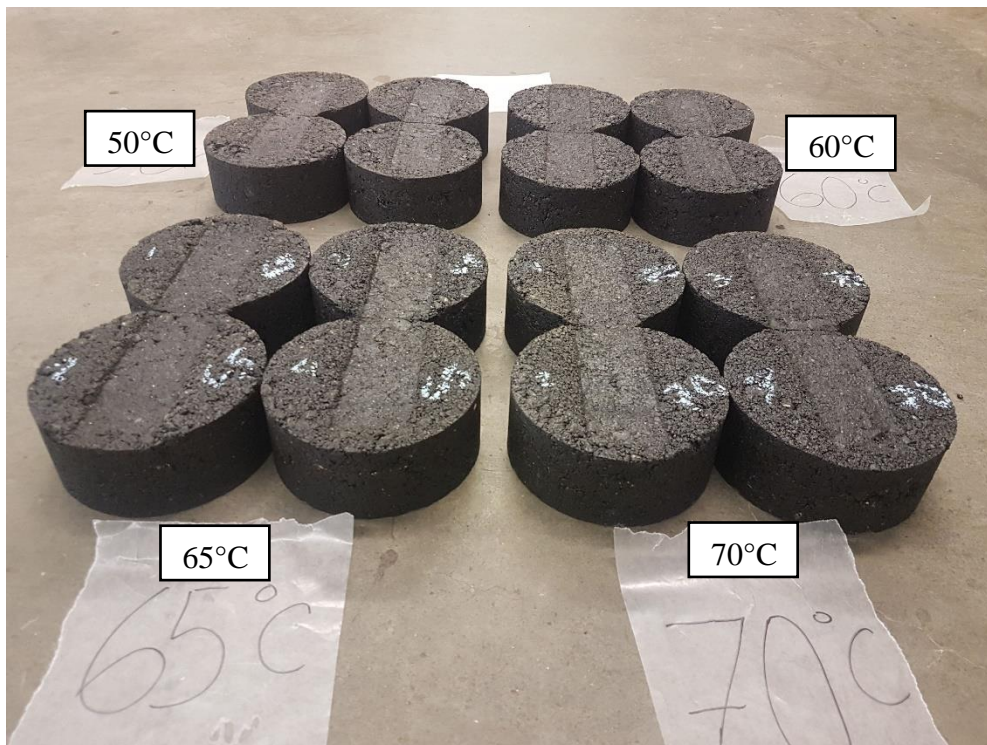


Image 5.3 Hamburg Wheel Tracking Test Samples Tested at Different Temperatures

5.3 Modified Lottman Test (AASHTO T 283)

The main purpose of this test is to measure the vulnerability of the compacted asphalt mix against moisture-induced damage and freeze-thaw cycles. To do so, the Superpave cylinder samples are compacted ($d=150\text{mm}$ and $h=95\pm 5\text{mm}$), the air voids are measured between 6.5 and 7.5 percent, and the control samples are separated from the ones that are meant to be conditioned. This conditioning consists of saturating the samples between 70 to 80%, freezing the samples at $18\pm 2\text{ }^\circ\text{C}$ for 24 hours, and then thawing the samples by submerging them into a water bath at 60°C for 16 hours.

As explained in the introduction of this chapter, some modifications were made to the AASHTO T-283 test. The main focus of the test was not on the asphalt mix itself but on the behaviour of it due to some conditioning modifications. In this case, the following 3 main modifications were made:

1. The number of cycles was increased. The test only requires the ratio of change to be calculated between the non conditioned samples and the samples that were subjected to one freeze-thaw cycle. Instead of only one, this project induced up to 3 freeze-thaw cycles to the samples to evaluate the ratio of change among them, exemplifying what climate, not necessarily climate change in this case, but the climate itself is causing to the pavement surface.
2. The constant rate of movement of the testing machine was boosted. The test requires the samples to be compacted at a rate of 50 mm/min. Once all the samples were tested, this project decided to move forward with an evaluation of how does freeze-thaw cycles impact the tensile strength on the areas of the runways that are subjected to a higher speed of loading; therefore, the departure and landing areas. Consequently, the speed of loading of the compaction machine was increased to 50 mm/sec.
3. [Figure 2.10](#) describes that many airport authorities have been noticing that not just the number of freeze-thaw cycles are changing but the intensity of them. Meaning that the timing between one freeze-thaw cycle and another is being perceived to be diminished. Hence, the freezing and thawing period were reduced by half; 12 hours of freezing and 8 hours of thawing. In another hand, the number of freeze-thaw cycles per year have not been increasing nor decreasing but simply varying sort of sinusoidal. Therefore, what matters is to compare the amount of cycles among the different provinces to understand how these cycles are impacting their specific airside infrastructure.

5.3.1 ITS's Variation due to Freeze-Thaw Cycles

Figure 5.6 presents the variation of the tensile strength caused by increasing the number of freeze-thaw cycles. Many statements can be made by evaluating this Figure, being the main ones that:

1. The tensile strength is significantly affected by freeze-thaw cycles in early stages; nonetheless, as it can be seen that the ITS difference between one cycle and the other is being reduced, it can be confirmed that the more freeze-thaw cycles the asphalt surface experience, the less effect these will induce to it.
2. Not just the maximum strength varied but also the deformation at which these maximum strengths were reached, indicating that the energy of fractures of the samples varied as well. These can be attributed to modification on the cracking resistance which will be further discussed.
3. Continuing the second statement, the concavity of the curves was becoming wider which indicates that the failure was less brittle; hence, the more freeze-thaw cycles, the softer the mix was becoming.

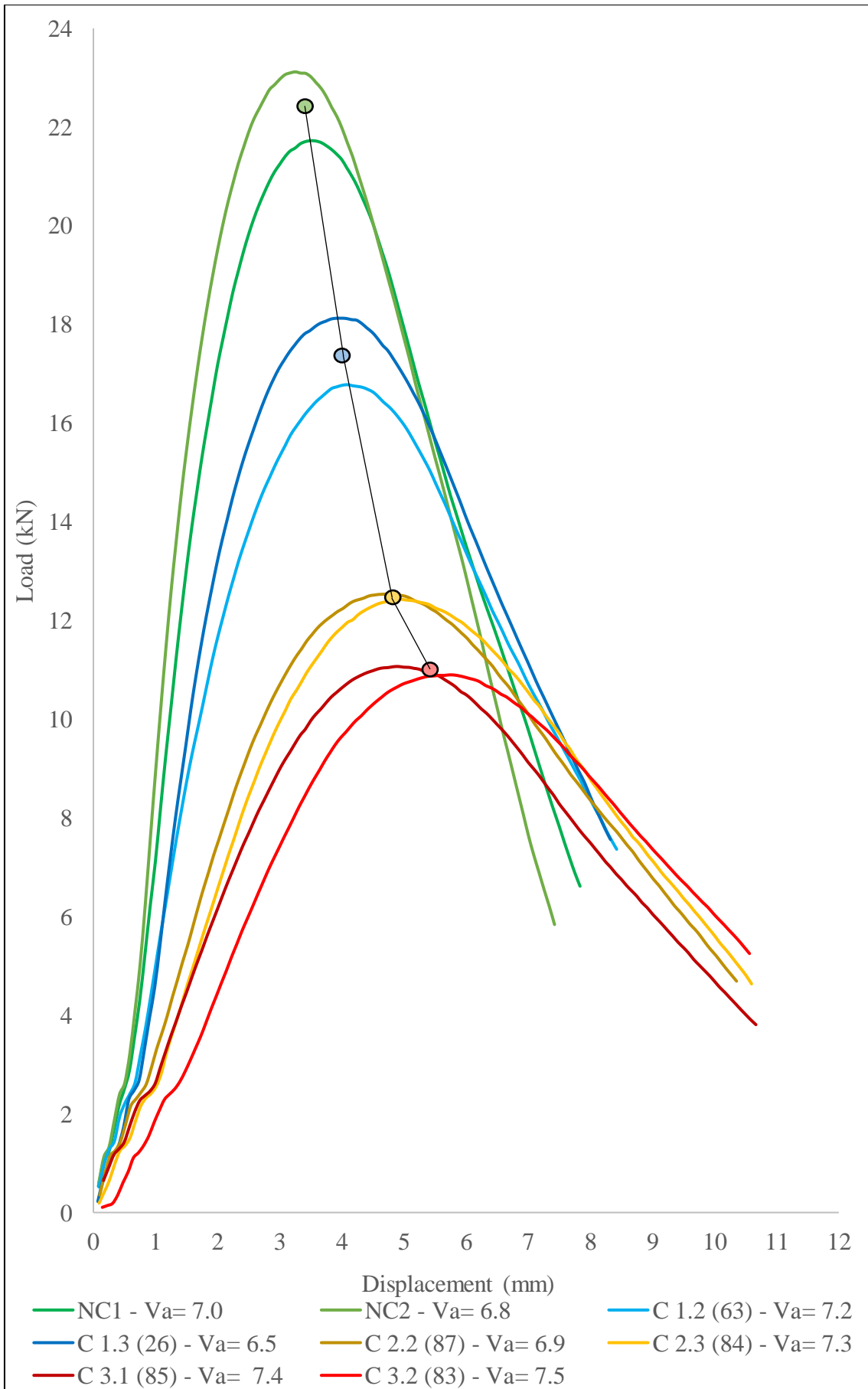


Figure 5.6 Tensile Strength Reduction due to Freeze-Thaw Cycles

Figure 5.7 summarizes what was described above and presents the relationship between the number of freeze-thaw cycles and the tensile strength. Consequently, the higher the number of cycles, the lower the influence these will have over the tensile strength.

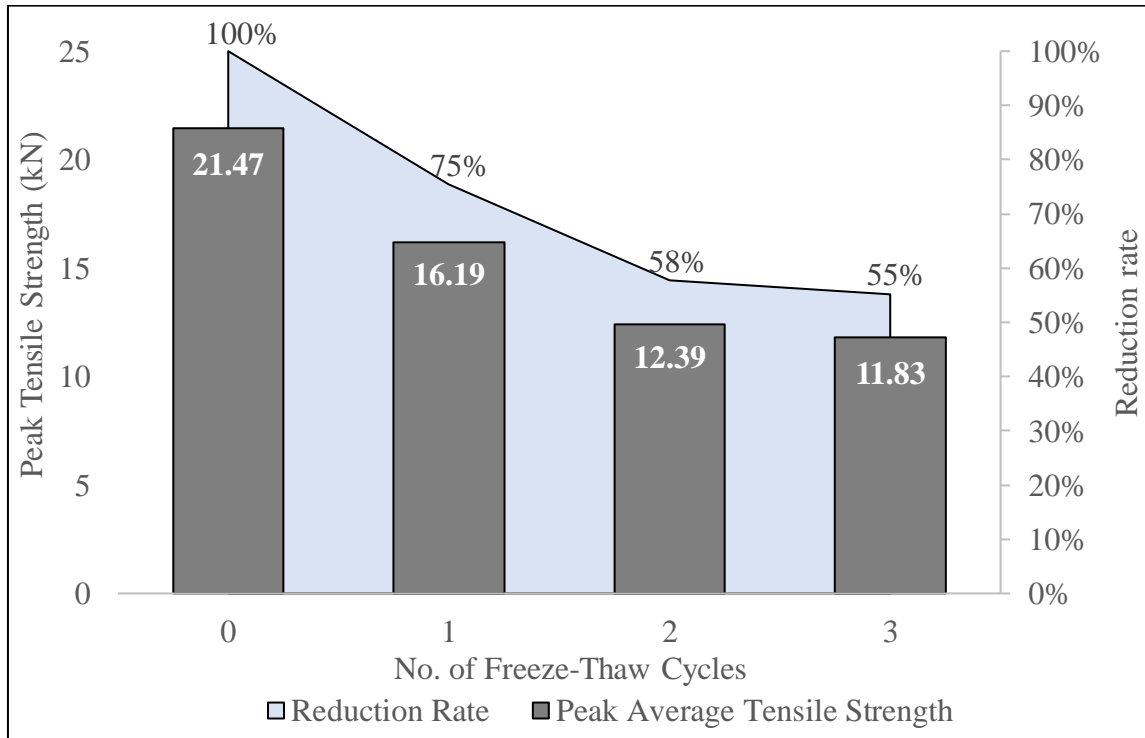


Figure 5.7 Tensile Strength versus Number of Freeze-Thaw Cycles

5.3.2 ITS's Variation due to Freeze-Thaw Cycles and Faster Compaction

Figure 5.8 shows the relationship between the ITS and the freeze-thaw cycles. It remains similar; however, it is valuable to notice that the tensile strength was increased approximately 18% by boosting the speed of loading to 50 mm/sec. This correlates to the viscoelastic properties of the asphalt mix of being highly susceptible against temperature and the speed of loading.

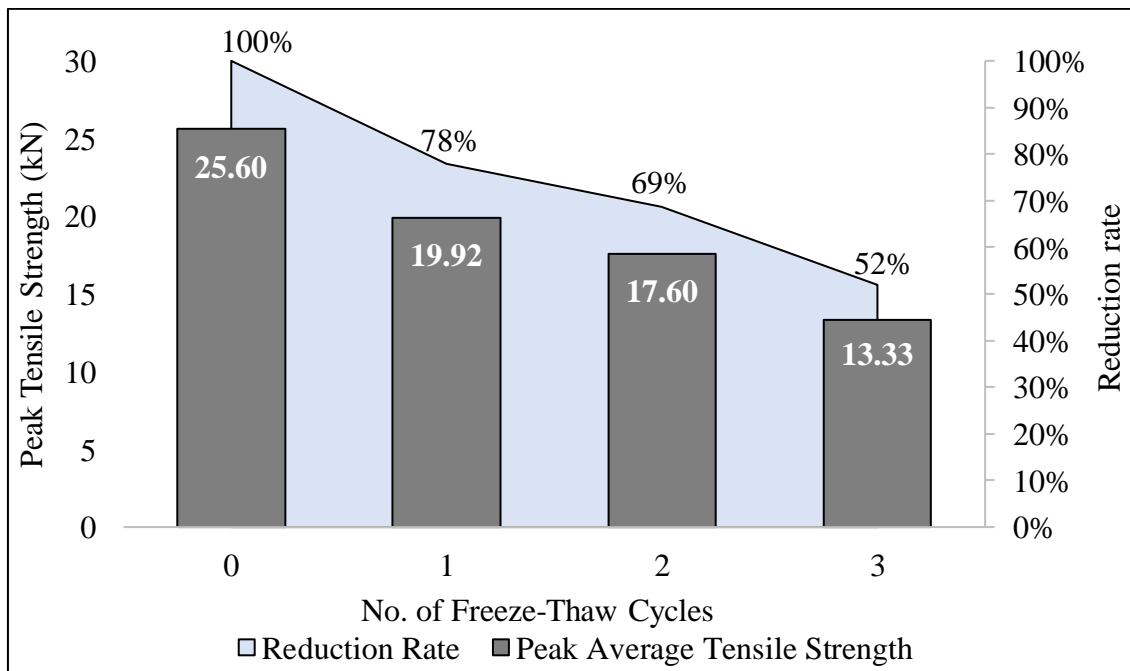


Figure 5.8 Indirect Tensile Strength with Faster Compaction vs Number of Freeze-Thaw Cycles

5.3.2 ITS's Variation due to the Reduction of the Freeze-Thaw Cycles' Period and Faster Compaction

The main purpose of performing this modification on the test was to evaluate the sensitivity of the pavements against the amount of freeze-thaw cycles per year, as all the provinces have distinct annual number of these cycles. What can be concluded is that if during the same period of time the pavement structure is subjected to double of the amount of freeze-thaw cycles, its tensile strength could be decreased by approximately 20 percent. Having said that, it can be confirmed that airports such as Halifax Stanfield or Calgary International can experience softer mixes due to freeze-thaw cycles compared to Yellowknife international or Iqaluit airport.

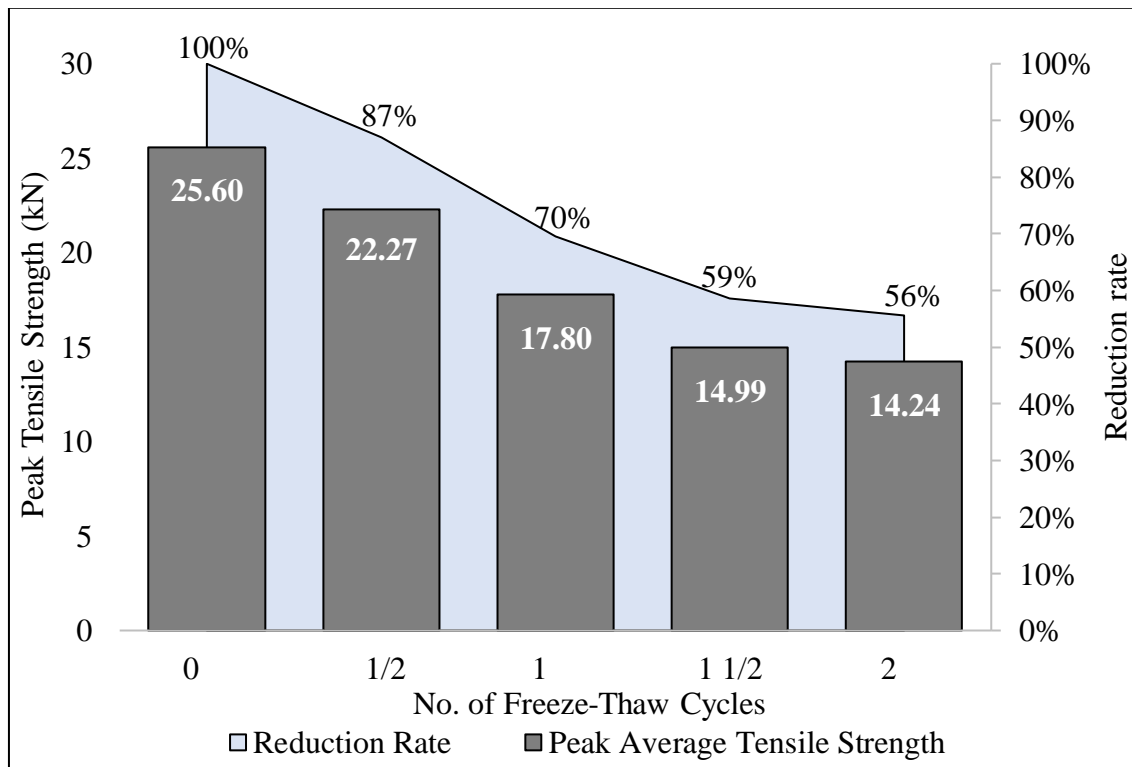


Figure 5.9 Tensile Strength with Faster Compaction and half period of Freeze-Thaw Cycles

5.4 Ideal Cracking Test

Figure 2.9 shows cracking severity as one of the main distresses affecting the Canadian airside infrastructures. By having the performance information of each of the samples that were tested for indirect tensile strength as well as the load versus displacement curves of each of them, the possibility of calculating a cracking index following the Ideal Cracking Test procedure was conceivable. This ideal cracking test index (CT-index), as described in [section 2.5.3](#), directly depends on fracture mechanics and it empirically correlates the load versus displacement curve with the crack propagation that is meant to happen on the field.

The higher the CT-index, the more resistant are the samples against crack propagation. Figure 5.10 presents that, as the number of freeze-thaw cycles increases, the cracking resistance rises too, meaning that the freeze-thaw cycles do not damage the asphalt samples but enhance them against cracking. This was an unexpected result because, theoretically, the expansion and contraction of the pavement surface during the freezing and thawing periods induce cracks, as it was explained in [section 2.4.4](#). [Figure 5.6](#) shows that the freeze-thaw cycles are not just causing a decrease in the tensile strength of the mix, it shows a reduction in the hardening of the mix; hence, making it softer and so, less susceptible to crack due to its less brittle behavior.

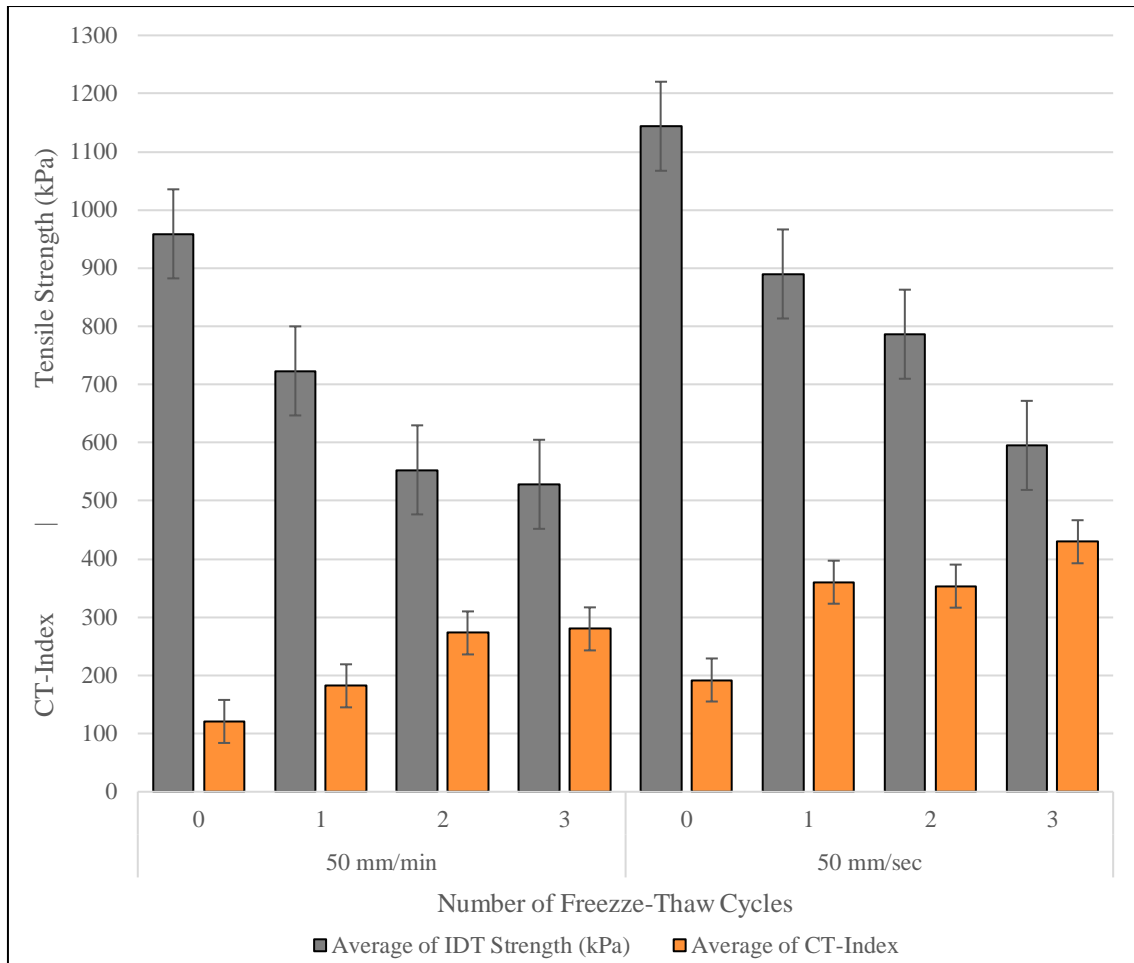


Figure 5.10 Indirect Tensile Strengths and Cracking Test Indexes

5.6 Chapter Summary

This chapter presented the performance of the described airfield asphalt mix (SP 12.5, PG 70-28J, and 5.2%AC) under different intensities of climate conditions such as saturation to induce moisture damage, freeze-thaw cycles, and temperature variations. Rutting and shoving, tensile strength, and crack propagation were the main focuses of this study.

As a result of the rutting analysis, it was demonstrated that freeze-thaw cycles and high temperatures induces the mix to become softer which makes it more susceptible to suffer rutting and shoving. It is important to acknowledge that freeze-thaw cycles induced a more premature rutting failure compared to the temperature variation on the range of 50°C to 70°C regardless the fact that the rutting values after 10,000-wheel passes were very similar.

Concerning the tensile strength of the samples, the main results expressed that apart from the fact that as the number of freeze-thaw cycles increased, the ITS was reduced, it is important to mention that the relationship was non proportional; hence, the higher the amount of freeze-thaw cycles induced, the less impact they will have on the mix.

Additionally, it is highly significant to recite that freeze-thaw cycles make the asphalt sample softer, also in a non-proportional way; which is the main explanation for having higher CT-indexes as the tensile strength was reduced due to freeze-thaw cycles. As the samples becomes softer, the energy of fracture dissipates which implies a less brittle performance; hence, less susceptibility for the cracks to propagate.

CHAPTER 6

Conclusions and Recommendations

The purpose of the following chapter is to present several considerations for mitigation and adaptation strategies as well as to conclude the perspective of this research towards climate change, its variations in different locations in Canada, and how are those changes impacting the airfield pavement infrastructure of its. Additionally, it provides several insights into the possible future work and recommendations.

6.1 Considerations for Mitigation and Adaptation Strategies

According to the Cambridge dictionary, to mitigate means to diminish the harm or unpleasantly of something; in the other hand, to adapt indicates a change to suit different conditions or needs. (Cambridge dictionary, 2019) Hence, in the scope of this research, mitigation and adaptation strategies refer to approaches, tactics, policies, or plans to decrease the main causes of climate change allowing the future consequences/impacts to be reduced, and, to adjust to the current changes to minimize the impacts in the present or near future, respectively.

As mentioned in [section 2.0](#) of the literature review, the main cause of climate change is the significant increment of GHG concentration in the atmosphere. This concentration, as it increases, it induces a variation in the balance between the absorption of solar radiation and the emission of infrared radiation, radiative forcing. More specifically, the absorption of solar radiation is higher than the emission of infrared radiation, positive radiative forcing. (Masters & Ela, 2008) Therefore, the key mitigation strategy against climate change, holistically, is to substantially reduce the emission of greenhouse gases.

The focus of this research has been in the airfield pavement infrastructure of Canadian airports; consequently, the major contributors to GHGs' emissions are the construction, reconstruction, and rehabilitation of the pavement, as well as the material's production. In this regard, reducing the amount of interventions in the airfield pavement as well as controlling the production of the construction materials embody the basics of the mitigation strategies. The challenge, however, is to find feasible solutions that can improve or meet the current requirements without compromising the environment and/or the society.

[Figure 2.12](#) presented that one of the main barriers faced by airport authorities against the development of mitigation and/or adaptation strategies, more than the lack of funding, is that the costs cannot be justified. Mostly due to the uncertainty of future climate events which eventually reduces the reliability of investing in new technologies or best practices. For this reason, it has been significantly beneficial to understand the changes of climate through time for each specific airport selected. That being said, with the obtained results of this research, the following mitigation and adaptation strategies' considerations are proposed for each specific airport case:

- Starting from YYZ (Toronto airport), several considerations for mitigation strategies can be proposed as this airport could be susceptible to more than one significant distress. It presented to be the one experiencing the highest temperatures and counting on 5 runways from which 4 have asphalt as surface layer, distresses such as rutting, but more importantly, shoving have and can continue to affect the pavement infrastructure. During the decade of 2000-2010, one of the main adaptation strategies that Toronto airport implemented was a change on the requirement for the performance grade of the asphalt cement varying from a conventional PG 64-28 with 5.5-5.8% of asphalt cement to a polymer modified asphalt PG 70-28 with a 4.8-5.2% of it. (Stewart, 2010)

Regardless the fact that, compared to the other airports evaluated, Toronto's is not experiencing a meaningful growth on its maximum temperatures; it is currently the busiest airport in Canada. Having such high temperatures and rainfall, but also having a significant reduction on its snowfall with a meaningful increment of its minimum temperature could plan for mitigation strategies that can be more focused on summer than winter operations. Nonetheless, due to the combination of high temperatures and the significant traffic that YYZ's runways receive, the new HMA P-601, accepted in 2018 by the FAA (Varamini, Corun, Bennert, Esenwa, & Kucharek, 2018), but now called FAA HMA P-404 can be considered as a superior long-term alternative.

- Continuing with YVR (Vancouver airport), reaching the highest amount of precipitation of all the airports evaluated, but also having the highest rate of grow, the drainage system and design ought to be evaluated or enhanced, specially to avoid future floods.
 - In the case of Halifax Airport (YHZ), referring to Figure 4.12, is the airport with the highest amount of annual freeze-thaw cycles as well as the greatest growth rate of its. [Section 5.2 to 5.4](#) presented that freeze-thaw cycles have a meaningful effect in the future performance of the pavement structure as they softer the mix, making it more susceptible to permanent deformations such as rutting and shoving; additionally, they cause a lost of tensile strength overtime which may lead to stripping and/or pumping.
 - Another airport with a distinctive case is YYC (Calgary airport) because, similar as YHZ, it experiences a high number of annual freeze-thaw cycles but combined with very high and low temperatures likewise YUL (Montreal airport). In the case of Calgary airport, the main runway is paved with concrete which is not significantly susceptible to high temperature, but it is to low temperatures and freeze-thaw cycles inducing cracks and other distresses such as curling, spalling, and /or scaling. (Adkins & Christiansen, 1989)
 - Furthermore, YZF (Yellowknife) have a significantly unique scenario. Although it was the airport with the lowest amount of freeze-thaw cycles, it is located in an intermediate permafrost area with an extensive discontinuous property, meaning that it is constantly varying over the years. Hence, having described in [sections 2.4.6](#) and [section 4.3](#) the possible distresses that can be generated in the airfield pavement due to the thaw of permafrost such as settlement which might rapidly lead to fatigue cracking as well, it may be a better decision to invest in mitigation strategies rather than adaptation ones. A rigid pavement would perform significantly better than the current flexible pavement against the thawing of permafrost and other pavement distresses' causes; however, the initial cost would be meaningfully high, not just due to the price of a rigid structure, but because of the unavailability of materials in northern Canada, making the strategy unjustifiable. New technologies that could mitigate the permafrost discontinuity are the use of thermosiphons to allow the subgrade heat to dissipate to the surface and not to accumulate. If necessary, artificial cooling could be used to maintain the subgrade frozen during the summer. In case of a future construction or reconstruction, an intentional thaw can be induced to eradicate the permafrost. (Emery, 2012)
- To mitigate fatigue distresses, superior mixing and compaction methods can be used to assure the proper content, distribution, and microstructure of air voids of the asphalt mix. According to Ma et al, having lower air voids content may lead to higher fatigue life. (Ma, Zhang, Zhang, Yan, & Ye, 2016) As the air void percentage decreases, the amount of asphalt cement increases. Hence, this technique may balance the hardening caused by the higher compaction energy induced to the pavement structure with the softening caused by the increment of asphalt cement.
- Lastly, it is important to acknowledge that, according to Rachel Burbidge, the main priorities towards an aviation climate resilience comes from understanding the problem, assessing it, find actions to adapt, and communicate. (Burbidge, 2016)

6.1 Conclusions

Once described and understood climate change holistically, it can be concluded that the main cause for it is the substantial augmentation of greenhouse gases produced by humanity since the industrial revolution; hence, anthropogenic reasons. The increment of the concentration of these gases have caused and will continue to cause positive radiative forcing, which mainly increases the temperature of the planet and, as a result, induces alterations on the weather events' location, intensity, and/or period of return. The IPCC has developed different future scenarios for year 2,100 on which the impacts of climate change are measured depending on the concentration of carbon dioxide equivalent gases. Currently, the concentration of these gases is at 407 ppm; therefore, best-case scenario, by year 2,100 the concentration will have decreased to its long-term average level of 260 ppm; worst-case scenario, it will have increased to 850 ppm on which life, as its known, will not be anymore.

The primary consequence of global warming is the precipitous melt of Arctic ice which is provoking a rapid increment of the sea level, putting in jeopardy coastal areas all over the world, but also reducing the albedo of the Earth, making it to warm exponentially. In the case of Canada, the sea level is rising up to 3mm per year conceivably reaching a meter in the next 100 years. The country has become warmer and also wetter as annual precipitation has increased in recent decades, annual snowfall has been reduced over most of southern Canada, and permafrost will continue warming/thawing exponentially. All these changes create or intensify pavement distresses and can generate disruption during flooding or hurricane events.

[Section 4.2](#) explained that the maximum and minimum temperatures of all Canadian airports are rising, specially for YZF and YHZ with an increment of 2°C on its maximum temperature since the 1950s, YYZ with approximately 4.4°C more on its minimum temperature, and YZF and YUL with roughly 2.2°C of augmentation in their minimum temperatures as well. Indeed, Canada is warming up. Furthermore, considering the relationship between the ambient temperature and the pavement surface temperature presented in Figure 4.9 and/or table 4.1, an approach to calculate the amount of annual freeze-thaw cycles was made. From the obtained results can be concluded that YHZ represent the airport with the highest amount of annual freeze-thaw cycles, moreover, growing considerably. That means that Halifax airport's airfield infrastructure is becoming more susceptible to an intensification of the pavement distresses due to the softening of the surface layer caused by the high number of freeze-thaw cycles. Additionally, it is important to mention that the airports located in northern Canada had lower amount of freeze-thaw cycles compared to those on southern Canada such as Calgary, Moncton, Toronto, and Montreal.

[Section 4.3](#) presented the permafrost distribution in Canada which varies on depth and continuity. It can be concluded that Iqaluit, the coldest airport from all the selected ones, is located in a continuous permafrost soil making it not pointedly prone to suffer pavement distresses associated with the melting of these; however, Yellowknife and Whitehorse, also being located in significantly cold regions, are indeed susceptible to experience settlements and fatigue cracks because of a lost on the bearing capacity on their subgrade due to the reduction of the effective stress caused by the melting or freezing of the discontinuous permafrost.

About the precipitation analysis shown in [section 4.4](#), YVR, YUL, and YYZ airports receive a significant amount of annual precipitation, specially in the case of Vancouver which reaches an average of approximately 100 mm/year compared to the 12 mm/year of YHZ being these two airports located in a very close latitude of the planet. Considering the snowfall, more than the rainfall, it can be concluded that the airports located at the south of Canada are experiencing a significant reduction of the snowfall, especially YUL which snowfall has decreased approximately 25% in just 70 years, making the winter operations fairly more manageable in the present and for the future. Nonetheless, Iqaluit, Saskatoon, and Winnipeg, are having more snow

falling during the winter season, mainly in the case of Winnipeg that has increased its snowfall nearly 50% in the past 70 years.

From the laboratory tests presented in [sections 5.2](#), [5.3](#), and [5.4](#) develop on a PG 70-28J airfield asphalt mix with 5.2% of asphalt cement and the gradation presented in Figure 5.1, and recognizing that this mix can serve as an example of a surface layer of the flexible airfield pavements located in most of southern Canada, being this part the most susceptible to high temperatures and freeze-thaw cycles, the following conclusions can be taken:

- As presented in Figure 5.6, freeze-thaw cycles make the asphalt mix softer and therefore more susceptible to both rutting and shoving.
- Figure 5.10 presented that as the number of freeze-thaw cycles increases, the resistance against crack propagation also rises due to the softening of the asphalt mix which make its to have a less brittle failure.
- It is important to mention that both for rutting and indirect tensile strength, as presented in Figures 5.3, 5.7, 5.8, and 5.9 it exists a non proportional relationship on which the more freeze-thaw cycles the pavement structure is subjected, the less impact these will induce to the mentioned distresses' resistance.
- In another hand, it can be concluded that flexible runway pavements subjected to massive impact of loadings; hence, the arrival and departure of large aircrafts, respond with meaningfully stiffer properties as for the viscoelastic properties of the asphalt cement of the mix. This can be noticed in Figure 5.8.
- Additionally, considering the comparison between the rutting due to freeze-thaw cycles and the rutting due to the rise of temperature, it can be concluded that freeze-thaw cycles induce a more premature longitudinal permanent deformation compared to that caused by the difference of pavement temperature in the range of 50-70°C.
- Concerning the rise of temperature, as evaluated and presented in [section 5.2.2](#), flexible pavements are susceptible to high temperatures as these cause the asphalt mix to exponentially become softer as the temperature rises. In the case of Toronto Pearson Airport, being the one subjected to the hottest temperatures evaluated, focusing on Figure 4.10 which indicated that YYZ is likely to experience a rise from 50.8°C to 51.4°C (half degree) of its surface maximum average temperature in the next 20 years. If the same asphalt mix design requirements are kept, its susceptibility to rutting will rise approximately 2%.

6.2 Future Work and Recommendations

This research developed a vast analysis on the Canadian climate at several airport locations. However, at the moment of examining the impacts of these variations of climate, only one airfield asphalt mix design was tested. Hence, it is recommended to evaluate these impacts on distinct asphalt mixes. Additionally, develop tests on airfield hydraulic concrete samples to assess the impacts on rigid pavements.

Concerning the laboratory tests, as it was presented in Figures 4.11 to 4.12, Canadian airports experience freeze-thaw cycles varying from 5 to 30 per year; therefore, approximately 100 to 600 freeze-thaw cycles per airfield pavement's life cycle (around 20 years) in a temperature range of -15°C to 15°C. Therefore, it will be significantly more accurate to evaluate the impacts of freeze-thaw cycles by inducing a meaningfully higher amount of them varying between the mentioned range.

REFERENCES

- ACPA. (2013). *American Concrete Pavement Association*. Retrieved from Frost Action and Frost Heave: http://overlays.acpa.org/concrete_pavement/technical/fundamentals/Frost.asp
- Adkins, D., & Christiansen, V. (1989, May). Freeze-Thaw Deterioration of Concrete Pavements. *Journal of Materials in Civil Engineering*, 1(2), 97-104.
- Aehnelt, R. (2016). <http://www.robertaehnelt.de>. Retrieved from PORTFOLIO (SELECTION): <http://www.robertaehnelt.de/index.php/infodesign/infografiken>
- American Association of State Highway and Transportation Officials. (2003). *Resistance of Compacted Asphalt Mixtures to Moisture-Induced Damage*. AASHTO.
- American Association of State Highway and Transportation Officials. (2014). *Standard Method of Test for Quantitative Extraction of Asphalt Binder from Hot Mix Asphalt (HMA)*. AASHTO.
- American Association of State Highway and Transportation Officials. (2014). *Standard Method of Test for Sieve Analysis of Fine and Coarse Aggregates*. AASTO.
- American Association of State Highway and Transportation Officials. (2016). *Standard Method of Test for Hamburg Wheel-Track Testing of Compacted Hot Mix Asphalt (HMA)*. AASHTO.
- Applegate, Z. (2013, 04 26). *Norfolk*. Retrieved from Guy Stewart Callendar: Global warming discovery marked: <https://www.bbc.com/news/uk-england-norfolk-22283372>
- Barral, M. (2019, 02 19). *Science*. Retrieved from Svante Arrhenius, the Man Who Foresaw Climate Change: <https://www.bbvaopenmind.com/en/science/leading-figures/svante-arrhenius-the-man-who-foresaw-climate-change/>
- Bone, C. (2019, 03 11). Permafrost Composition. Retrieved from <https://www.arcgis.com/home/item.html?id=043d953a00874b85a28c6c3b5f8d245b>
- Burbidge, R. (2016). Adapting European Airports to a Changing Climate. *Transportation Research Procedia*, 14, 14-23. doi:10.1016/j.trpro.2016.05.036
- Bush, E., & Lemmen, D. (2019). *Canada's changing climate report*. Ottawa, ON: Government of Canada. Retrieved from https://www.nrcan.gc.ca/sites/www.nrcan.gc.ca/files/energy/Climate-change/pdf/CCCR_FULLREPORT-EN-FINAL.pdf
- Cambridge dictionary. (2019). *Dictionary*. Retrieved from Mitigate and Adapt: <https://dictionary.cambridge.org/dictionary/english/mitigate> | <https://dictionary.cambridge.org/dictionary/english/adapt>
- Cambridge Dictionary. (2019). *Dictionary*. Retrieved from Shove: <https://dictionary.cambridge.org/dictionary/english/shoving>
- Cambridge Dictionary. (2019). *Dictionary Cambridge*. Retrieved from Precipitation: <https://dictionary.cambridge.org/dictionary/english/precipitation>
- Chang, S.-W. (2015). Crosswind-based optimization of multiple runway orientations. *Journal of Advance Transportation*, 49, 1-9.

- Cipione, C. A., Davrson, R. R., Burr, B. L., Glover, C. J., & Bullin, J. A. (1991). Evaluation of Solvents for Extraction of Residual Asphalt from Aggregates. *Transportation Research Record*(1323), 47-52.
- Climate Atlas of Canada. (2019). Retrieved 03 13, 2019, from Climate vs. Weather: <https://climateatlas.ca/climate-vs-weather>
- Cook, J. (2010, 07 09). *How reliable are CO2 measuments*. Retrieved from Skeptical Science: <https://skepticalscience.com/co2-measurements-uncertainty.htm>
- Emery, J. (2012). CLIMATE CHANGE IMPACTS ON ASPHALT PAVEMENTS, global perspective, adaptation and opportunities. *CUPGA*. Edmonton: CTAA. Retrieved from <https://www.ctaa.ca/wp-content/uploads/2012/02/Climate-Change-Impacts-on-Asphalt-Pavements-Global-Perspective-J.-Emery.pdf>
- Environment Canada. (2019, 03 28). *Canada.ca*. Retrieved 03 30, 2019, from Causes of climate change: <https://www.canada.ca/en/environment-climate-change/services/climate-change/causes.html>
- Google Earth Pro. (2019). NOAA. London, Ontario, Canada. Retrieved 07 14, 2019
- Gopalakrishnan, K., Steyn, W., & Harvey, J. (2014). *Climate Change, Energy, Sustainability, and Pavements*. Heildeberg, Germany: Springer.
- Government of Canada. (1995). *Natural Resources Canada*. Retrieved from Permafrost: <https://www.nrcan.gc.ca/earth-sciences/geography/atlas-canada/selected-thematic-maps/16886#physicalgeography>
- Government of Canada. (2010, 02 03). *National Airport Policy*. Retrieved from The National Airport System: <https://www.tc.gc.ca/eng/programs/airports-policy-nas-1129.htm>
- Government of Canada. (2018, December). *Aeronautics Act*. Ottawa: Minister of Justice. Retrieved from Justice Laws: <https://laws-lois.justice.gc.ca/eng/acts/A-2/page-1.html#h-7489>
- Haas, R., Falls, Macleod, & Tighe, a. S. (2004). Climate impacts and adaptations on roads in Northern Canada. *Cold Climates Conference*, (p. 18). Regina.
- Holdren, J., Daily, G., & Ehrlich, P. (1995). *The Meaning of Sustainability: Biogeophysical Aspects*. Washington DC: United Nations University and the World Bank.
- James Hansen, M. S.-E. (2006). Global temperature change. *Proceedings of the National Academy of Sciences of The United States of America (PNAS)*, 14288–14293.
- Khan, S., Nagabhushana, M., Tiwan, D., & Jain, a. P. (2013). Rutting in Flexible Pavement: An approach of evaluation with Accelerated Pavement Testing Facility. *Social and Behavioral Sciences*, 149-157. doi:10.1016/j.sbspro.2013.11.107
- Konarski, K. (2014). *Mitigation of Climate Change Impacts on Runway Friction, Kuujjuaq Airport*. Waterloo: University of Waterloo.
- Leanne Whiteley, S. T. (2006, 10 13). Pavement Thickness Design for Canadian Airports. Waterloo, Ontario, Canada.
- Lu, D., & Dutton, D. (2017). Summary of Climate Change and Airfield Pavements Survey. *CAPTG*. Halifax: CAPTG. Retrieved from

<http://www.captg.ca/docs/pdf/17Presentations/Tuesday%20PM/Summary%20of%20Climate%20Change%20and%20Airfield%20Pavements%20Survey.pdf>

- Ma, T., Zhang, Y., Zhang, D., Yan, J., & Ye, Q. (2016). Influences by airvoids on fatigue life of asphalt mixture based on discrete element method. *Construction and Building Materials*, 785-799.
- Masters, G. M., & Ela, W. P. (2008). *Introduction to Environmental Engineering and Science* (Third ed.). Prentice Hall.
- Masters, W. P. (2010). *Introduction to Environmental Engineering and Science*. Pearson, PHI.
- Mills, B., Tighe, S., Andrey, J., Smith, J., & Huen, K. (2009). Climate Change Implications for Flexible Pavement Design and Performance in Southern Canada. *Journal of Transportation Engineer*, 135(10), 773-782. Retrieved from <https://ascelibrary.org/doi/pdf/10.1061/%28ASCE%290733-947X%282009%29135%3A10%28773%29>
- Mills, B., Tighe, S., Andrey, J., Smith, J., Parm, S., & Huen, a. K. (2007). *The Road Well-Traveled: Implications of Climate Change for Pavement Infrastructure in Southern Canada*. Waterloo.
- Minnesota Department of Transportation. (2013, 11 01). *MnDOT | Frost damage in pavement*. Retrieved from youtube.com: <https://www.youtube.com/watch?v=fkrrSys03qQ&t=145s>
- Mohamed, E.-S., Osman, M. E., & El-monem, R. (2011, November). Investigation in Selecting the Optimum Airport Runway Orientation with Special Reference to Egyptian Airports. *Journal of Engineering Science*, 39(6), 1261-1280.
- Morse, P. D. (2017, 12 15). *Natural Resources Canada*. Retrieved from Permafrost: <https://www.nrcan.gc.ca/earth-sciences/sciences/earth-sciences-permafrost-ice-and-snow/permafrost/10990>
- Murmakova, N. (2017, 09 08). Empty runway at airport during a foggy sunrise. istockphoto. Retrieved from <https://www.istockphoto.com/il/photo/empty-runway-at-airport-during-a-foggy-sunrise-gm844702598-138235277>
- NASA. (2016, 10 28). *Scientific Visualization Studio*. Retrieved from Weekly Animation of Arctic Sea Ice Age with Graph of Ice Age By Area: 1984 - 2016: <https://svs.gsfc.nasa.gov/4510>
- National Oceanic and Atmospheric Administration. (2018, 08 01). *www.climate.gov*. Retrieved from NOAA Climate.gov: <https://www.climate.gov/news-features/understanding-climate/climate-change-atmospheric-carbon-dioxide>
- National Oceanic and Atmospheric Organization. (2019, 10 02). *Earth System Research Laboratory*. Retrieved from Recent Daily Average Mauna Loa CO2: <https://www.esrl.noaa.gov/gmd/ccgg/trends/monthly.html>
- NSIDC/NASA. (2019, 05 2018). *Global Climate Change*. Retrieved from climate.nasa.gov: <https://climate.nasa.gov/vital-signs/arctic-sea-ice/>
- Ozborn, L. (2019). *Current Results, Weather and Science Facts*. Retrieved 09 29, 2019, from Hottest Places in Canada: <https://www.currentresults.com/Weather-Extremes/Canada/hottest.php>

- Pavement Interactive. (2019). *Pavement Interactive*. Retrieved from Stripping: <https://www.pavementinteractive.org/reference-desk/pavement-management/pavement-distresses/stripping/>
- PPRA. (2018). *Pavement Preservation and Recycling Alliance*. Retrieved from Explore by pavement photos: <https://roadresource.org/toolbox/photos>
- Public Works Canada. (1992). *Manual of Pavement Structural Design ASG-19*. Quebec: Public Works and Government Services Canada.
- Reggin, A. (2019). Modeling the Progression of Runway Boing Bump Index. *SWIFT* (p. 38). Vancouver: TetraTech.
- Robert E. Hom and J. C. Orman, P. M. (1974). AIRPORT AIRSIDE AND AIRSIDE INTERACTION. *Transportation Research Record*, 196-208. Retrieved from <http://onlinepubs.trb.org/Onlinepubs/sr/sr159/159-018.pdf>
- Solaimanian, M., Bonaquist, R., & Tandon, V. (2007). *Improved Conditioning and Testing Procedures for HMA Moisture Susceptibility*. Washington: Transportation Research Board. doi:978-0-309-09906-6
- Stewart, C. (2010). Best Practices in the Design and Construction of Airfield Asphalt Pavements. *Canadian Airfield Pavement Technical Group*. Calgary, Alberta: CAPTG.
- TAC Urban Transportation Council. (1998). *A Primer on Urban Transportation and Global Climate Change*. Ottawa: TAC.
- Transport Canada. (2017). *Transportation in Canada, National Overview Report, 2017*. Transport Canada. Retrieved 11 2018
- Uzarowski, L., & Tighe, S. (2016). Comparison of Airport Paving Specification Requirements in Canada & USA. *SWIFT*. Minneapolis: CAPTG.
- Varamini, S., Corun, R., Bennert, T., Esenwa, M., & Kucharek, A. (2018). Development and Field Evaluation of High Performance and Fuel Resistant Asphalt Mixture. *Canadian Technical Asphalt Association*. Vancouver: CTAA. Retrieved from <https://www.ctaa.ca/download/abstracts-2018/Abstract-2018-018-Varamini.pdf>
- Walabita, L., Faruk, Zhang, Komba, Alrashyidah, & Simate, a. G. (2018). The Hamburg Rutting Test (HWTT) alternative data analysis methods and HMA screening criteria. *International Journal of*, 110-116. doi:10.1007/s42947-019-0014-3
- Warren and Lemmen. (2014). *Canada in a Changing Climate: Sector Perspectives on Impacts and Adaptation*. Ottawa: Government of Canada.
- White, G. (2018). State of the art: Asphalt for airport pavement surfacing. *International Journal of Pavement Research and Technology*, 77-98.
- Zhou, F., Im, S., Sun, L., & Scullion, a. T. (2017). Development of an IDEAL Cracking Test for Asphalt Mix Design and QC/QA. *Road Materials and Pavement Design*, 18. doi:<https://doi.org/10.1080/14680629.2017.1389082>

APPENDIX A

Environmental Analysis Results

Temperature Results

Toronto Pearson International Airport

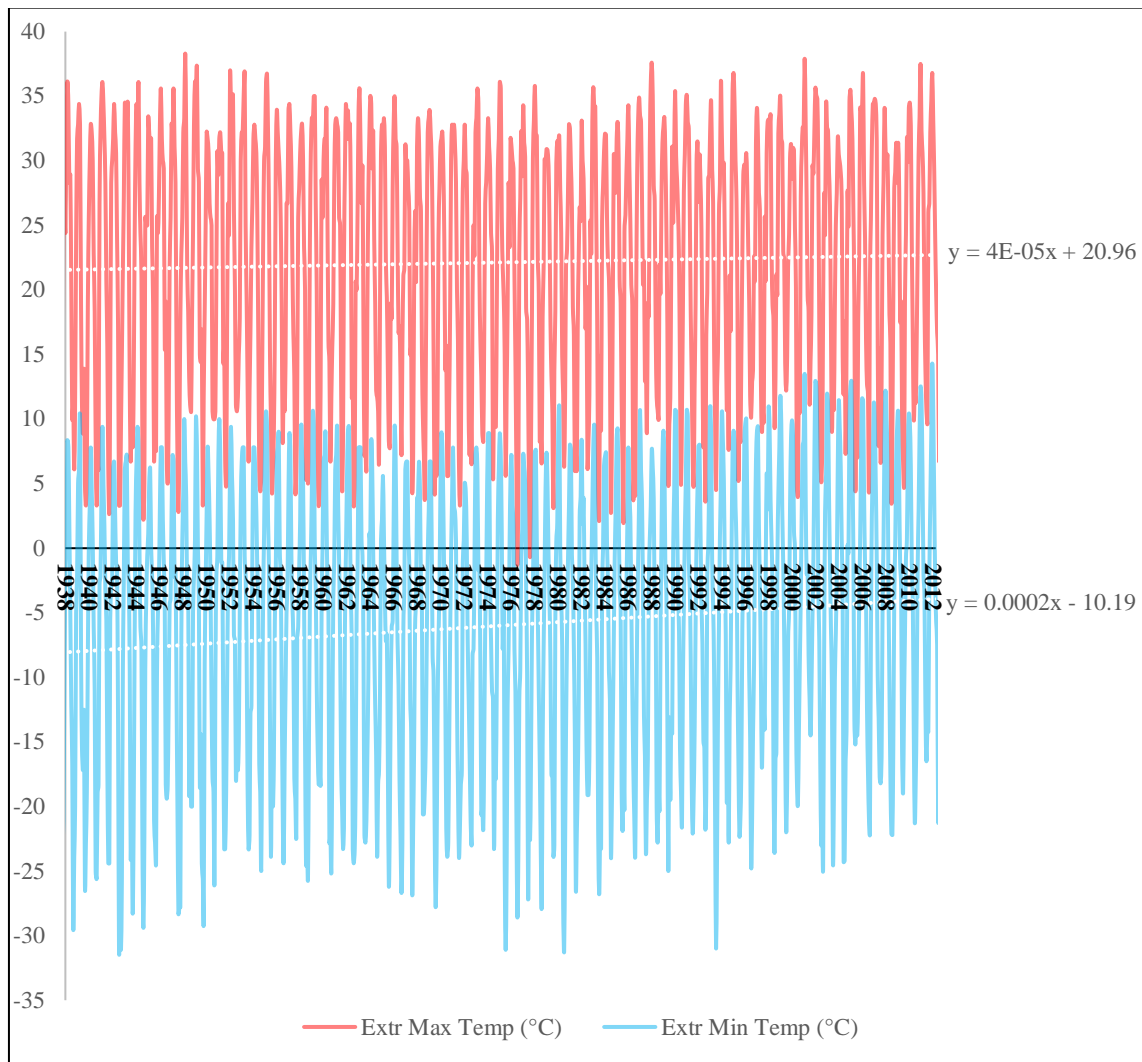


Figure A.1 Monthly Ambient Temperature at YYZ from 1938 to 2012

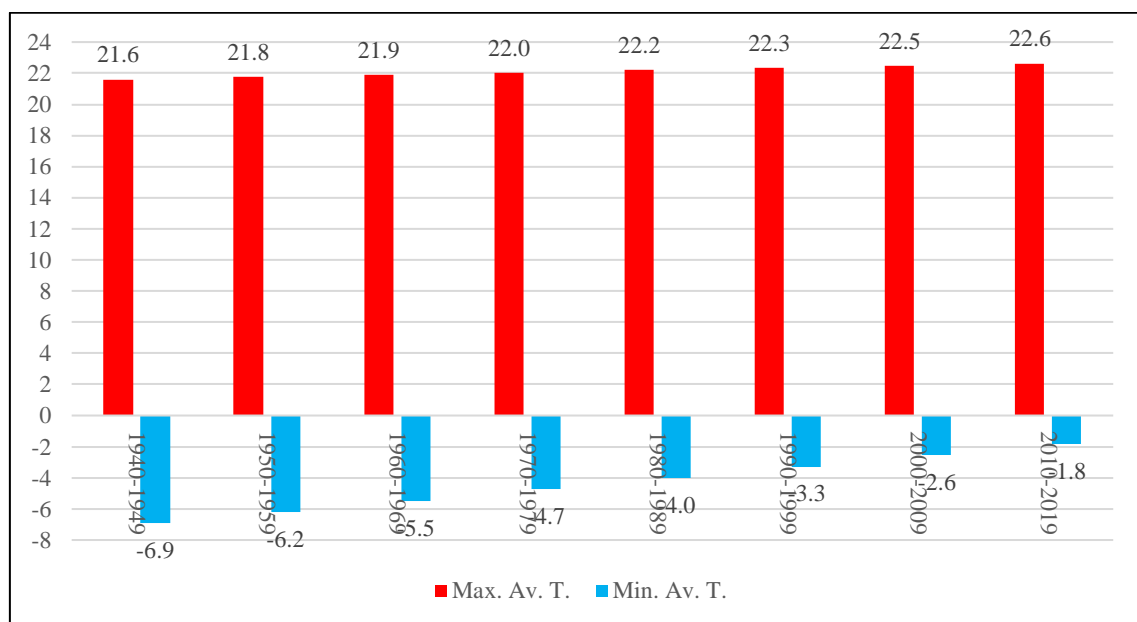


Figure A.2 Decade Average Temperature Trendlines for YYZ from 1940-1949 to 2010-2019

Vancouver International Airport

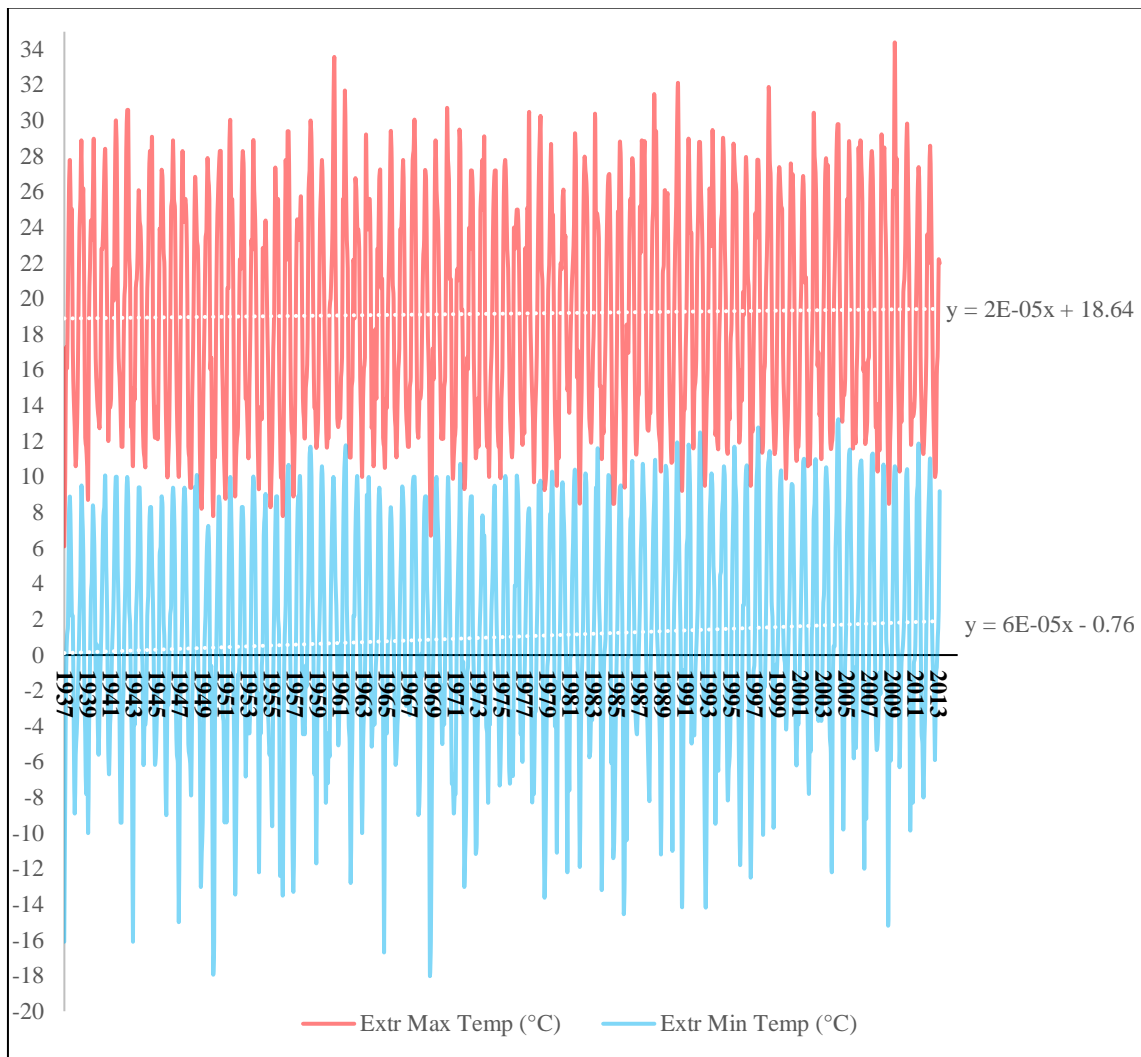


Figure A.3 Monthly Ambient Temperature at YVR from 1937 to 2013

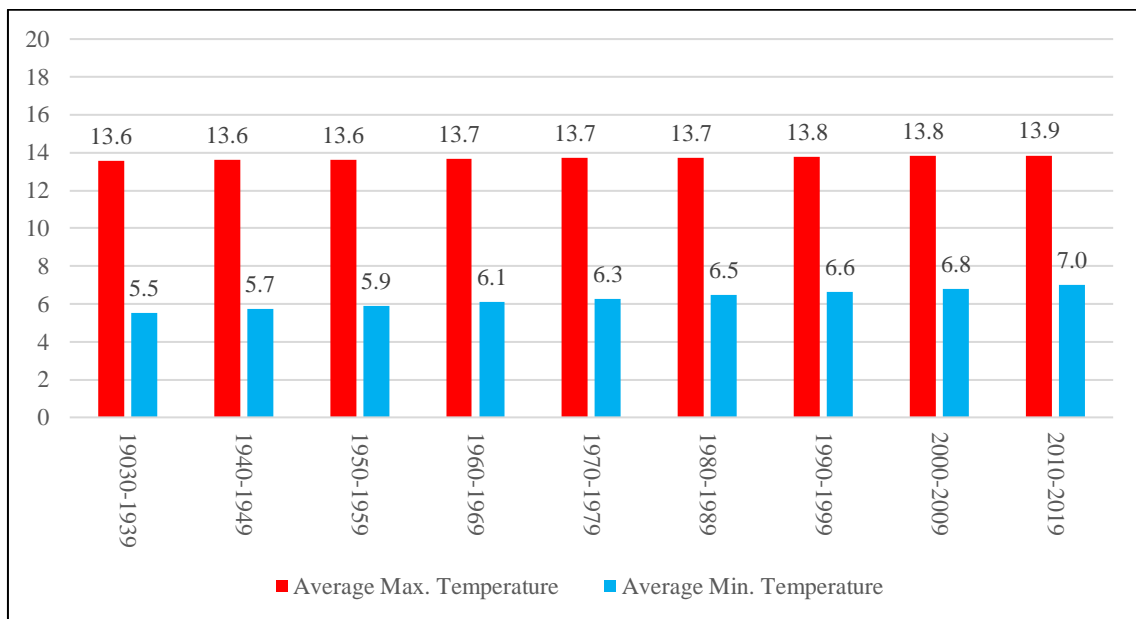


Figure A.4 Decade Average Temperature Trendlines for YVR from 1930-1939 to 2010-2019

Montreal Trudeau International Airport

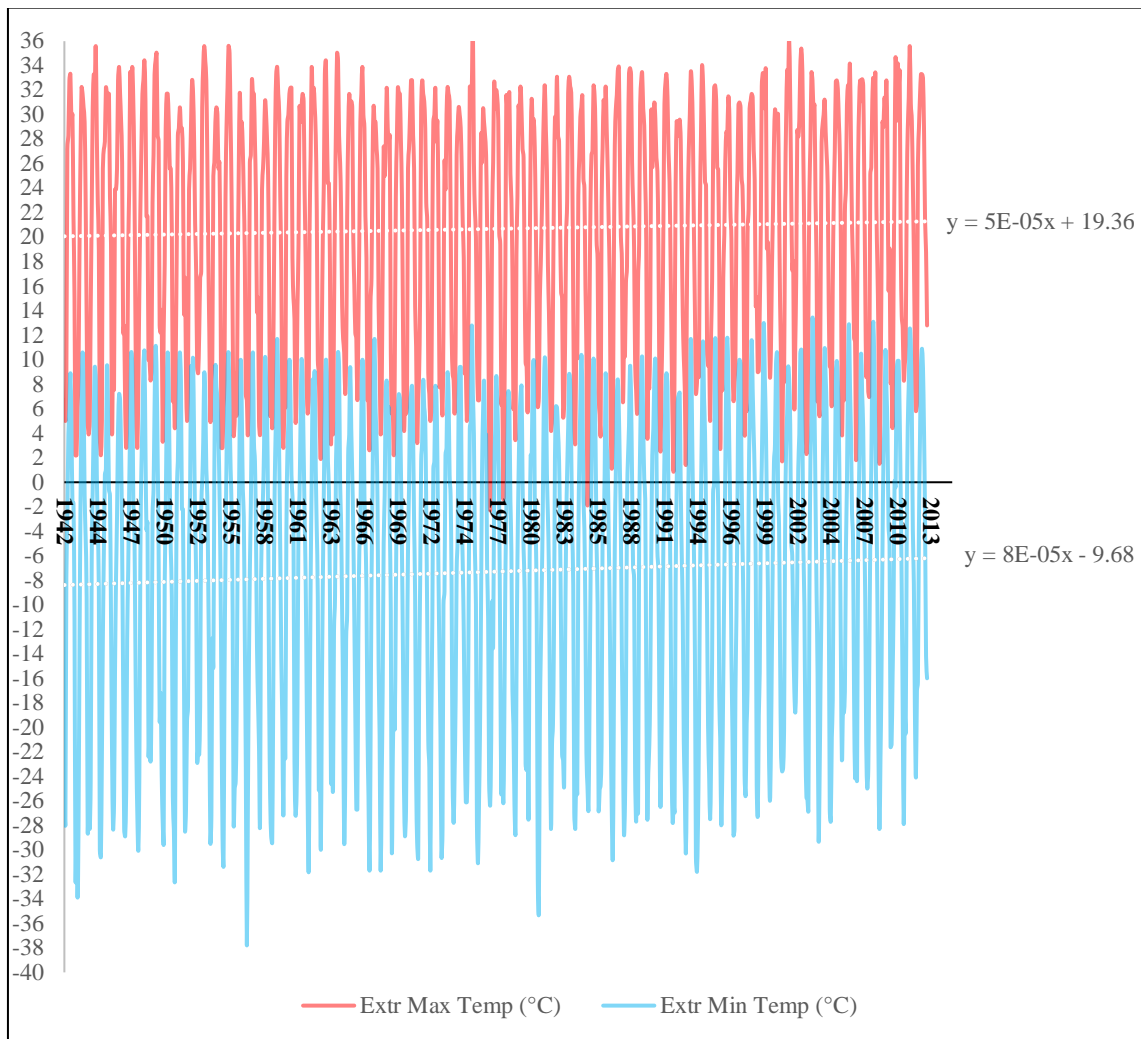


Figure A.5 Monthly Ambient Temperature at YUL from 1942 to 2013

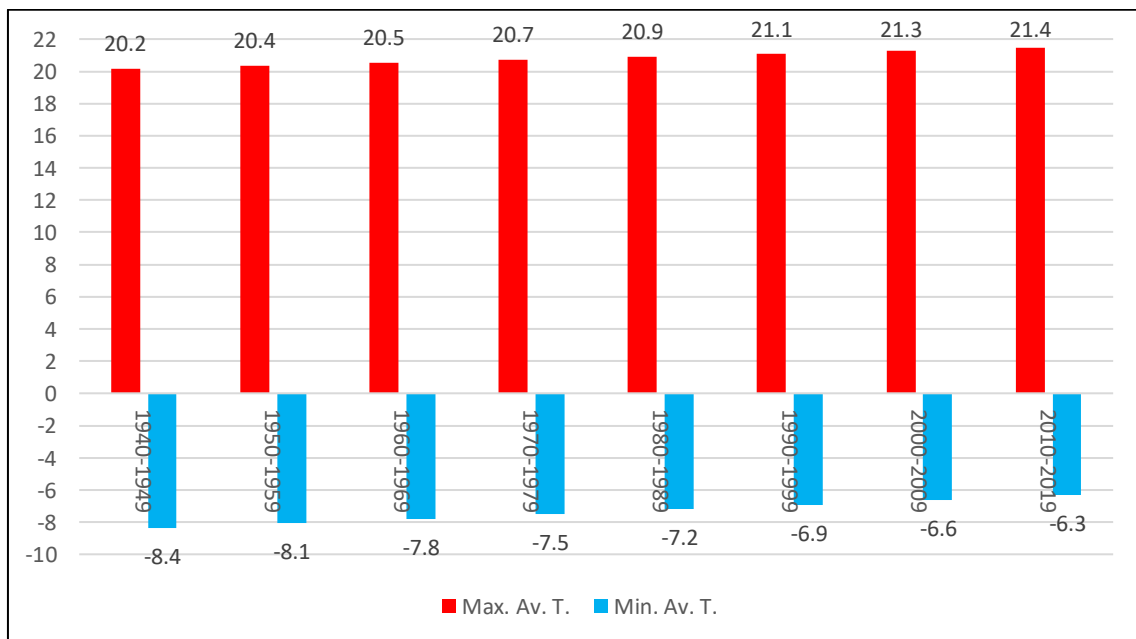


Figure A.6 Decade Average Temperature Trendlines for YUL Since 1940-1949 to 2010-2019

Halifax Stanfield International Airport

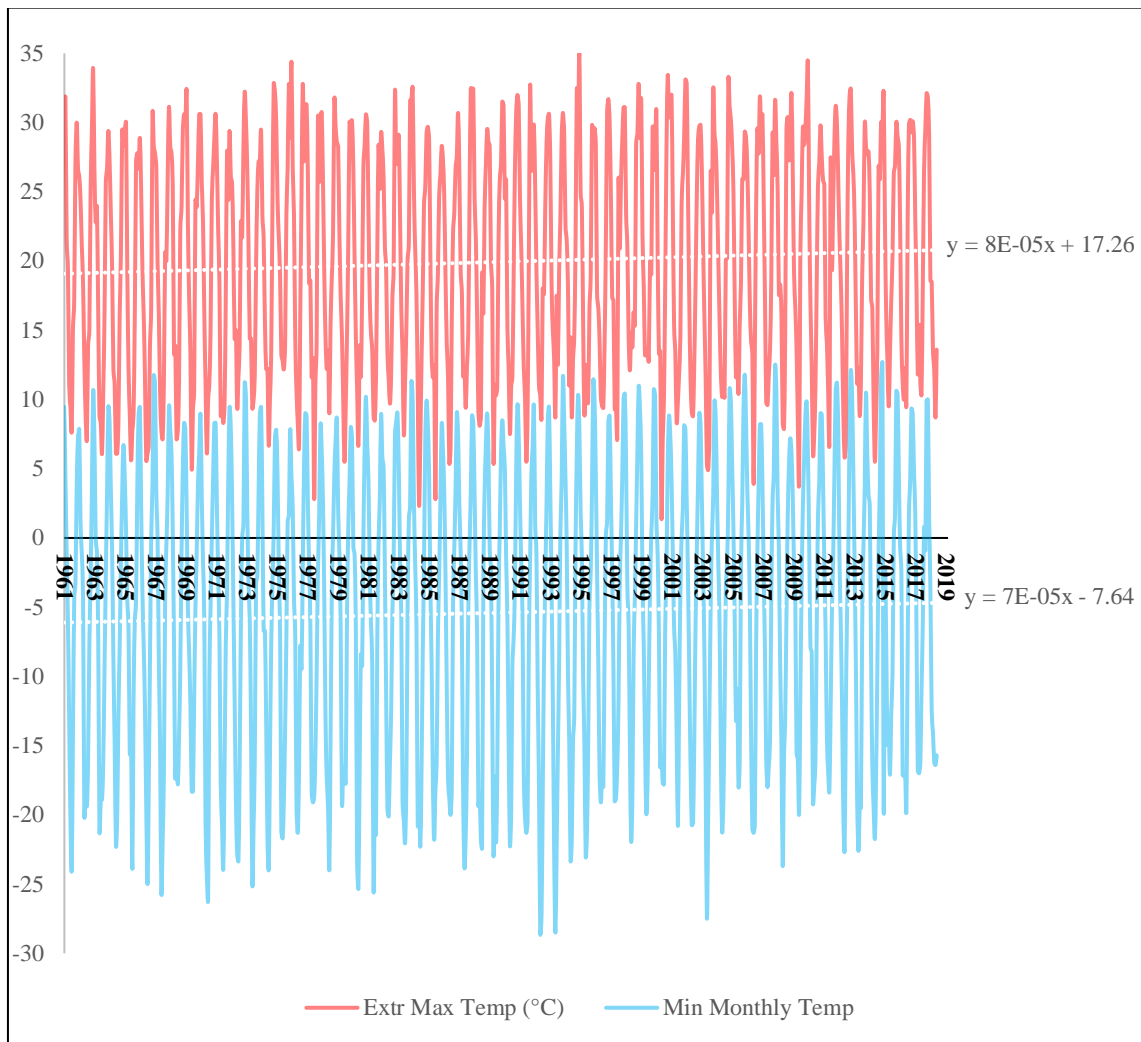


Figure A.7 Monthly Ambient Temperature at YHZ from 1961 to 2019

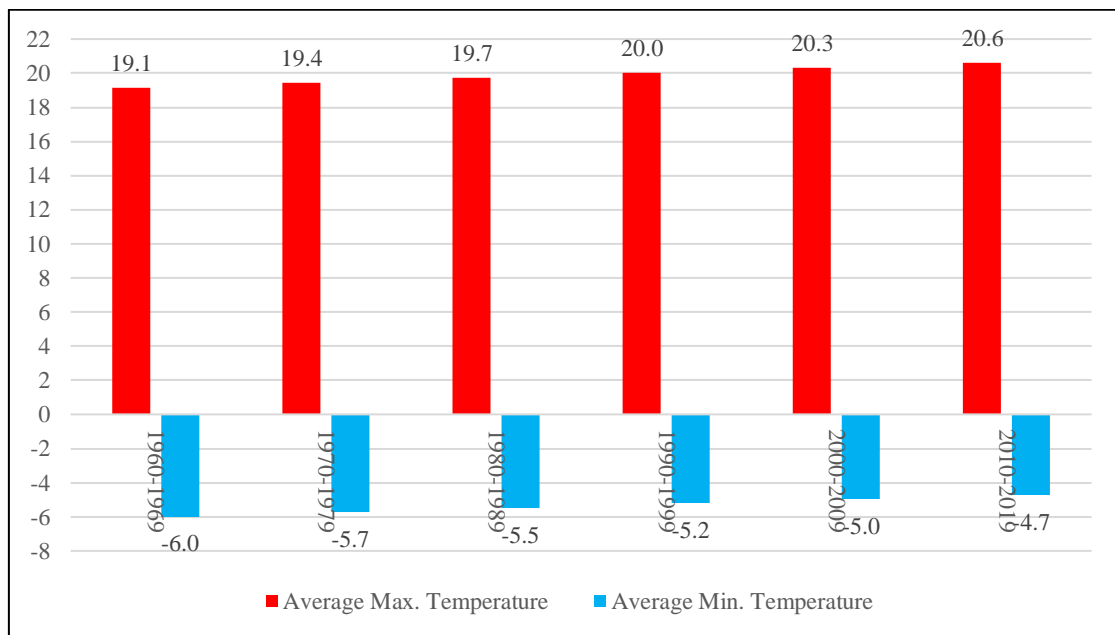


Figure A.8 Decade Average Temperature Trendlines for YHZ from 1960-1969 to 2010-2019

Calgary International Airport

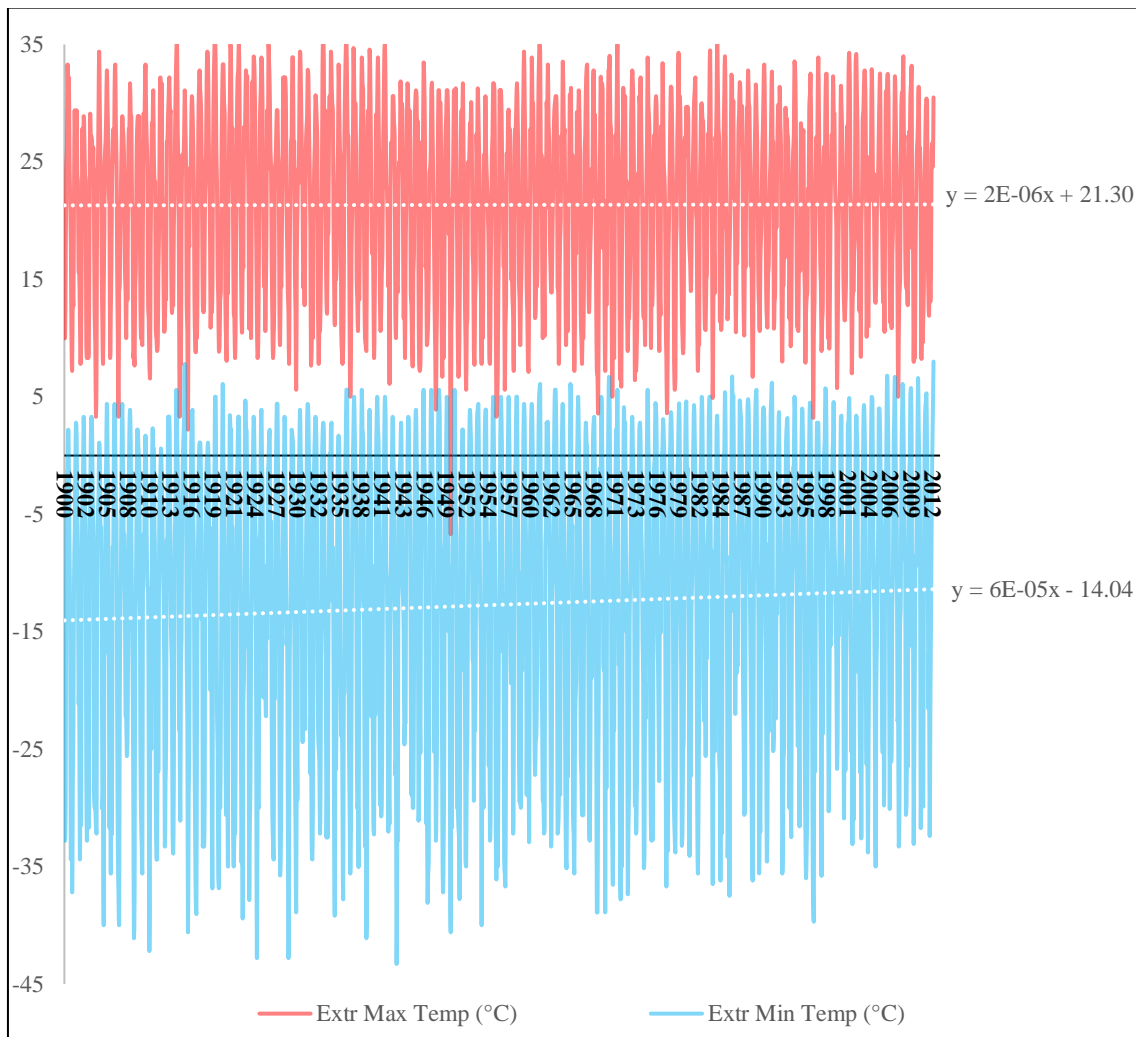


Figure A.9 Monthly Ambient Temperature at YYC from 1900 to 2012

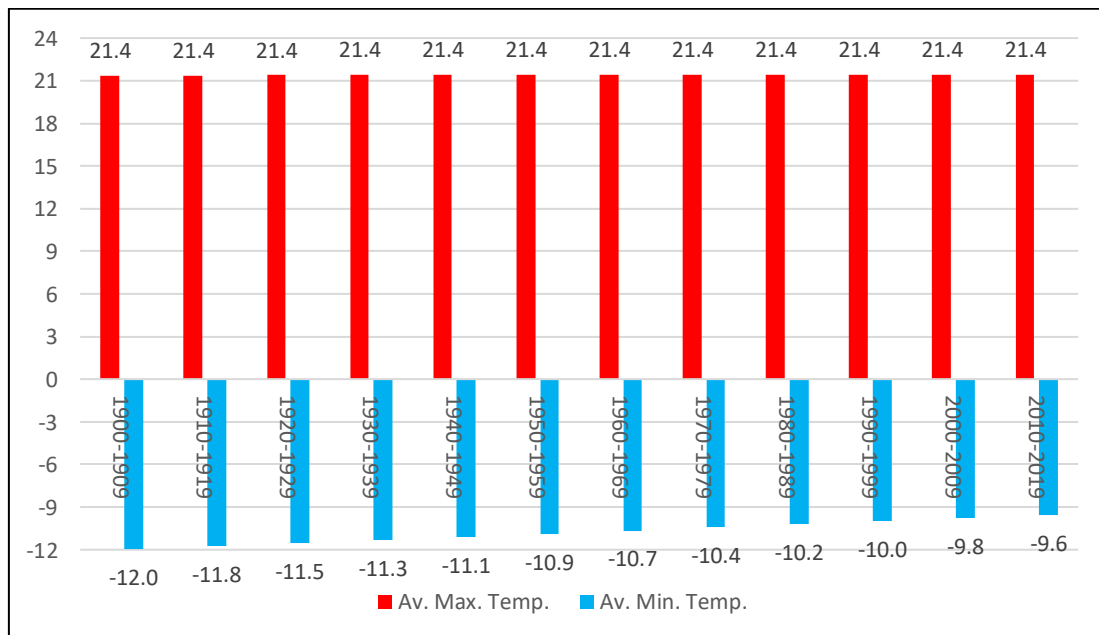


Figure A.10 Decade Average Temperature Trendlines for YYC Since 1900-1909 to 2010-2019

Saskatoon International Airport

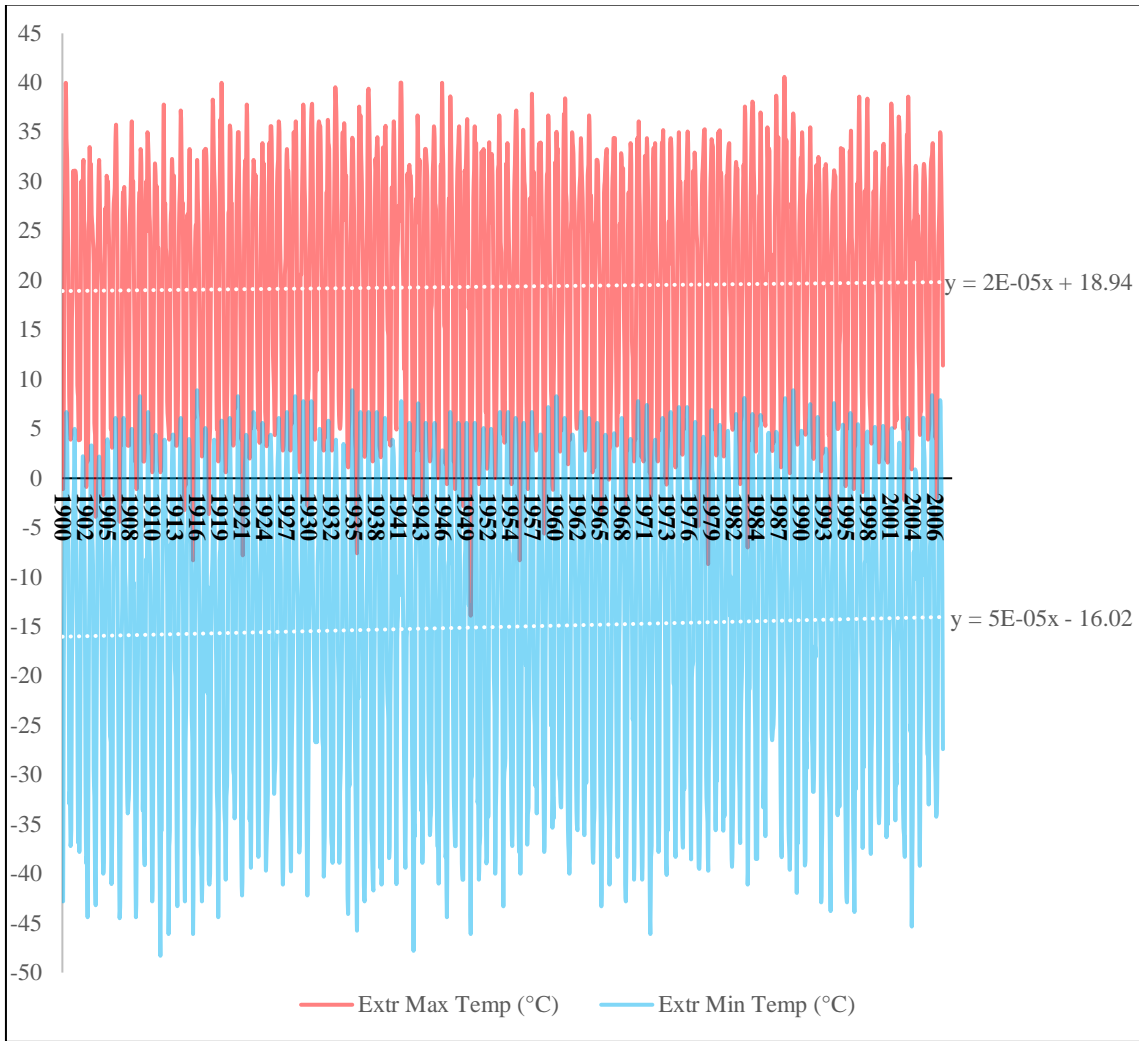


Figure A.9 Monthly Ambient Temperature at YXE from 1900 to 2006

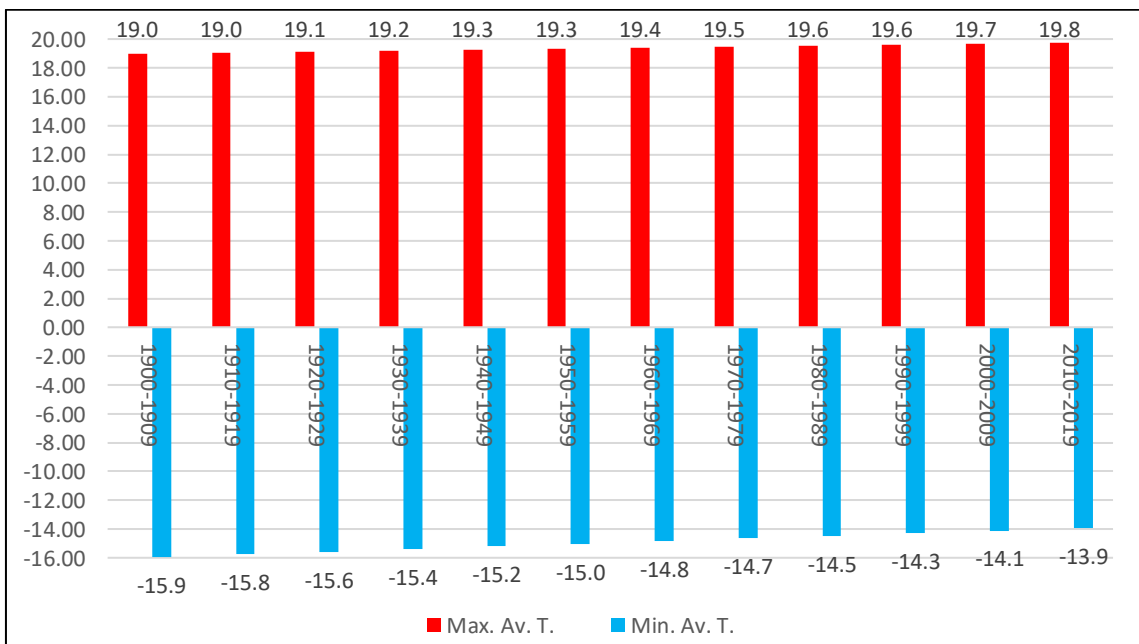


Figure A.10 Decade Average Temperature Trendlines for YXE Since 1900-1909 to 2010-2019

Winnipeg International Airport

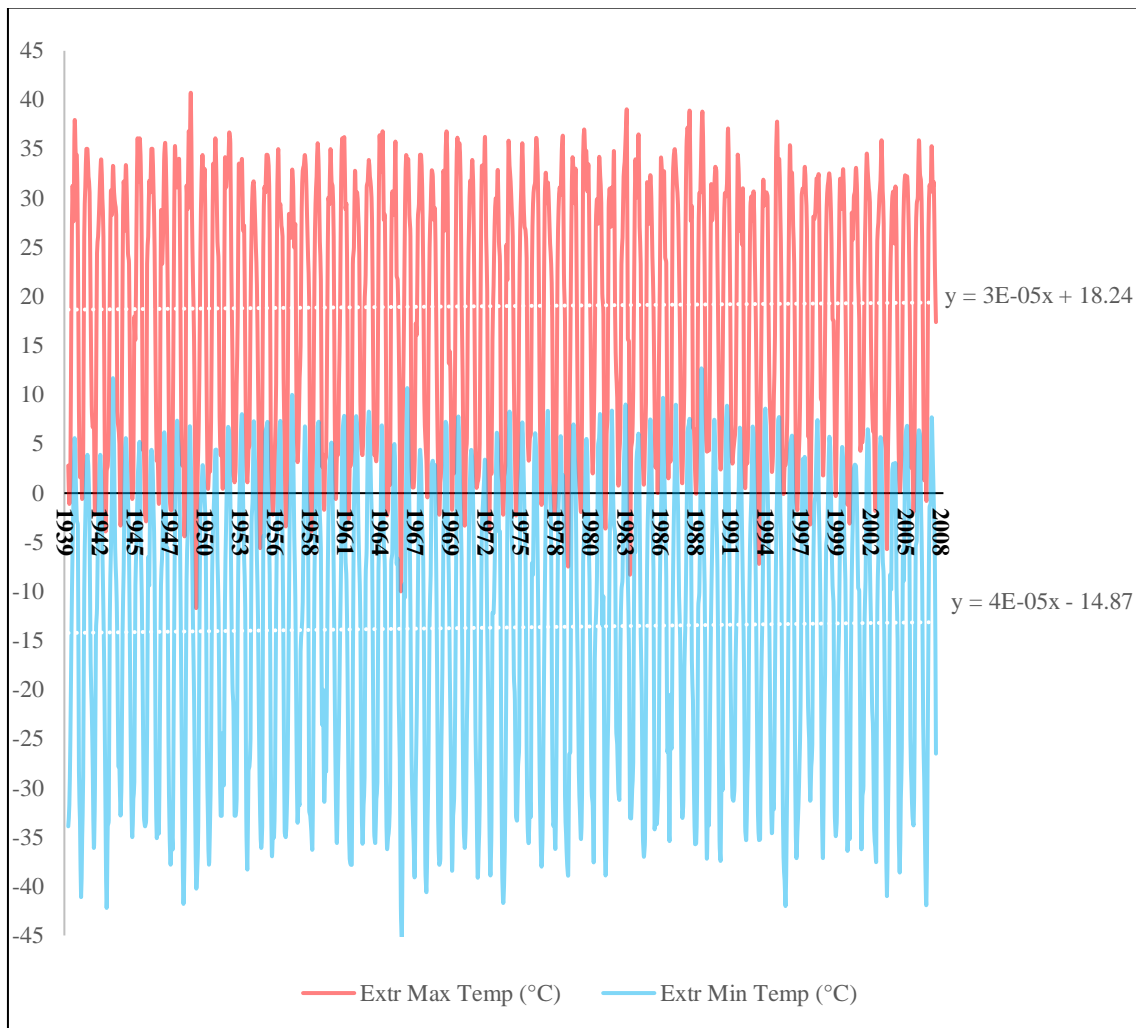


Figure A.11 Monthly Ambient Temperature at YWG from 1939 to 2008

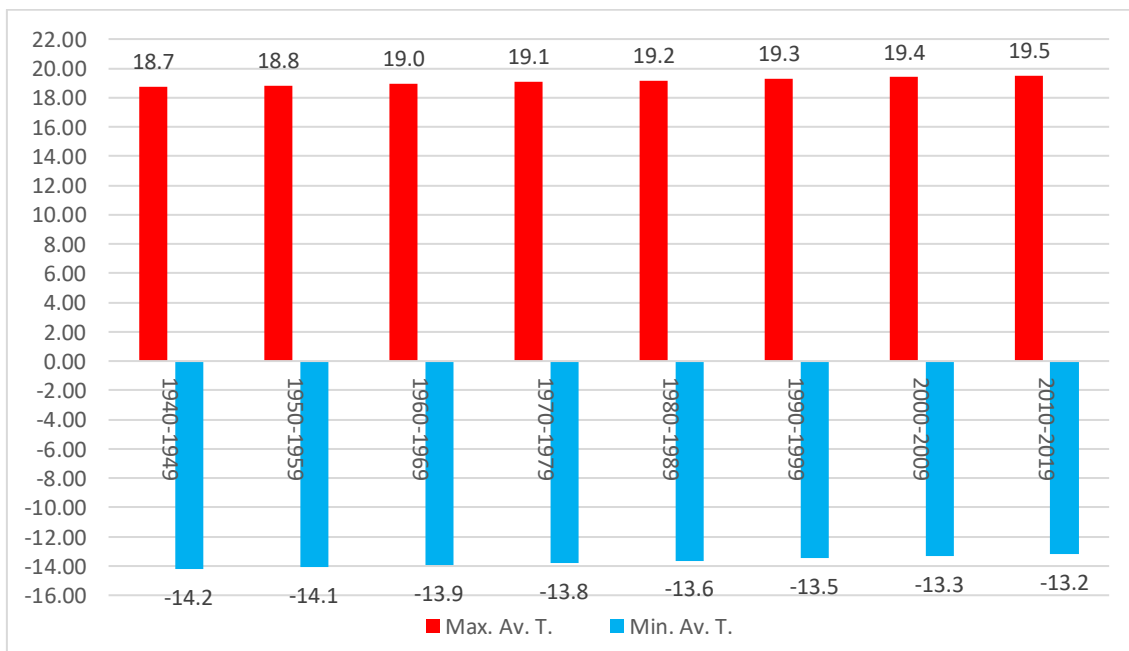


Figure A.12 Decade Average Temperature Trendlines for YWG Since 1940-1949 to 2010-2019

Moncton International Airport

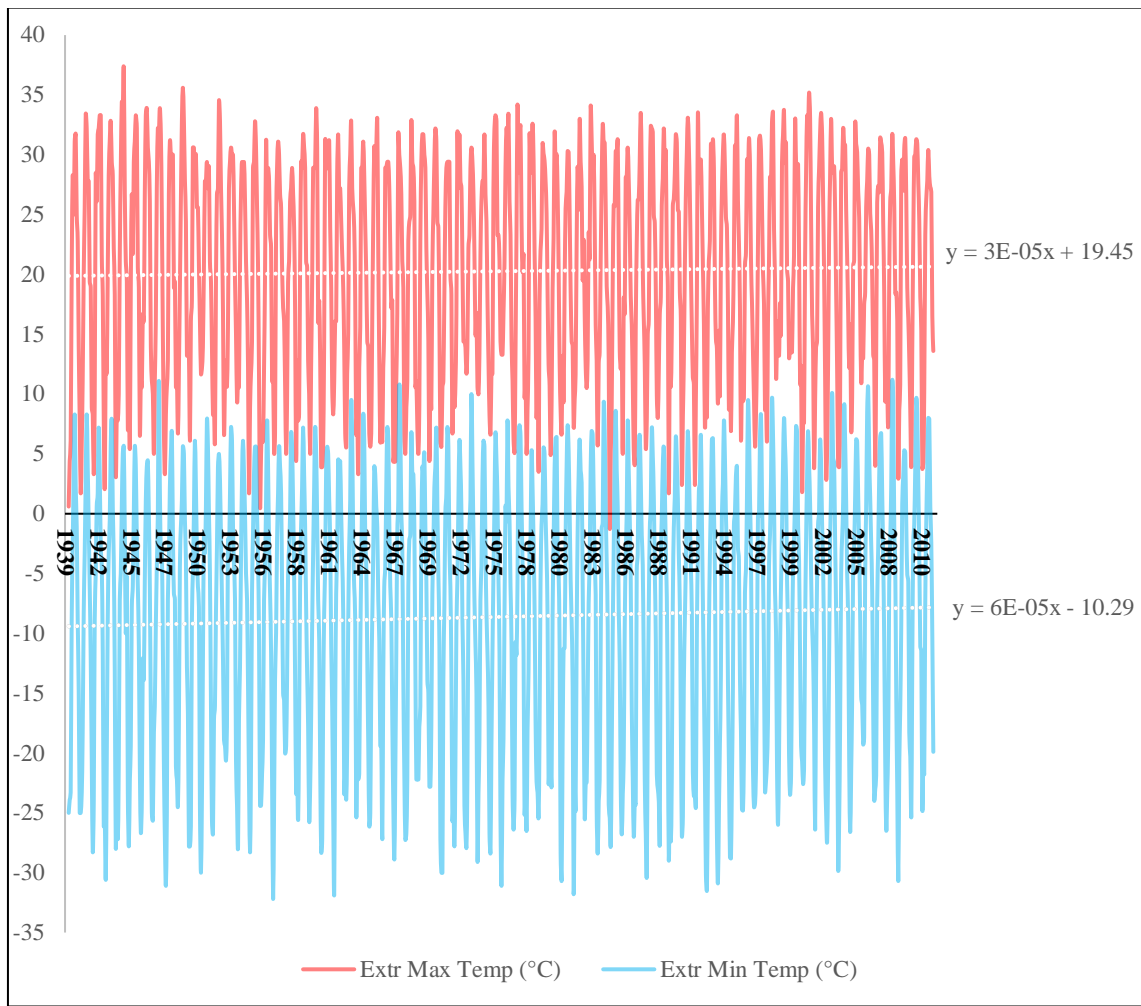


Figure A.13 Monthly Ambient Temperature at YQM from 1939 to 2010

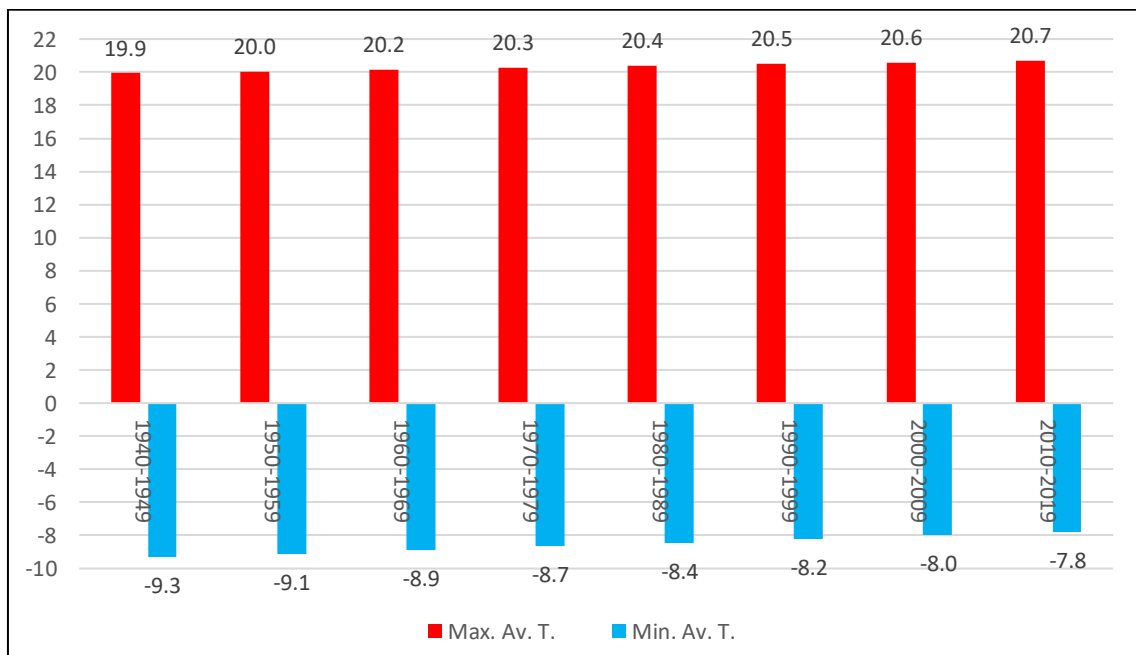


Figure A.14 Decade Average Temperature Trendlines for YQM Since 1940-1949 to 2010-2019

Whitehorse International Airport

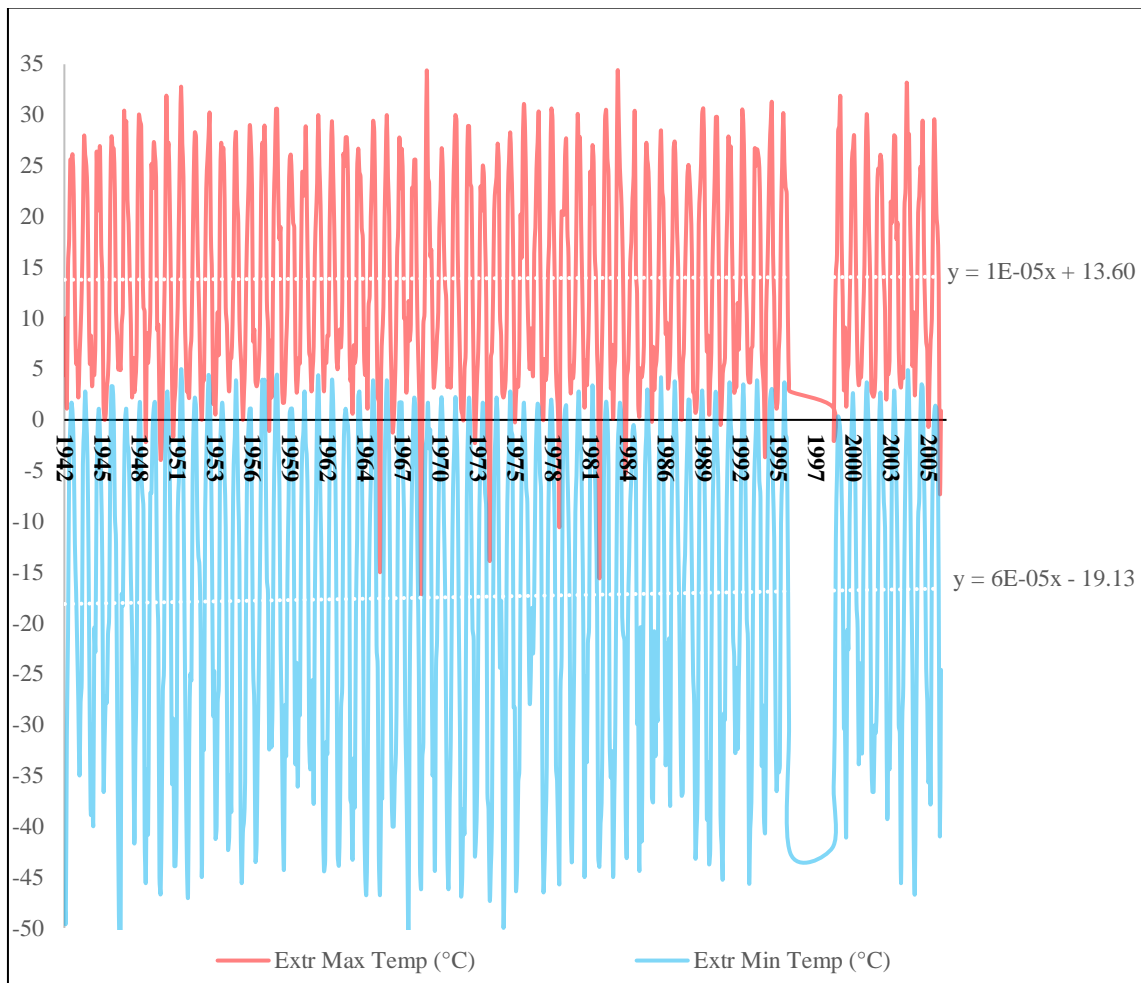


Figure A.15 Monthly Ambient Temperature at YXY from 1942 to 2009

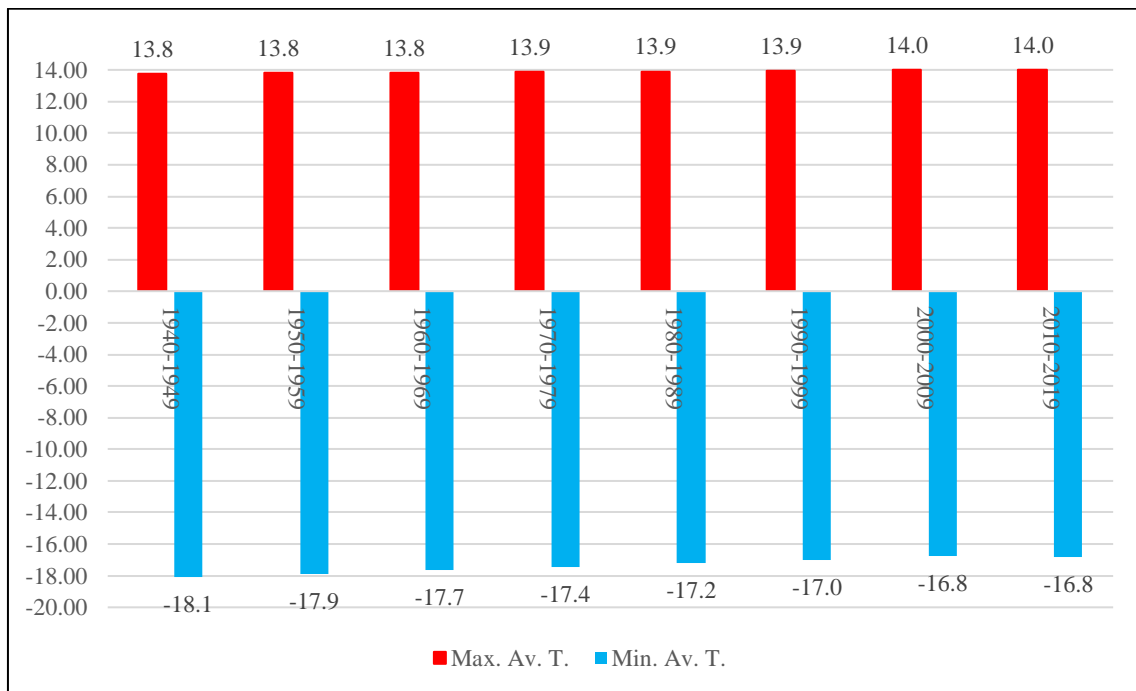


Figure A.16 Decade Average Temperature Trendlines for YXY Since 1940-1949 to 2010-2019

Yellowknife International Airport

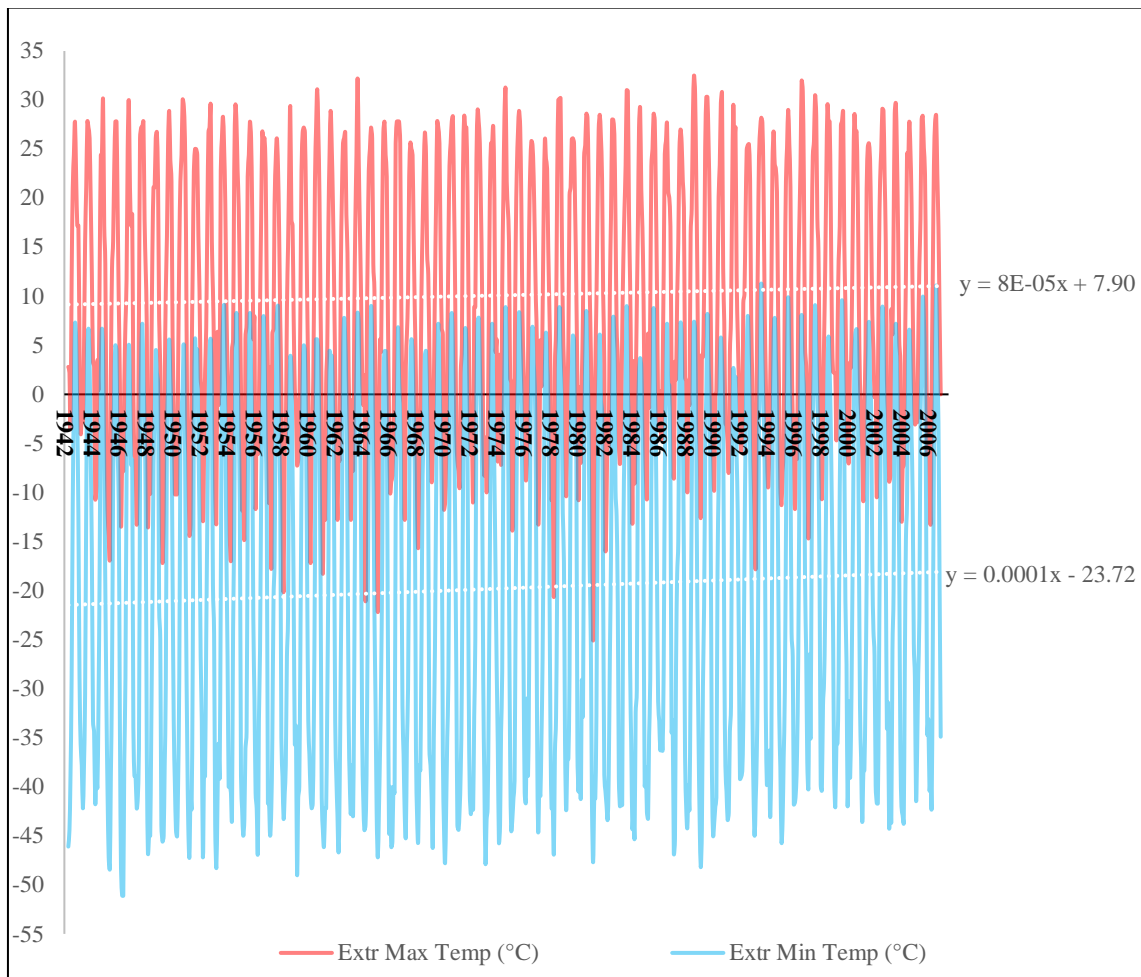


Figure A.17 Monthly Ambient Temperature at YZF from 1942 to 2006

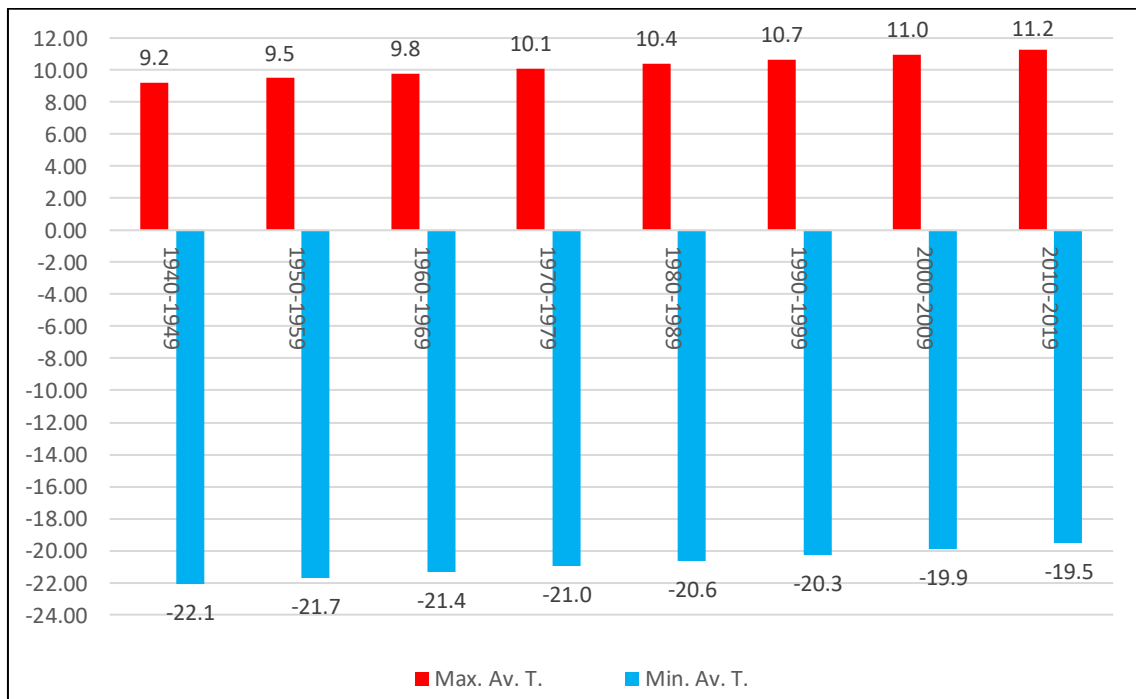


Figure A.18 Decade Average Temperature Trendlines for YXY Since 1940-1949 to 2010-2019

Iqaluit Airport

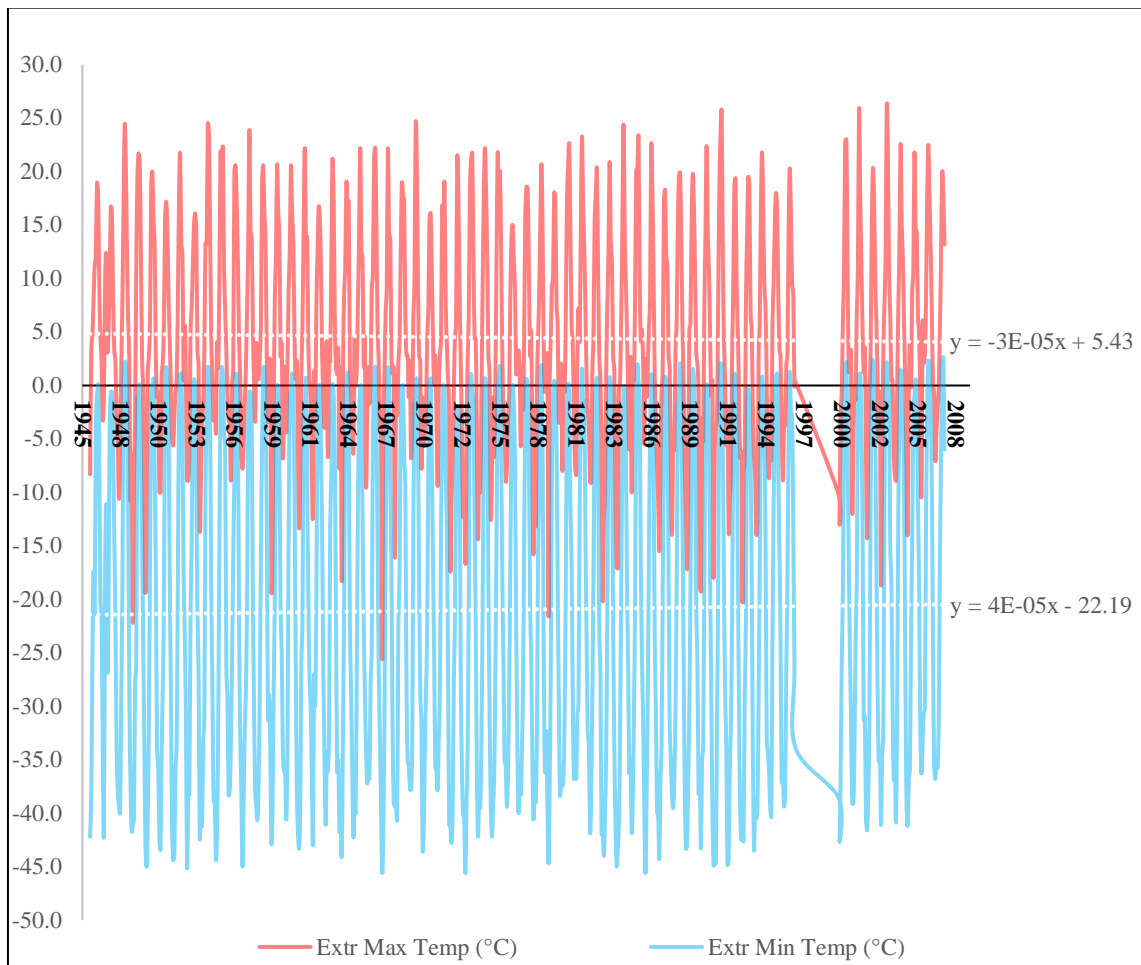


Figure A.19 Monthly Ambient Temperature at YFB from 1945 to 2008

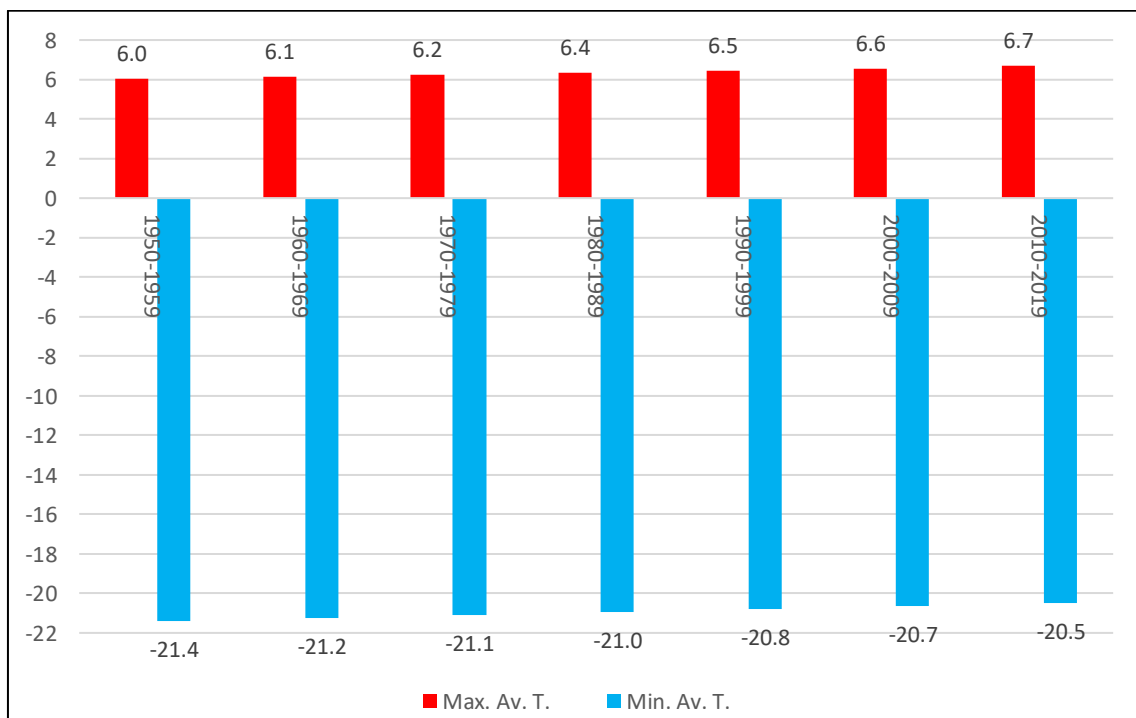


Figure A.20 Decade Average Temperature Trendlines for YFB Since 1950-1959 to 2010-2019

Freeze-Thaw Cycles Algorithm

Values' Description:

Tm1= Mean Temperature current day [Given value]

Tm2= Mean Temperature next day1 [Given value]

Ts1= Surface Temperature current day

Ts2= Surface Temperature next day

Tr= Temperature range = -15°C to 15°C [subjective]

dt= Temperature difference between current day and next day > 0.2°C [subjective]

TC= Temperature Check

dTC= dT Check

FS= Freeze Search

TS= Thaw Search

Excel Algorithm:

Ts1= 0.0065*Tm1^2 + 1.1828*Tm1 + 1.7533

TC= IF(Ts1>=(-15); IF(Ts1<=15;1;0);0)

dTC= IF(TC =1;IF((ABS(Ts2-Ts1))>0.2;1;0);0)

IF(TC + dTC =2;IF(Ts2<0;IF(Ts1>0;"Freeze";"none");"none");"none")

IF(TC + dTC =2;IF(Ts2>0;IF(Ts1<0;"Thaw";"none");"none");"none")

Freeze Count= IF(FS="Freeze";1;0)

Thaw Count= IF(TS="Thaw";1;0)

Freeze-Thaw Cycles/day= Average(Freeze Count; Thaw Count) [0 or 0.5]

Freeze-Thaw Cycles/year= Sum(Freeze-Thaw Cycles/day) [for the entire evaluated year]

Freeze-Thaw Cycles Results

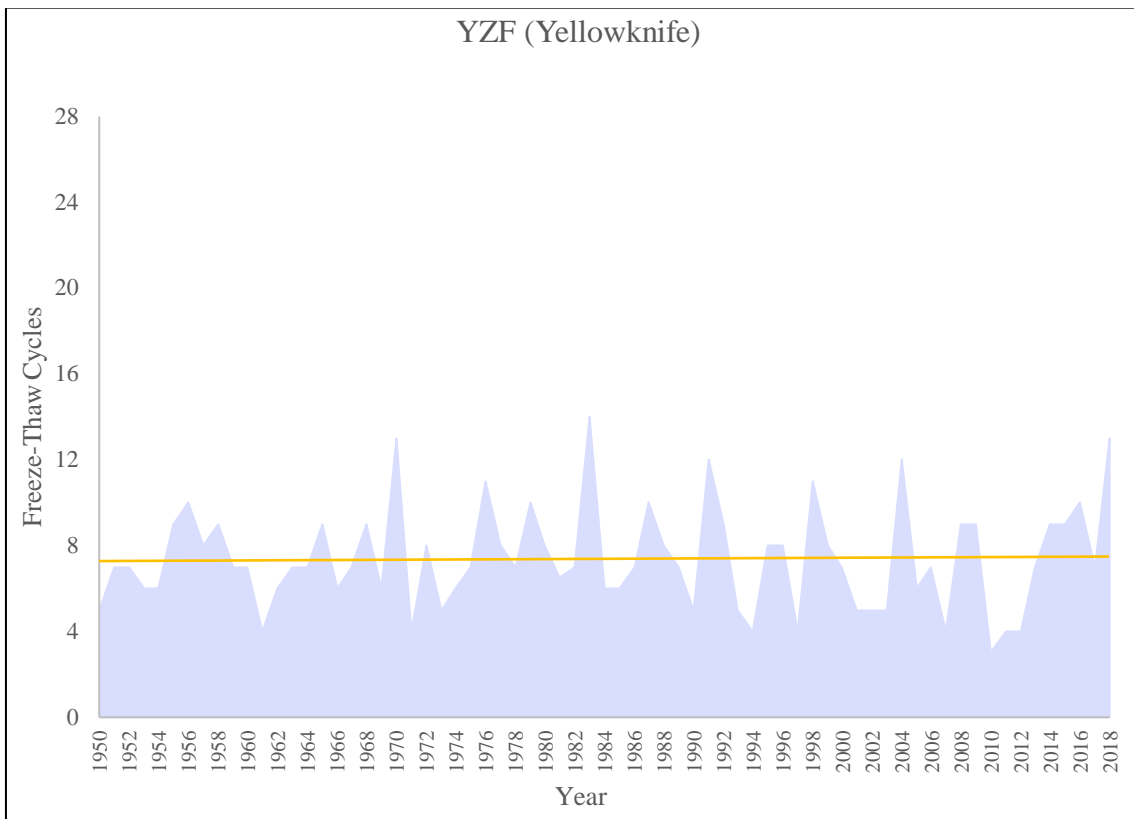


Figure A.21 Annual Freeze-Thaw Cycles for Yellowknife International Airport

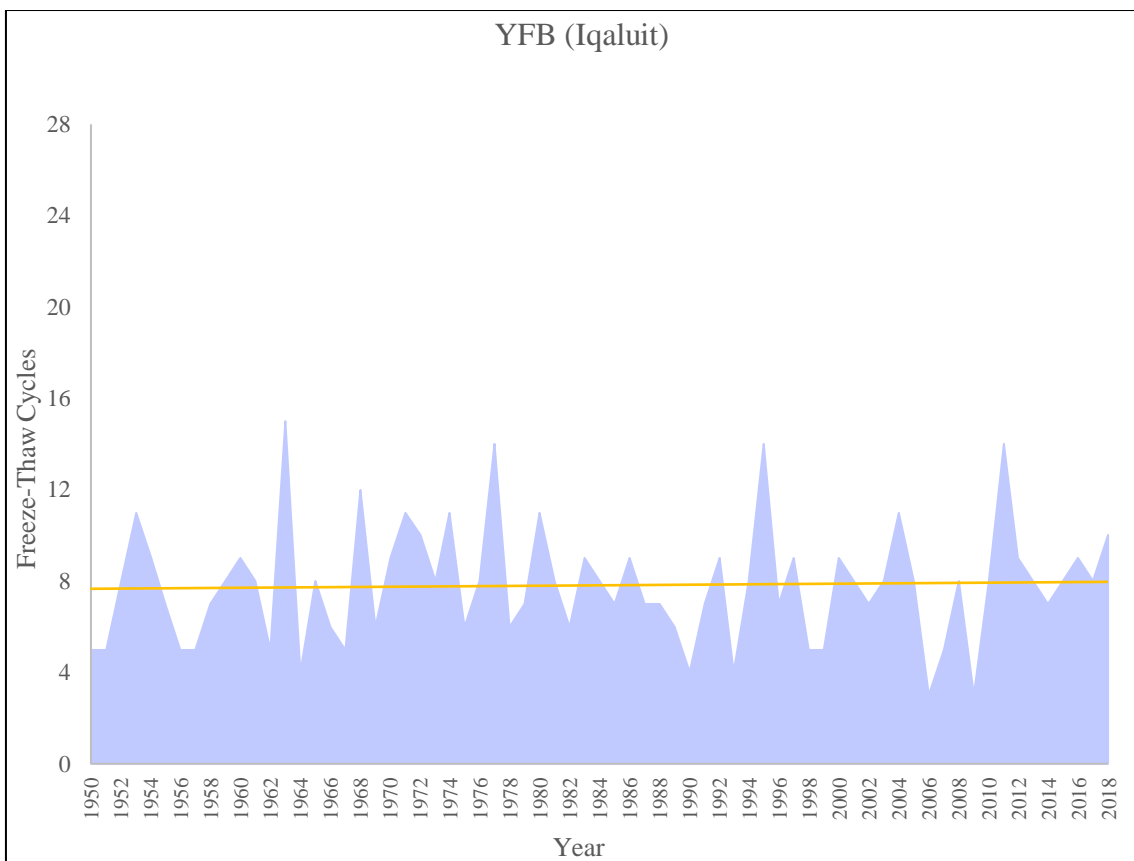


Figure A.22 Annual Freeze-Thaw Cycles for Iqaluit Airport

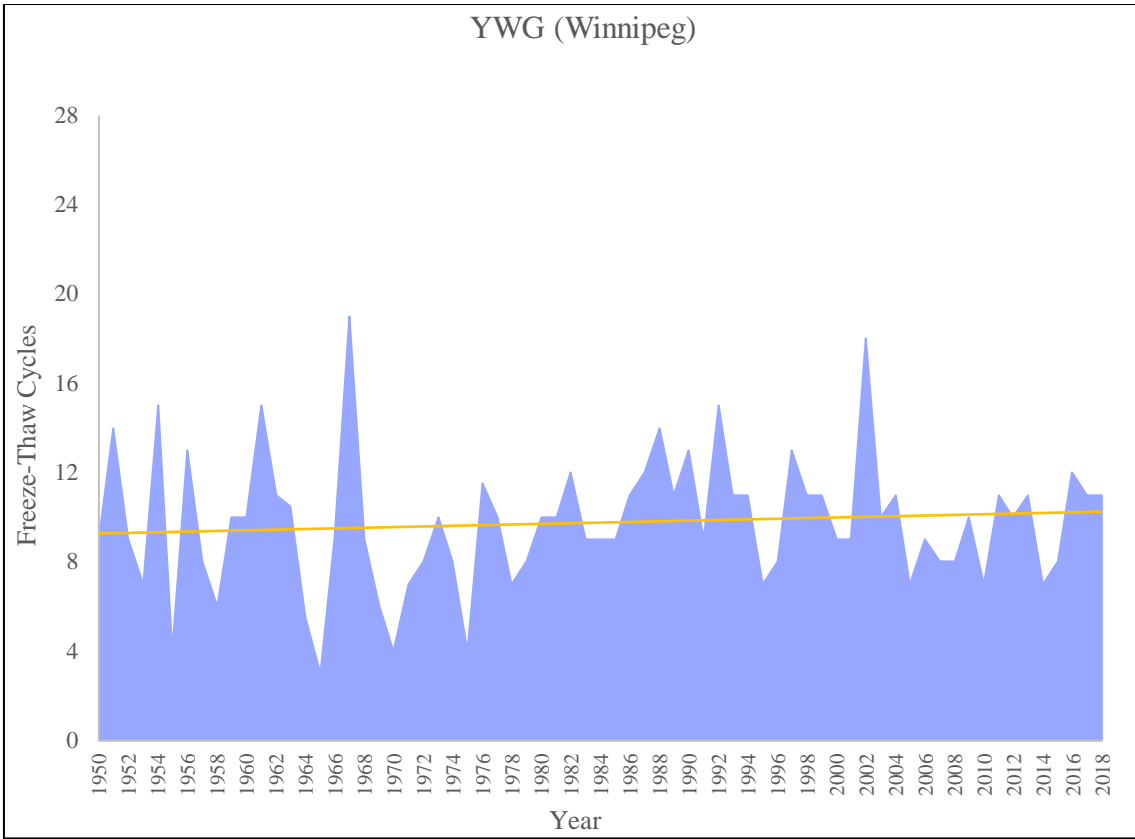


Figure A.23 Annual Freeze-Thaw Cycles for Winnipeg International Airport

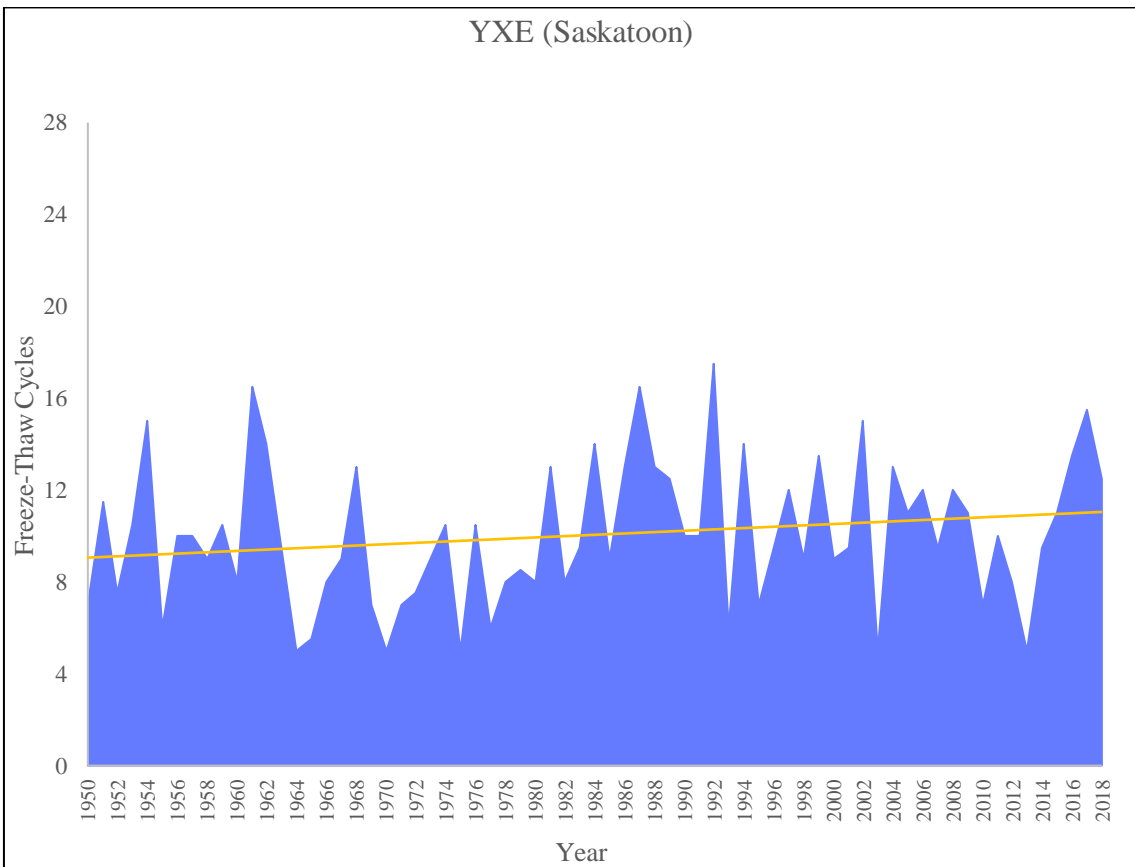


Figure A.24 Annual Freeze-Thaw Cycles for Saskatoon International Airport

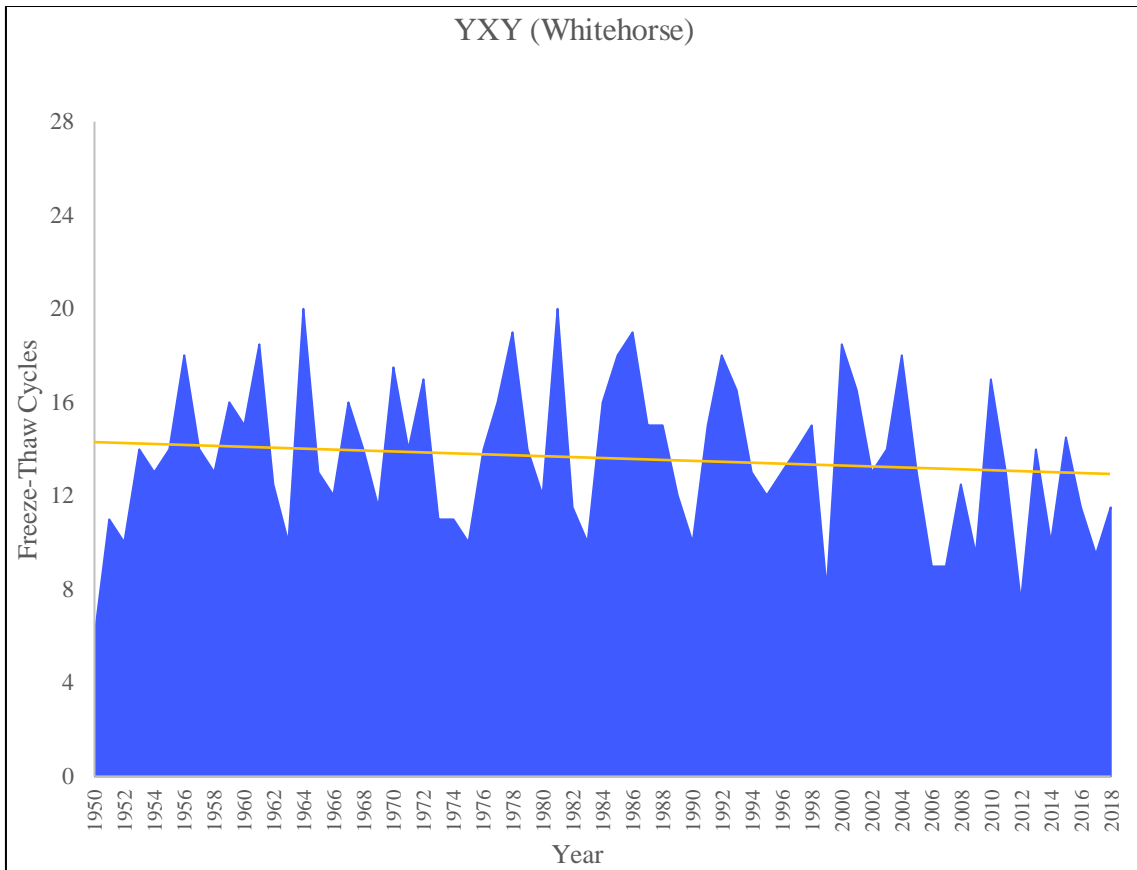


Figure A.25 Annual Freeze-Thaw Cycles for Whitehorse International Airport

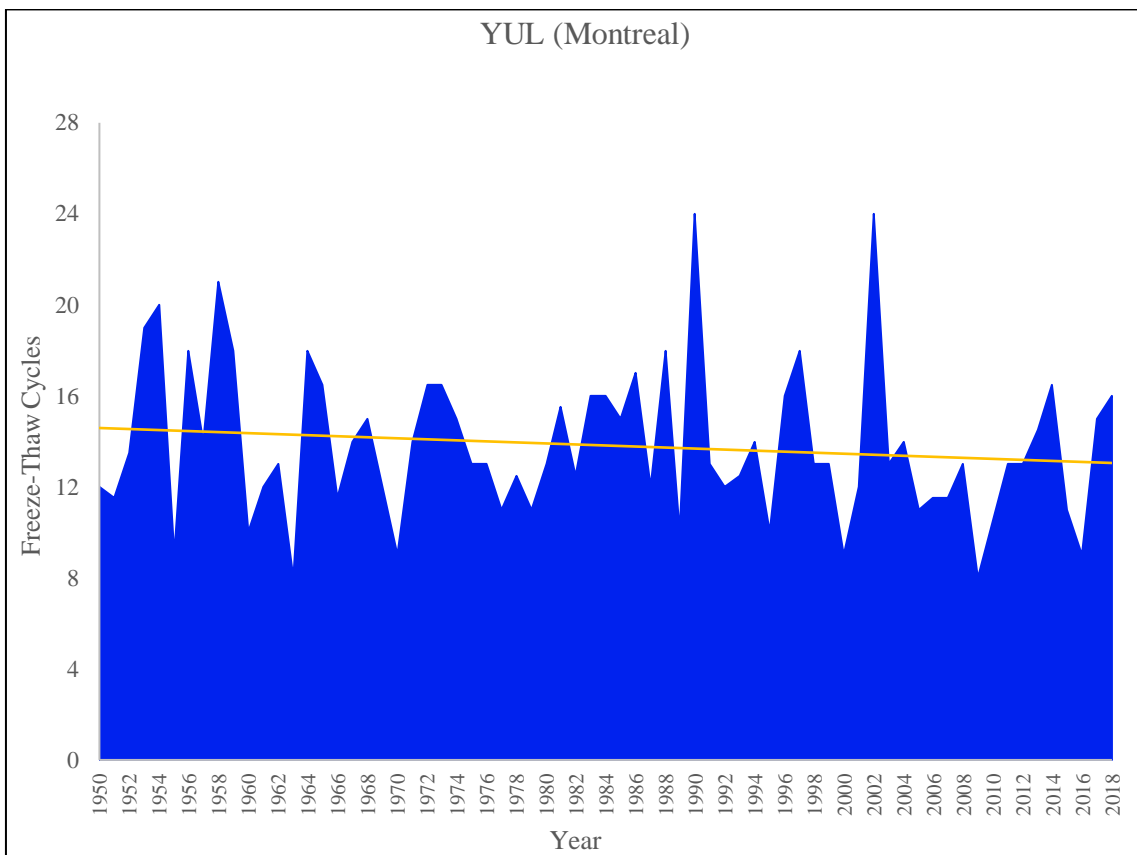


Figure A.26 Annual Freeze-Thaw Cycles for Montreal Trudeau International Airport

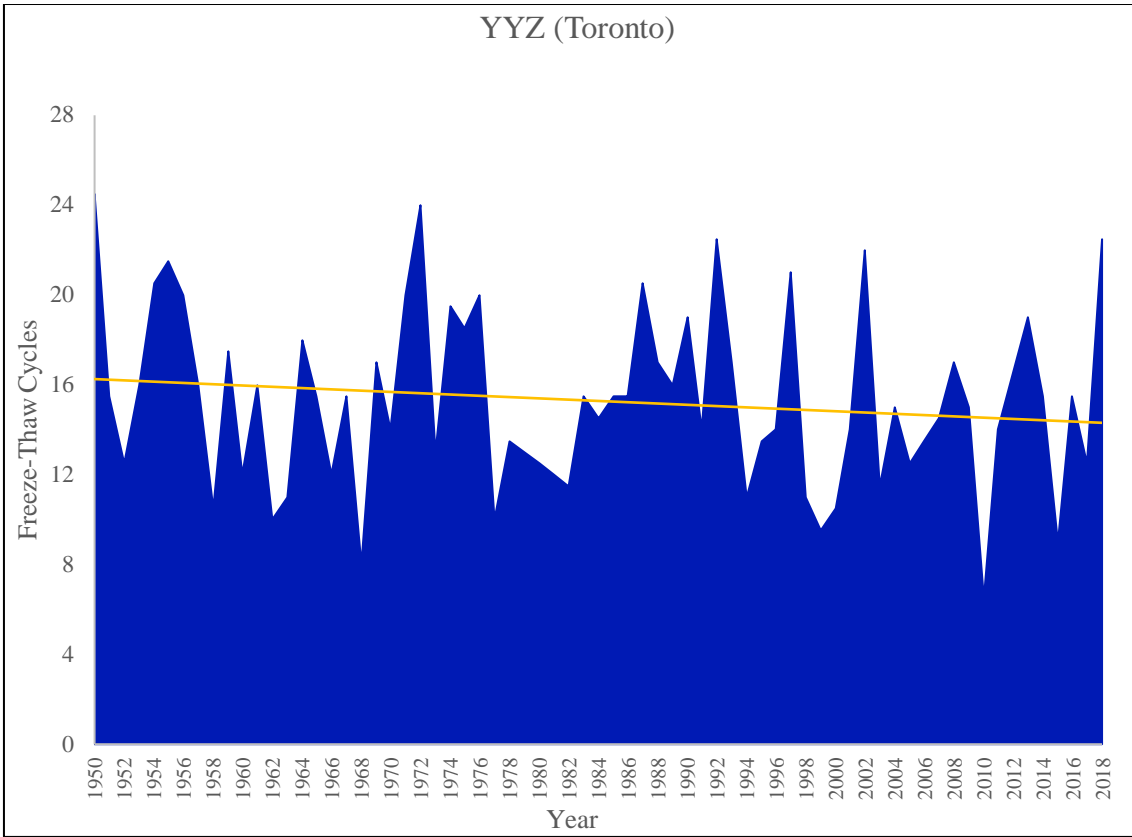


Figure A.27 Annual Freeze-Thaw Cycles for Toronto Pearson International Airport

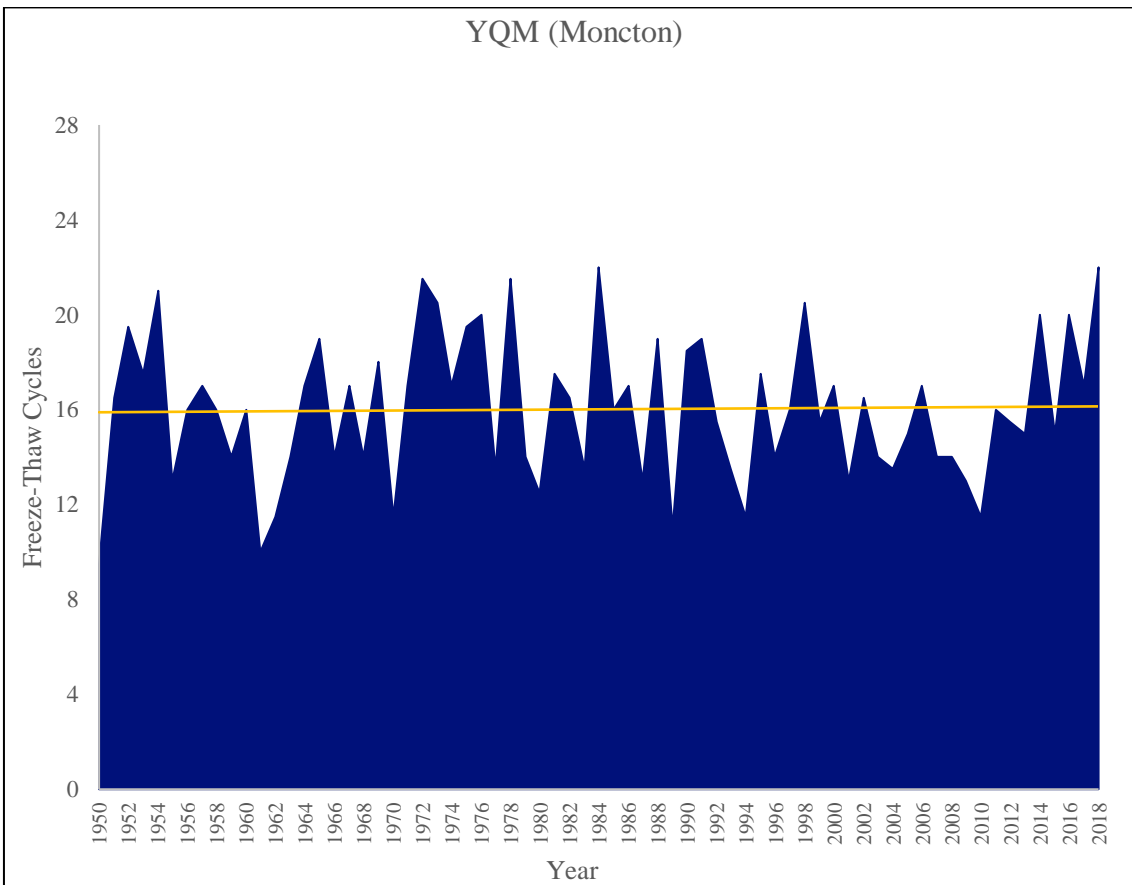


Figure A.28 Annual Freeze-Thaw Cycles for Moncton International Airport

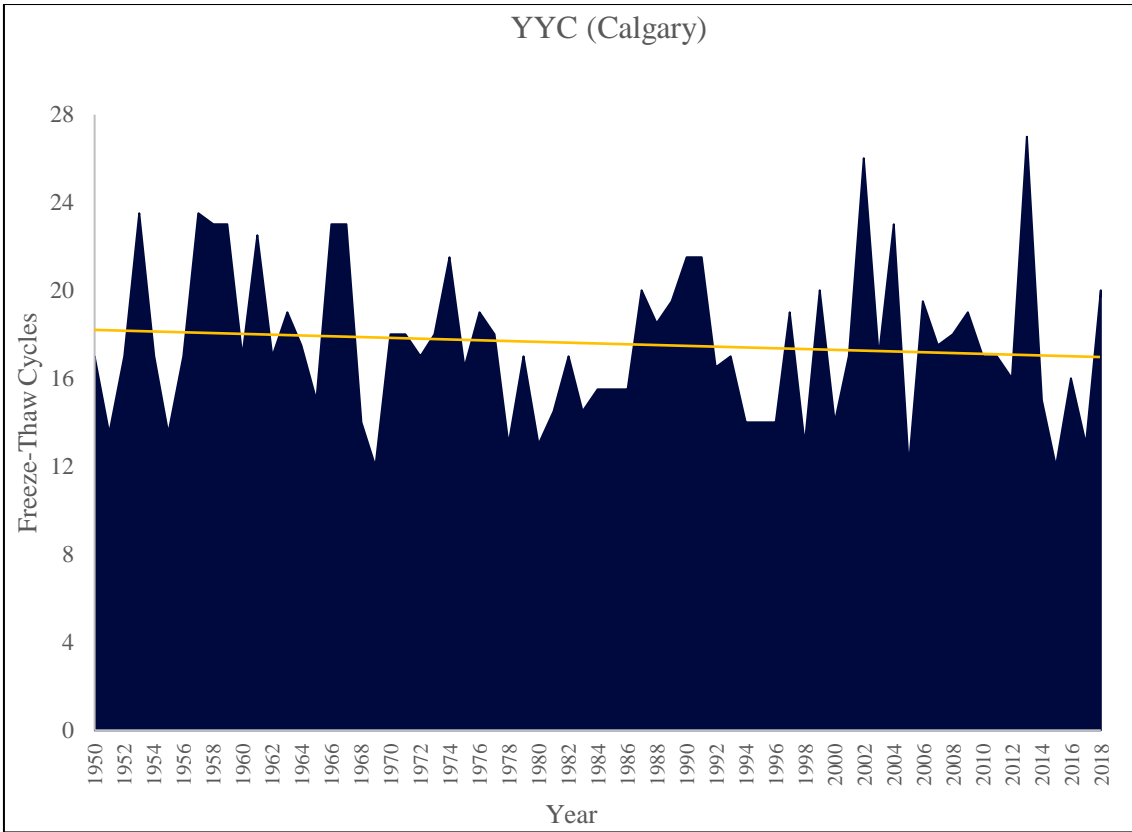


Figure A.29 Annual Freeze-Thaw Cycles for Calgary International Airport

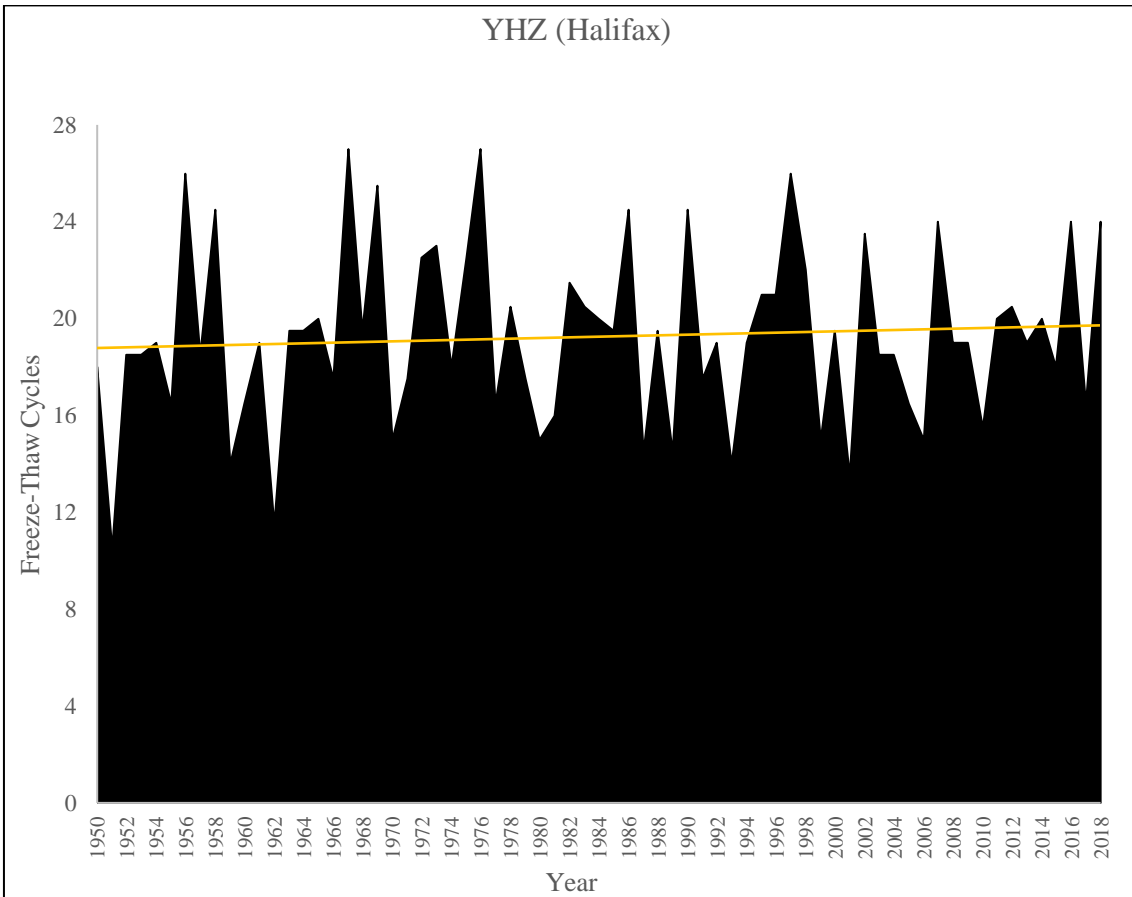


Figure A.30 Annual Freeze-Thaw Cycles for Halifax Stanfield International Airport

Precipitation Results

Toronto Pearson International Airport

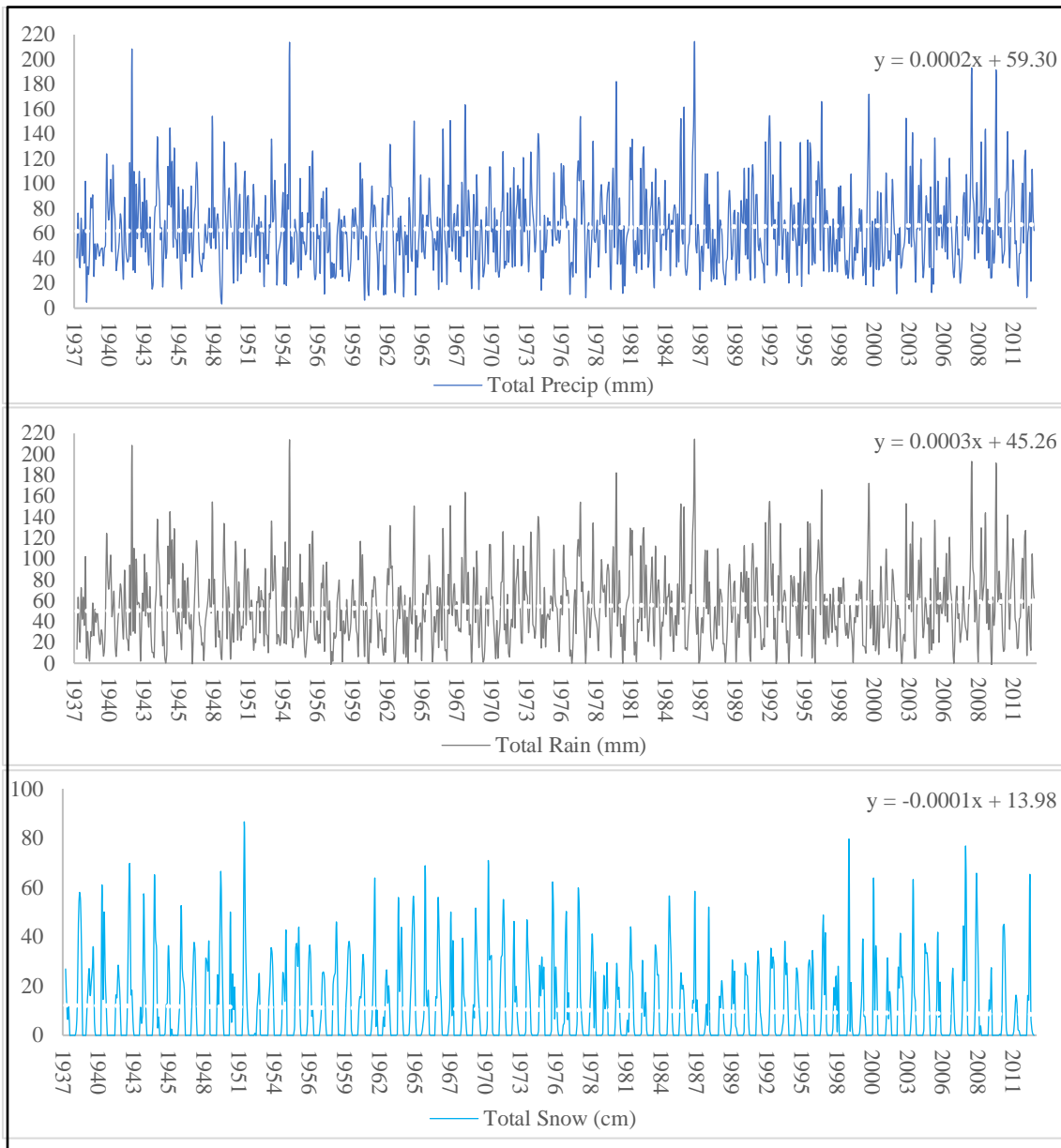


Figure A31 Annual Precipitation, Rainfall, and Snowfall for YYZ from 1937 to 2011

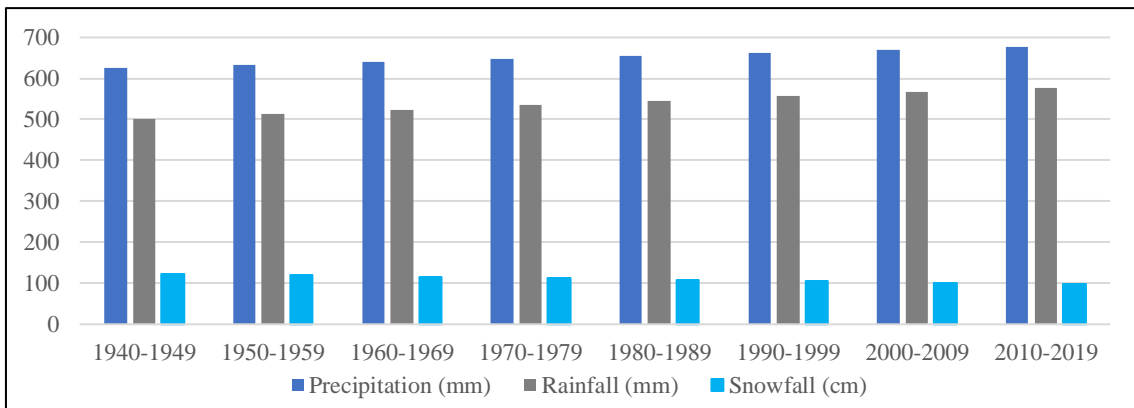


Figure A32 Annual Precip, Rainfall, and Snowfall Trends from YYZ from 1940-1949 to 2010-2019

Vancouver International Airport

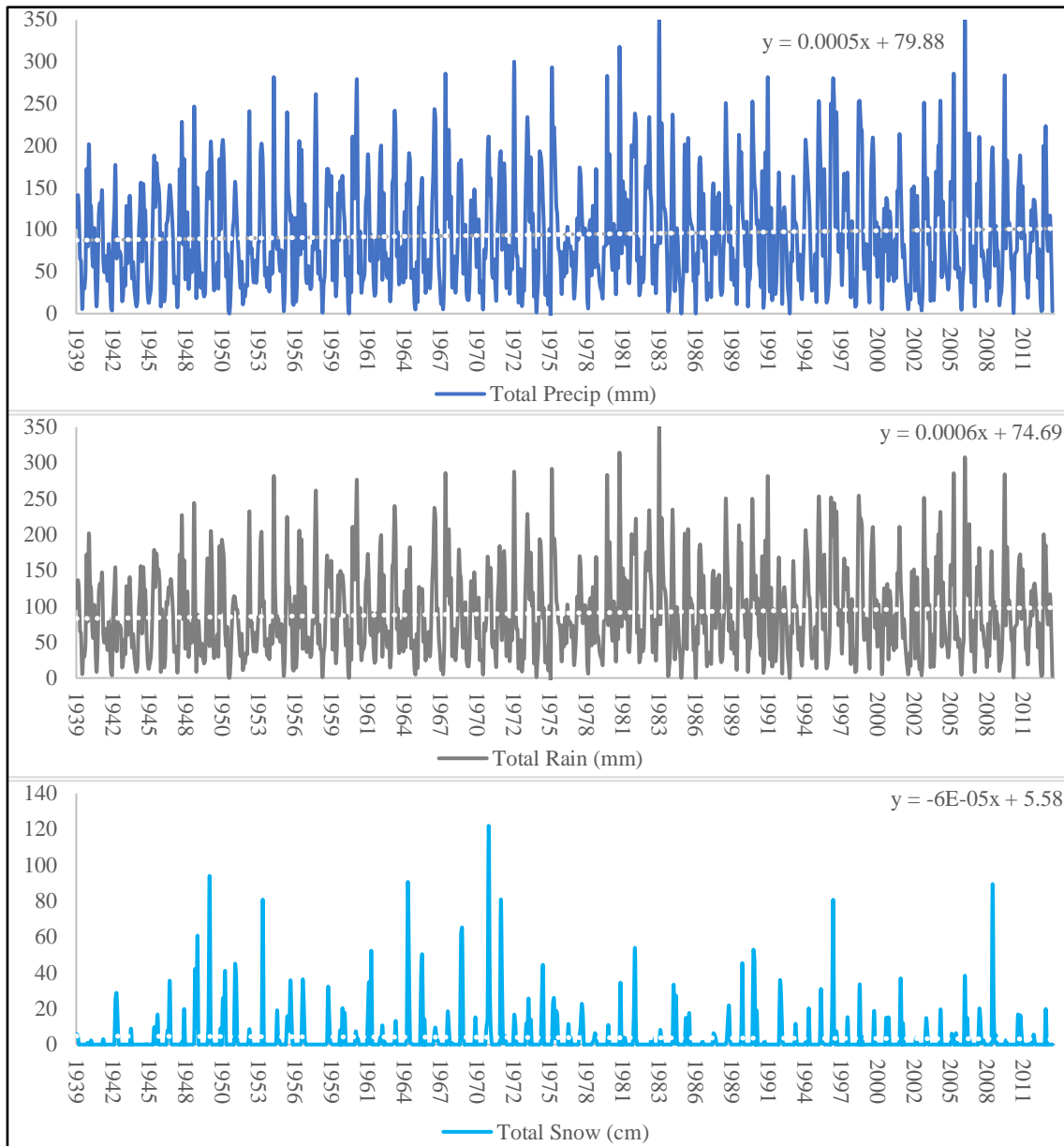


Figure A33 Annual Precipitation, Rainfall, and Snowfall for YVR from 1939 to 2011

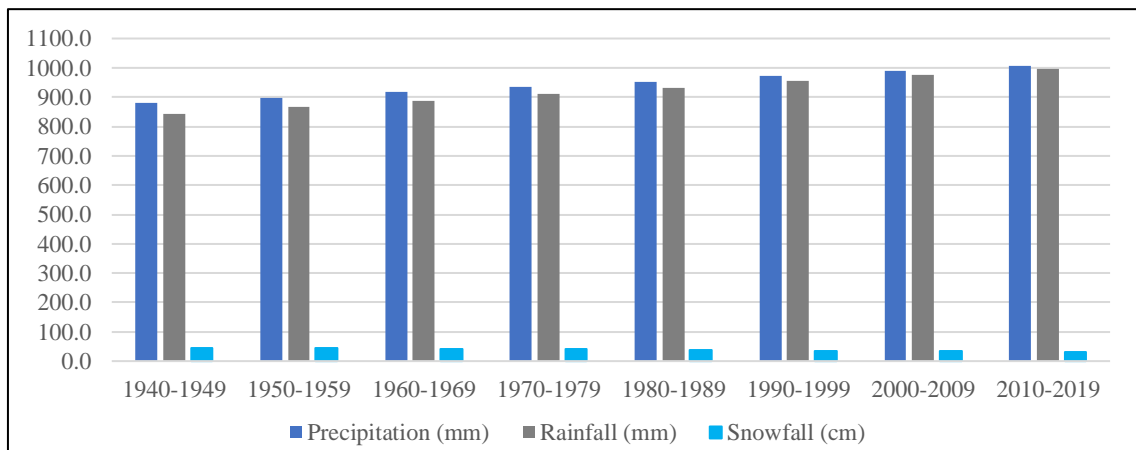


Figure A34 Annual Precip, Rainfall, and Snowfall Trends from YVR from 1940-1949 to 2010-2019

Montreal Trudeau International Airport

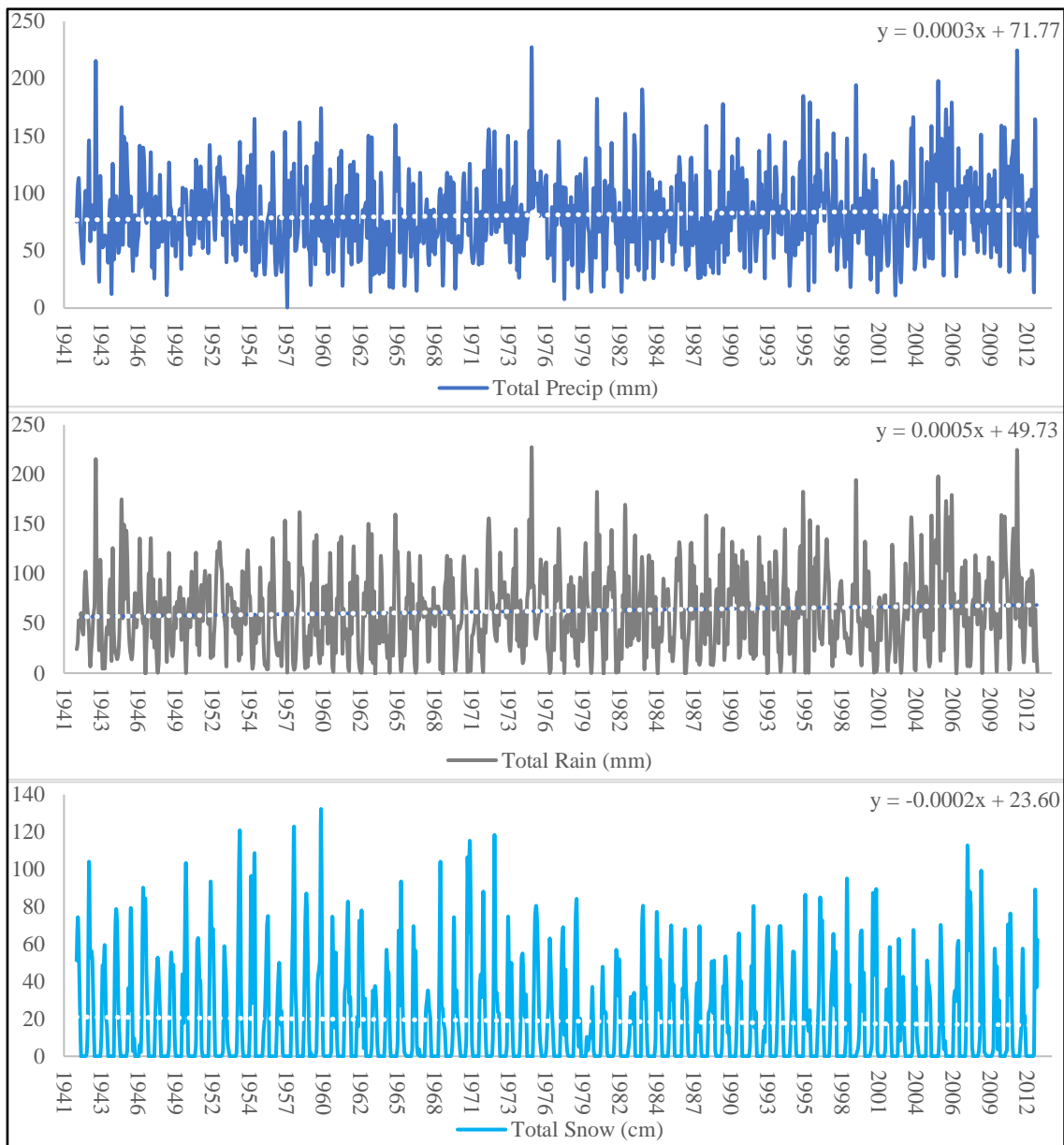


Figure A35 Annual Precipitation, Rainfall, and Snowfall for YUL from 1941 to 2012

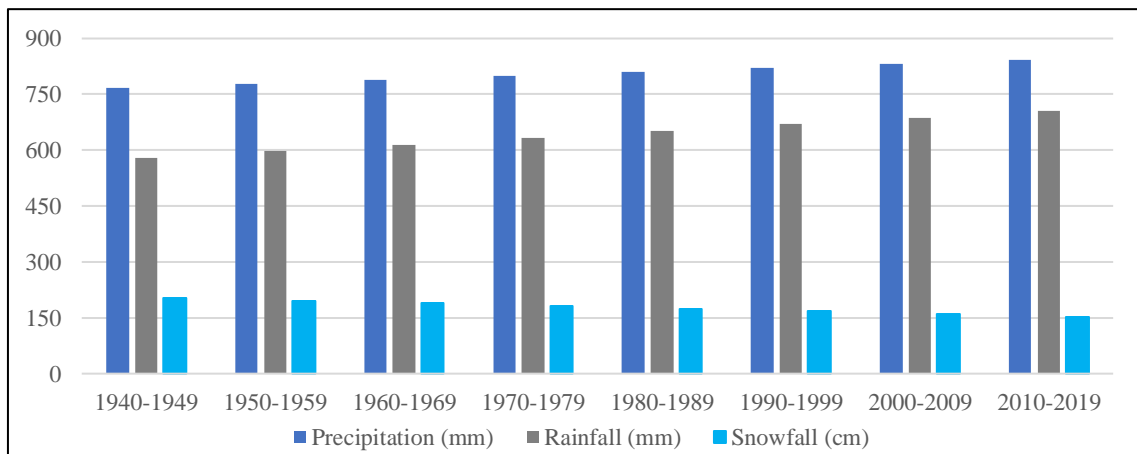


Figure A36 Annual Precip, Rainfall, and Snowfall Trends from YUL from 1940-1949 to 2010-2019

Halifax Stanfield International Airport

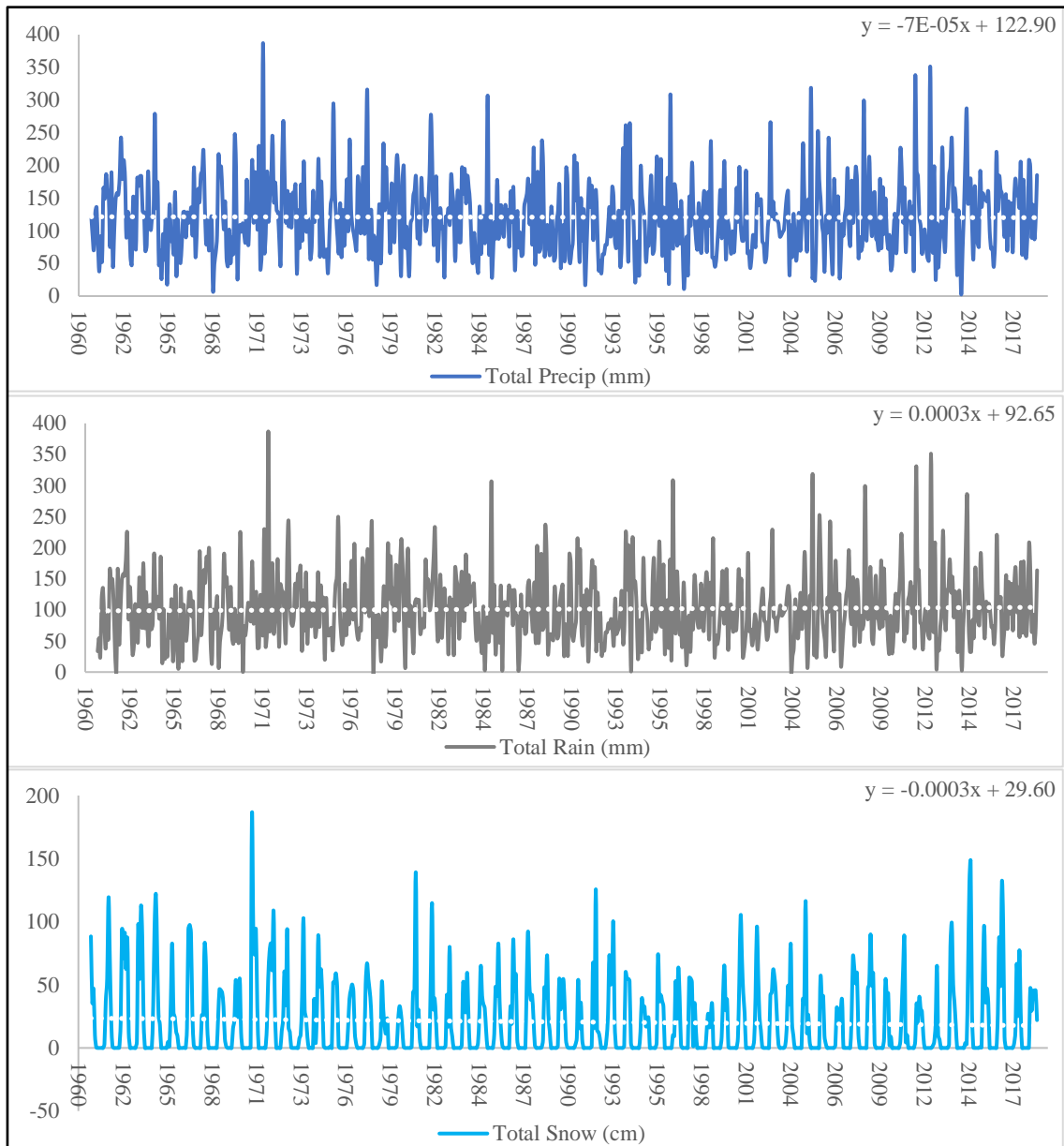


Figure A37 Annual Precipitation, Rainfall, and Snowfall for YHZ from 1960 to 2017

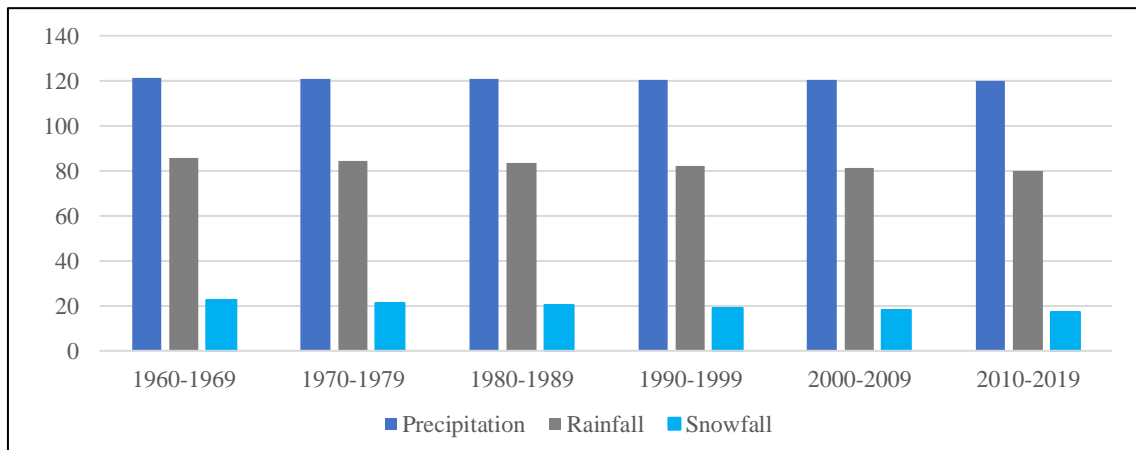


Figure A38 Annual Precip, Rainfall, and Snowfall Trends from YHZ from 1960-1969 to 2010-2019

Calgary International Airport

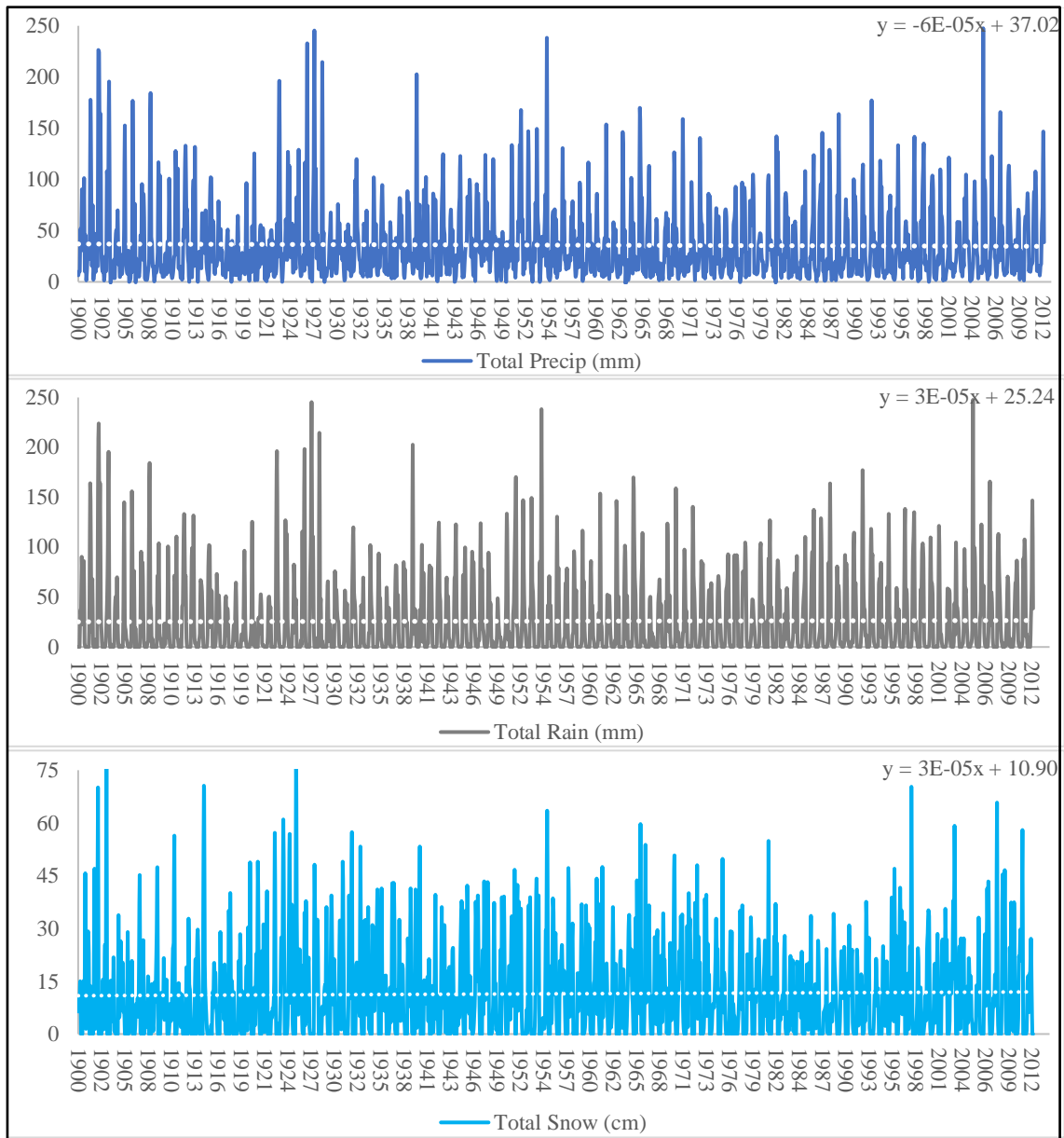


Figure A39 Annual Precipitation, Rainfall, and Snowfall for YYC from 1900 to 2012

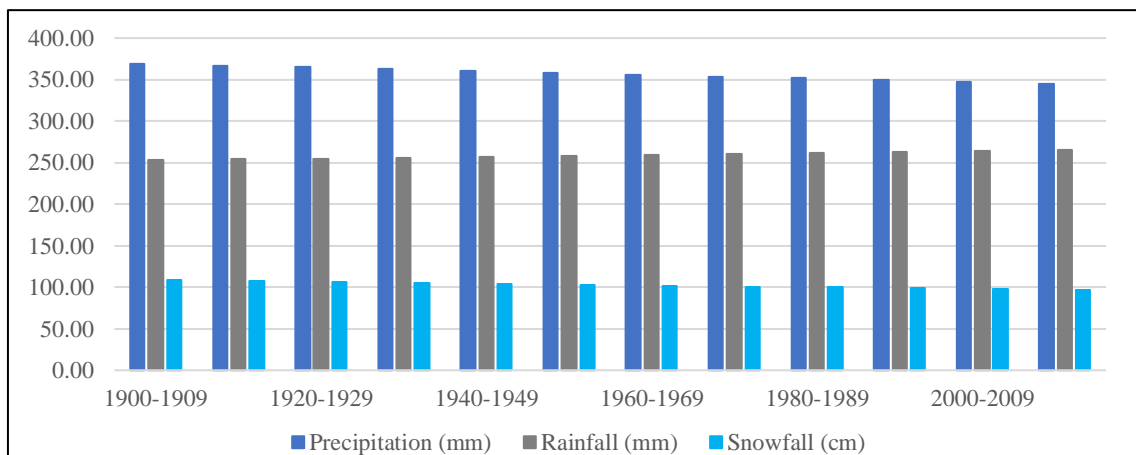


Figure A40 Annual Precip, Rainfall, and Snowfall Trends from YYC from 1940-1949 to 2010-2019

Saskatoon International Airport

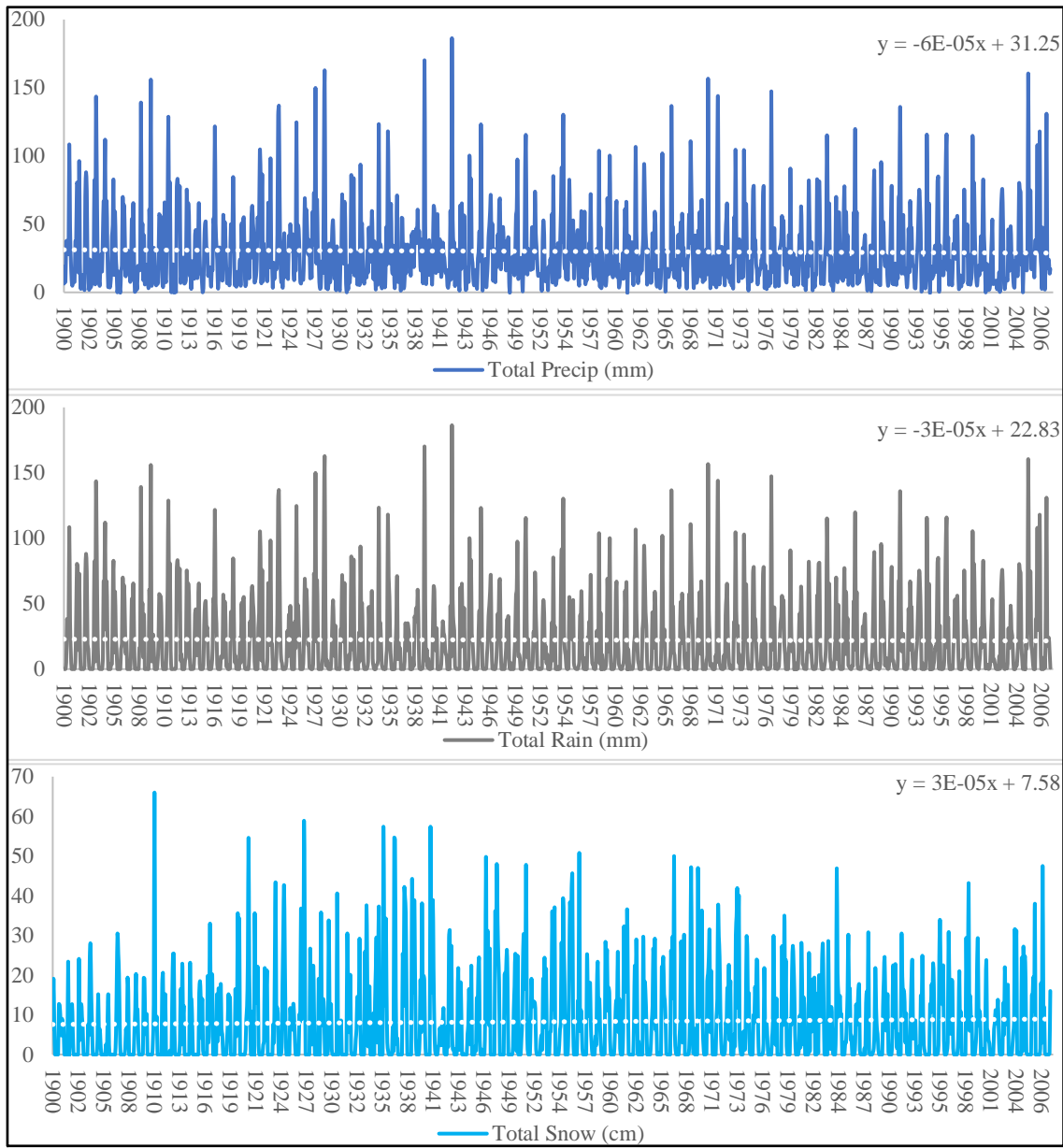


Figure A41 Annual Precipitation, Rainfall, and Snowfall for YXE from 1900 to 2006

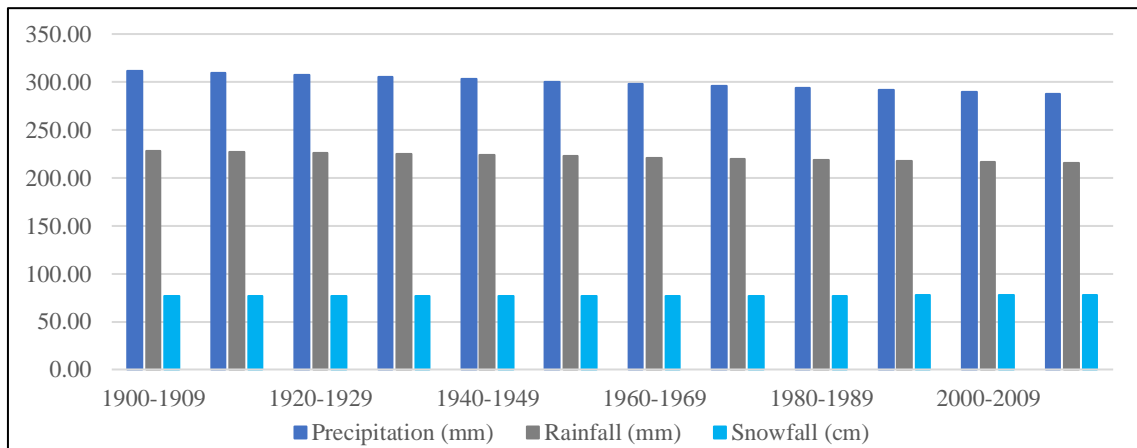


Figure A40 Annual Precip, Rainfall, and Snowfall Trends from YXE from 1900-1909 to 2010-2019

Winnipeg International Airport

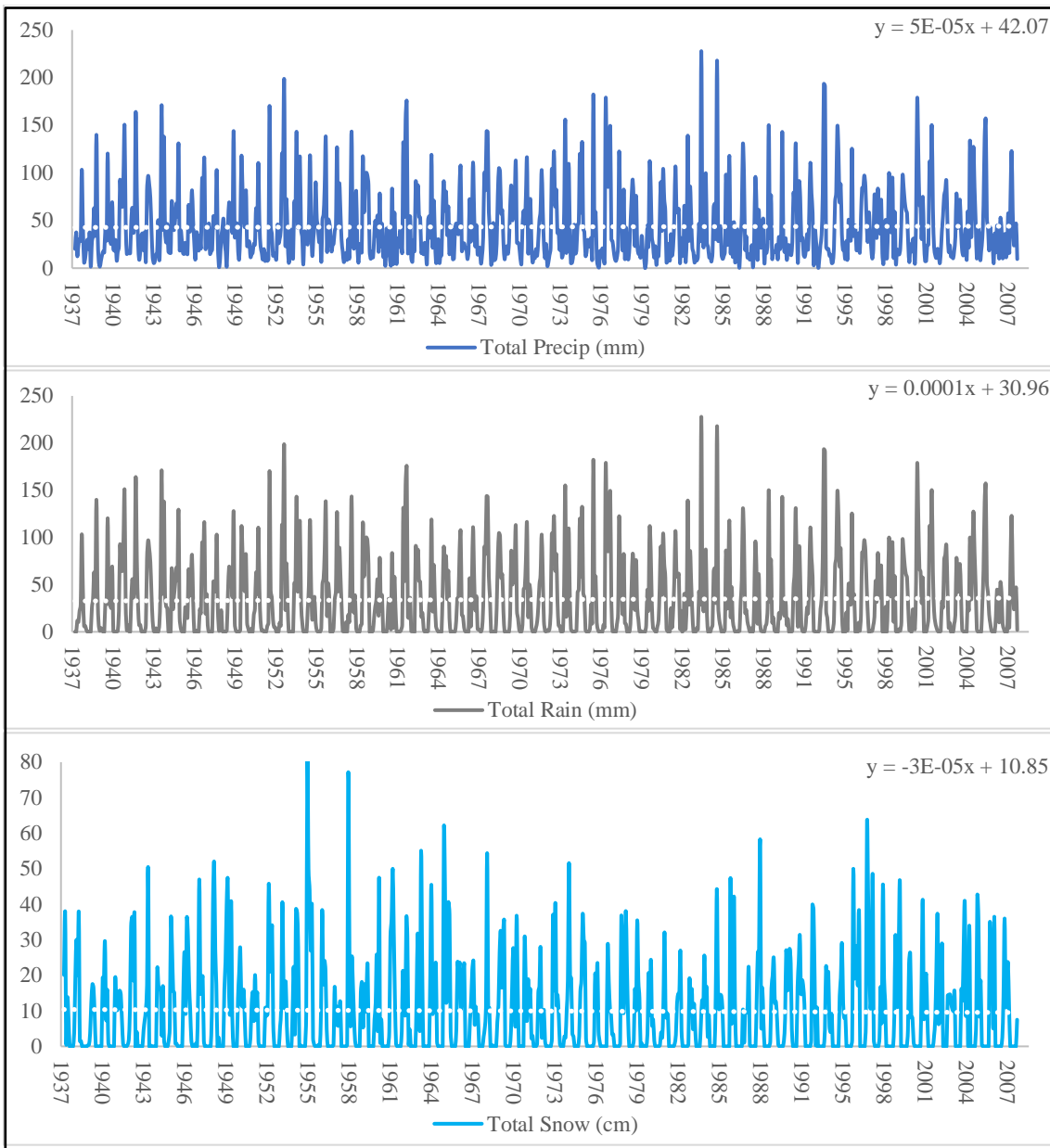


Figure A43 Annual Precipitation, Rainfall, and Snowfall for YWG from 1937 to 2007

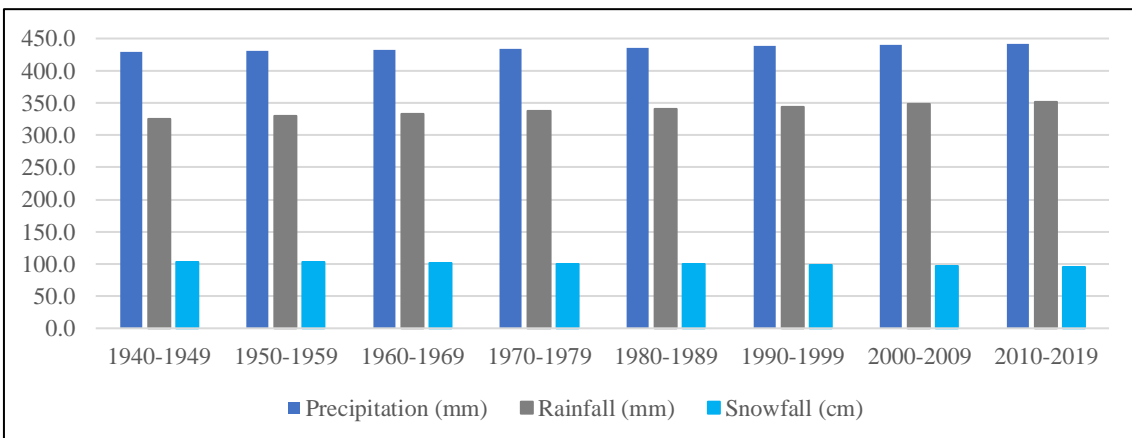


Figure A44 Annual Precip, Rainfall, and Snowfall Trends from YXE from 1940-1949 to 2010-2019

Moncton International Airport

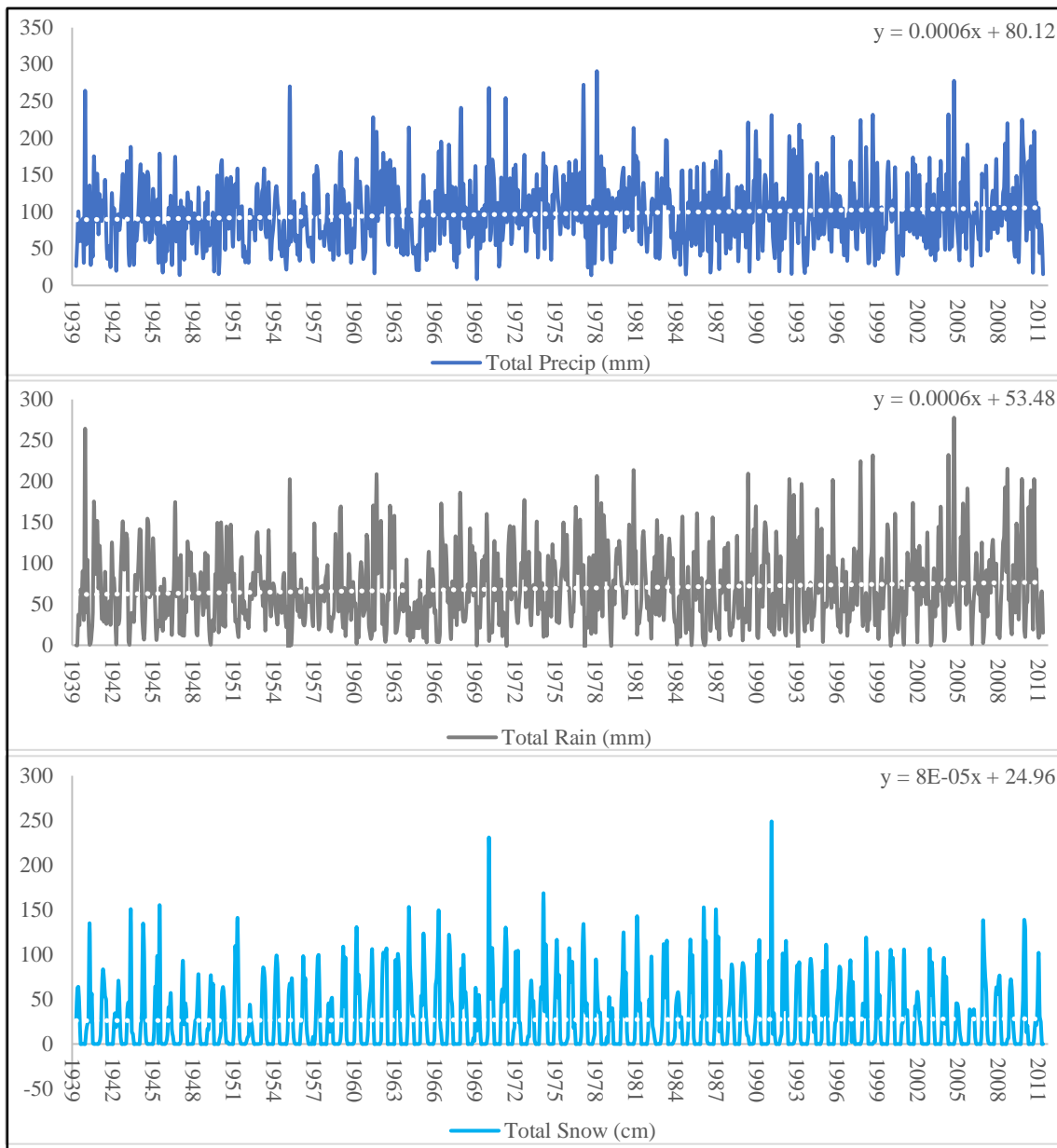


Figure A45 Annual Precipitation, Rainfall, and Snowfall for YQM from 1939 to 2011

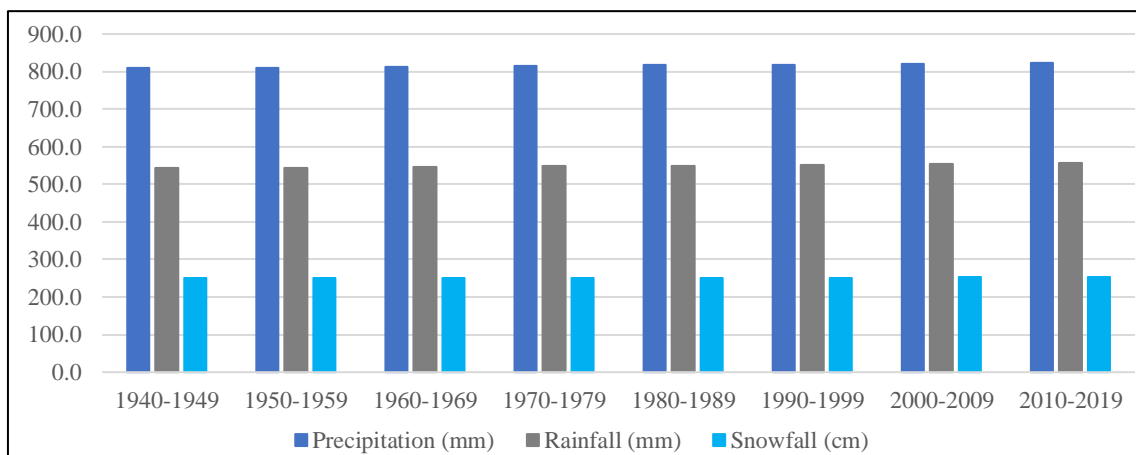


Figure A46 Annual Precip, Rainfall, and Snowfall Trends from YQM from 1940-1949 to 2010-2019

Whitehorse International Airport

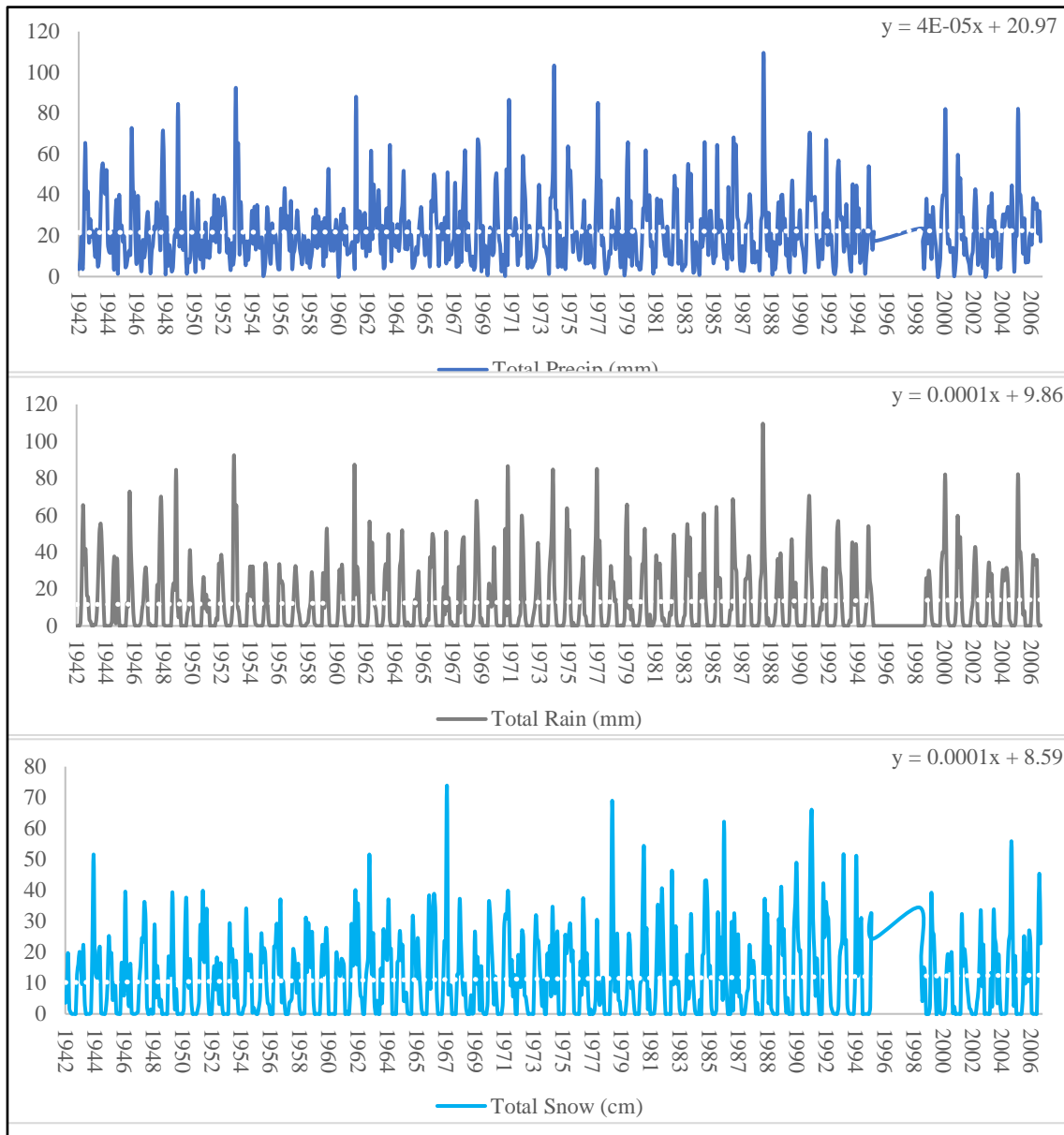


Figure A47 Annual Precipitation, Rainfall, and Snowfall for YXY from 1942 to 2006

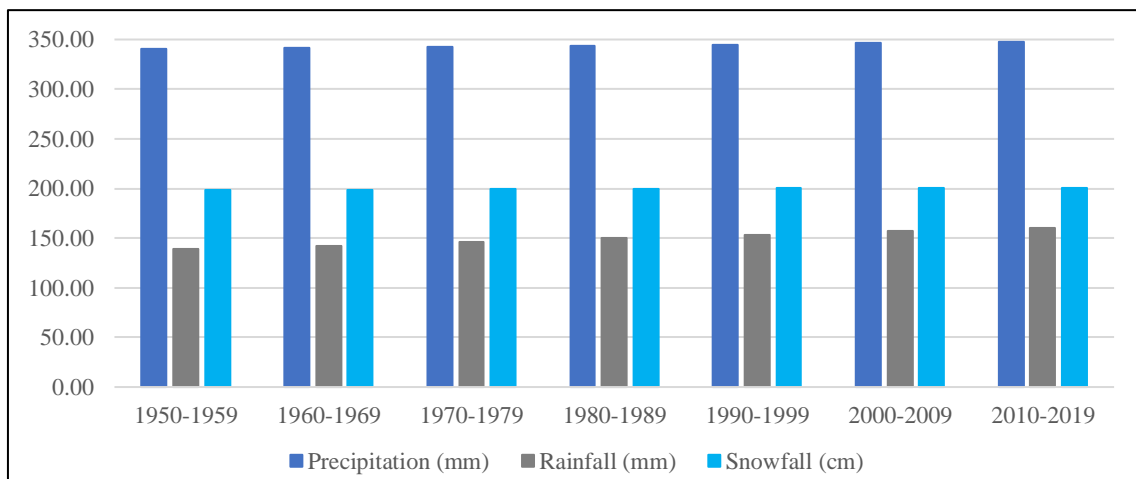


Figure A48 Annual Precip, Rainfall, and Snowfall Trends from YXY from 1950-1959 to 2010-2019

Yellowknife International Airport

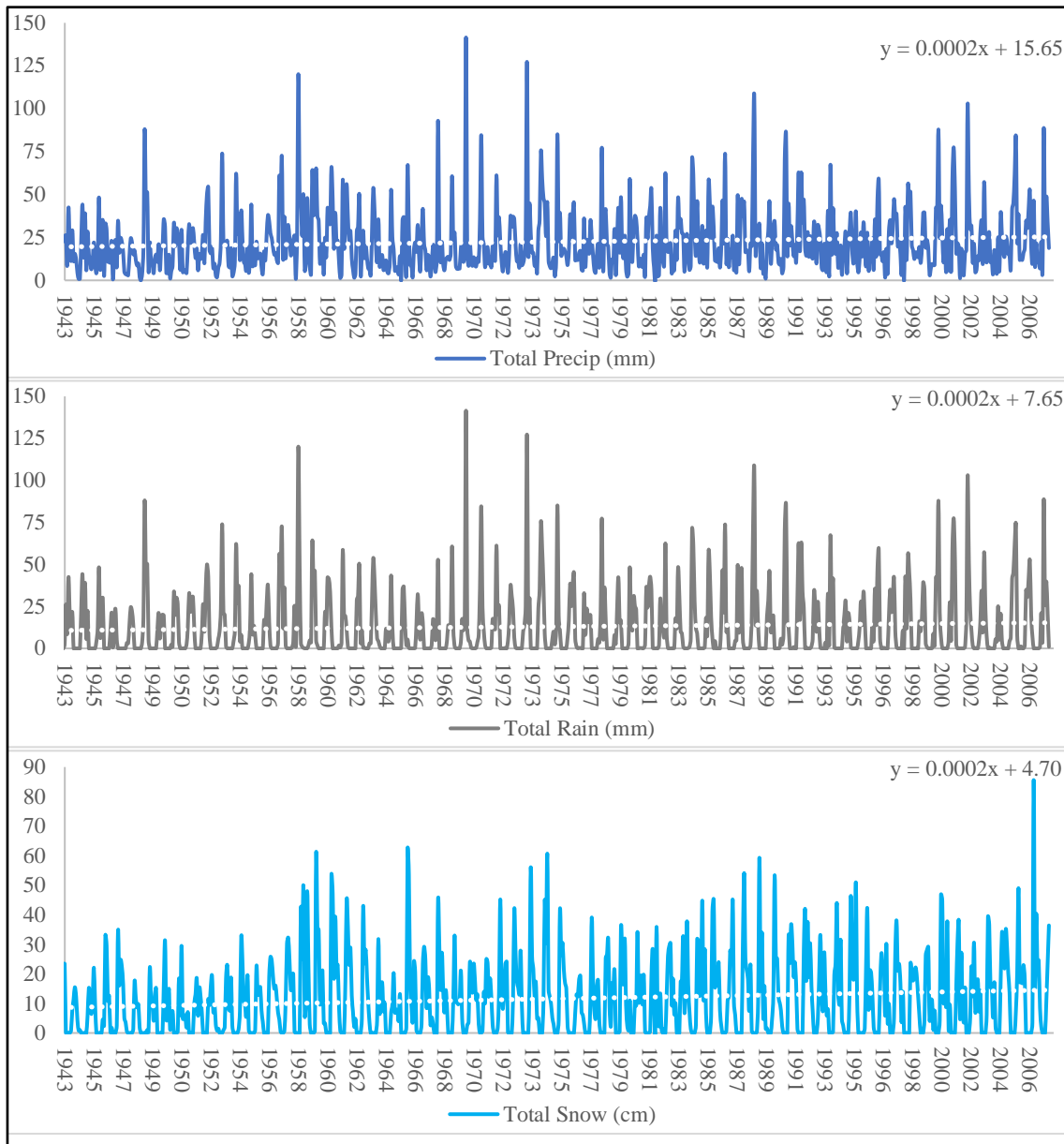


Figure A49 Annual Precipitation, Rainfall, and Snowfall for YZF from 1943 to 2006

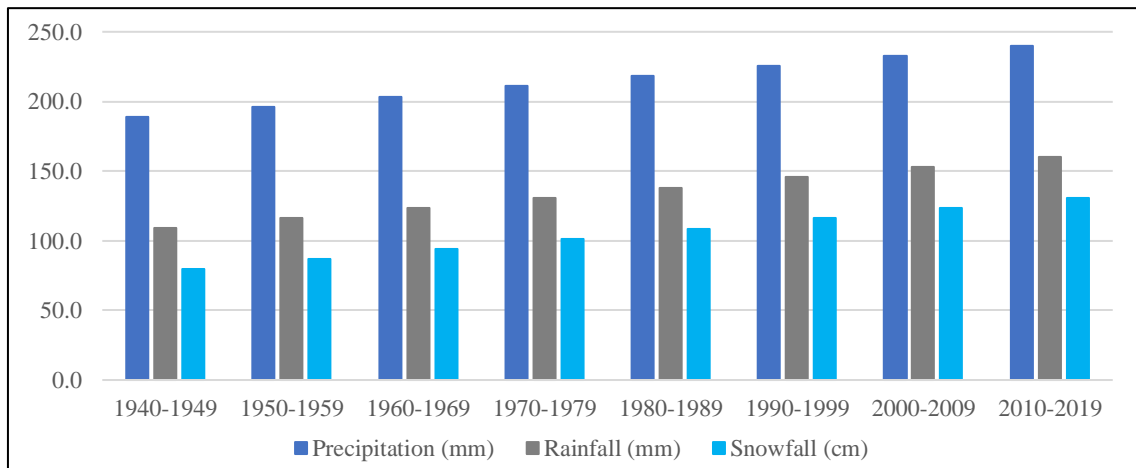


Figure A50 Annual Precip, Rainfall, and Snowfall Trends from YZF from 1940-1949 to 2010-2019

Iqaluit Airport

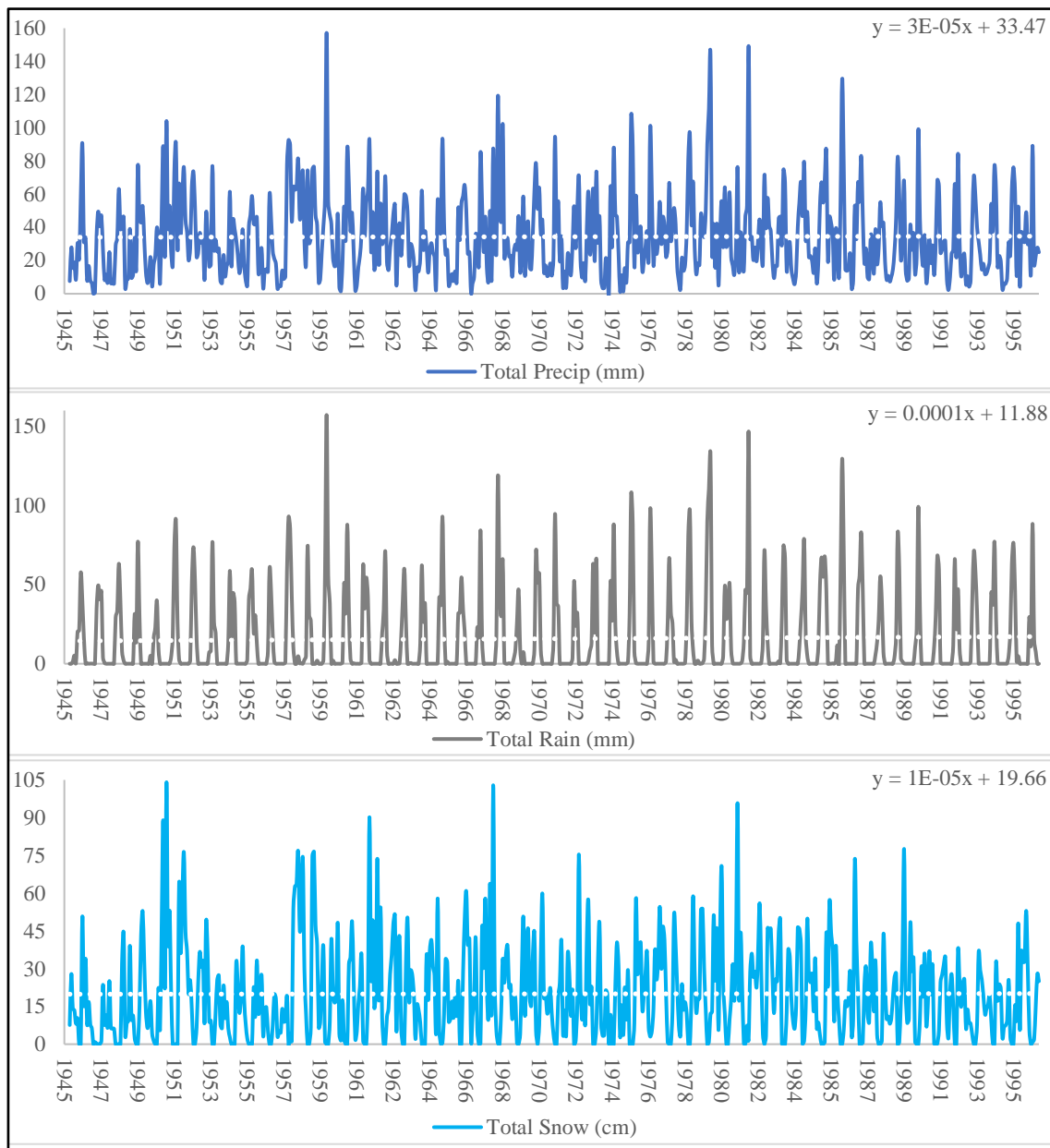


Figure A51 Annual Precipitation, Rainfall, and Snowfall for YFB from 1945 to 1995

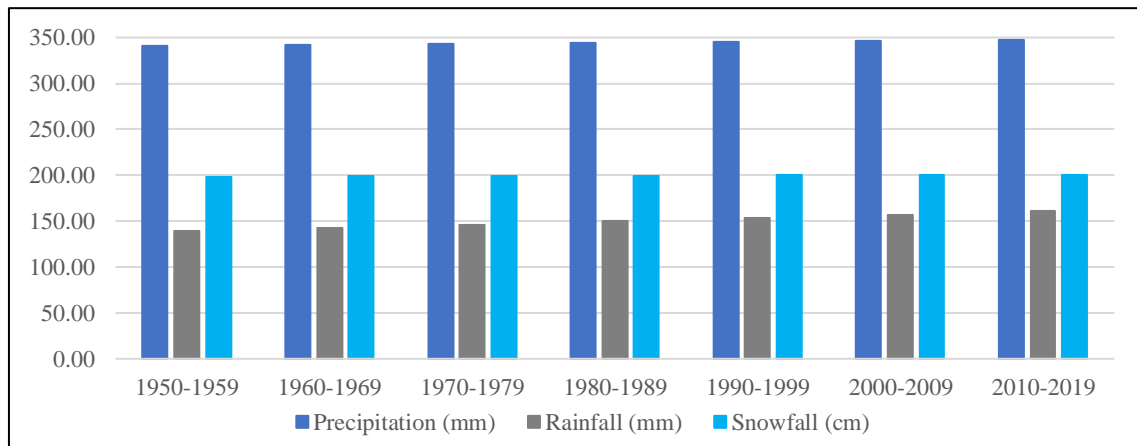


Figure A52 Annual Precip, Rainfall, and Snowfall Trends from YFB from 1950-1959 to 2010-2019

APPENDIX B

Laboratory Results

Hamburg Wheel Tracking Test Results

Temperature Variation

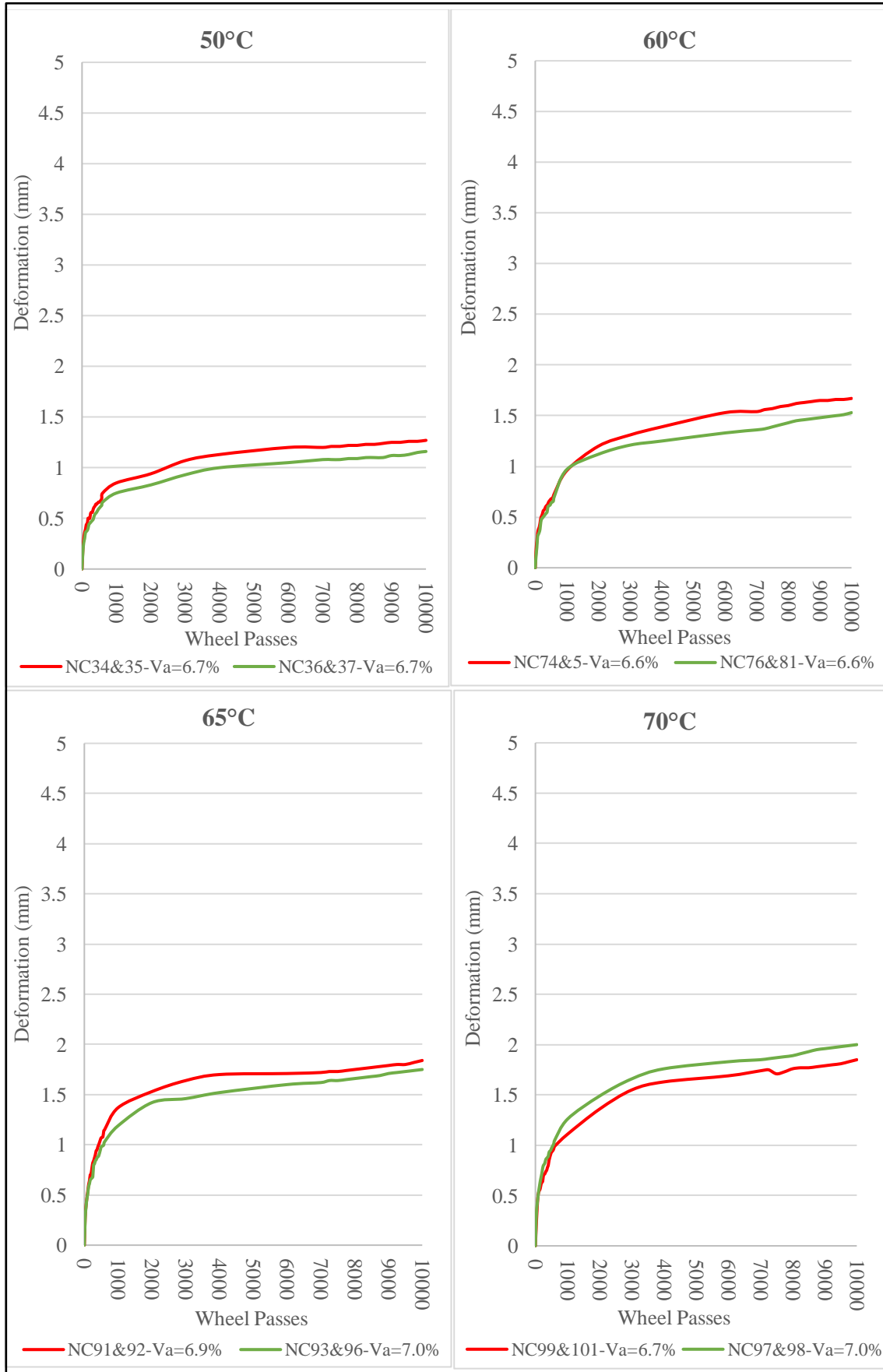


Figure B.1 Rutting Propagation versus Temperature Variation

Freeze-Thaw Cycles Variation

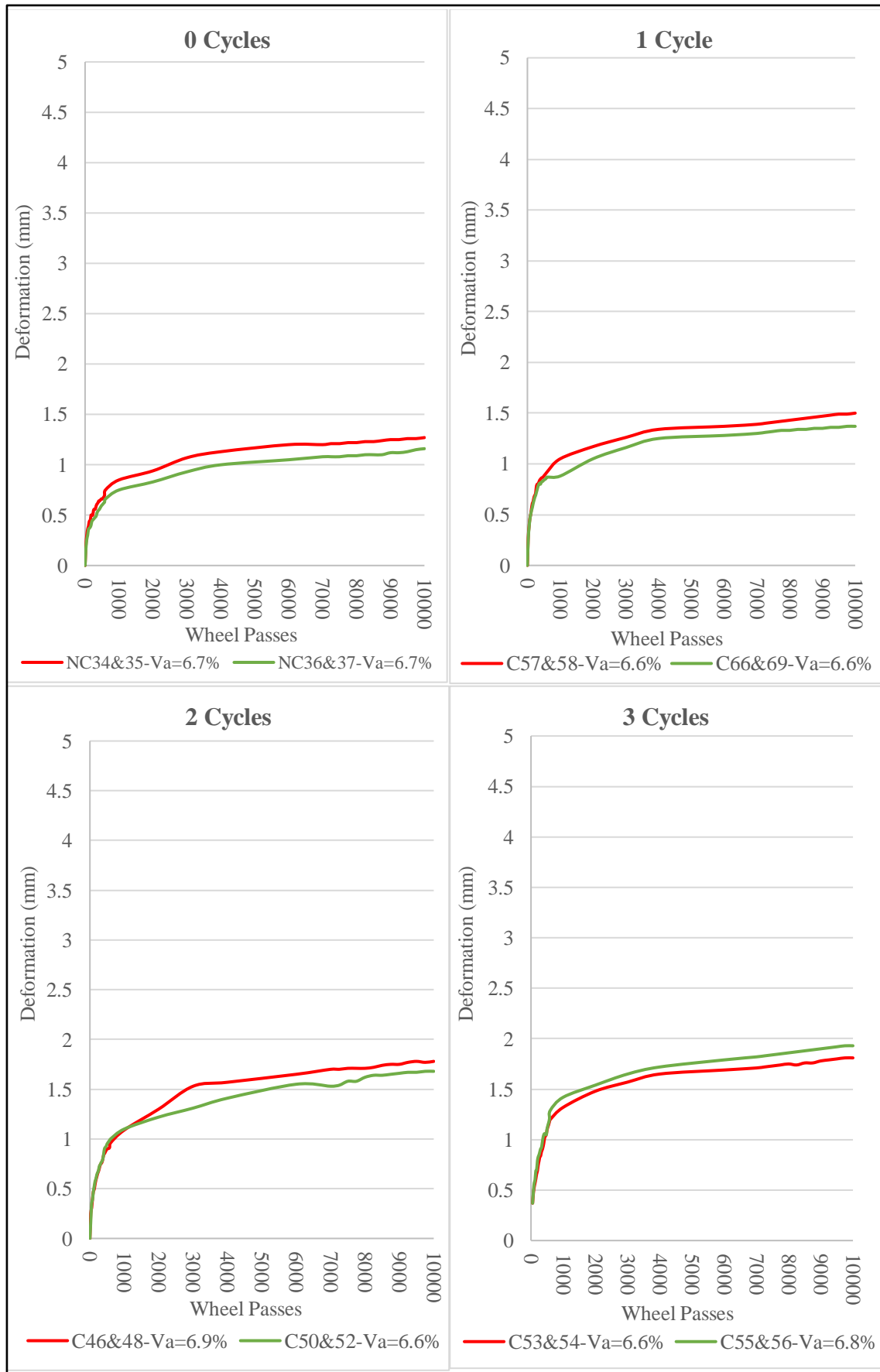


Figure B.2 Rutting Propagation versus Freeze-Thaw Cycles' Variation

Tensile Strength Ratio Results

Modified Lottman Test – 50 mm/min – Freeze-Thaw Cycles Variation

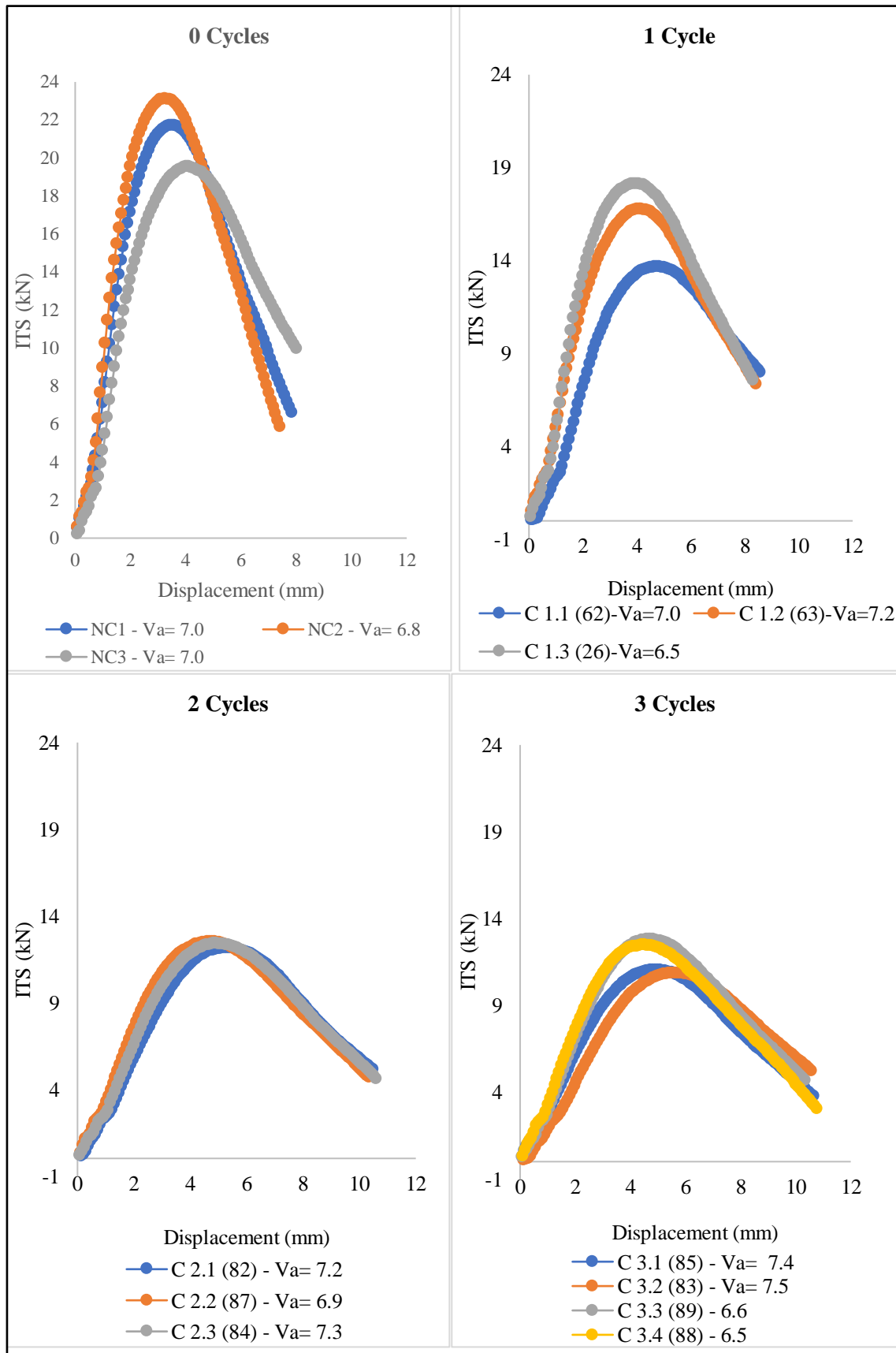


Figure B.3 ITS versus Displacement Variations due to F-T Cycles

Modified Lottman Test – 50 mm/sec – Freeze-Thaw Cycles Variation

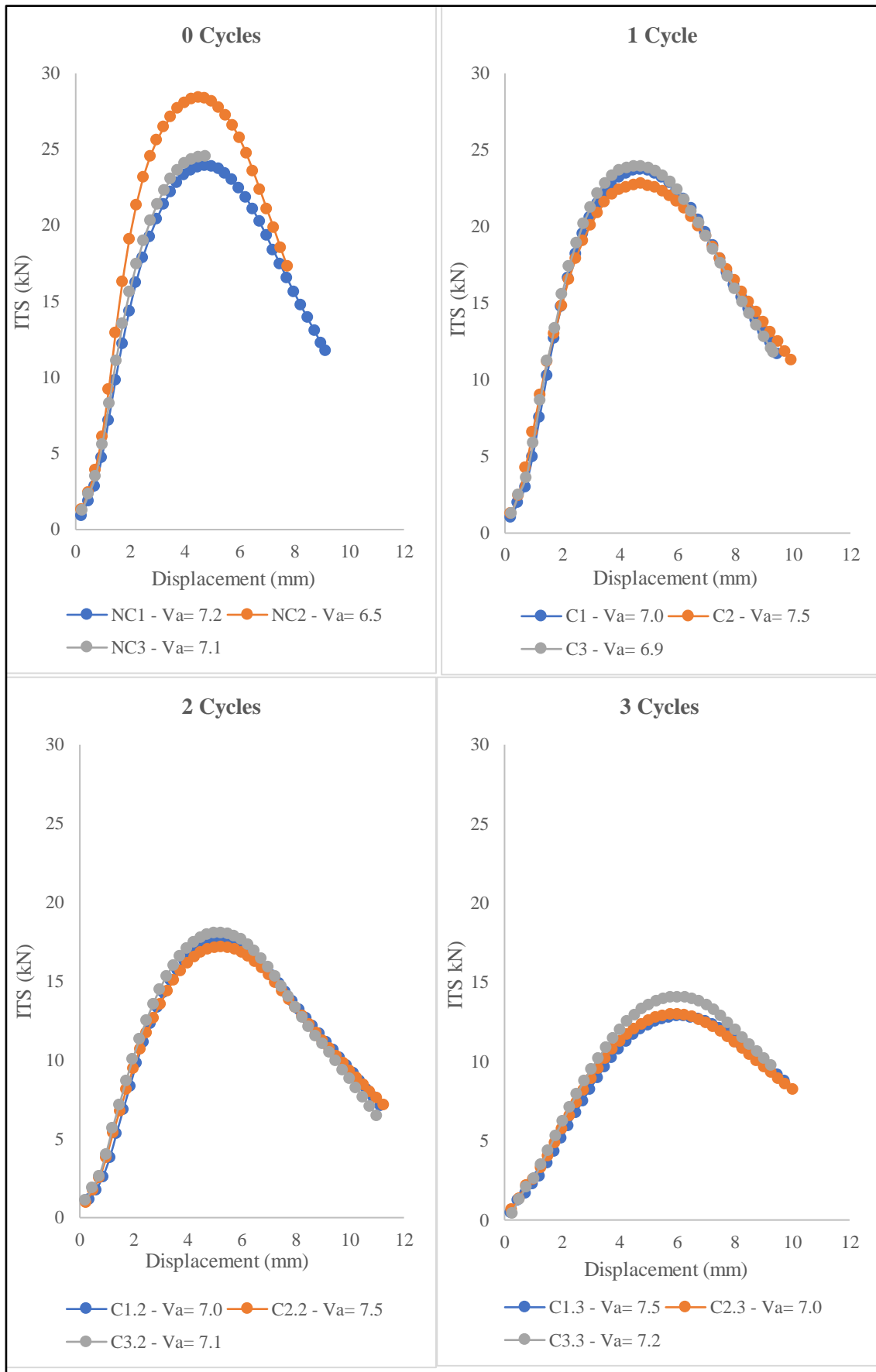


Figure B.4 ITS versus Displacement Variations due to F-T Cycles (Higher Speed of Loading)

Modified Lottman Test – 50 mm/sec – Half Freeze-Thaw Cycles Variation

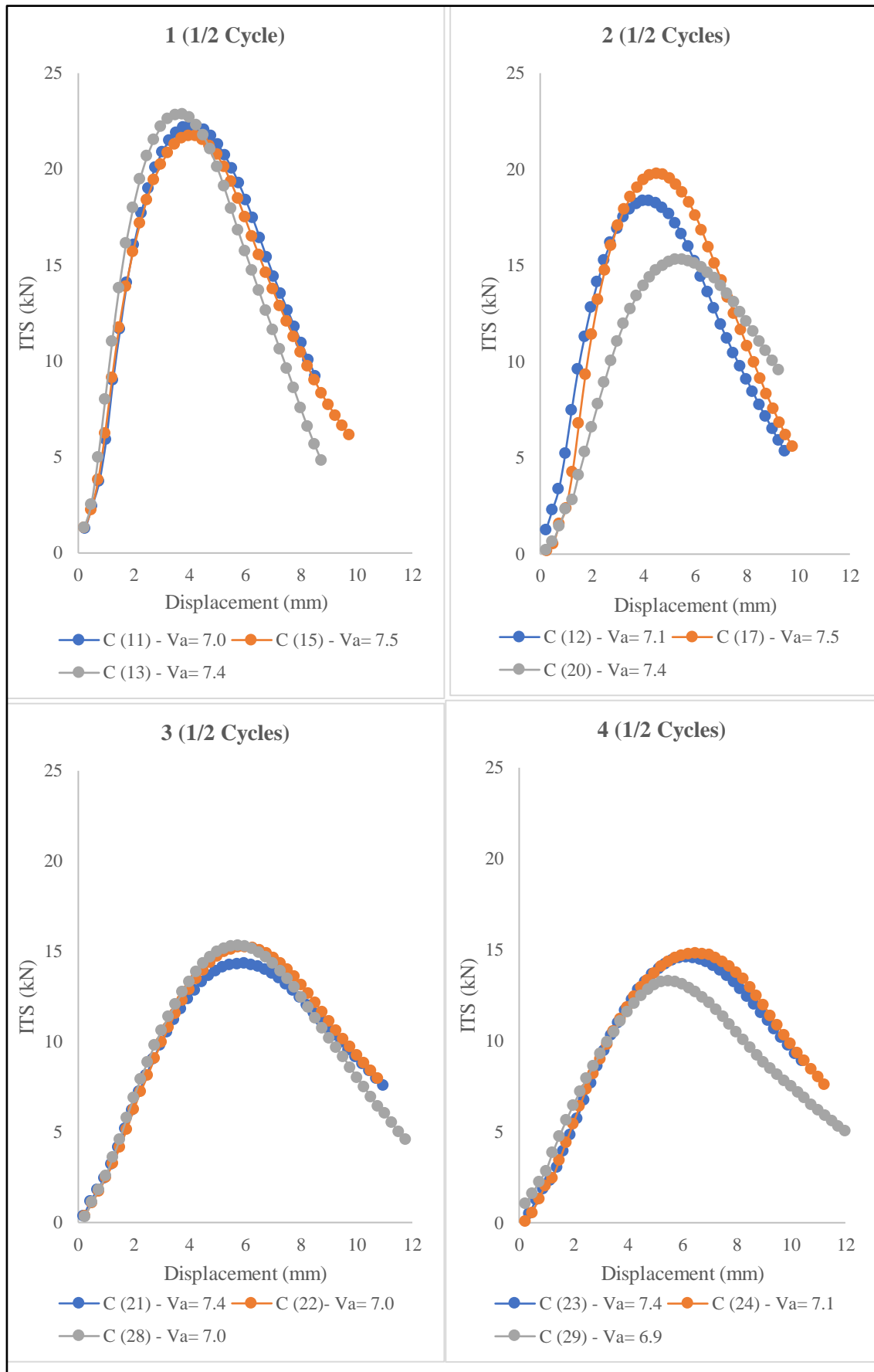


Figure B.5 ITS versus Displacement Variations due to Half F-T Cycles (Higher Speed of Loading)

Ideal Cracking Test Results

Table B.1 Tensile Strength and Ideal Cracking Test Average Results

Row Labels	Average of Tensile Strength (kPa)	Average of CT-Index
No. of Freeze-Thaw Cycles (50mm/min)		
0	958.87	120.83
1	723.30	182.03
2	553.20	272.98
3	528.40	279.89
No. of Freeze-Thaw Cycles (50mm/sec)		
0	1143.80	192.06
1	889.92	360.15
2	786.37	353.37
3	595.27	429.68

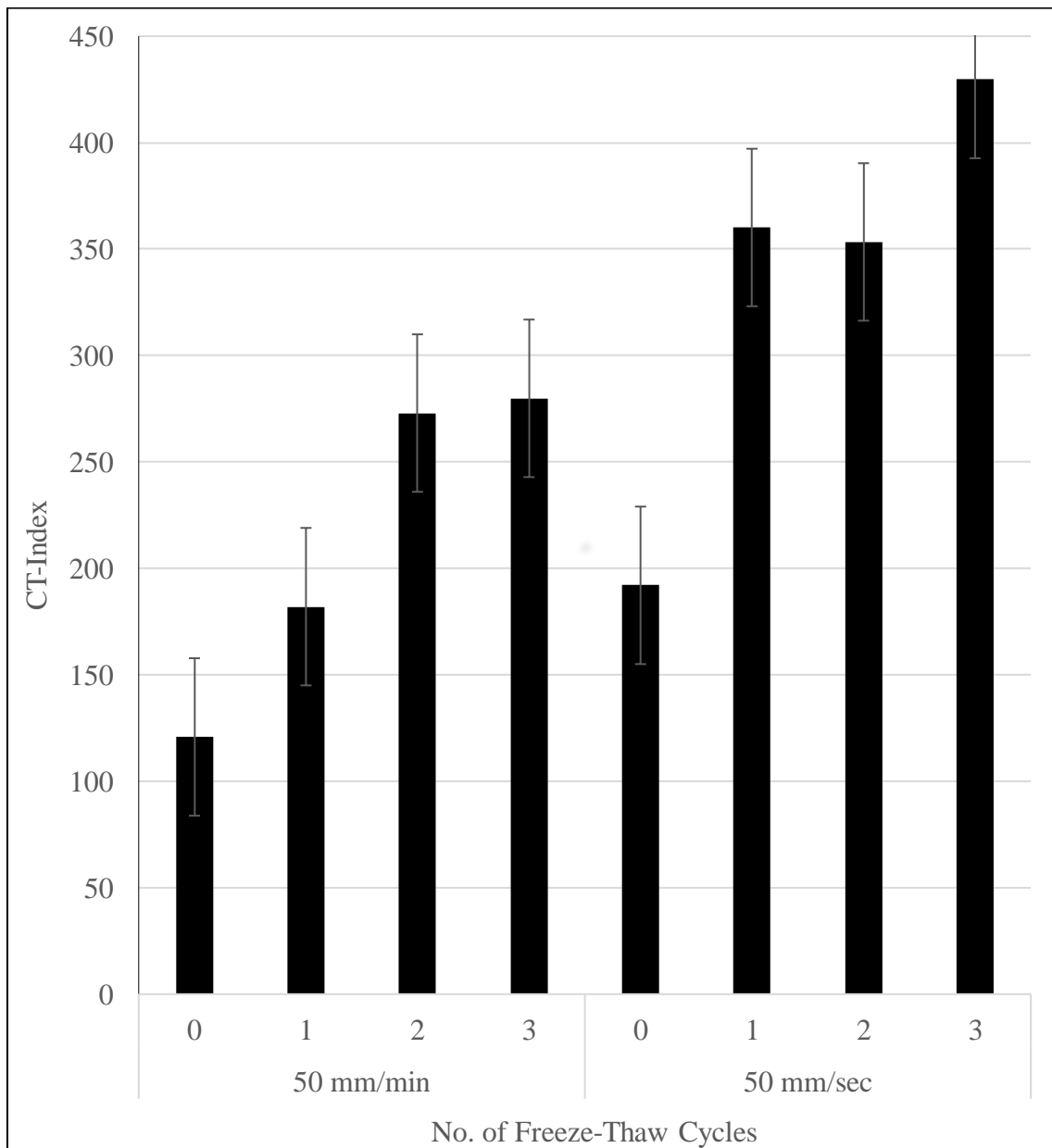


Figure B.6 Ideal CT Index Variations due to F-T Cycles and Speed of Loading



Load Report

Project ID:	Specimen ID:
Date / Time: 01-01-01 00:00	Stability (Peak Load): 21.72 kN
Specimen Diameter: 150.00 mm	IDT Strength: 970.3 kPa (140.7 PSI)
Specimen Thickness: 95.00 mm	Peak Displacement: 3.5 mm
Starting Load: 0.53 kN	Flow (0.01 inch units): 13.8
Stopping Load: 6.6 kN	Total Energy: 110.81 Joules
Max Specific Gravity:	Energy to Peak: 46.05 Joules
% Voids:	Temperature: 22 °C
% AC: %	IDEAL-CT Index: 96.532 Data did not reach 0.1kN load limit
Project ID:	Specimen ID:
Date / Time: 01-01-01 00:00	Stability (Peak Load): 23.1 kN
Specimen Diameter: 150.00 mm	IDT Strength: 1032.9 kPa (149.8 PSI)
Specimen Thickness: 95.00 mm	Peak Displacement: 3.25 mm
Starting Load: 0.6 kN	Flow (0.01 inch units): 12.8
Stopping Load: 5.8 kN	Total Energy: 111.24 Joules
Max Specific Gravity:	Energy to Peak: 45.79 Joules
% Voids:	Temperature: 22 °C
% AC: %	IDEAL-CT Index: 85.267 Data did not reach 0.1kN load limit
Project ID:	Specimen ID:
Date / Time: 01-01-01 00:00	Stability (Peak Load): 19.6 kN
Specimen Diameter: 150.00 mm	IDT Strength: 873.4 kPa (126.7 PSI)
Specimen Thickness: 95.00 mm	Peak Displacement: 4.09 mm
Starting Load: 0.2 kN	Flow (0.01 inch units): 16
Stopping Load: 5.3 kN	Total Energy: 126.27 Joules
Max Specific Gravity:	Energy to Peak: 48.13 Joules
% Voids:	Temperature: 22 °C
% AC: %	IDEAL-CT Index: 180.693 Data did not reach 0.1kN load limit

Technician:

Signature: _____

Figure B.7 Ideal CT Report for the Non-Condition Samples



Load Report

Project ID:	Specimen ID:
Date / Time: 01-01-01 00:00	Stability (Peak Load): 18.13 kN
Specimen Diameter: 150.00 mm	IDT Strength: 810 kPa (117.5 PSI)
Specimen Thickness: 95.00 mm	Peak Displacement: 3.99 mm
Starting Load: 0.22 kN	Flow (0.01 inch units): 15.7
Stopping Load: 7.6 kN	Total Energy: 102.91 Joules
Max Specific Gravity:	Energy to Peak: 44.45 Joules
% Voids:	Temperature: 22 °C
% AC: %	IDEAL-CT Index: 149.99 Data did not reach 0.1kN load limit
Project ID:	Specimen ID:
Date / Time: 01-01-01 00:00	Stability (Peak Load): 13.7 kN
Specimen Diameter: 150.00 mm	IDT Strength: 610.3 kPa (88.5 PSI)
Specimen Thickness: 95.00 mm	Peak Displacement: 4.75 mm
Starting Load: 0.1 kN	Flow (0.01 inch units): 18.7
Stopping Load: 8.0 kN	Total Energy: 80.55 Joules
Max Specific Gravity:	Energy to Peak: 37.34 Joules
% Voids:	Temperature: 22 °C
% AC: %	IDEAL-CT Index: 233.237 Data did not reach 0.1kN load limit
Project ID:	Specimen ID:
Date / Time: 01-01-01 00:00	Stability (Peak Load): 16.8 kN
Specimen Diameter: 150.00 mm	IDT Strength: 749.6 kPa (108.7 PSI)
Specimen Thickness: 95.00 mm	Peak Displacement: 4.09 mm
Starting Load: 0.5 kN	Flow (0.01 inch units): 16
Stopping Load: 7.4 kN	Total Energy: 96.9 Joules
Max Specific Gravity:	Energy to Peak: 42.25 Joules
% Voids:	Temperature: 22 °C
% AC: %	IDEAL-CT Index: 162.862 Data did not reach 0.1kN load limit

Technician: _____

Signature: _____

Figure B.8 Ideal CT Report for the Samples with one Freeze-Thaw Cycle



Load Report

Project ID:	Specimen ID:
Date / Time: 01-01-01 00:00	Stability (Peak Load): 12.18 kN
Specimen Diameter: 150.00 mm	IDT Strength: 544.1 kPa (78.9 PSI)
Specimen Thickness: 95.00 mm	Peak Displacement: 5.23 mm
Starting Load: 0.18 kN	Flow (0.01 inch units): 20.6
Stopping Load: 5.2 kN	Total Energy: 85.14 Joules
Max Specific Gravity:	Energy to Peak: 37.27 Joules
% Voids:	Temperature: 22 °C
% AC: %	IDEAL-CT Index: 266.576 Data did not reach 0.1kN load limit
Project ID:	Specimen ID:
Date / Time: 01-01-01 00:00	Stability (Peak Load): 12.4 kN
Specimen Diameter: 150.00 mm	IDT Strength: 555.3 kPa (80.5 PSI)
Specimen Thickness: 95.00 mm	Peak Displacement: 4.84 mm
Starting Load: 0.2 kN	Flow (0.01 inch units): 19.1
Stopping Load: 4.6 kN	Total Energy: 88.07 Joules
Max Specific Gravity:	Energy to Peak: 35.51 Joules
% Voids:	Temperature: 22 °C
% AC: %	IDEAL-CT Index: 279.385 Data did not reach 0.1kN load limit
Project ID:	Specimen ID:
Date / Time: 01-01-01 00:00	Stability (Peak Load): 12.5 kN
Specimen Diameter: 150.00 mm	IDT Strength: 560.2 kPa (81.3 PSI)
Specimen Thickness: 95.00 mm	Peak Displacement: 4.77 mm
Starting Load: 0.4 kN	Flow (0.01 inch units): 19
Stopping Load: 4.7 kN	Total Energy: 87.95 Joules
Max Specific Gravity:	Energy to Peak: 37.45 Joules
% Voids:	Temperature: 22 °C
% AC: %	IDEAL-CT Index: 272.977 Data did not reach 0.1kN load limit

Technician: _____

Signature: _____

Figure B.9 Ideal CT Report for the Samples with two Freeze-Thaw Cycles



Load Report

Project ID:	Specimen ID:
Date / Time: 01-01-01 00:00	Stability (Peak Load): 10.9 kN
Specimen Diameter: 150.00 mm	IDT Strength: 487 kPa (70.6 PSI)
Specimen Thickness: 95.00 mm	Peak Displacement: 5.73 mm
Starting Load: 0.11 kN	Flow (0.01 inch units): 22.6
Stopping Load: 5.3 kN	Total Energy: 77.5 Joules
Max Specific Gravity:	Energy to Peak: 36.58 Joules
% Voids:	Temperature: 22 °C
% AC: %	IDEAL-CT Index: 330.234 Data did not reach 0.1kN load limit
Project ID:	Specimen ID:
Date / Time: 01-01-01 00:00	Stability (Peak Load): 11.1 kN
Specimen Diameter: 150.00 mm	IDT Strength: 494.6 kPa (71.7 PSI)
Specimen Thickness: 95.00 mm	Peak Displacement: 4.91 mm
Starting Load: 0.7 kN	Flow (0.01 inch units): 19.3
Stopping Load: 3.8 kN	Total Energy: 78.39 Joules
Max Specific Gravity:	Energy to Peak: 33.42 Joules
% Voids:	Temperature: 22 °C
% AC: %	IDEAL-CT Index: 260.267 Data did not reach 0.1kN load limit
Project ID:	Specimen ID:
Date / Time: 01-01-01 00:00	Stability (Peak Load): 12.5 kN
Specimen Diameter: 150.00 mm	IDT Strength: 558.4 kPa (81 PSI)
Specimen Thickness: 95.00 mm	Peak Displacement: 4.43 mm
Starting Load: 0.4 kN	Flow (0.01 inch units): 17
Stopping Load: 3.1 kN	Total Energy: 87.32 Joules
Max Specific Gravity:	Energy to Peak: 33.54 Joules
% Voids:	Temperature: 22 °C
% AC: %	IDEAL-CT Index: 263.713 Data did not reach 0.1kN load limit
Project ID:	Specimen ID:
Date / Time: 01-01-01 00:00	Stability (Peak Load): 12.8 kN
Specimen Diameter: 150.00 mm	IDT Strength: 573.6 kPa (83.2 PSI)
Specimen Thickness: 95.00 mm	Peak Displacement: 4.58 mm
Starting Load: 0.3 kN	Flow (0.01 inch units): 18.0
Stopping Load: 5.2 kN	Total Energy: 88.54 Joules
Max Specific Gravity:	Energy to Peak: 34.27 Joules
% Voids:	Temperature: 22 °C
% AC: %	IDEAL-CT Index: 265.361 Data did not reach 0.1kN load limit

Technician:

Signature: _____

Figure B.10 Ideal CT Report for the Samples with three Freeze-Thaw Cycles